

**THE INFLUENCE OF OsAUX1 ON ROOT SYSTEM ARCHITECTURE AND
PHOSPHORUS UPTAKE IN RICE (ORYZA SATIVA)**

Susan Christine Zappala, BSc. (Hons)

Thesis submitted to the University of Nottingham for the
degree of Doctor of Philosophy

July 2014

Abstract

Rice (*Oryza sativa* L.) provides up to 50% of the total calories consumed in countries such as India, Madagascar and Nigeria. As a crop, rice can require significant fertiliser inputs to maintain the required yields. Additionally, climate change has increased the need for rice varieties with improved drought resistance, tolerance to pests and more efficient acquisition of nutrients from soil. One major fertiliser input for rice is phosphate; reducing phosphorus (P) fertiliser use would have environmental and economic implications.

Root traits linked to P acquisition in crops include shallow root angle, lateral root proliferation and increases in root hair length and density. Two T-DNA knockout alleles with reduced gravitropic response, *Osaux1-1* and *Osaux1-2*, were used to investigate the influence of shallow root angle on P uptake. OsAUX1 is a rice ortholog for the *Arabidopsis thaliana* gene AUX1, which controls lateral root growth and gravitropic response.

The wildtype and mutant rice plants were grown in soil and non-destructively imaged using X-ray micro Computed Tomography (X-ray CT). In Chapter Three, visualisation of rice roots in soil using X-ray CT was optimised by determining the ideal soil moisture content that would produce the best images. Water in soils has a similar X-ray attenuation density to that of plant roots and can influence segmentation of roots from soil in X-ray CT images. It was found that soil at nominal field capacity (ca. 3 days of drainage) produced the best contrast between soil fractions (organic matter, minerals and pore space) and root material. In Chapter Four, the impact of X-ray dose on root growth was quantified because the experimental design included repeated scanning of the same sample (Chapter Five). It was found that even under repeated scanning, the X-ray doses involved in this work (ca. 15 Gy

per sample) did not significantly affect the root architecture and overall plant growth in rice cultivars used.

In Chapter Five, *Osaux1-1* and *Osaux1-2* retained the agravitropic phenotype that was observed on agar-based systems when plants were grown in loamy sand soil. However, when subject to various soil P concentrations and distributions (Chapter Six), *Osaux1-1* had similar gravitropic response and P uptake as wildtype. It was unclear what role gravitropism and topsoil foraging played in P uptake for these rice cultivars, if any. OsAUX1 could be linked to P uptake as well as responses to soil P concentration and distribution. Under uniformly low soil P wildtype had a shallower root system distribution than *Osaux1-1*. Of most interest were the results when sufficient soil P was sequestered to the top 4 cm of the soil column and low P was maintained in the bottom 6 cm. Under these conditions, wildtype took up more overall P, had almost twice the biomass, twice the total root length and twice the surface area when compared to *Osaux1-1*. This provides evidence that OsAUX1 can be linked to adaptation to P stress and distribution of P in soil through control of fine root characteristics and not necessarily its impact on gravitropic response.

Chapter Seven describes the investigation into the impact of OsAUX1 on sub-architectural effects of the root system that could influence P uptake. It was determined that OsAUX1 was involved in root hair density and elongation under varying P availability for agar grown plants. In comparison to wildtype, *Osaux1-1* had significant variation in root hair phenotype that seemed unrelated to a P stress response. In flooded environments, root hairs influence the potential for root:soil contact that is integral to P uptake in rice paddies which have reduced soil conditions and mass water flow that can transport plant available soluble P. This reinforces the potential for an interaction between OsAUX1 and P uptake in paddy rice.

Publications arising from this work

Refereed journal articles included in the thesis

Zappala, S., Mairhofer, S., Tracy, S., Sturrock, C. J., Bennett, M., Pridmore, T., & Mooney, S. J. (2013). Quantifying the effect of soil moisture content on segmenting root system architecture in X-ray computed tomography images. *Plant and Soil*, 370 (1-2), 35-45.

Zappala, S., Helliwell, J. R., Tracy, S. R., Mairhofer, S., Sturrock, C. J., Pridmore, T., Bennett, M. & Mooney, S. J. (2013). Effects of X-Ray Dose On Rhizosphere Studies Using X-Ray Computed Tomography. *PloS one*, 8(6), e67250.

Other related refereed journal articles not included in the thesis

Hill, K., Porco, S., Lobet, G., **Zappala, S.**, Mooney, S.J., Draye, X., Bennett, M. (2014). Root Systems Biology: Bridging regulatory networks to rhizosphere-scale processes. *Plant Physiology*, 164:1619-1627.

Mairhofer, S., **Zappala, S.**, Tracy, S., Sturrock, C., Bennett, M. J., Mooney, S. J., & Pridmore, T. P. (2013). Recovering complete plant root system architectures from soil via X-ray μ -Computed Tomography. *Plant Methods*, 9(1), 8.

Mairhofer, S., **Zappala, S.**, Tracy, S. R., Sturrock, C., Bennett, M., Mooney, S. J., & Pridmore, T. (2012). RooTrak: Automated recovery of three-dimensional plant root architecture in soil from X-ray microcomputed tomography images using visual tracking. *Plant Physiology*, 158(2), 561-569.

Lucas, M., Swarup, R., Paponov, I. A., Swarup, K., Casimiro, I., Lake, D., Peret, B., **Zappala, S.**, Mairhofer, S., Whitworth, M., Wang, J., Ljung, K., Marchant, A., Sandberg, G., Holdsworth, M., Palme, K., Pridmore, T., Mooney, S. J. & Bennett, M. J. (2011). Short-Root regulates primary, lateral, and adventitious root development in Arabidopsis. *Plant Physiology*, 155(1), 384-398.

Acknowledgements

A PhD thesis is meant to be the culmination of work solely completed by the author, however it would be impossible to create without the support of so many others. First, I'd like to thank my supervisors Sacha J. Mooney, Malcolm J. Bennett and Tony Pridmore for giving me this opportunity to work at the cutting edge of plant and soil science, patiently providing support throughout the PhD process and allowing me enough leeway to truly implement the scientific method. This work would not have been possible without financial support from University of Nottingham and the Engineering and Physical Sciences Research Council.

There are so many practicalities with working in a lab and learning new techniques. Thank you to my colleagues for being so open with your knowledge and enthusiasm. In particular, thank you to Silvana Porco, Antoine Larrieu and Helen Parker for taking time to help me navigate the wonderful world of plant molecular biology and discussing the good (and sometimes not so good) results. For the technical support from Morag Whitworth, Craig Sturrock, Sue Golds, Mark Meacham and Darren Hepworth, I am positive this PhD would not have happened without your help and guidance.

Thank you to my lab members, family and friends who provided much needed emotional support and enough laughs to get me to this point; Saoirse, Jon, Radek, Amin and Katy. Finally thank you to my mother, father and husband for supporting me once I decided to undertake this challenge. It has been a wondrous ride.

Table of Contents

1.0	General Introduction	1
1.1	Agricultural and research significance of rice (<i>Oryza sativa</i> L.)	1
1.2	Phosphorus in agriculture	2
1.2.1	Environmental aspects.....	3
1.2.2	P distribution and transformation in agricultural soil	4
1.2.3	Effects of flooding on P availability to plants	6
1.3	Root responses to variation in soil phosphate.....	7
1.3.1	Root gravitropism and increasing soil exploration	8
1.3.2	Increasing root:soil contact through fine roots, root hairs and mycorrhizal associations	9
1.3.3	Mycorrhizal associations.....	11
1.4	Molecular mechanisms controlling root angle	12
1.5	Observing root development in soil with X-ray CT	16
1.6	Literature review summary	20
1.7	Aims and hypothesis	21
2.0	Materials and Methods.....	23
2.1	Seed preparation.....	23
2.2	Growth conditions.....	24
2.3	Soil collection and properties.....	24
2.4	Soil preparation	25
2.4.1	Sieving and sterilisation	25
2.5	Column preparation	26
2.5.1	Altering P content and distribution	26
2.5.2	Column packing.....	27
2.5.3	Planting and nutrient supplement.....	28
2.6	Agar-based growth media	29
2.6.1	Nutrient agar growth medium.....	29
2.6.2	Agar with varying P content.....	29
2.6.3	pH indicator.....	30
2.7	Plating protocol	30
2.8	3-D Root measurement.....	32
2.8.1	X-ray CT Scanning.....	32

2.8.2	Segmentation of roots	32
2.8.3	3-D measurement with VG Studio Max and RooTrak.....	33
2.9	Destructive analysis and 2-D measurements.....	34
2.9.1	WinRHIZO measurements	35
2.9.2	Specific root length	35
2.9.3	Image J	35
2.10	Chemical analysis	37
2.10.1	Soil pH	37
2.10.2	Plant phosphate	37
2.11	Statistical analysis.....	38
3.0	Quantifying the effect of soil moisture content on segmenting root system architecture in X-ray Computed Tomography images.....	40
3.1	Description and author contributions.....	40
3.2	Abstract	40
3.2.1	Aims.....	40
3.2.2	Methods.....	41
3.2.3	Results.....	41
3.2.4	Conclusions	41
3.3	Introduction.....	41
3.4	Materials and Methods	43
3.4.1	Sample preparation	43
3.4.2	Visualisation of Root System Architecture in Soil using X-ray CT	45
3.4.3	Calculation of X-ray Dose	47
3.4.4	Root Segmentation Efficiency.....	47
3.5	Results	50
3.6	Discussion	54
3.7	Conclusions.....	59
3.8	Acknowledgments.....	60
4.0	Effects of X-ray dose on rhizosphere studies using X-ray Computed Tomography	61
4.1	Description and author contributions.....	61
4.2	Abstract	61
4.3	Introduction.....	62
4.3.1	Dose to sample in X-ray CT Investigations.....	62
4.3.2	X-ray Dose and Plants	66

4.3.3	The influence of X-ray radiation on soil microbial populations.....	67
4.4	Materials and Methods	68
4.4.1	Data Collection	68
4.4.2	Dose Calculations derived from the literature	70
4.4.3	Soil and Plant Sample Preparation and Treatment	71
4.4.4	Soil and Microbe Sample Preparation and Treatment	72
4.4.5	X-ray CT Imaging	73
4.4.6	Statistical Analysis.....	73
4.5	Results	73
4.5.1	Literature analysis.....	73
4.5.2	Impact of Repeated Scanning on Plant Roots in Soil	75
4.5.3	Impact of Repeated Scanning on Microbes in Soil	75
4.6	Discussion.....	76
4.7	Conclusion	81
5.0	Phenotyping of OsAUX1 related root system architecture (RSA)	82
5.1	Introduction.....	82
5.2	Materials and Methods	84
5.3	Results	84
5.3.1	3-D root volume and comparison of VGSM and RooTrak	84
5.3.2	X-ray CT derived indicators of root angle	86
5.3.3	Non-root angle related RSA measured by X-ray CT.....	89
5.3.4	Comparison of X-ray CT and WinRHIZO analysis	93
5.3.5	Destructive WinRHIZO analysis.....	93
5.4	Discussion	97
5.5	Conclusion	99
6.0	Influence of root gravitropism and OsAUX1 on RSA and subsequent P uptake	100
6.1	Introduction.....	100
6.2	Materials and Methods	102
6.3	Results	104
6.3.1	Biomass accumulation and P uptake	104
6.3.2	3-D root exploration in relation to soil P concentration and distribution.....	105
6.3.3	Destructively sampled RSA and P soil concentration	108
6.4	Discussion.....	113
6.5	Conclusion	117

7.0	Unravelling the role of OsAUX1 in P uptake	119
7.1	Introduction.....	119
7.1.1	Increasing the likelihood of encountering soil P.....	119
7.1.2	Root induced changes to the rhizosphere to make P more available.....	120
7.2	Materials and Methods	122
7.2.1	OsAUX1: pro β -glucuronidase marker	122
7.2.2	Real time quantitative polymerase chain reaction (RT-qPCR)	122
7.2.3	Root hair and RSA characterisation on agar with varying P	124
7.2.4	Iron rhizosheath SEM/EDX.....	124
7.2.5	pH under varying phosphate	125
7.2.6	Aerenchyma measurement	128
7.3	Results	129
7.3.1	Osaux1 genotype and potential indicators for P uptake.....	129
7.3.2	Primary root elongation and lateral root development on agar.....	132
7.3.3	Root hair phenotype in agar	134
7.3.4	Iron rhizosheath development in soil grown plants.....	136
7.3.5	pH under varying P concentration in agar	138
7.3.6	Aerenchyma in soil grown plants.....	140
7.4	Discussion	143
7.5	Conclusions.....	148
8.0	General discussion and conclusion	149
8.1	OsAUX1 as a target gene for improvement of phosphorus uptake in paddy rice..	149
8.1.1	Root angle effects on encountering soil P in rice paddies.....	150
8.1.2	Fine roots: Increasing the ability to take-up phosphate from soil	152
8.1.3	OsAUX1 and RSA plasticity in relation to P uptake.....	154
8.1.4	Optimisation of X-ray CT for imaging soil-grown rice roots	156
8.2	Conclusions.....	157
8.3	Further investigation	159
9.0	Bibliography	161

Abbreviations and Acronyms

2-D	Two dimensional
3-D	Three dimensional
AUX1	abbreviation of AtAUX1; Arabidopsis auxin influx carrier gene
OsAUX1	Rice ortholog gene of AtAUX1
<i>Osaux1</i>	T-DNA mutant with loss of function of the rice gene OsAUX1
ANOVA	Analysis of variance
ca.	circa
cv	cultivar
DAS	days after sterilisation
DNA	deoxyribonucleic acid
EDX	electron dispersive X-ray microanalysis
FAO	Food and Agriculture Organisation of the United Nations
Fe	the element iron
Fig.	Figure
GUS	<i>E. Coli</i> enzyme β -glucuronidase
Gy	Gray, SI unit of absorbed radiation dose
IAA	indole-3-acetic acid
MS	Murishage and Skoog nutrient medium
MRI	Magnetic Resonance Imaging
NMR	Nuclear Magnetic Resonance
NS	not statistically significant
P	Phosphorus
PET	Positron Emission Tomography
Pi	Orthophosphate
PUE	Phosphorus uptake efficiency
RGB	red-green blue colour assignment for images
RNA	ribonucleic acid
ROI	Region of interest
RRes	Rothamsted Research Station
RSA	Root system architecture
RT-qPCR	Rela-time quantitative polymerase chain reaction

SEM	scanning electron microscopy
<i>ssp</i>	sub-species
UK	United Kingdom
US	United States of America
VGSM	VG StudioMax (image analysis software)
X-Gluc	5-bromo-4-chloro-3-indolyl glucuronide
X-ray CT	X-ray micro Computed Tomography

List of Tables

Table 1-1: Selection of rice genes that influence root angle.....	13
Table 2-1: Soil properties summary.....	25
Table 2-2: Selection of ranges for published low and high P treatments in non-agar based studies of root architecture in relation to P concentration for crop plants.....	27
Table 2-3: Quantities of nutrient solution used to create agar with varying P levels.....	30
Table 2-4: Summary of interactions for experimental results analysed by Analysis of Variance (ANOVA).....	39
Table 4-1: X-ray CT scan parameters	73
Table 6-1: Biomass and colorimetric P measurements for wildtype and <i>Osaux1-1</i> under uniform P distribution for low, sufficient and high P.	104
Table 6-2: Biomass and colorimetric P measurements for wildtype and <i>Osaux1-1</i> under stratified P distribution for sufficient and high P..	105
Table 6-3: X-ray CT derived measurements for wildtype and <i>Osaux1-1</i> under uniform P distribution for low, sufficient and high P.	107
Table 6-4: X-ray CT derived root measurements for wildtype and <i>Osaux1-1</i> under stratified P distribution for sufficient and high P..	108
Table 6-5: WinRHIZO measurements for wildtype and <i>Osaux1-1</i> under uniform P distribution for low, sufficient and high P.	110
Table 6-6: WinRHIZO derived measurements for wildtype and <i>Osaux1-1</i> under stratified P distribution for sufficient and high P..	113
Table 7-1: Comparison of colour segmentation algorithms.....	127

List of Figures

Fig. 1-1: Phosphorus demand will eventually outstrip supply.....	4
Fig. 1-2: Phosphorus cycles through soils in organic forms that are primarily unavailable to plants.....	5
Fig. 1-3: Rhizosphere interaction with flooded soils..	7
Fig. 1-4: Soil nutrient status affects root architecture and varies with nutrient type.....	11
Fig. 1-5: Auxin transport and involvement with root gravitropism.....	14
Fig. 1-6: Genotype and phenotype of <i>O. sativa</i> cv. Dongjin and the loss of function mutants <i>Osaux1-1</i> and <i>Osaux1-2</i>	15
Fig. 1-7: Setup for X-ray CT scanner to visualise root architecture of a rice plant in soil.....	17
Fig. 1-8: Representative sample of an X-ray CT slice for a scan of a rice plant grown in loamy sand soil.	19
Fig. 1-9: Environmental stress and soil characteristics are linked to root architecture through biochemistry.	20
Fig. 2-1: Rice seed de-husking protocol and germination setup.	23
Fig. 2-2: Representation of experimental design investigating the distribution of P.....	28
Fig. 2-3: Plating rice seeds in square petri dishes filled with agar growth media.	31
Fig. 2-4: Schematic representation of measurements available in RooTrak 0.2 measured from segmented X-ray images of root systems.....	34
Fig. 2-5: Example of a destructively sampled root system that was imaged on a flatbed scanner and the resulting WinRHIZO output	36
Fig. 3-1: Soil moisture release curves for Loamy sand and Clay loam soils.....	44
Fig. 3-2: Representative cross-section of the 3-D X-ray CT volume of a rice root in soil.	46
Fig. 3-3: An illustration of the difficulties in segmenting roots from soils.	49
Fig. 3-4: Three-dimensional rice root system architecture X-ray images.....	52
Fig. 3-5: X-ray CT segmented root volume as a function of volumetric soil water content....	53
Fig. 3-6: Segmentation efficiency ratio as a function of soil water content.....	53
Fig. 3-7: X-ray CT segmented root volume and soil water content as a function of time.....	55
Fig. 3-8: Example X-ray CT images of horizontal slices through loamy sand (A) and clay loam (C) soil columns	57
Fig. 3-9: Air-filled macroporosity increasing with drying in soil	58
Fig. 4-1: Flowchart depicting meta-analysis protocol.....	69
Fig. 4-2: X-ray dose in plant and soil studies	70
Fig. 4-3: Impact of X-ray CT on rice root growth	77

Fig. 4-4: Influence of X-ray CT on soil microbial biomass after 24 weeks	78
Fig. 5-1: Root volume measurement of root systems segmented from X-ray CT images.....	85
Fig. 5-2: Root volume at weekly measurement points.....	86
Fig. 5-3: Root angle from X-ray CT images of soil and agar grown rice	88
Fig. 5-4: Centroid Z-value for wildtype, <i>Osaux1-1</i> and <i>Osaux1-2</i>	89
Fig. 5-5: Weekly measurement of maximum root system depth and the minimum enclosing circle.....	90
Fig. 5-6: Convex hull and root system solidness derived from X-ray CT.....	91
Fig. 5-7: Root system surface area measured by RooTrak from X-ray CT derived images.....	92
Fig. 5-8: Comparison of X-ray CT and WinRHIZO (root washing derived) root volumes.....	93
Fig. 5-9: Rice root system components.....	94
Fig. 5-10: Root washing derived root volume and root surface area.....	95
Fig. 5-11: WinRHIZO derived total root length and mean root diameter	96
Fig. 5-12: Number of root tips for wildtype, <i>Osaux1-1</i> and <i>Osaux1-2</i>	96
Fig. 6-1: Root systems obtained by X-ray CT for plants under uniform P distribution.....	106
Fig. 6-2: X-ray CT of root systems grown with P in the top 4 cm of soil.....	106
Fig. 6-3: X-ray CT of root systems grown with P in the bottom 6 cm of soil	107
Fig. 6-4: Representative images of roots washed after being grown in uniform low P, sufficient P and high P.....	109
Fig. 6-5: Washed root systems of plants grown in sufficient and high P sequestered to the top 4 cm of the soil column	111
Fig. 6-6: Representative images of RSA for plants grown with P in the bottom 6 cm of the soil column	112
Fig. 7-1: Influence of P uptake itself, release of O ₂ from aerenchyma and root exudates on the pH of the rhizosphere in submerged soils.....	121
Fig. 7-2: Colour segmentation setup.....	126
Fig. 7-3: X-ray CT cross section of a segmented rice root and subsequent isolation of intra-root air space (aerenchyma).....	129
Fig. 7-4: <i>OsAux1</i> :GUS expression in the tip of the primary root, crown root and large lateral root.....	130
Fig. 7-5: Expression of <i>OsAUX1</i> in both shoot and root of wildtype and <i>Osaux1-1</i>	131
Fig. 7-6: Coarse root development under uniform P conditions.....	133
Fig. 7-7: Root hair length and root hair density in response to available phosphate	135
Fig. 7-8: Rice root hair length under varying phosphate concentration	136
Fig. 7-9: EDX measured concentrations of elemental P and Fe on root surfaces	137

Fig. 7-10: Area of root system influence in agar doped with pH indicator	139
Fig. 7-11: The total volume of air space within roots grown in P amended soil	141
Fig. 7-12: Root air space as a proportion of total root volume air	142
Fig. 8-1: Representation of P signalling pathway and in planta and ex planta responses to P stress	149

1.0 General Introduction

1.1 Agricultural and research significance of rice (*Oryza sativa* L.)

In order to feed the world population at current growth rates, it is estimated that global rice (*Oryza sativa* L.) production will need to increase 40% by 2030 (Khush 2005). Even in China where rice production is increasing, Cai and Chen (2000) found that to keep pace with Chinese population growth, domestic rice production must increase 20% by 2030. To meet this challenge, growers must increase production in a changing climate and under pressure to utilise sustainable methods requiring less fertiliser, less land and less water (Van Nguyen and Ferrero 2006).

In the post green revolution era, there has been a call to develop new rice varieties that are drought and disease resistant as well as highly efficient at acquiring nutrients from soils without addition of fertiliser. Peng et al. (2009) highlight the need in China for more (i) diverse genetic resources, (ii) development of drought, heat, disease and pest resistant varieties, (iii) reducing the occurrence of over-fertilisation and excessive pesticide use and (iv) incorporating the use of integrated crop management. In Japan, the need for improved water and nutrient management has led researchers to investigate how root systems in particular can be optimised through seedling spacing and using wet-dry cycles to conserve water to improve yield (Chapagain and Yamaji 2010). Sub-Saharan Africa presents similar challenges with water consumption, however economic restraints (lack of capital) and soil qualities such as acidity and P-fixing contribute to reduced rice yields (Balasubramanian et al. 2007).

Although advances in agronomic practice will be required to ensure yields of rice reach those needed for global food security, improved plant lines will be critical for adaptation to climate change as well as the need to reduce resource use. Khush (2005) argued that the availability of the rice genome would revolutionise rice yield through improved selection for nutrient and water efficiency, improved root architecture and the likelihood of more successful genetic engineering. When the full *japonica* (Goff et al. 2002) and *indica* (Yu et al. 2002) rice genomes were published in 2002, rice became a model plant for genetic research.

Quantitative trait loci (QTLs) have been identified on the rice genome by linking common gene sequences with phenotypic traits of rice adapted to phosphorus stress (Shimizu et al. 2004; Wissuwa et al. 2002), drought tolerance (Hazen et al. 2005) and salinity tolerance (Lin et al. 2004; Ren et al. 2005). By pinpointing areas of the genome that are potentially involved in stress responses, reverse genetic approaches, among others, can be used to manipulate the plant phenotype and likely increase yield under the chosen stress conditions (de Dorlodot et al. 2007; Ismail et al. 2007). Comprehensive mapping of QTLs can direct researchers to candidate genes to test for agronomically valuable traits (Nguyen et al. 2004) and are considered to be accurate enough to enhance the discovery of these genes (Price 2006).

1.2 Phosphorus in agriculture

All plants require phosphorus (P) for biomass accumulation, plant signalling and reproduction (López-Bucio et al. 2002). P is an integral part of the nucleic acids, metabolic intermediates and phospholipids that are inherent to plant biochemistry and tissue development (Abel et al. 2002). However, if agricultural soils are not supplemented with P

inputs such as such as raw phosphate rock or chemical fertilisers derived from it, the bioavailable inorganic P (P_i) fraction declines as P is removed in harvested crops (Syers et al. 2001). Additionally, P_i is quickly transformed in soil to forms of P unavailable to plants (Kirkby and Johnston 2008).

1.2.1 *Environmental aspects*

At current consumption rates, the supply of phosphorus-containing rock appropriate for use as fertiliser will be depleted within the next 100 years and by 2030 production will surpass demand (Fig. 1-1) (Cordell et al. 2009). More than half of P fertiliser applied to crops was used on cereals (Potter et al. 2010). Despite this likely shortage of rock phosphate, there are severe imbalances between the amount of applied P and the P requirements and uptake of crops. MacDonald et al. (2011) found this was linked to spatial distribution with the largest deficits being in Argentina and Paraguay, the northern United States and Eastern Europe. Alternatively, the largest surplus or overuse of P fertiliser was in eastern Asia, south-western Europe, southern Brazil and the coastal United States. The extra applied P does not increase yield after the plant has reached critical internal P concentrations (Hammond and White 2008).

Not only will P become scarcer and more expensive, but overuse of P can have detrimental environmental impacts on freshwater and marine environments (Smith et al. 1999). P is often the primary limiting nutrient in aquatic ecosystems (Carpenter 2005; Conley et al. 2009). P-containing run-off from agricultural fields can enter waterways and is a major cause of eutrophication in waterways (Sims and Sharpley 2005; White and Hammond 2009). Eutrophication is the nutrient loading of a nutrient deficient environment and in waterways

can cause algal and bacterial blooms that consume the available oxygen and subsequently suffocate larger aquatic life. A balanced approach is required to ensure sustainable use of P-containing fertiliser whilst ensuring sufficient food supplies.

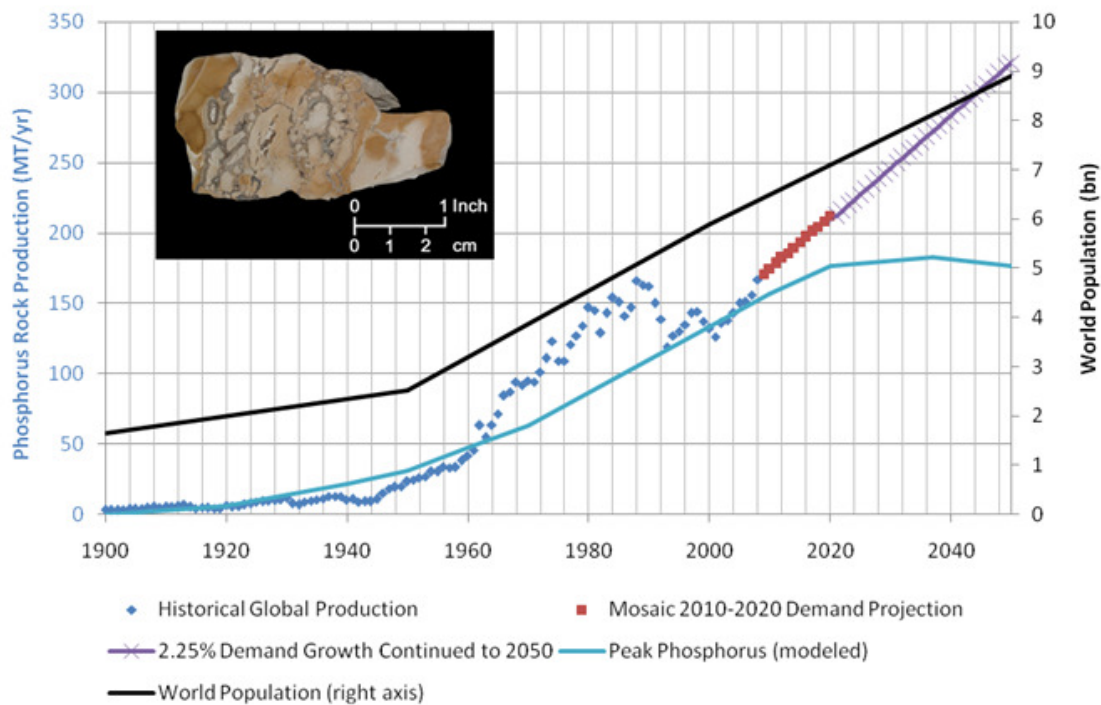


Fig. 1-1: Phosphorus demand will eventually outstrip supply. Around 2030, the demand (blue diamonds, red squares and purple cross hash) for phosphorus containing rock (inset picture) will likely surpass supply (solid blue line). If world population (black solid line) continues to increase at current rates, this could become a significant problem for agricultural production. Figure from Cordell et al. (2009).

1.2.2 P distribution and transformation in agricultural soil

Phosphorus is most abundant in the upper layers of soil. P is a negligibly mobile element in the soil profile and often resides in the top 15 cm of the soil profile and is greatest in the top 5 cm (Owens et al. 2008; Page et al. 2005). The major mode of P distribution to any notable depth in soil is through anthropogenic sources such as fertilisation or incorporation of crop residues into the soil which then release P from lysed cells (Larsen 1967).

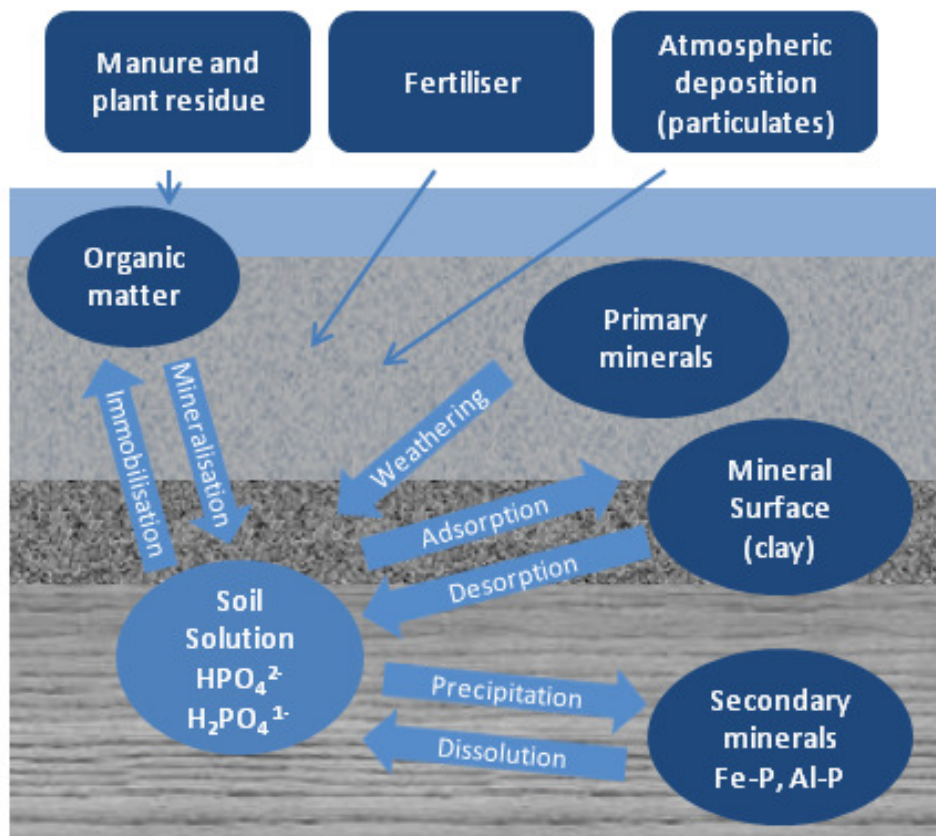


Fig. 1-2: Phosphorus cycles through soils in organic forms that are primarily unavailable to plants. Through dissolution, desorption, weathering and mineralisation P transforms to inorganic forms that are soluble in soil solution and bioavailable. Figure adapted from <http://msucares.com/crops/soils/images/phosphorus.gif>.

P is supplied to the root system through diffusion and generally does not migrate quickly through the soil profile when compared to more soluble nutrients such as N (Jianguo and Shuman 1991). Up to 90% of fertiliser applied P is not taken up by plants and is lost to complexing with soil organic matter, sorbing on soil minerals (Fig. 1-2) as well as movement through soil water and runoff (Shahandeh et al. 2003; Smil 2000; Stevenson and Cole 1999).

The form of P applied also affects mobility and bioavailability of P in the soil profile. Incorporation of organic matter such as manure and plant biomass influences availability of P in soils (Irshad et al. 2008; Ohno et al. 2007; Pheav et al. 2005). P applied to soils as triple superphosphate will generally reside in the upper 20-35 cm of soil which is the typical

plough depth (Shepherd and Withers 1999) and does not migrate much past this depth. Eghball et al. (1996) found that manure derived P reached depths of up to 1.8 m whereas fertiliser derived P reached a maximum depth of 1.1 m. Differences in soil mineral and organic matter content as well as microbial communities can significantly influence P cycling in agricultural soils (Blake et al. 2000; Richardson et al. 2009).

1.2.3 *Effects of flooding on P availability to plants*

In combination with soil properties, water management can affect soil chemistry and subsequent availability of soil phosphorus (Patrick et al. 1985; Ponnampereuma 1984). Flooding of very clayey soils with high aluminium content can lead to sequestration of phosphates that bind to the aluminium in preference to iron or calcium although over time (Patrick Jr and Mahapatra 1968). This balance shifts toward formation of iron phosphates which become unavailable to plants (Mengel 1985).

Additionally, flooding creates reducing conditions which increase pH in soils and immobilise previously bioavailable P through adsorption, immobilisation and precipitation with elements like iron (Ponnampereuma 1972). Diffusion of gases through water is much slower than through air thus oxygen becomes limited in waterlogged soils because it is consumed faster than it can diffuse into the soil (Gotoh and Patrick 1974). Regions of oxygen containing soil and anoxic soil become stratified (Fig. 1-3). In an adaptation to waterlogging, some plants form aerenchyma which are air spaces that form within roots to enhance gas exchange with the rhizosphere (Justin and Armstrong 1987). In aerenchyma forming plants such as rice, gases can disperse into the area adjacent to the root system through root tips

and areas of the lateral root (Bodegom et al. 2001). This alters local pH and resulting P chemistry, making nutrients more available (Jackson and Armstrong 1999).

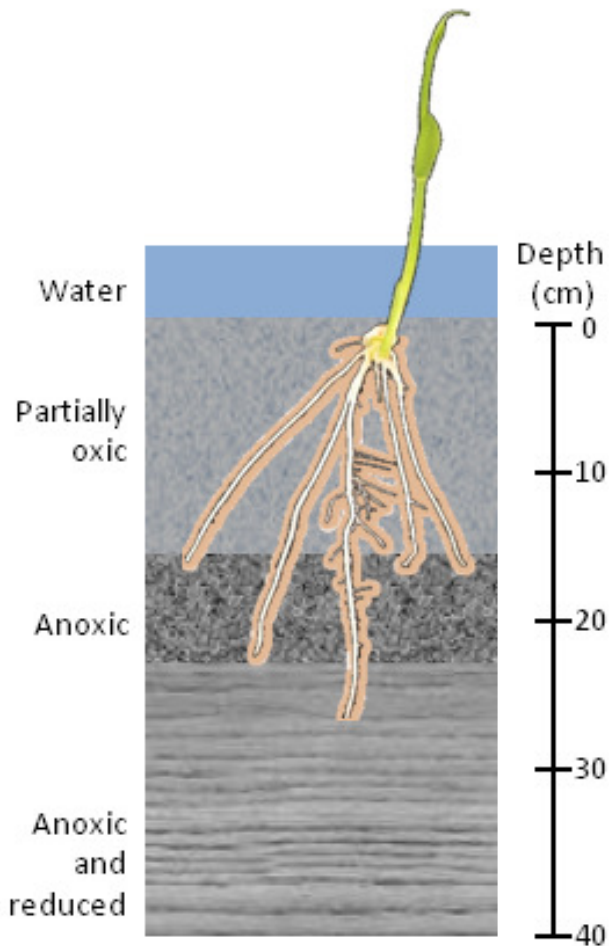


Fig. 1-3: Rhizosphere interaction with flooded soils. In flooded soils, oxygen becomes depleted due to waterlogging and slow gas diffusion in comparison to soils which have air-filled pores. The rhizosphere can be oxic in flooded soils with the influence of aerenchymatous roots. Adapted from Patrick et al. (1985).

1.3 Root responses to variation in soil phosphate

A plant that focuses root growth at the soil surface may be more likely to encounter phosphorus. Agravitropic root systems explore shallower soil and have more roots in the phosphorus rich areas. Proliferation of adventitious roots and an increase in lateral root

formation has been linked with adaptation to low P in common bean (*Phaseolus vulgaris* L.) (Miller et al. 2003).

However, root architecture alone may not be the determining factor for phosphorus use efficiency. Availability of phosphorus for plant uptake has also been linked to organic matter content of soil and microbial activity (Kirkby and Johnston 2008). There are significant variations between plant species and genotypes in both utilization and acquisition of P (White and Hammond 2008). Root plasticity is critical for adaptation to changes in nutrient availability and has been linked to heterogeneity of the soil environment (Hutchings and John 2004; Kembel and Cahill 2005).

1.3.1 *Root gravitropism and increasing soil exploration*

One documented response to P deprivation is shallower rooting and adventitious root formation which is commonly termed topsoil foraging (Lynch and Brown 2001). In general, shallower root systems are more successful at acquiring P because of the distribution of P in the agricultural soil profile and its generally immobile nature (Ge et al. 2000; Robinson 1994; 1996). The shallow root system explores the soil volume by increasing its root system width.

In order to achieve shallower rooting depth, the initiation angle of the root is obtuse. Root angle appears to have optimum values for anchorage; 90° between a lateral and primary root and $< 20^\circ$ between primary and secondary lateral roots (Robinson 1996). However, in the case of very mobile nutrients such as nitrogen, ideal root architecture and angle can vary with time (Campbell et al. 1991; Grime et al. 1991).

Root angle and thus, gravitropic response, have been linked to an increase in biomass and plant P concentrations in rice and soybean (*Glycine max* L.) (Fang et al. 2009; Zhu et al.

2005). However, some plants do not favour shallow root distributions under P stress. Wheat (*Triticum aestivum* L.) was found to dedicate more root biomass to deeper portions of the root system under P stress which may be related to the allocation of biomass to deal with potential drought deficiency in preference to topsoil foraging (Manske et al. 2002).

Another factor that has been linked to P stress is aerenchyma formation. Aerenchyma are air spaces that form within roots to enhance gas exchange with the rhizosphere (Justin and Armstrong 1987). There are two main types of aerenchyma, schizogenous and lysigenous. Schizogenous aerenchyma form through species specific regulation of cell separation and expansion that is generally considered constitutive, however their development can be induced by environmental stress as well (Jackson and Armstrong 1999). Lysigenous aerenchyma are created through programmed cell death within cortical cells and is often associated with crop plants under nutrient and oxygen stress such as maize (Drew et al. 2000).

1.3.2 *Increasing root:soil contact through fine roots, root hairs and mycorrhizal associations*

Within the explored soil volume, plants can maximise the amount of soil exploited by increasing the root system surface area and root:soil contact. This is achieved by increasing the number and length of lateral roots and root hairs and varies depending on which nutrient is being supplied (Fig. 1-4). Fine roots and root hairs are critical for nutrient acquisition from soil by plants because they increase the surface area of the root system which increases the likelihood of nutrient uptake.

Hutchings et al. (2003) argued that fine roots are the primary route for acquisition of nutrients in soil and that this makes the distribution of fine roots more relevant to understanding of nutrient acquisition than the coarser root structure. This is debatable because the transitory nature of most fine roots means they either expire quickly or develop into coarser roots (Wells and Eissenstat 2002). However, root plasticity is often exhibited at the local level in reaction to distribution of nutrients and the heterogeneity of soils (Wijesinghe et al. 2001). These local reactions to soil heterogeneity are at scales smaller than that of the whole plant because they involve reactions such as proliferation of fine roots in a patch of nutrient rich soil. There is a feedback loop between root architecture, root growth and soil properties. Nutrient concentration and water content related to porosity can greatly affect plant survival (Hodge 2004; Hutchings and John 2003). Additionally, plant roots can alter soil structure and excrete compounds that alter the water-holding capacity of soils after several drying and wetting cycles (Carminati et al. 2010).

Lateral root growth is necessary for secondary and tertiary root initiation, which gives architectural agility to root systems under nitrogen and phosphorus stress (Linkohr et al. 2002). Phosphorus stress can increase root diameter and root hair density in *Arabidopsis*; P deficiency increased root hair elongation by 500% (Ma et al. 2001). This architectural adaptability driven by fine root development has been linked to the plant's ability to acquire nutrients necessary for biomass accumulation, competition and general plant functions (Nibau et al. 2008). Thus, nutrient conditions can alter root architecture.

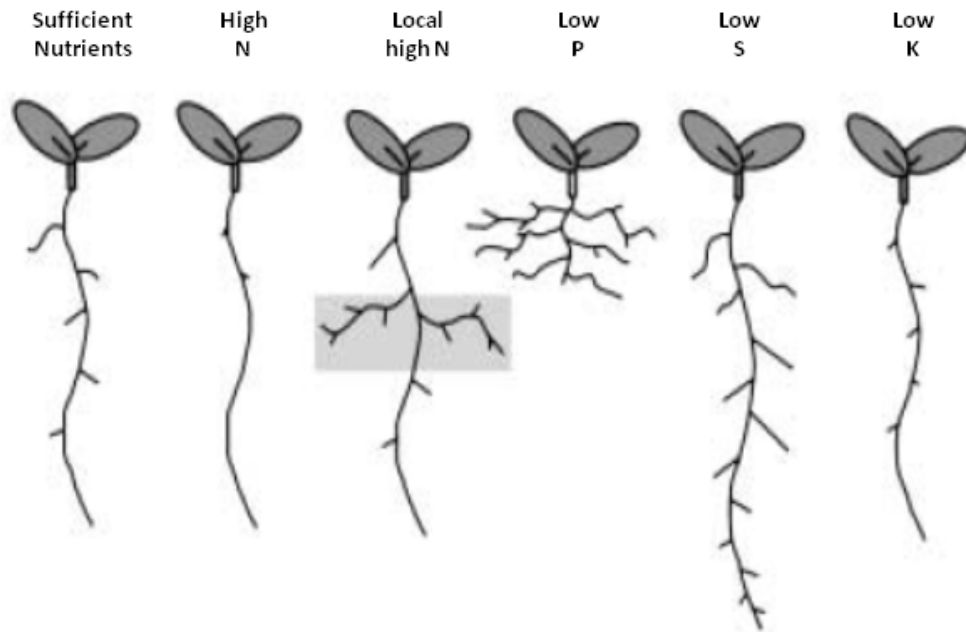


Fig. 1-4: Soil nutrient status affects root architecture and varies with nutrient type. In localised nitrogen (N) patches, lateral root formation increases. In low phosphorus (P) conditions, lateral roots tend to explore the upper soil where P is most prolific. Limiting nutrients such as sulphur (S) and potassium (K) can have dramatic impacts on lateral root formation. Image from Nibau et al. (2008).

1.3.3 Mycorrhizal associations

Root hairs interact with soil microbes (bacterial/fungal) that can influence P uptake and biomass accumulation in wetland ecosystems (Khan 2004a). Particularly in young rice, P solubilising bacteria can significantly influence growth and the size of the rhizosphere in flooded soils (Raghu and MacRae 1966). AMF can influence expression of P transporters and ultimately total P uptake in aerobic sand media for the rice cultivar Nipponbare (Chen et al. 2012a). In sterilised paddy soil, inoculation with arbuscular mycorrhiza fungi (AMF) at the plant nursery stage (four weeks old; *O. sativa* cv. Nipponbare) increased biomass and nutrient uptake including grain P content (Solaiman and Hirata 1995). Solaiman and Hirata (1995) found significant infection by AMF and other endophytic fungi under aerobic soil conditions and this was independent of rice genotype. AMF infection does not always provide an agronomic advantage for some Italian rice varieties as shown by Vallino et al.

(2009). P uptake and root growth have been linked to AMF inoculation in flooded conditions for the rice cultivar Shafagh (Hajiboland et al. 2009b). However, Hajiboland et al. (2009b) found that AMF colonisation of rice roots under flooded conditions was difficult to achieve.

1.4 Molecular mechanisms controlling root angle

A large number of genes have been identified that influence root angle in plants such as rice (Table 1-1) and Arabidopsis. Many are related to auxin metabolism, efflux and influx and form part of the Aux/IAA gene family described by Jain et al. (2006). Whilst the function of these genes is becoming clearer, the underlying mechanism for gravity perception, signalling and response are unestablished (Baluška and Volkmann 2011). Roots sense changes in their orientation relative to the direction of gravity through sedimentation of starch-filled amyloplasts that are present in root cap cells called statocytes (Harrison and Masson 2008).

Mutants of Arabidopsis lacking starch can disrupt the formation of a lateral auxin gradient following gravity stimulus. Band et al. (2012) recently demonstrated that the starchless mutant *pgm* disrupted function of the gravity induced auxin gradient triggered by statolith sedimentation (Fig. 1-5 A to C) which is dependent on the angle of the root tip (Fig. 1-5 D to F). The mechanisms behind gravitropic response in rice roots are less clear. A starchless mutant of rice was identified by Jing et al. (2004) that did not respond under gravistimulus which is consistent with an impaired gravitropic response.

Root responses to gravistimulus have been linked to distribution of the plant hormone auxin/IAA in various species (Bai et al. 2013; Brunoud et al. 2012; Ge et al. 2000; Marchant et al. 1999; Swarup et al. 2005). This gravity-induced auxin gradient is dependent on PIN3 auxin efflux activation which causes auxin accumulation on the lower side of the root

(Kleine-Vehn et al. 2010). The mechanism for local activation of the PIN3 auxin efflux carrier on the lower sides of the root cells has yet to be resolved. However, the auxin influx and efflux carriers AUX1 and PIN2 in *Arabidopsis thaliana* cv. Columbia (Bennett et al. 1996; Swarup et al. 2005) have been shown to play a critical role in mobilising auxin to the elongation zone where the hormone induces differential cell expansion and subsequent root bending (Swarup et al. 2005). In *Arabidopsis*, the AUX1-dependent lateral auxin gradient alters pH and Ca²⁺ levels in the cytosol during this differential root growth (Monshausen et al. 2011). These changes to pH and Ca²⁺ likely impact differential cell elongation and promote root bending via secondary signal transduction (Monshausen and Haswell 2013).

Table 1-1: Selection of rice genes that influence root angle.

Gene name	Root angle phenotype	Citation
OsAEM1	Agravitropic, auxin efflux	Rani Debi et al. (2005)
OsCRL1	Impaired root gravitropism, lateral root formation and no crown root primordia	Inukai et al. (2005) and Coudert et al. (2011)
OsCRL4	Shallow rooting angle, agravitropic	Kitomi et al. (2008)
OsDRO1	Deep rooting QTL	Uga et al. (2011)
OsIAA1	Auxin-brassinosteroid crosstalk, loose architecture	Song et al. (2009)
OsIAA3	Agravitropic, auxin insensitive	Nakamura et al. (2006)
OSIAA13	Agravitropic, less lateral roots and root hairs	Kitomi et al. (2012)
OsLRT1	No lateral roots and reduced gravitropic response	Chhun et al. (2003)
OsPIN1 (previously OsREH1)	Impacts adventitious root growth and lateral roots; Auxin efflux	Xu et al. (2005)

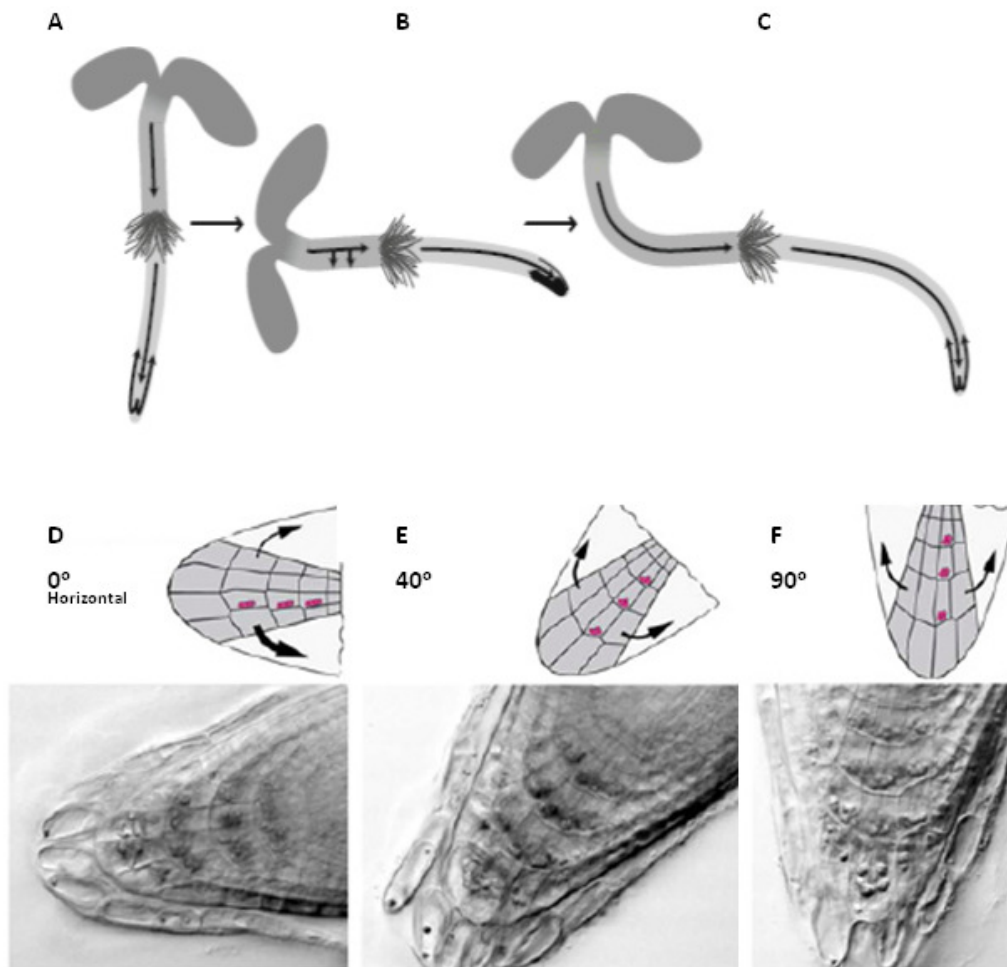


Fig. 1-5: Auxin transport is involved in root gravitropic response. Auxin movement (indicated by arrows) becomes polarised after sedimentation of starch amyloplasts in root cells when the root is placed horizontally (A and B). This creates the characteristic root curvature attributed to gravitropism (C). When the root is placed horizontally (D), 40° from horizontal (E) and 90° from horizontal (F), the starch statoliths trigger this mechanism and alter the auxin gradient. Figure adapted from Stanga et al. (2009) and (Band et al. 2012).

With the strong ties between AtAUX1 and gravitropism in mind, an AtAUX1 gene ortholog was identified in the model plant rice (*Oryza sativa* ssp. *Japonica* cv. Dongjin) and as expected the *Osaux1* loss of function mutant had an impaired gravitropic response (Parker 2010). Bioinformatic analysis revealed two rice sequences (termed Os01g63770 and Os05g37470) that were very closely related to AtAUX1. To test the *in planta* function of OsAUX1, these two independent rice T-DNA insertion lines were isolated. The two OsAUX1

T-DNA knockout mutants, known as *Osaux1-1* and *Osaux1-2*, were differentiated by the

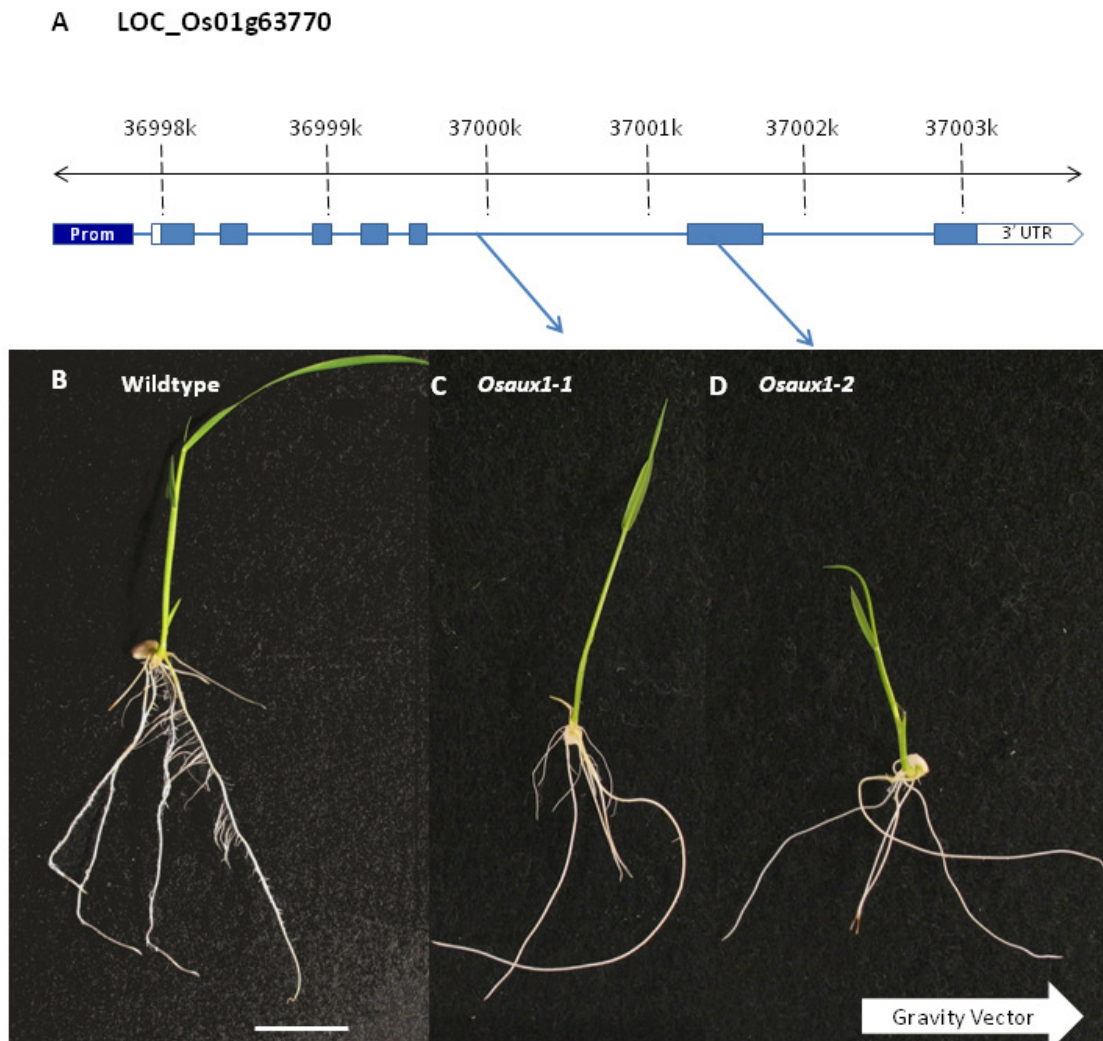


Fig. 1-6: Genotype and phenotype of *O. sativa* cv. Dongjin and the loss of function mutants *Osaux1-1* and *Osaux1-2*. In the schematic of the *OsAUX1* gene (A), introns are represented by lines and exons by boxes with arrows for location of T-DNA insertions for each mutant. Wildtype (B) had the expected gravitropic response under gravistimulus for fully functioning *OsAUX1* whereas *Osaux1-1* (C) and *Osaux1-2* (D) were agravitropic. Scale bar is equivalent to 2 cm.

location of the T-DNA insertions (Fig. 1-6 A). Only one member (*Os1g63770*) was able to complement the *Arabidopsis aux1* mutant, providing genetic evidence that it was orthologous (i.e. equivalent function). This condition was further strengthened when promoter:GUS reporter fusions for the *OsAUX1* gene were observed to be expressed in an equivalent tissue pattern to the *Arabidopsis* ortholog. The *Osaux1-2* allele exhibited a more severe gravitropic defect than *Osaux1-1* consistent with the exonic versus intronic genomic

insertion positions (Fig. 1-6 A). Most compellingly, when the Os1g63770 gene was disrupted using T-DNA insertion, several of the T-DNA insertion lines exhibited an agravitropic root phenotype (Fig. 1-6 B to D).

1.5 Observing root development in soil with X-ray CT

The ability to visualise roots, water and the soil matrix simultaneously and repeatedly over time opens new avenues for in situ investigation of plant water uptake, nutrient uptake and root development (Bakker et al. 2012). Further understanding of root architecture (Tracy et al. 2012b; Tracy et al. 2012e), root growth (Flavel et al. 2012a), root decomposition (Haling et al. 2013b) and soil properties (Helliwell et al. 2013) at the microscale have been possible with X-ray micro-Computed Tomography (X-ray CT). Researchers have increasingly utilised non-destructive analytical techniques such as X-ray CT and Nuclear Magnetic Resonance (NMR) to measure RSA in situ (Gregory et al. 2003a; Pálsdóttir et al. 2005).

Before the introduction of micro X-ray CT, plant samples were scanned in medical grade scanners that were developed for imaging of the human body, which produced low resolution images (mm scale) that made root material difficult to distinguish from the growth medium (Moran et al. 2000). The X-ray CT methodology provides the opportunity for non-destructive analysis of root growth and architecture. Under the right circumstances, X-ray CT allows repeated measurement of root and soil properties over time to reveal root development under abiotic and biotic stress such as compaction and moisture stress (Tracy et al. 2012b; Tracy et al. 2012e; Zappala et al. 2013b).

Theoretically, X-ray CT can be used with any object that allows X-rays to completely penetrate it on a plane perpendicular to the axis of rotation. Fig. 1-7 shows the X-ray tube

that releases X-rays in a fan beam which completely covers the object as it rotates. The X-rays lose energy as they move through the sample object and are attenuated by the sample. A detector records the X-rays that pass through the sample object. The attenuated X-rays recorded by the detector are directly related to the density of the object that the X-rays pass through. Image slices perpendicular to the single axis of rotation are created as the sample object is rotated in steps that are usually of less than one degree.

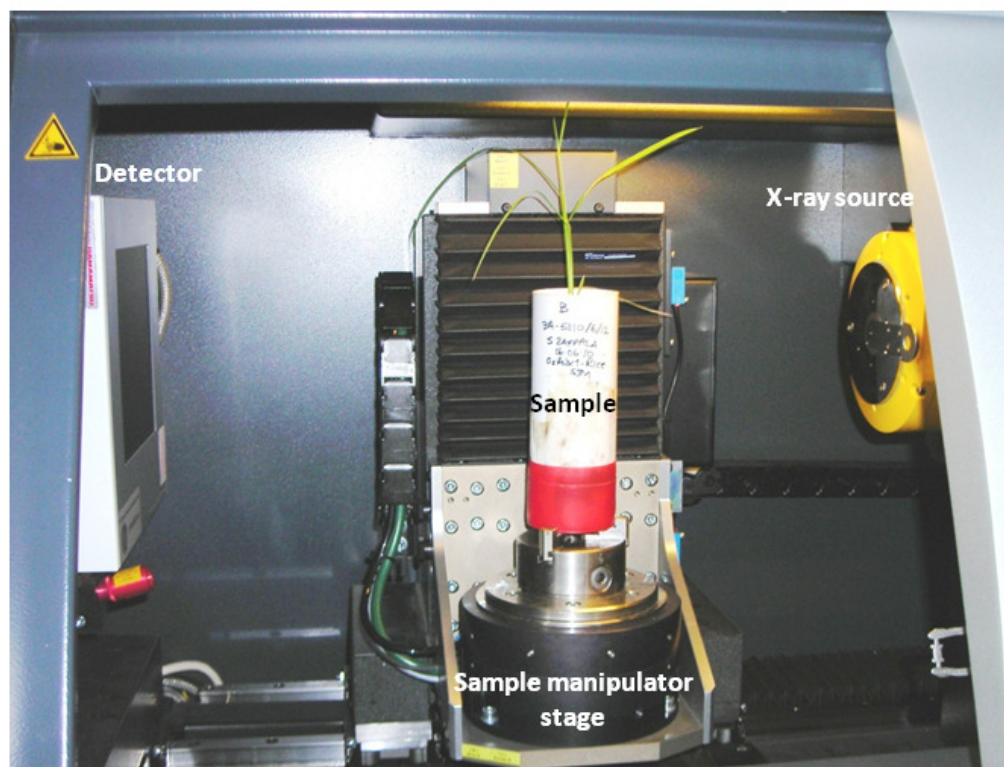


Fig. 1-7: Setup for X-ray CT scanner to visualise root architecture of a rice plant in soil. The X-rays are produced by the X-ray source. They pass through the sample and are recorded on the detector.

A computer is used to numerically stack the slices. Each pixel stack is compiled into volume units called voxels. Each voxel is like a 3-D pixel and is associated with an averaged greyscale related to the density of the registered area. Voxel size can reach $0.2 \mu\text{m}$ in nano-focus tube systems. The 3-D volume of voxels can then be analysed to extract features of interest. For

in situ, non-destructive imaging of plants in soil, features of interest could include soil solids, air-filled pores, water-filled pores and plant roots (Fig. 1-8).

Root systems are usually composed of larger primary roots and finer lateral roots that branch off of the primary root. Fine roots (< 0.5mm diameter) often account for a large proportion of the total root volume (Eissenstat 1992; Fitter 1991). The high resolution, microscale images characteristic of X-ray CT can enable imaging of the majority of the root system because it enables imaging of these fine roots if sample size is small enough to ensure the resolution is sufficient to visualise fine roots (Tracy et al. 2012b).

The resolution of images can restrict analysis to that of coarse roots as found by (Flavel et al. 2012a) and Zappala et al. (2013b). Analysis of coarse roots provides a starting point for understanding of fine root architecture because fine roots originate from coarse roots. Coarse root architecture has been linked to further understanding of plant nutrient acquisition from soils such as adventitious rooting in common bean (Rubio et al. 2003) and maize (Zhu et al. 2005).

X-ray CT as a method is most informative because of its non-destructive quality which allows observation of root and soil development, particularly in 3-D. The published literature contains few examples of experiments where X-ray CT is solely utilised as a tool to non-destructively visualise the changes in root growth and architecture when the plant is subject to an altered environment. However, as X-ray CT has advanced as a tool in soil and plant science, the number of studies combining abiotic factors with root development is growing (Mooney et al. 2012b; Tracy et al. 2010). One of the few examples was an osmotic potential experiment performed on lupin (*Lupinus angustifolius* L.) and radish (*Raphanus sativus* L.)

roots (Hamza et al. 2007; 2008). X-ray CT was used to determine root diameter and changes in density related to salinity stress. Root width, root angle and root tortuosity can be measured from the root architecture extracted from the reconstructed image of the 3-D soil

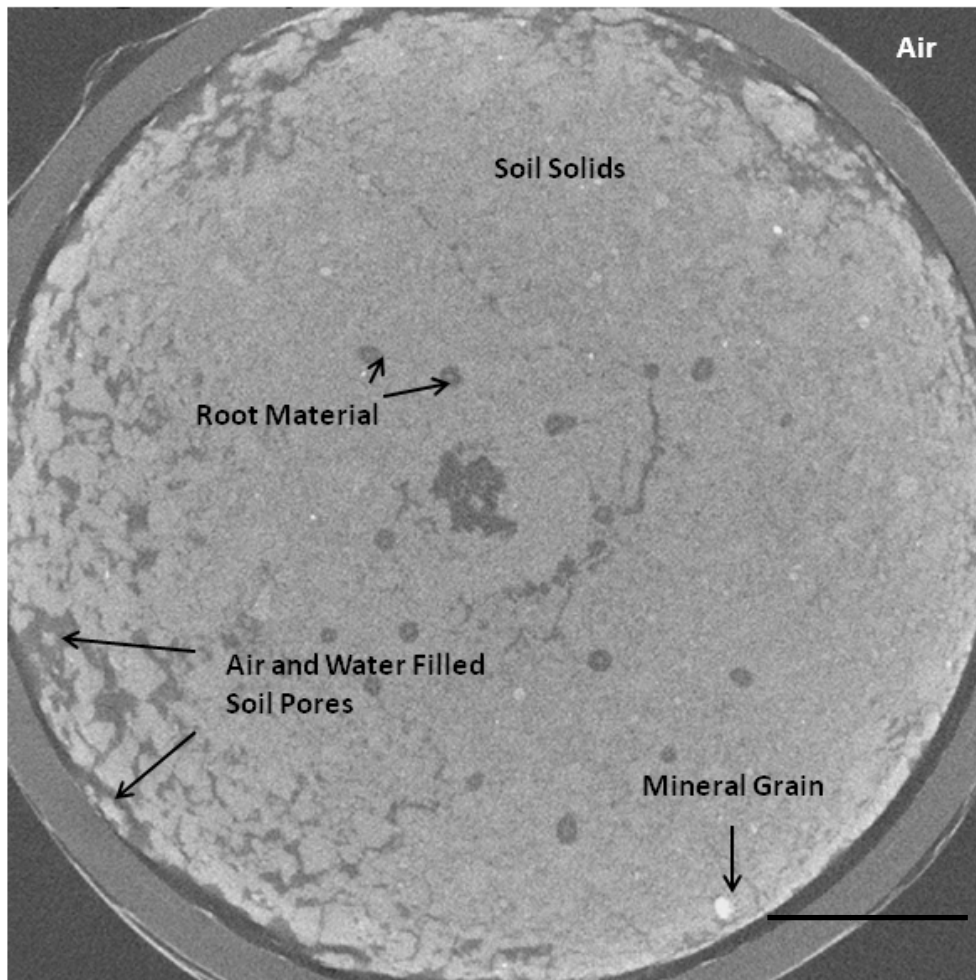


Fig. 1-8: Representative sample of an X-ray CT slice for a scan of a rice plant grown in loamy sand soil. Example locations of root material, air/water-filled pores and mineral grains are labelled. Higher X-ray attenuating materials appear lighter or white (minerals) whereas less dense materials tend toward black (air). Scale bar is 2 cm.

volume. The root architecture of barley phenotypes was successfully compared between different growth media by Hargreaves et al. (2009) with plants grown in 2-D gel chambers, 2-D soil sacs and 3-D X-ray soil pots for comparison. Tracy et al. (2013) utilised X-ray CT to understand how root architecture development in tomato is influenced by soil texture and

bulk density. X-ray CT has also been used to estimate root:soil contact at the microscale (Schmidt et al. 2012).

1.6 Literature review summary

The ability to visualise plant roots in soil enables researchers to combine knowledge about the biochemical functions related to plant root architecture with changes in root architecture over time. This is because root architecture, root development and biochemical activity are directly related to environmental stresses and soil characteristics (Fig. 1-9).

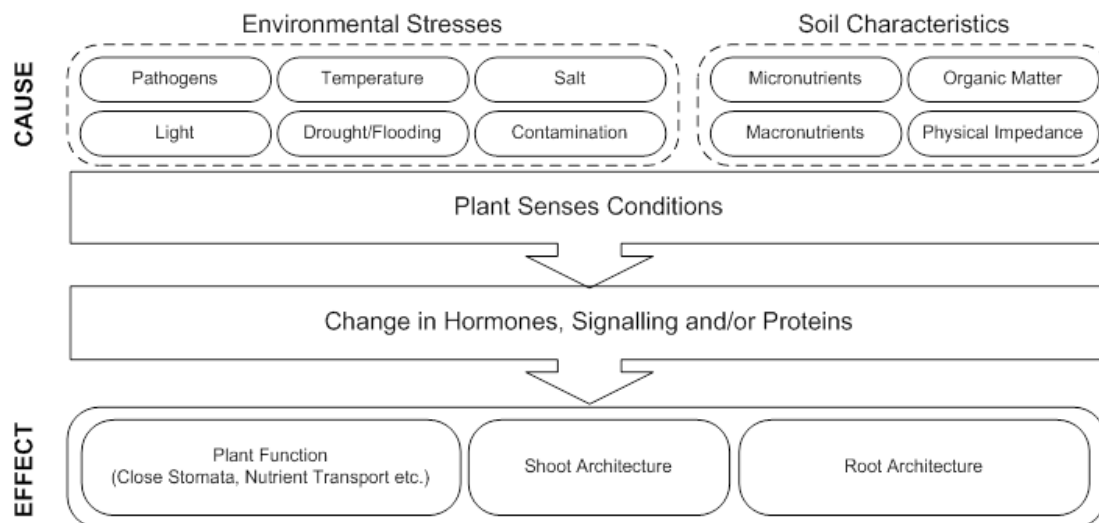


Fig. 1-9: Environmental stress and soil characteristics are linked to root architecture through biochemistry.

In general, X-ray CT studies solely link root architecture traits with environmental stresses or soil characteristics. Whereas this work takes a step further and investigates the influence of environmental stress on RSA and specifically, the role of the gene *OsAUX1*.

The relationship between the model plant rice, root gravitropism and P uptake from soil has not been established. This research project aimed to gain further understanding of phosphorus uptake in relation to *OsAUX1* associated changes to root system architecture in

rice. Knowledge gained through interdisciplinary research opportunities will contribute to improvement of crop species for adaptation to harsh environmental conditions or poor soils.

1.7 Aims and hypothesis

The overarching hypothesis for this work is that gravitropism improves P uptake in rice. As part of this hypothesis the following questions were considered:

1. Does reduced *OsAUX1* expression impact root gravitropism in soil (Chapter Five)?
2. Does root gravitropism influence P uptake in rice (Chapter Six)?
3. Do *OsAUX1* regulated root traits influence P uptake (Chapters Six and Seven)?
4. Does P availability and distribution influence gravitropic response or any other root traits in soil-grown rice (Chapters Six and Seven)?

The aims and sub-aims of this work were to:

- i. investigate the RSA development of *Osaux1* reduced function mutants in relation to wildtype when they are grown in soil and observed via X-ray CT by:
 - a. understanding the influence of soil moisture on segmenting roots from soil in X-ray CT images (Chapter Three), and
 - b. quantifying the effects of X-ray dose on RSA development and plant growth in samples repeatedly scanned with X-ray CT (Chapter Four), and
 - c. quantifying RSA development in loamy sand soil of wildtype and *Osaux1* T-DNA knockouts (Chapter Five),

- ii. assess the influence of root gravitropism and root distribution in the vertical soil profile on P uptake from soil with varying P concentration and distribution by:
 - a. using X-ray CT to quantify global RSA development in wildtype and *Osaux1* T-DNA knockouts grown in soil with low, sufficient and high P concentrations that have uniform vertical P distribution in the soil column (Section 6.3),
 - b. assessing local changes in RSA of these plants under split vertical P distribution with P concentrations sequestered to the top 4 cm or bottom 6 cm of the soil column (Section 6.3), and
- iii. quantify the influence of P availability on root morphological traits in relation to auxin influx or the lack thereof by:
 - a. quantifying root length, lateral root number, crown root number (Section 7.3.2) and root hair characteristics (Section 7.3.3) for plants grown on agar with low, sufficient and high P,
 - b. quantifying root rhizosheath P and Fe concentrations with SEM/EDX (Section 7.3.4),
 - c. understanding pH changes induced by wildtype and *OsAUX1* knockout mutants on agar with low, sufficient and high P (Section 7.3.5), and
 - d. quantifying intra-root air space (aerenchyma) in X-ray CT images of wildtype and *Osaux1-1* grown under varying P concentration and distribution (Section 7.3.6).

2.0 Materials and Methods

This section presents detailed descriptions of methods used for seed preparation, growth media preparation (soil and agar), planting in soil, plating on agar as well as 2-D and 3-D RSA measurement techniques. Methods specific to each chapter such as molecular methods are described in the Chapters themselves.

2.1 Seed preparation

The husk of the rice seed was removed by loosening the lower lamella to separate the seed kernel and husk (Fig. 2-1 A). The dehusked kernel was surface sterilised with a 50% solution of sodium hypochlorite (NaClO ; CAS 7681-52-9; Sigma Aldrich reagent grade) and sterile water for 30 min. The sterilised seed material was rinsed three times with sterilised water.

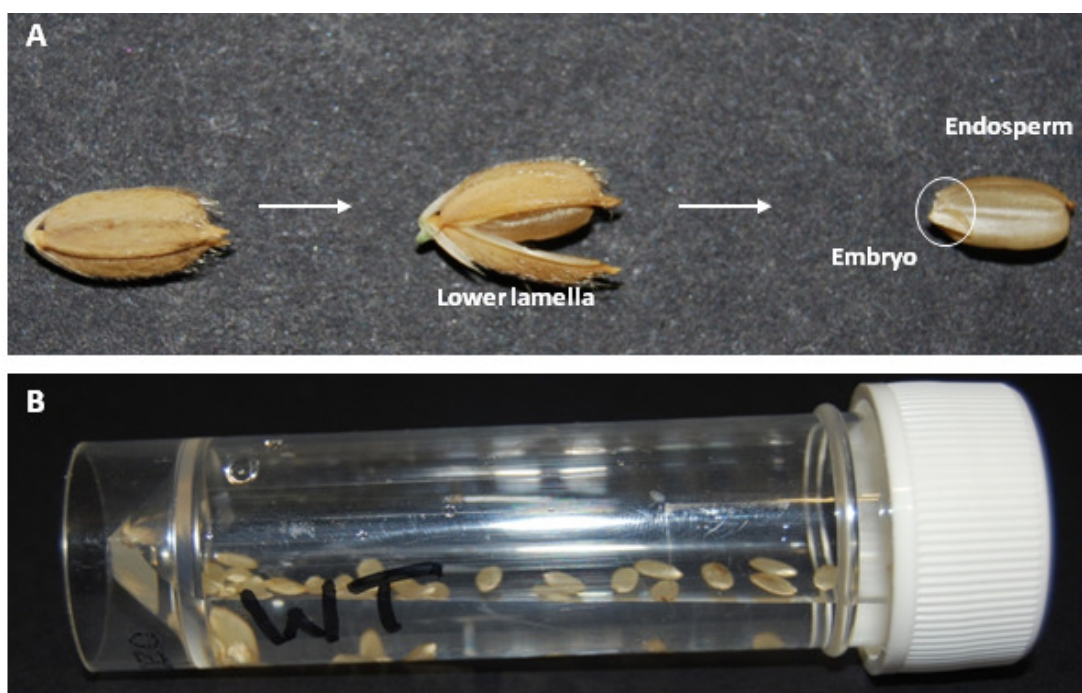


Fig. 2-1: Rice seed de-husking protocol (A) and germination setup (B).

The rinsed seeds were transferred to a universal tube and germinated in 25 mL sterilised water for 72 h to ensure emergence of the coleoptile (Fig. 2-1 B). The germinated seeds

were then transferred to the growing media as described in the following sections; specifically Section 2.5.3 describes planting in soil and Section 2.7 describes plating on agar.

2.2 Growth conditions

All plants were grown in a controlled growth environment room (Fitotron® Standard Growth Room, Room C103, University of Nottingham Sutton Bonington Facility) set at 28°C daytime temperature and 20°C night-time temperature with a 12 hour day/night cycle. Plants were grown in pots held in trays on 80 cm high benches. Fluorescent lights were in fixed suspension 1.2m above the bench tops. At 1 m distance from the light source, average light intensity was measured with a photosynthetically active radiation meter (Skye Instruments, PAR Quantum, Powys, Wales) as $220 \mu\text{mol m}^{-2} \text{s}^{-1}$.

2.3 Soil collection and properties

Three soils were used in this work; two typical UK soils of contrasting soil texture from the University farm at Bunny, Nottinghamshire used in Chapters Three, Four and Five and a specially sourced low P UK soil from Rothamsted Research Station (RRes) used in Chapter Six. The soil was low P because for over 100 years, the plot has undergone repeated planting and harvest of wheat without addition of P fertiliser (RRes 2006). This was undertaken to ascertain the impact of P application and crop management on soil P concentrations. Soil characteristics are summarised in **Table 2-1**. The two typical UK soils were a loamy sand (Brown soil, Newport series) and a clay loam (Argillic pelosol, Worcester series) collected from the University of Nottingham Farm at Bunny, Nottinghamshire, UK (52.86 °N, 1.13 °W). The low P soil from Rothamsted was a silty clay loam (Chromic luvisol) hand cored from the

top 10 cm of plot 14 from the Hoosfield Exhaustion Land Winter Wheat (Little Hoos) experimental field at Rothamsted Research Station in Harpenden, UK (51.81°N, 0.37°W).

Table 2-1: Soil properties summary. Compiled from original chemical analysis and information from Mooney and Morris (2008) designated with * and information provided by Chris Watts designated with **.

Soil sample	pH	Olsen P (mg kg ⁻¹)	Organic Matter (%)	Sand (%)	Silt (%)	Clay (%)
Newport Series	6.7	50	4.7	78.7*	9.4*	11.9*
Worcester Series	7.2	69	5.7	31.1*	34.5*	34.4*
Rothamsted low P	6.1	4.1	5.4**	18.9**	50.4**	30.6**

Bunny soil samples were collected using a spade; samples were taken from the top 20 cm of the soil profile at locations away from the edge of the field to avoid areas that had been frequented by farm machinery. The contrasting Bunny soils had too much Pi to induce P starvation in rice (> 5 mg kg⁻¹ Pi) thus low P soil collected from the Hoosfield Exhaustion Land at RRes was used in the P experiments (Chapter Six). The Exhaustion Land experiment has been underway since the mid-nineteenth century and was initiated to assess the influence on soil nutrient content of fertiliser application (phosphorus as triple superphosphate (TSP) and potassium as muriate of potash) and annual alternation of winter wheat and fallow. Soil samples were collected by Chris Watts from RRes.

2.4 Soil preparation

2.4.1 Sieving and sterilisation

Soil was air dried, manually sieved to < 2 mm then sterilised by autoclave (Phoenix 40E Bench Top, Rodwell Scientific Instruments, UK). Autoclaving was performed twice on each bag of sieved soil to minimise potential fungal and microbial activity in the soil columns

(Carter et al. 2007). This ensured any residual weed and wheat seeds were killed and did not interfere with assessment of RSA. A temperature probe (integrated into the autoclave) was placed in the centre of the soil mass to ensure that the autoclave temperature reading was representative of the entire bag of soil. The autoclave was held at 121 °C at 120 kPa for 30 min. Autoclaving was performed over two days with the soil being autoclaved once each day. Autoclaved soils were then oven dried (50 °C for 24 h) and stored in sealed containers at room temperature in preparation for packing into columns.

2.5 Column preparation

2.5.1 Altering P content and distribution

Phosphate amendment was achieved by segregating the desired amount of soil in plastic bags and adding crushed TSP (44% P₂O₅) in 50 mL of deionised water then thoroughly mixing. The amended soil was sieved to < 2 mm to ensure the mixture was homogenised. The soil was then air dried for four hours and subsequently used in packing.

Three P levels were composed from the soil (i) low P with no added TSP, (ii) sufficient P (replete) with 50 mg kg⁻¹ P and (iii) high P (toxic) with 150 mg kg⁻¹. The sufficient P treatment was achieved by adding 0.378 g TSP kg⁻¹ soil and the high treatment by adding TSP at 1.13 g kg⁻¹ soil. These P levels were established as being consistent with literature soil P treatments to starve rice (< 5 mg P kg⁻¹ soil) and also with low and high P treatments published in the literature and presented in Table 2-2. These three P levels (low, sufficient, high) were used in three different experiments exploring how RSA changed in relation to P distribution within the soil profile. The first experiment explored uniform P distribution where the P was evenly incorporated throughout the entire soil column (Fig. 2-2 A). The second experiment explored RSA changes under conditions where P was in the top 4 cm of soil (Fig. 2-2 B). The

final experiment investigated RSA when P was distributed in the bottom 6 cm of the column (Fig. 2-2 C).

Table 2-2: Selection of ranges for published low and high P treatments in non-agar based studies of root architecture in relation to P concentration for crop plants.

Low P (mg P kg ⁻¹ soil)	High P (mg P kg ⁻¹ soil)	Growth medium as described	Citation
0	40	sand	Lambers et al. (2006)
0	136.1	soil	He et al. (2003)
0.3	17.4	Paddy soil	Kirk et al. (1998)
0.9	56.2	< 2mm sieved soil	Ohno et al. (2007)
25	150	Loam, clay loam and silt	Kristoffersen and Riley (2005)
40.7	152.1	Field soil	Hammond et al. (2009)
79	285	Paddy soil	Irshad et al. (2008)
100	400	Paddy soil	Jianguo and Shuman (1991)
206	580	Silty sand	Blake et al. (2000)

2.5.2 Column packing

Polypropylene columns (5.5 cm internal diameter, 10 cm height and 0.23 cm thickness) were packed with prepared soil to 1.2 g cm⁻³ packing density. Each column had a mark in it at nine cm height to mark the target soil height. Each column received 217 g of dry sieved soil unless TSP was added. Then the target amount of soil was adjusted for the amount of water added with the TSP. All columns were packed in one cm sections, compressed with a ram and then scarified before addition of another layer. After all of the soil was in the column, the column was tapped to settle the soil below the nine cm line. There was no evidence that this technique created packing layers.

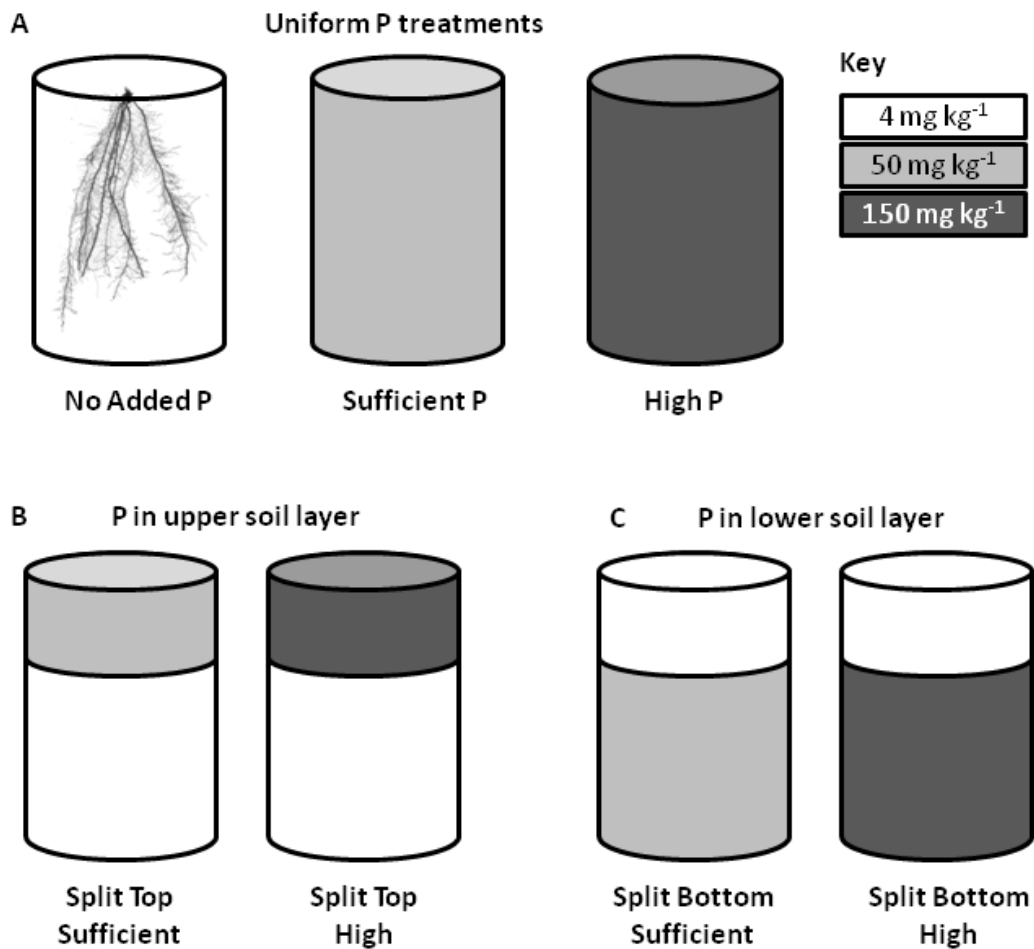


Fig. 2-2: Representation of experimental design investigating the distribution of P. Experiments used P in three levels (low/no added P, sufficient P and high P) distributed uniformly throughout the soil column (A), isolated to the top layers of soil (B) and isolated in the bottom layers of soil (C).

2.5.3 Planting and nutrient supplement

The packed columns were placed in five cm of deionised water until moisture was visible at the soil surface and the soil was saturated. Saturated columns were then planted with germinated rice seed when the coleoptile and radicle were least 1 cm in length. Columns were kept at saturation in the tray of deionised water under controlled growth conditions as described in Section 2.2. Weekly, 10 mL of nutrient solution was added to each column. In the phenotyping experiment (Chapter Five), nutrient solution containing phosphate was used (pH 6.0; 136g L⁻¹ KH₂PO₄, 0.94 mL L⁻¹ K₂SO₄ and KOH, 2 mL L⁻¹ MgSO₄ * 7H₂O and CaCl₂ * 2H₂O, 2 mL L⁻¹ Fe NaEDTA, 4 mL L⁻¹ NH₄NO₃, 1 mL L⁻¹ H₃BO₃, 1 mL L⁻¹ MnSO₄ * 4H₂O,

1 mL L⁻¹ ZnSO₄ * 7H₂O, 1 mL L⁻¹ CuSO₄ * 5H₂O, 1 mL L⁻¹ Na₂MoO₄ * 2H₂O) and 5 mL of mL L⁻¹ Ca(NO₃)₂ * 4H₂O). For the phosphorus experiments in Chapter Six, P-free nutrient solution with the same composition excluding KH₂PO₄ was applied weekly to each of the soil columns.

2.6 Agar-based growth media

2.6.1 Nutrient agar growth medium

For 1 L of basic nutrient agar medium, 2.15 g Murishage and Skoog Basal Salt Mixture (MS; M 5524, Sigma Aldrich) and 10 g Bacto™ agar (CAS 9002-18-0, Dickinson and Company, Sparks, MD, USA) were added to a 1 L glass bottle with polypropylene screw top lid. The MS-agar solution was adjusted to pH 5.8 with HCl or NaOH as needed. pH was determined with a calibrated combination pH electrode (Hannah Instruments HI110). The media was autoclaved in a benchtop unit (Prestige Classic 2100 benchtop autoclave) at 126 °C, 15 psi for 15 min and allowed to cool in an incubator oven to 50 °C.

2.6.2 Agar with varying P content

Agar with varying P content was comprised of three nutrient solutions instead of the MS nutrient mixture used in Section 2.6.1. The first nutrient solution was the P-free base mixture comprised of 0.41 g L⁻¹ NH₄NO₃, 0.002 g L⁻¹ H₃BO₃, 0.083 g L⁻¹ CaCl₂, 6.9*10⁻⁶ g L⁻¹ CoCl₂, 6.2*10⁻⁶ g L⁻¹ Cu₂SO₄, 0.09 g L⁻¹ Na-EDTA, 0.007 g L⁻¹ FeSO₄, 0.045 g L⁻¹ MgSO₄, 0.004 g L⁻¹ MnSO₄, 6.2*10⁻⁵ g L⁻¹ Na₂MoO₄ * 2 H₂O, 2.7*10⁻⁴ g L⁻¹ KI, 0.47 g L⁻¹ KNO₃, 0.002 g L⁻¹ ZnSO₄. The second solution was used to adjust phosphate levels and was 0.042 g L⁻¹ KH₂PO₄. The final solution was used to adjust potassium levels in the absence of KH₂PO₄ and was composed of 0.023 g L⁻¹ KCl. Proportions used of each solution for mixing the various P level

agar media are presented in Table 2-3. The nutrient solution was then supplemented with 10g bacto agar and adjusted to pH 5.8 as described in Section 2.6.1.

Table 2-3: Quantities of nutrient solution used to create agar with varying P levels.

P Concentration ($\mu\text{M PO}_4$)	Solution 1 Nutrient 100x (mL)	Solution 2 Phosphate (mL)	Solution 3 Potassium (mL)	Sterile water (mL)
3.12 (low P)	10	0.1	9.9	980
31.2 (replete P)	10	1	9	980
62.4 (high P)	10	2	8	980
312 (toxic P)	10	10	0	980

2.6.3 pH indicator

In order to assess the root induced pH changes in relation to P availability, pH indicator was added to agar with different P levels. Agar growth media (pH 5.8) with four P concentrations was prepared as described in Section 2.6.3. Before sterilisation, the agar was doped with bromocresol green powder at 0.006% (CAS 76-60-8; British Drug Houses Lab Chemicals Division, UK). The powder readily dissolved into the acidic media. Bromocresol green is a pH indicator that changes yellow at pH 3.6 and darkens to blue at pH 5.4. This is an adaptation of the method used by Mulkey and Evans (1981) with bromocresol purple and maize roots.

2.7 Plating protocol

Two polystyrene plate types were utilised for agar-based work (i) small disposable square plates (125 mm x 125 mm x 13mm; Thermo Scientific) and (ii) large reusable square plates (245 mm x 245 mm x 25 mm deep; Thermo Scientific). Small plates required 100 mL of medium and large plates required 300 mL of medium to ensure the seeds remained in the plate.

Reused large trays and lids were cleaned with phosphate-free detergent and then allowed to dry. The trays were then flooded with 100% EtOH in a laminar flow hood. A paper towel was used to rub the ethanol into all corners to ensure they were sterile. The ethanol was allowed to evaporate under the laminar flow hood.

Sterile plates were filled with autoclaved agar whilst in a laminar flow hood. Media was carefully poured in at one corner of the plate slowly, being careful to avoid development of air bubbles. If air bubbles did form, a sterile pipette tip was used to move the bubbles to the sides of the plate. Filled plates were left for 3 h in the laminar flow hood to solidify and dry.

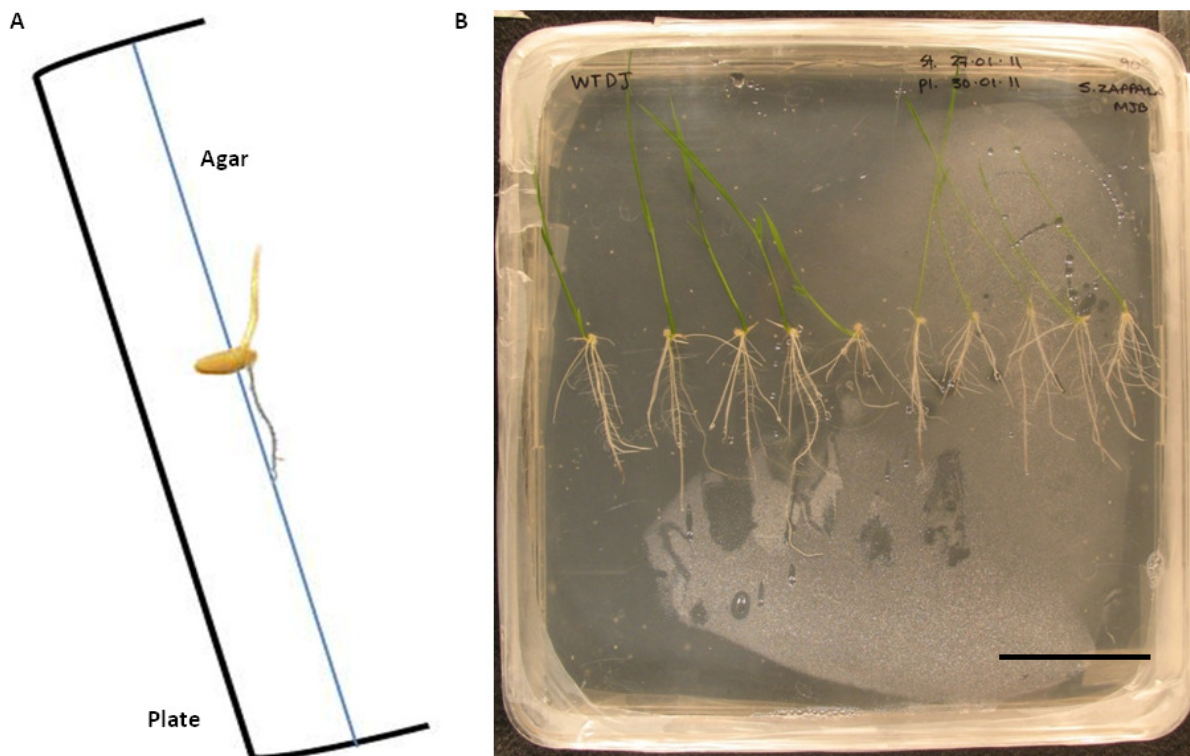


Fig. 2-3: Plating rice seeds in square petri dishes filled with agar growth media. Rice seeds are positioned with the endosperm embedded in the agar and grown for the first 24h at a 45° angle (A). The plates are then repositioned on vertical and large plates can hold ca. 10 plants for 12 days of growth (B). Panel A is not to scale. Scale bar in panel B represents 5 cm.

Germinated seeds were plated in a laminar flow hood. Germinated seed was grasped with sterile tweezers and placed approximately halfway down the plate. Seeds were positioned

with the endosperm of each seed in the agar and the emerged radicle and coleoptile pointing out of the agar. Once the desired number of seeds has been plated (for small plates between three and five; for large plates approximately ten), plates were sealed with plastic film (Parafilm, Cole-Parmer). The planted plates were kept at a 45° angle to prevent the roots growing into the surface of the agar in the first 24-36 h. After this time, the plates were re-positioned to vertical.

2.8 3-D Root measurement

2.8.1 X-ray CT Scanning

Radiographs of the soil and root volumes were obtained with a Phoenix Nanotom X-ray CT scanner (GE Sensing and Inspection Technologies, GmbH, Wunstorf, Germany) using a tungsten transmission target, mode zero with a spot size of approximately 3 µm. Scanner settings and scan frequency varied between scan setups and are described in the applicable Chapters. X-ray CT generated radiographs were reconstructed into 3-D volumes with Datos|x 2.0 (GE Sensing and Inspection Technologies, GmbH, Wunstorf, Germany). Individual adjustments in reconstruction were made for any sample movement that occurred during scanning.

2.8.2 Segmentation of roots

RooTrak is capable of automatically segmenting roots from soil in X-ray CT images (Mairhofer et al. 2012). In particular, root systems have been successfully segmented for tomato (Tracy et al. 2013) and wheat (Tracy et al. 2012a). In the case of rice, RooTrak was not optimised for the similarity of greyscale variation within the rice root and outside of the rice root. RooTrak depends on differences between the greyscale distribution of roots and soil to automatically distinguish between the two. Therefore, VG StudioMax 2.0 (VGSM) was

used to manipulate the X-ray CT volumes and to segment the root systems from the root-soil images. Manual segmentation took around 20 min for simple root systems and up to 6 hours for the very complicated root systems. The X-ray CT volumes were median filtered to 3x3 pixel prior to root segmentation. The roots were segmented with the VGSM region growing tool because it includes user-defined pixels within the root region of interest (ROI). The segmented root systems were finished with the VGSM open-close function (five pixels) to include any un-segmented airspace within the root. This was critical to ensure that X-ray CT root systems could be compared to the root system measurements obtained via flatbed scanning (WinRHIZO), which would include air spaces within the root.

2.8.3 3-D measurement with VG Studio Max and RooTrak

The software packages VGSM and RooTrak (Mairhofer et al. 2012) were used to quantify aspects of the RSA extracted from X-ray CT images. VGSM was used to measure root volume by pixel counting. RooTrak provided values for root volume, surface area, centroid (Fig. 2-4 A), maximum depth (Fig. 2-4 B), minimum enclosing circle (Fig. 2-4 C) and convex hull (Fig. 2-4 D). RooTrak primarily utilises voxel counting or area calculations from a triangle mesh generated around the segmented root system to provide quantification of these traits. Measurement of the segmented volumes took between 10 and 20 min depending on the image sizes and computer processing capability. Solidness was calculated via the ratio of root volume to convex hull volume to express the amount of root that was exploring the soil volume where root was present.

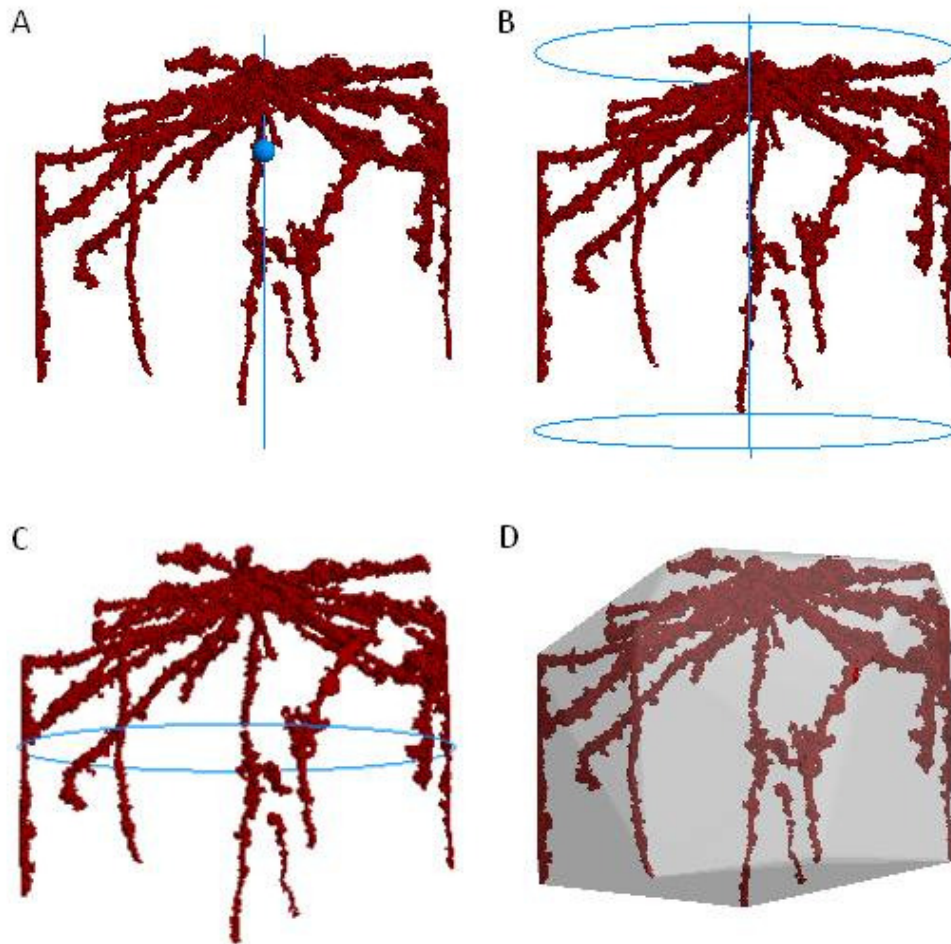


Fig. 2-4: Schematic representation of measurements available in RooTrak 0.2 measured from segmented X-ray images of root systems (Mairhofer et al. 2012). Centroid (A), maximum depth (B), minimum enclosing circle (C) and convex hull volume (D) provide indicators of the root distribution in the soil profile. RooTrak quantifies root systems from segmented greyscale images, in this case obtained by X-ray CT, through voxel counting and calculations based on a triangle mesh of the extracted root system.

2.9 Destructive analysis and 2-D measurements

After scanning, shoot material was excised with scissors and set aside for oven drying (80 °C for 48 h). Rice plants were then removed from the polypropylene soil columns and then carefully washed of soil with DI water. The destructively sampled root systems were rinsed several times and visible soil was removed with aid of a small paintbrush. The cleaned roots were imaged using a flatbed scanner, which is part of the WinRHIZO (Regent Instruments Inc., Canada) system described in Section 2.9.1. After WinRHIZO analysis, shoot and root

material was oven dried at 80 °C for 48 h in preparation for P analysis. Dry mass was recorded.

2.9.1 *WinRHIZO measurements*

The destructively sampled root systems were then scanned on a flatbed scanner in water-filled Perspex® trays designed to fit the WinRHIZO system. The resulting images were analysed in WinRHIZO Regular 2002[©] software. WinRHIZO provided total root system measurements of root length, projected root surface area, root volume and number of tips. These measurements were also provided in distribution by root diameter class (e.g. total root length within classes 0 to 0.5 mm diameter, 0.5 to 1.0 mm diameter, 1.0 to 1.5 mm diameter, etc.). Root diameter extrapolation (algorithm not provided by WinRHIZO) was used by WinRHIZO to calculate root surface area and root volume from root length. Root length was calculated from a skeletonisation of the scanned root system. Fig. 2-5 provides an example of WinRHIZO output in relation to the scan of the original system with colour denoting root diameter class assigned by WinRHIZO.

2.9.2 *Specific root length*

Specific root length (SRL) was calculated from the ratio between total root length obtained in WinRHIZO and the root dry mass.

2.9.3 *Image J*

Images for analysis in Image J (National Institute of Health, rsb.info.nih.gov/ij/) were captured with a digital camera (Cannon Powershot). For measurement of primary root length and lateral root number, the plates were photographed with fixed lighting and a ruler for scaling. The camera was mounted on an adjustable stand and the plates were placed on

a neutral black cloth background. For root hair images, the digital camera was mounted on a microscope (Zeiss Steri SV6). A ruler photographed at the microscope settings was used for

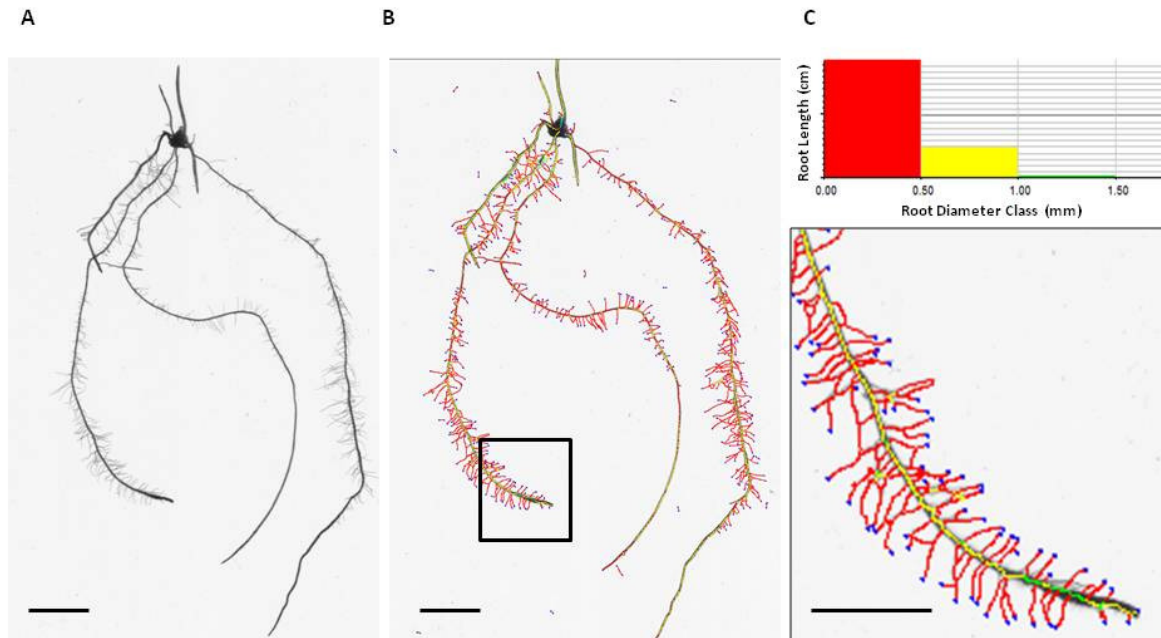


Fig. 2-5: Example of a destructively sampled root system that was imaged on a flatbed scanner (A) and the resulting WinRHIZO output (B). Each root is skeletonised and assigned a colour according to root diameter. A subsection of the output image has been magnified (C). The histogram shown applies to root length (cm) where red is the total length for roots of diameter 0 to 0.5 mm, yellow is 0.5 to 1.0 mm and green is 1.0 to 1.5 mm (C). Root tips are shown in blue (C). Scale bar is equivalent to 1 cm.

scaling the root hair images. Lighting was provided by a Zeiss KL1500 adjustable cold light. Images were captured using Zoom Browser EX software.

Images were loaded into Image J and then the scale was adjusted by drawing a line (straight) over the ruler to obtain a pixel to mm ratio. Using the Image J Analyze>>Set Scale function, the known distance pertaining to the pixel length of the line was entered to provide a pixel mm^{-1} scale for the image. Then length was measured by drawing a freehand line over the root feature of interest (primary root or root hair) and then using the measure tool (Analyze>>Measure) to produce a scaled measurement. Ten replicate length

measurements were performed for each sample. Lateral roots were counted manually in Image J.

2.10 Chemical analysis

2.10.1 Soil pH

Approximately 5 g of prepared soil (autoclaved, sieved to < 2mm) was added to a 50 mL plastic centrifuge tube with screw on cap with 12.5 mL of DI water. The centrifuge tubes were placed in an end-over-end shaker for 30 min. The tip of a combined pH electrode (HI110; Hannah Instruments from Fisher Scientific, Loughborough, UK) was submerged into the soil-water slurry and allowed to equilibrate for up to 5 min. The electrode was calibrated using pH 4.01, pH 7.00 and pH 10.01 calibration solutions (SLS Select buffer series).

2.10.2 Plant phosphate

Oven dried (80°C for 48 h) root and shoot material was weighed before being ground by centrifugal plant mill (stainless steel housing and grind barrel). The ground samples were decanted into individual porcelain crucibles and ashed in a cold muffle furnace gradually brought to 550 °C and then kept at this temperature for 8 h. The ashed material was digested for 20 min with 5 mL of 0.2M HCl. This digestate was filtered through Whatman No. 1 filter paper suspended in plastic funnels over 25 mL glass volumetric flasks. The crucibles were rinsed with a further 10 mL of deionised water and this was also filtered into the flasks. The filtrate was brought to 25 mL with deionised water to create the sample solution.

In new 25 mL volumetric flasks, 10 mL of sample solution was mixed with 10 mL of colour forming reagent, brought to 25 mL with deionised water and allowed to stand for 30 min.

The colour forming ammonium vanadomolybdate reagent was made with 56.3 g L⁻¹ (NH₄)₆Mo₇O₂₄* 4 H₂O, 4.17 g L⁻¹ NH₄VO₃ and 25% concentrated HNO₃. This method was adapted by adjusting solution amounts for small samples (approx 0.1 g dried material) from colorimetric protocols described by Cavell (1955) and Pearson (1976).

1 mL of this reacted yellow-coloured solution was transferred to a disposable plastic cuvette. The absorbance was measured at 410 nm wavelength by spectrophotometer. A calibration curve was created from absorption values for samples with known P concentration generated from a 0.22 g L⁻¹ (50 ppm) KH₂PO₄ stock solution. A deionised water blank and method blank (from empty crucible) were also included.

The percent of plant P was calculated using the following equation:

$$\% P_{\text{plant}} = \text{ppm P (from calibration curve)} \times \frac{R}{Wt} \times \frac{100}{10000}$$

where *R* = ratio between volume of the digest (25 mL) and amount used for measurement (10 mL) and *Wt* = the dry mass of plant tissue.

2.11 Statistical analysis

All statistics were calculated using Genstat 15th Edition (VSN International Ltd., Hemel Hempstead, UK). Randomisation for block design and selection of samples for X-ray CT scanning was achieved through assignment of random numbers in Microsoft Excel. General Analysis of Variance (ANOVA) was used to evaluate differences for all possible interactions as applicable including moisture content, P concentration and genotype. A summary of interactions is presented in Table 2-4. For all tests, the data was normally distributed which satisfied assumptions of general ANOVA. Normality was confirmed through analysis of residual plots. When comparing results from repeatedly scanned columns (week one, two,

three and four) a polynomial contrast was included to provide the most conservative statistical result for time related interactions. This was most appropriate for analysis of repeated measurements performed on the same sample.

Table 2-4: Summary of interactions for experimental results analysed by Analysis of Variance (ANOVA). Polynomial contrast was used to delineate interactions for repeated measurement of the same sample and is designated by an asterisk in the table.

Chapter	Experiment	ANOVA Interactions
3	Soil Moisture effects on X-ray CT	Day after removal from water*, Soil type
4	X-ray effects on root growth	X-ray CT treatment
5	Phenotyping <i>Osaux1</i> in soil	Week*, Genotype
6	P uptake and <i>Osaux1</i>	P concentration, Genotype
7	<i>Osaux1</i> expression	Tissue, Genotype
7	<i>Osaux1</i> traits and available P	P concentration, Genotype
7	Fe rhizosheath SEM/EDX	Location on root, Genotype

3.0 Quantifying the effect of soil moisture content on segmenting root system architecture in X-ray Computed Tomography images

3.1 Description and author contributions

This chapter is a reformatted version of a paper published in *Plant and Soil* (Zappala et al. 2013b) that describes how soil moisture can influence the ability to visualise and ultimately, distinguish roots from soil in X-ray CT images. Having soil that is very wet can be as detrimental to segmentation of roots from soil in X-ray CT images as using soil which is dry.

Author contributions are as follows:

- Project supervision was provided by M. Bennett, T. Pridmore and S. J. Mooney.
- General advice and draft editing was given by S.J. Mooney
- Image analysis assistance was provided by S. Mairhofer
- Water release curves were provided by S. Tracy
- Literature review, experimental design, practical work and paper construction were completed by S. Zappala.

3.2 Abstract

3.2.1 Aims

A commonly accepted challenge when visualising plant roots in X-ray CT images is the similar X-ray attenuation of plant roots and soil phases. Soil moisture content remains a recognised, yet currently uncharacterised source of segmentation error. This work sought to quantify the effect of soil moisture content on the ability to segment roots from soil in X-ray CT images.

3.2.2 *Methods*

Rice (*Oryza sativa*) plants grown in contrasting soils (loamy sand and clay loam) were X-ray CT scanned daily for nine days whilst drying from saturation. Root volumes were segmented from X-ray CT images and compared with volumes derived by root washing.

3.2.3 *Results*

At saturation the overlapping attenuation values of root material, water-filled soil pores and soil organic matter significantly hindered segmentation. However, in dry soil (ca. six days of drying post-saturation) the air-filled pores increased image noise adjacent to roots and impeded accurate visualisation of root material. The root volume was most accurately segmented at nominal field capacity (soil water content 2 to 3 days after irrigation).

3.2.4 *Conclusions*

Root volumes can be accurately segmented from X-ray CT images of undisturbed soil without compromising the growth requirements of the plant providing soil moisture content is kept at field capacity. We propose all future studies in this area should consider the error associated with scanning at different soil moisture contents.

3.3 Introduction

X-ray micro Computed Tomography (X-ray CT) has been used in the non-destructive study of plant-soil interactions for a number of years (Gregory 2006; Heeraman et al. 1997; Mooney et al. 2012b; Moran et al. 2000; Perret et al. 2007). A recent review of applications in Brazilian soil research by Pires et al. (2010) highlighted that soil solids, pore space and water have often been the focus of rhizosphere research involving X-ray CT because they are

easier to identify and segment than plant roots, however plant roots play a critical role in the root-soil-microbe system and cannot be ignored.

X-ray CT can be used for the non-destructive observation of plant root development in soil over short time periods (Tracy et al. 2012b). At present, the application of X-ray CT for high throughput root phenotyping is limited by several challenges including the trade-off between spatial resolution and sample size. Dhondt et al. (2010a) has recently illustrated that X-ray CT can be successfully employed to visualise the physiology of plant aerial tissues. However, several challenges exist when capturing plant root development in soil using X-ray CT (see Mooney et al. 2012b for detail).

Improvements in X-ray detector technology have advanced the ability to distinguish soil microstructure and finer roots at ever decreasing scales (Mees et al. 2003). Despite this, contrast in X-ray attenuation between the soil matrix, air-filled pores, water-filled pores, plant material and organic matter is frequently poor. The X-ray attenuation of these materials varies with several factors including soil type (Pálsdóttir et al. 2005), proximity of roots to organic matter or air-filled pores (Perret et al. 2007) and root water status (Hamza et al. 2007). The main challenge is to increase the difference in density between the soil matrix and plant roots in natural plant-soil systems without altering the biochemical status of the system. Previous work has achieved this to an extent by using non-soil or pseudo-soil growing media, using extremely small sample columns, drying out the sample (Seigneur et al. 2010) or growing plants that have very coarse, easily distinguishable below-ground structures such as potato (Ferreira et al. 2010). However each of these techniques, to an extent, compromises our ability to examine root behaviour under field-like soil conditions.

Recently, Mairhofer et al. (2012) demonstrated great potential for segmenting roots using object tracking approaches but the success of this method is also influenced by soil moisture content.

For plant-soil systems, soil moisture content plays an integral part in the plant growth rate, root development and soil strength (Whalley et al. 2008). Additionally, soil moisture content influences the difference between the linear attenuation coefficients of the plant roots and soil fractions during the X-ray scanning, thus influencing image quality as X-ray CT images are a reflection of the material density and X-ray attenuation of the sample. As such, the moisture content at the point of scanning has a profound influence on the ability to segment plant roots from soil by image analysis. This is to a large extent well known, however as Flavel et al. (2012a) recently observed water-filled pores can confound segmentation algorithms and cause misclassification of roots in X-ray CT images. To date the nature of the error caused by soil moisture content has not been quantified. This work aimed to quantify the influence of soil moisture on the segmentation of plant roots in CT images of rice (*Oryza sativa*) in natural soil at high resolutions with the intention of identifying a preferred working condition for future studies.

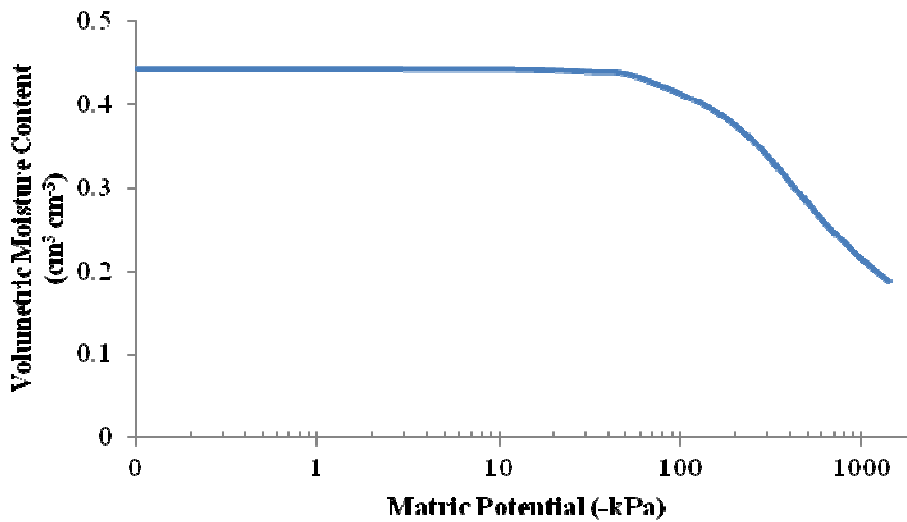
3.4 Materials and Methods

3.4.1 Sample preparation

Polypropylene (due to low X-ray attenuation) columns (55 mm diameter and 15 mm high) were filled in triplicate with both sieved (< 2 mm) loamy sand soil (Newport Series, FAO Class Brown soil) and a clay loam soil (Worcester Series, FAO Stagnogleyic Lovisol). The columns were packed to a representative field bulk density of 1.1 g cm^{-3} and 1.3 g cm^{-3} respectively. A water release curve for each soil type was prepared using a combination of

sand tables and a pressure membrane apparatus. The Van Genuchten-Mualem model was fitted to the experimental data using RETC software (www.scisoftware.com) (Fig. 3-1).

(A) Loamy Sand



(B) Clay Loam

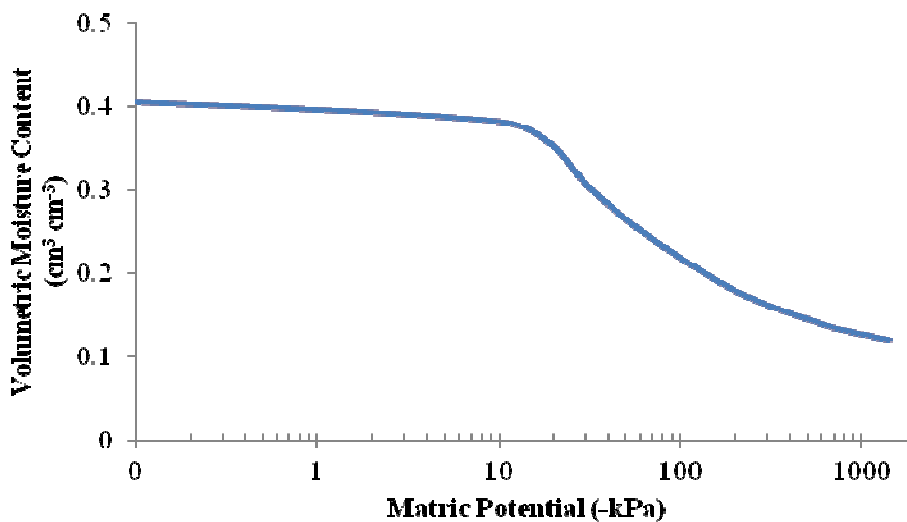


Fig. 3-1: Soil moisture release curves for (A) Loamy sand and (B) Clay loam soils fitted to the Van Genuchten-Mualem Model derived in RETC (Retention Curve Program for Unsaturated Soils) (www.scisoftware.com).

The columns were saturated from the bottom upwards with deionised (DI) water and planted with germinated rice seeds (*O. sativa cv. Azucena*; 5 days after germination and

with emergence of the coleoptile and radicle). The plants were grown for 29 days in a controlled growth room with 12 hours of daylight at temperatures of 28 °C during the day and 20 °C at night. DI water was provided continuously by placing columns in a tray with approximately 2 cm DI water ponded in the bottom. In preparation for X-ray CT scanning, all columns were removed from the tray several hours before the start of the scanning regime and no further water was added. The soil moisture content was gravimetrically determined for each column before and after scanning to record any moisture losses during the scanning process. Each column was scanned daily for nine days to represent a large range of the water release curve as shown in Fig. 3-1. An equal number of columns were prepared that were treated in exactly the same way with the exception of X-ray CT scanning so that any effect on the plants from exposure to X-rays could be detected at the end of the experiment.

3.4.2 *Visualisation of Root System Architecture in Soil using X-ray CT*

A Phoenix Nanotom micro X-ray CT scanner (GE Sensing and Inspection Technologies, GmbH, Wunstorf, Germany) was used to obtain 2-D images of root and soil structure and 3-D root volumes for each column. Each day for nine consecutive days, columns were scanned and soil moisture content determined. The columns were placed directly in the X-ray CT scanner without any alteration. The X-ray CT scan position and settings were kept constant for each column. Each column was scanned at a 57.3 µm voxel size over 73 min. Note that scan times significantly faster than this are possible (< 10 minutes) however longer scan times are usually associated with greater image quality (e.g. less random variation in pixel brightness known as image noise) which was the main consideration here. The range of settings for scanning was 110 – 130 kV, 320 µA, 500-750 ms timing. The centre of the

sample was positioned 22.5cm distance from the X-ray source and 1080 projection images were taken. The detector size was 2300 X 2300 pixels (1150 X 1150 pixels in binning mode) and spot size of the X-ray beam was ca. 3 μ m. A tungsten transmission target was used with a 0.2 mm copper filter.

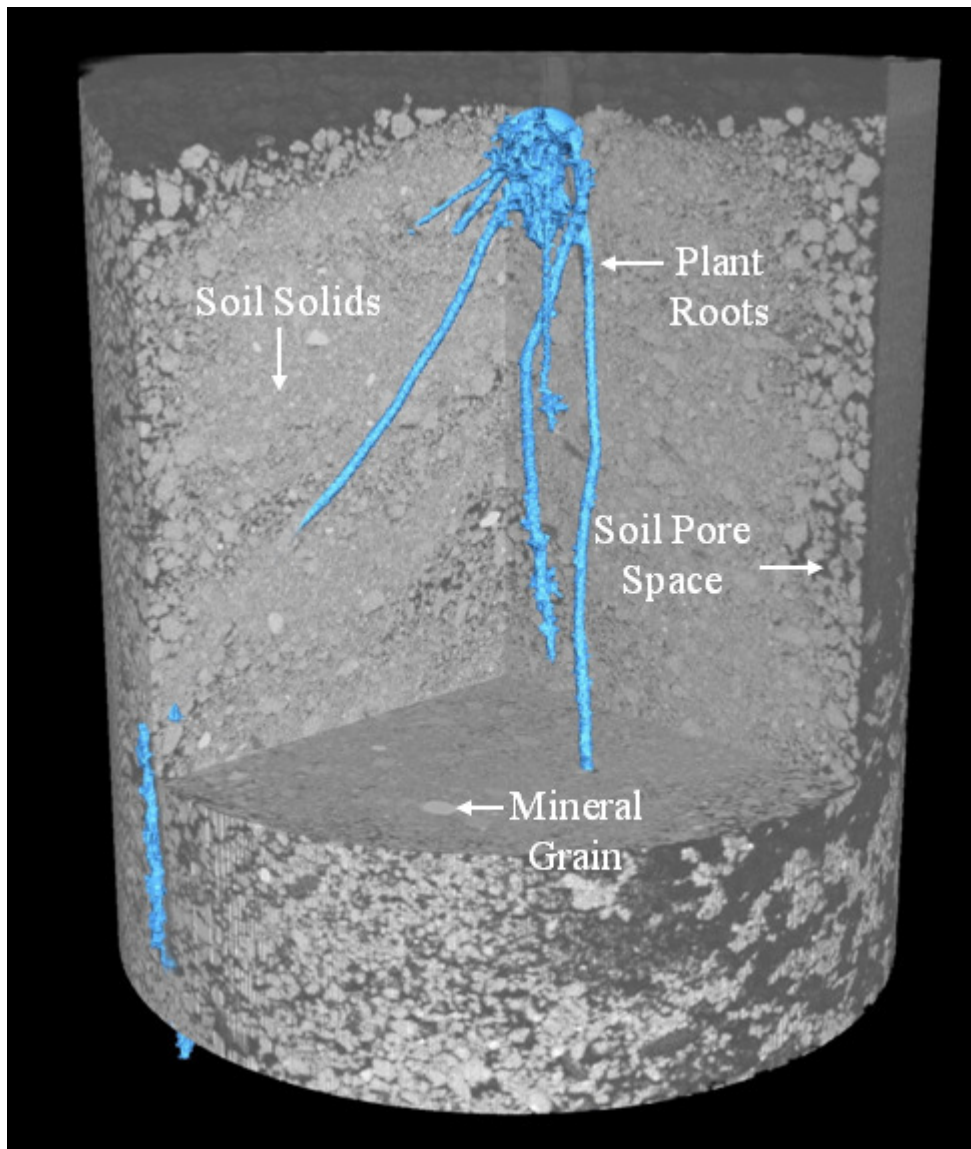


Fig. 3-2: Representative cross-section of the 3-D X-ray CT volume of a rice root-soil sample. Examples of mineral grains, air/water-filled pores and soil solids are highlighted in greyscale. The segmented root system is shown in false colour. Scale bar = 1 cm.

On some occasions, slight variation in the scan parameters was required to optimise the image quality/greyscale histogram, associated with the difference in bulk density between

the two soil types. There were a total of 72 scans. The volumes were reconstructed in Datos|x 2.0 (GE Sensing and Inspection Technologies, GmbH, Wunstorf, Germany) with a beam hardening correction set at 8 and individual adjustments for minor sample displacement. All reconstructed volumes were firstly filtered with a median filter (radius of 3.0 pixel) before the root systems were segmented using the region growing tool in VGStudioMax v 2.0 (Volume Graphics GmbH, Heidelberg, Germany). A 3-D volume to illustrate the range of X-ray attenuation values for different materials within the sample is shown in Fig. 3-2. The effect of soil water content is shown by the overlap in X-ray attenuation observed between root material and water-filled pores at the point of segmentation (Fig. 3-3).

3.4.3 *Calculation of X-ray Dose*

Dose was calculated using the free-online RadPro Dose Calculator (McGinnis, R; <http://www.radprocalculator.com/XRay.aspx>). The calculator uses formulae and X-ray empirical data from British Standard BS 4094-2:1971 (Recommendation for data shielding from ionizing radiation – Part 2: Shielding from X-radiation) to provide a dose approximation defined by user inputs. The calculated X-ray dose for each sample was 1.41 Gy with a total dose for each sample accumulated over 9 scans of 12.71 Gy per column.

3.4.4 *Root Segmentation Efficiency*

On the final scan day (day nine), each soil-root system was removed from the columns and the soil was gently washed away from the intact root systems with DI water. The destructively sampled root systems were scanned using WinRHIZO (Regent Instruments Inc., Canada) to determine the root volume of the intact root system. WinRHIZO calculates total

root volume from average root diameter and root length determined from the 2-D scanned root image through pixel counting. X-ray CT root volumes were calculated from the segmented root region of interest (ROI) determined in VGStudioMax v 2.0. The root system was segmented from the greyscale CT images of soil with VGStudioMax v 2.0 region-growing tool. A user defined root pixel (seed pixel) is selected and then the region-growing tool tolerance is adjusted to select visible root material within a defined radius of the seed pixel (This process is similar to the process of dilation, but based on greyscale values). The dynamic mode of the region-growing tool was utilised to actively adapt to minor fluctuations between each CT slice. Automated tracking algorithms such as those found in Mairhofer et al. (2012) were tested but not effective for rice roots because of noise within each rice root image caused by water/air-filled aerenchyma. After segmentation, the VGStudioMax v 2.0 filling function (open-close 1 pixel) was used to fill un-highlighted areas within the root ROI boundary.

The root segmentation efficiency, which we define as the ratio of the 3-D segmented X-ray CT root volume derived by VGStudioMax v 2.0 to the destructively determined root volume derived by WinRHIZO, was measured for each sample and expressed as a percentage. This calculation assumes X-ray CT observable root growth was minimal between day one and day nine of the experiment which is why the scanning was undertaken on well established

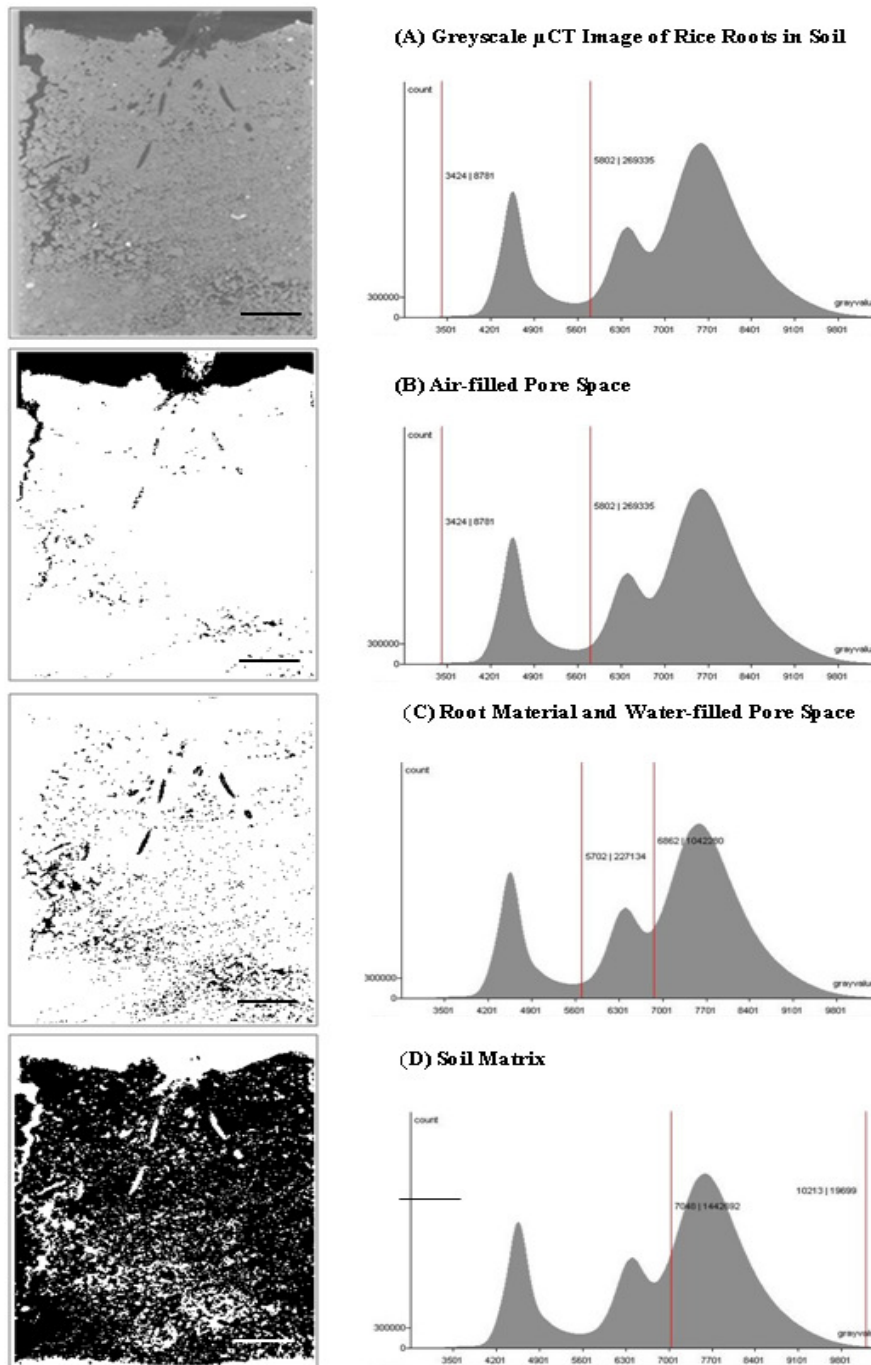


Fig. 3-3: An illustration of the difficulties in segmenting roots from soils. A 2-D CT slice of rice roots grown in soil (A) has been thresholded and binarised to show in black (B) air-filled pores, (C) root material/water-filled pores and (D) soil matrix; the corresponding greyscale histogram (frequency distribution) for the thresholded areas is at the right of each image for B, C and D respectively. Lines on the greyscale histograms denote the greyscale values included in the dark grey portion of the sample. Numbers to the right of the lines detail the greyscale values on left and frequency of occurrence on right. Scale bars = 1 cm.

plants (i.e. 34 DAG) and a cultivar (*O. sativa* cv. Azucena) with reduced branching in the observation zone (Clark et al. 2011). Soil macroporosity (pores >115 μ m effective diameter)

was measured from the X-ray CT images with ImageJ (<http://rsbweb.nih.gov/ij/>). The image stack was median filtered with a 0.5 pixel radius. Pore space was segmented with the Otsu thresholding algorithm (multi-threshold plugin). The segmented area was binarised and pore space parameters were measured with the ImageJ “Analyse Particles” function. Macroporosity was characterised because this was the pore size visible within the resolution of the X-ray CT images.

The results were subjected to an analysis of variance (ANOVA) containing soil type and time and all possible interactions as explanatory variables using Genstat 13.1. Regression analysis was used to explore the relationships between root volume and soil moisture content. Normality was tested by interpreting the plots of residuals; in all cases the data were normally distributed, satisfying the assumptions underlying general ANOVA.

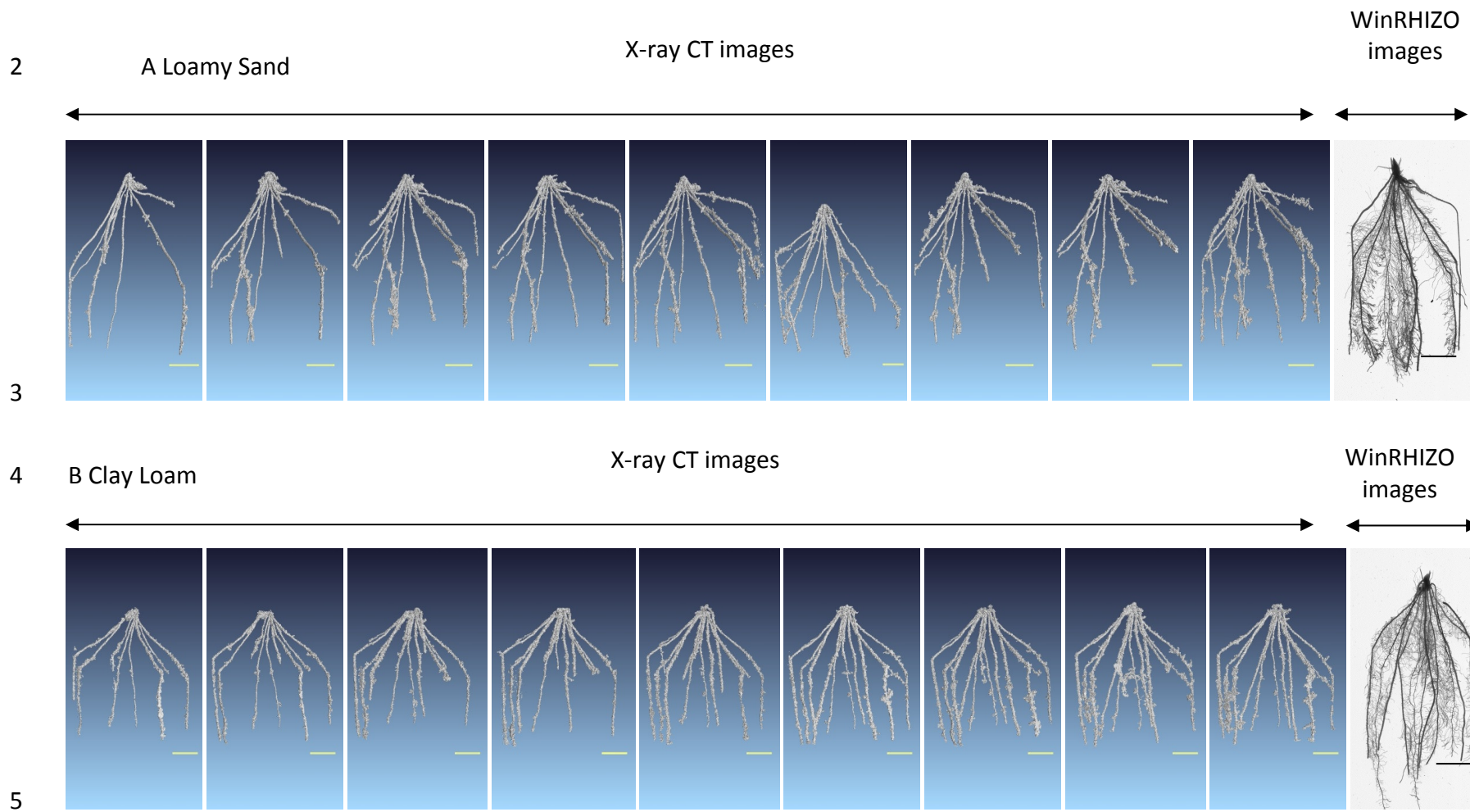
3.5 Results

Accurately observing root system architecture (RSA) development in soil through X-ray CT requires a balance of the trade-off between soil water content and image quality. We aimed to quantify this trade-off. The experiment successfully yielded high quality images of the undisturbed RSA of rice plants grown in soils with two contrasting textures. The root volumes were significantly ($p < 0.001$) greater in the clay loam soil compared to the loamy sand (0.512 vs. 0.369 cm³ respectively). As expected a larger volume of roots were recorded in the WinRHIZO images (Fig. 3-4) as the X-ray CT derived volumes are restricted by the resolution of the scan (57 µm) and the aforementioned difficulties in segmenting the root material, however the X-ray CT and WinRHIZO measurements of root volume were still significantly correlated ($R^2=0.61$; $p < 0.01$).

As hypothesised there was a significant effect of soil moisture content on the ability to segment the RSA in the X-ray CT images (Fig. 3-4). As soil water content decreased through the drying period, the ability to segment the RSA increased ($R^2=0.47$) (Fig. 3-5). There was no significant difference in the ability to segment root material as the soil dried between the contrasting soil textures.

In order to explore this further the root segmentation efficiency ratio (ratio of X-ray CT root volume: WinRHIZO root volume) was calculated for each sample. This was also significant illustrating the same trend albeit with a smaller R^2 of 0.39 (Fig. 3-6). However in this instance there was also a significant difference between the soil types (loamy sand $R^2=0.23$ and clay loam $R^2=0.66$) which may be attributed to the relative abundance of fine roots (< 0.2mm diameter) in the loamy sand samples which would not be visible via X-ray CT at the 57 μm voxel size. The average total length of fine roots was 556 cm in the sandy loam and 465 cm in the clay loam.

The experiment required continuous assessment of the same plant as the soil dries and could potentially include root growth which would skew results. However, mature plants were used to minimise the possibility of significant coarse root growth for the duration of the experiment (only roots > 57.3 μm effective diameter are included). As an additional precaution, the rice cultivar *Azucena* was used because it has been shown to have little branching in the upper root system due to its deep rooting nature (Clark et al. 2011).



6 Fig. 3-4: Three-dimensional rice root system architecture (RSA) images as obtained by both X-ray CT and WinRHIZO for (A) Loamy sand and (B) Clay Loam
7 soils. Scale bars = 1 cm.

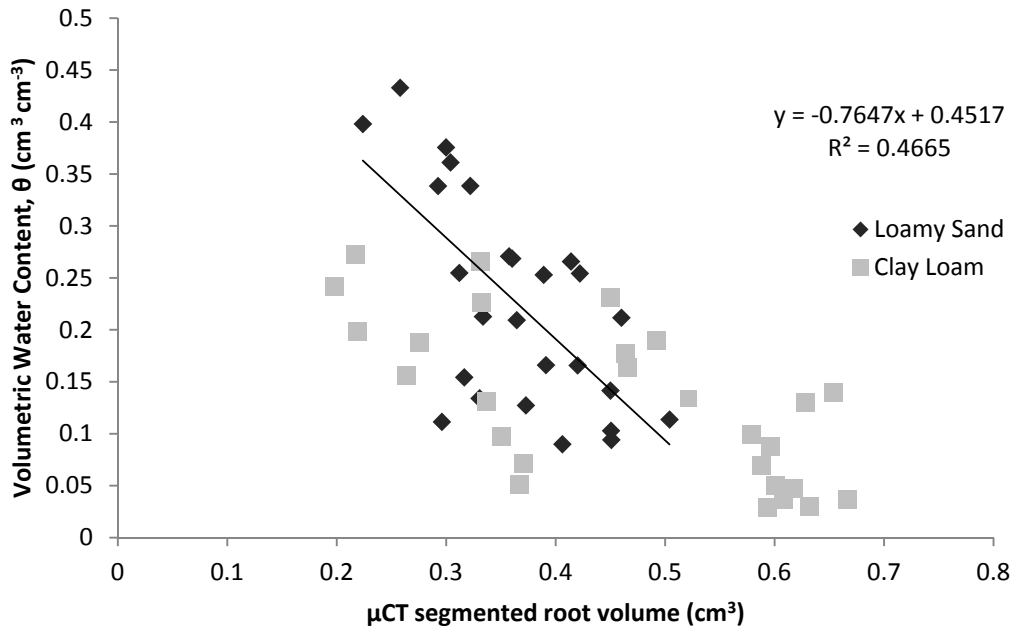


Fig. 3-5: X-ray CT segmented root volume as a function of volumetric soil water content for both loamy sand (diamonds) and clay loam soil (squares).

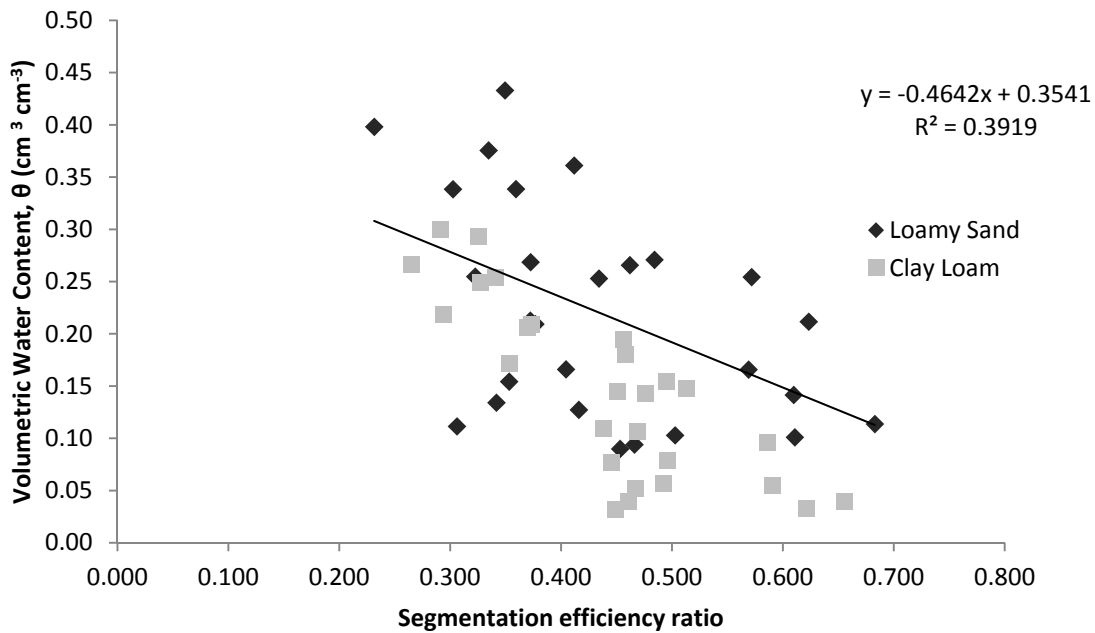


Fig. 3-6: Segmentation efficiency ratio as a function of soil water content for both a loamy sand (diamonds) and clay loam soil (squares). Segmentation efficiency is defined as the ratio between root volume segmented from X-ray CT images and the root volume determined through root washing.

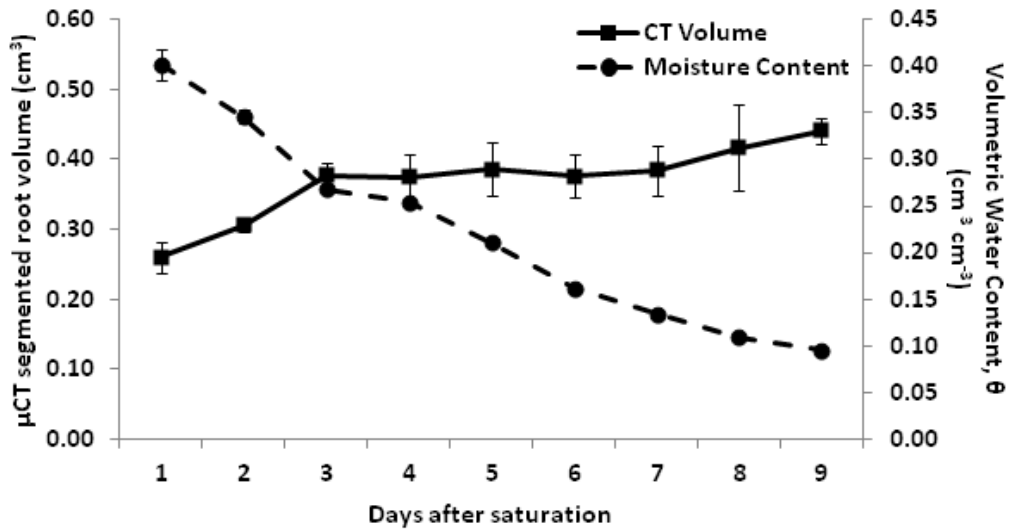
Assuming root growth between scan days one and nine is negligible, the soil moisture content at scanning had a clear significant impact on the ability to discriminate root material

in X-ray CT images, especially between days one and three where the effect was most pronounced ($p < 0.01$) (Fig. 3-7). However after three days, there were no significant differences in the segmented root volumes although a slight increase (not significant) was recorded between day seven and eight. Interestingly this is consistent across two very different soil textures which was not as hypothesised. In order to ensure that repeated X-ray exposure did not have an effect on plant development, an equivalent number of columns were prepared that were not subject to scanning at any stage. All unscanned plants were removed from the growth chamber for the same duration as the scan time and treated the same as the scanned plants apart from the scanning itself. At the end of the experiment these columns were also root washed and the total root volume compared with the scanned columns. No significant difference ($p = 0.752$) was found between the scanned and unscanned root volumes.

3.6 Discussion

These results show that segmentation of root material in X-ray CT images is indeed influenced by soil moisture content and that this should be a key consideration in future studies. This was expected and might explain why many previous researchers who have tried to employ X-ray CT as a tool to visualize roots in soil have preferred to work with coarse, dry porous media (e.g. Heeraman et al. 1997) where possible. However X-ray CT as a tool for the plant-soil scientist is becoming more popular due to recent improvements in image quality, scan and reconstruction speeds and root segmentation software (see Mooney et al. 2012b for more detail). With this will come new opportunities to work with porous media that more closely resembles field soil and as such the moisture content at the time of scanning is a crucial experimental consideration.

A Loamy Sand



B Clay loam

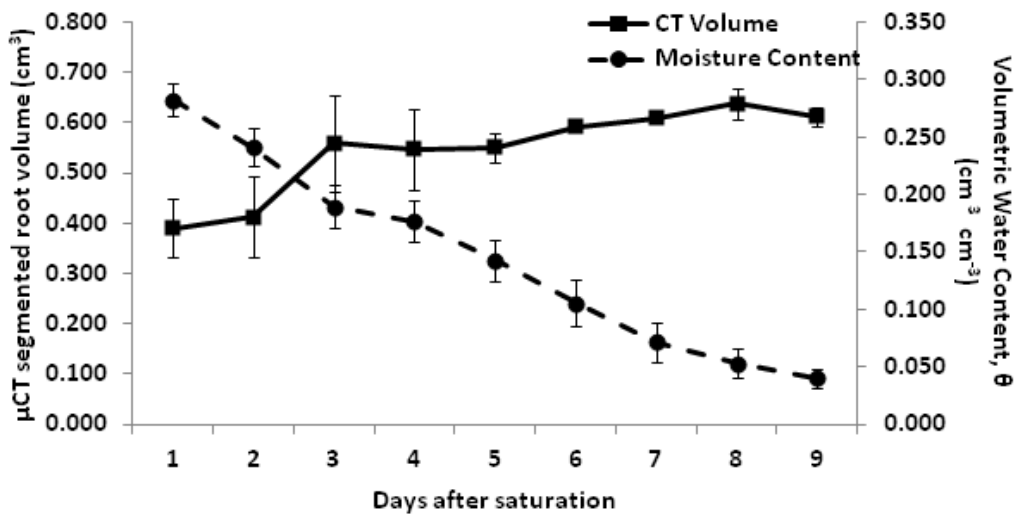


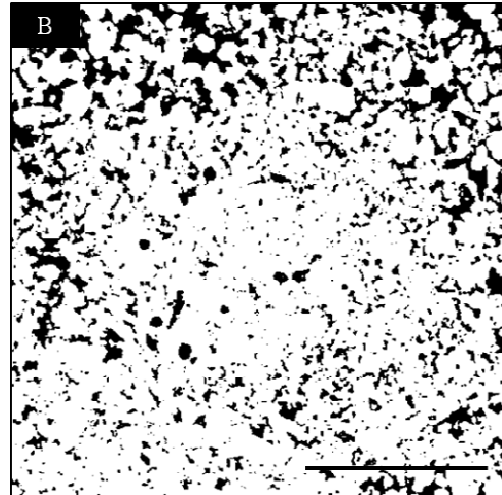
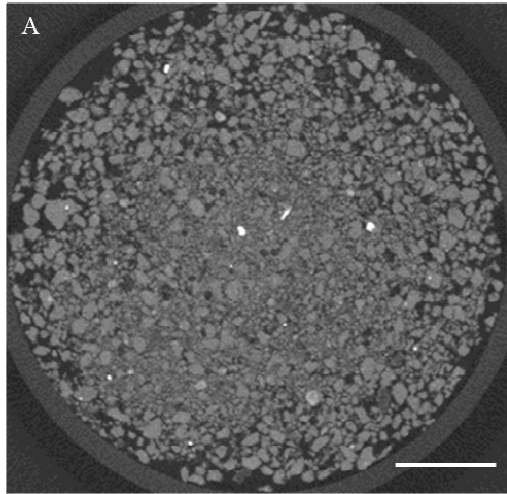
Fig. 3-7: X-ray CT segmented root volume and soil water content as a function of time for both a loamy sand (A) and clay loam soil (B). Soil volumetric water content (secondary axis) decreases with time in loamy sand and clay loam. Error bars represent standard error of the mean. Note significant differences between day one and three ($p < 0.01$); thereafter this was not significant for either soil type.

Here we have shown that the wetter the soil, the more difficult it is to segment roots in X-ray CT images of soils. However to dry soil prior to scanning introduces the risk of creating structural artifacts such as crack shaped pores which negatively impact on image processing. Further, drying leads to the possibility of drought stress in the plant. Our results show that

in order to optimize the image processing of segmenting root material in soil images it is preferable to scan soil columns approximately three days after saturation, which was -50 kPa for the loamy sand and between -1100 and -1200 kPa for the clay loam. We hypothesize in our experiment that this was approximately just below the field capacity moisture status of the soil.

Interestingly, further drying after three days did not appear to have any significant effect. Although we did record some minor increases in segmented root volume after seven days, visual examination suggested that the 'extra' root material that was segmented at this stage is most likely air at the root-soil interface as the effects of shrinkage take place (Carminati et al. 2009). Additionally, as the soils in this study were sieved < 2 mm but the resolution limited to 57 μm , the measurable porosities were actually greater in the loamy sand soil (11%) than in the clay loam (5%). The increased macroporosity in the loamy sand soil appears to have impacted on segmentation efficiency of roots from X-ray CT images, possibly because it provided less root-soil contact increasing root growth in the finer root fraction (<0.2mm) that was not visible at the X-ray CT scanning resolution (Fig. 3-8). Air-filled macroporosity significantly increased in both soil types between day one and day nine as expected (Fig. 3-9). The influence of air-filled macropores on segmentation means that sections of the macropore network can potentially be included as root material because of their similar X-ray attenuation.

Loamy Sand



Clay Loam

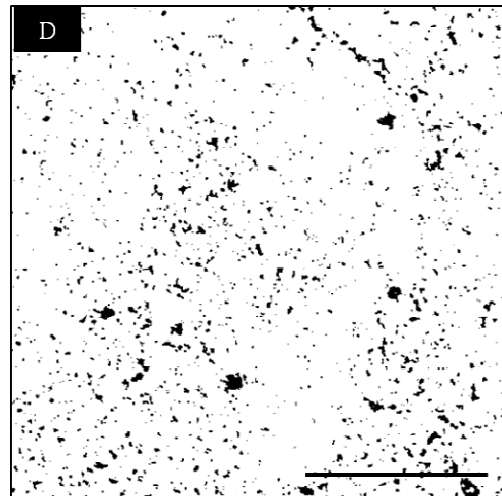
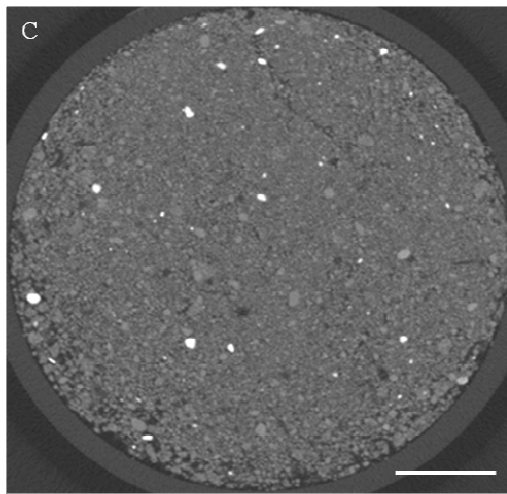


Fig. 3-8: Example X-ray CT images of horizontal slices through loamy sand (A) and clay loam (C) soil columns was used to analyse pore space through segmentation and binarisation (B and D). 1 pixel = 57.3 μm . Scale bars = 1 cm.

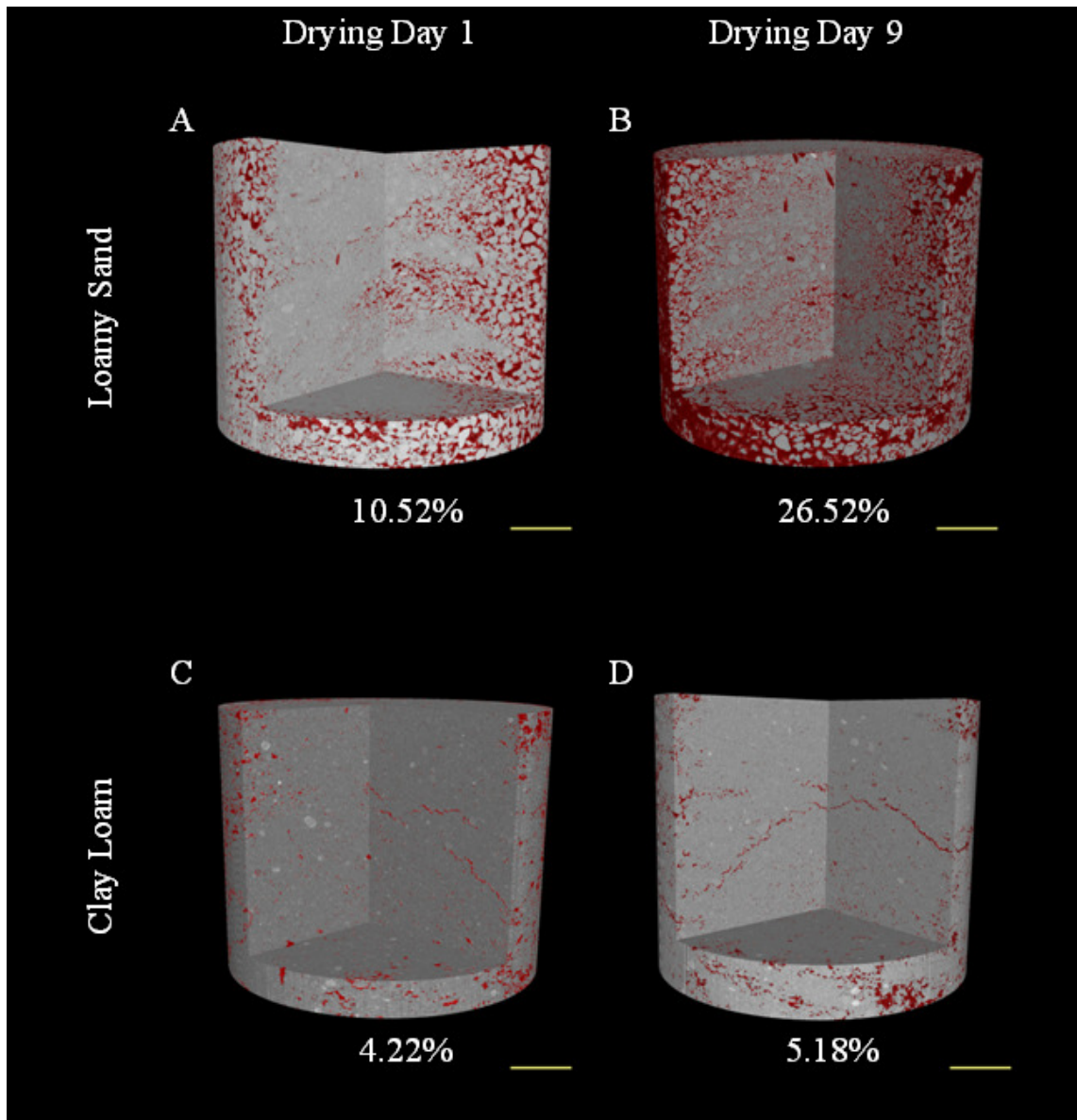


Fig. 3-9: Three-dimensional visualisations of air-filled macroporosity increasing with drying in loamy sand (A and B) and clay loam (C and D). Air-filled macroporosity has been segmented and false coloured red in the X-ray CT images with soil solids remaining in greyscale. Scale bar = 1cm.

As the hardware and software associated with X-ray CT develops in the future it can be expected that the correlation with root measurements obtained by other methods will improve. For example, the images recently obtained in Mairhofer et al. (2012) suggest that the very fine root volume that has to date been out of reach for X-ray CT studies will soon be able to be visualised. The regression values reported here for X-ray CT and WinRHIZO derived root measurements are similar to previously published work (Flavel et al. 2012a;

Tracy et al. 2012b; Tracy et al. 2012e). However when considering this one has to be mindful that while X-ray CT has its limitations, so do approaches like WinRHIZO. For example WinRHIZO has the potential to underestimate root volume as it calculates volume from average root diameter. This is because the average root diameter is biased toward the finer root fraction because the majority of most root systems are composed of fine roots (Ryser 2006). There is also a discrepancy between the standard WinRHIZO method and Tennant's method of measurement for root length (Wang and Zhang 2009; Zobel 2008), surface area and root diameter (Himmelbauer 2004).

A further potential impediment to the development of X-ray CT as a tool for root-soil studies, especially root phenotyping, is the potential of the X-rays to affect root growth. This is an area that has not been considered until very recently, however the advent of 4-D imaging (e.g. Tracy et al. 2012e) mean that it is probably more relevant now than ever before. Recently Flavel et al. (2012a) has also found that the effect of exposure of X-ray radiation to the plants did not have a significant effect on the roots measured by WinRHIZO. However as X-ray CT develops as a root phenotyping tool with faster scanning, the potential effects of X-rays on plant growth will need to be carefully monitored.

3.7 Conclusions

Here we highlight the importance of soil moisture content at the point of X-ray CT scanning as a critical parameter which significantly affects the performance of subsequent image processing steps used to acquire images of 3-D RSA. The optimum soil moisture content shown here was at, or just below, an approximated field capacity (i.e. 3 days drainage) and although not shown in this study this may vary between different soil types. Scanning

samples at moisture contents greater than this will lead to the total RSA being underestimated. Scanning up to a week after drainage should also be avoided as the drying process can cause cracks to form which leads to overestimating the total RSA after segmentation, not to mention potential negative influences on the plant caused by water stress.

3.8 Acknowledgments

This work was supported by an Engineering and Physical Sciences Research Council (EPSRC) Doctoral Training Award to SZ. The authors wish to acknowledge the help of Pedro Carvalho for his part in the WinRHIZO volume measurements.

4.0 Effects of X-ray dose on rhizosphere studies using X-ray Computed Tomography

4.1 Description and author contributions

This chapter is a reformatted version of a paper published in *PLOS One* (Zappala et al. 2013b) that describes the effect of X-ray dose on root growth and soil biota when visualising the rhizosphere using X-ray CT. X-rays have the potential to impact soil root development depending on the sensitivity of the plant and the total dose the sample receives.

Author contributions are as follows:

- Project supervision was provided by M. Bennett, T. Pridmore and S. J. Mooney.
- General advice and draft editing was given by S.J. Mooney and C.J. Sturrock.
- Image analysis assistance was provided by S. Mairhofer.
- Literature review, experimental design, practical work and data analysis was completed by J. Helliwell for soil microbe studies and S. Zappala for plant studies.
- Paper construction was completed by S. Zappala, J. Helliwell and S. Tracy.

4.2 Abstract

X-ray CT is a non-destructive imaging technique originally designed for diagnostic medicine, which was adopted for rhizosphere and soil science applications in the early 1980s. X-ray CT enables researchers to simultaneously visualise and quantify the heterogeneous soil matrix of mineral grains, organic matter, air-filled pores and water-filled pores. Additionally, X-ray CT allows visualisation of plant roots in situ without the need for traditional invasive methods such as root washing. However, one routinely unreported aspect of X-ray CT is the

potential effect of X-ray dose on the soil-borne microorganisms and plants in rhizosphere investigations. Here we aimed to i) highlight the need for more consistent reporting of X-ray CT parameters for dose to sample, ii) to provide an overview of previously reported impacts of X-rays on soil microorganisms and plant roots and iii) present new data investigating the response of plant roots and microbial communities to X-ray exposure. Fewer than 5% of the 126 publications included in the literature review contained sufficient information to calculate dose and only 2.4% of the publications explicitly state an estimate of dose received by each sample. We conducted a study involving rice roots growing in soil, observing no significant difference between the numbers of root tips, root volume and total root length in scanned versus unscanned samples. In parallel, a soil microbe experiment scanning samples over a total of 24 weeks observed no significant difference between the scanned and unscanned microbial biomass values. We conclude from the literature review and our own experiments that X-ray CT does not impact plant growth or soil microbial populations when employing a low level of dose (< 30 Gy). However, the call for higher throughput X-ray CT means that doses that biological samples receive are likely to increase and thus should be closely monitored.

4.3 Introduction

4.3.1 Dose to sample in X-ray CT Investigations

X-ray CT is a non-destructive imaging technique commonly used to observe and quantify aspects of the soil environment including plant root development (Flavel et al. 2012b; Karahara et al. 2012; Tracy et al. 2012a; Tracy et al. 2012d), fungal influences (Kravchenko et al. 2011; Martin et al. 2012), changes to pore structure (Munkholm et al. 2012) and the influence of microbial activity (Nunan et al. 2006). One often overlooked aspect of X-ray CT

studies involving soil is the influence of X-ray dose on the biological subject of interest (e.g. plants and animals) in these studies. For those studies that have included unscanned controls and reported X-ray dose or parameters enabling calculation of dose, there has been no discernible influence on plant root growth (Flavel et al. 2012b; Gregory et al. 2003b), fungal (Kravchenko et al. 2011) or microbial activity (Bouckaert et al. 2012). However, it should be noted that these samples have received relatively small X-ray dose to sample (i.e. < 1.5 Gy). With the advent of higher throughput X-ray CT techniques (Yang et al. 2011), which often involve multiple scans of the same sample over longer periods of time, total dose and therefore potential influence of the received dose will increase for individual samples. Stuppy et al. (2003) argued that X-ray CT was not feasible for living systems due to repeated exposure to X-rays. However, Dutilleul et al. (2005) stated that given the right precautions to limit and assess dose effects, X-ray CT is suitable for repeated observation of living organisms and particularly plants.

Dose is the quantity of energy absorbed by an object after exposure to radiation, making it a critical factor for consideration in X-ray CT studies and thus something that should be closely monitored (Gregory et al. 2003b; Johnson 1936b). However, many of the previously published X-ray CT studies do not report X-ray dose or provide insufficient information to calculate dose and its subsequent impact on plant growth or microbial activity. X-ray dose is estimated from tube current, voltage, exposure time and distance (r) from source, and has an exponential relationship to the distance between the X-ray source and the sample, as described by Gauss' Law. Dose decreases in air by $1/r^2$, making source to sample distance a critical determinant of intensity. This ratio was found to be true for energies between 50 kV and 150 kV and with currents between 1 μ A and 400 μ A (Stupian 2007), which is consistent

with most recent X-ray CT investigations involving soil and plants. Filters can influence the dose received by the sample, by progressively attenuating the highest and lowest X-rays, producing a narrower spectrum X-ray beam. Some filters composed of metals with low attenuation have little effect on dose. For example, Stupian (2007) observed no effect on radiation dose using a 1.6 mm aluminium filter. Furthermore sample composition and size play a key role in resultant doses. Common artefacts such as streaks and ‘shadowing’ behind the constituent of interest occur during photon starvation, when X-rays have insufficient velocities to penetrate certain sample constituents (Mori et al. 2012; Wildenschild et al. 2002). Likewise container composition and thickness can play a critical role in shielding samples from X-ray exposure (Yardin et al. 2000), and so need to be carefully evaluated before dose calculations can be applied.

The accurate calculation of dose is notoriously difficult due to the complex nature of radiation interaction with matter. For example, X-rays can interact with matter in several ways that are themselves difficult to predict. Primarily, X-ray attenuation by a material is determined by processes such as absorption, scattering, refraction and reflection, as well as magnetic interactions, although these are quite rare (Als-Nielsen and McMorrow 2011). In an effort to quantify the minimum dose required to acquire a tomographic image, Jenneson et al. (2003) describe a method for estimating these X-ray interactions, and thus dose to the centre of a sample as:

$$\text{Dose} = \frac{2.26E_x (\text{SNR})^2 f_c}{\rho\mu\eta\epsilon h} \exp\left[\frac{\mu d}{2}\right]$$

where E_x is the beam energy; SNR the signal-to-noise ratio; f_c the Compton factor (normalisation parameter reflecting photon energy after inelastic scattering (Als-Nielsen and McMorrow 2011)); ρ the density of the sample; μ the attenuation coefficient; η the detector efficiency; ε the planar pixel size; h the slice thickness; d the diameter of the reconstruction.

However, it is unusual for many of these measures to be reported in publications. In an effort to establish actual dose rather than an estimation, Stupian (2007) measured dose directly with a Radcal[®] 2026°C ionisation chamber meter. Whilst this is preferable as it gives a near-instantaneous reading of dose at the sample boundary, it relies on laboratories using X-ray CT scanners to have the required equipment. A simpler indication of dose can be made using freely available online calculators such as the Rad Pro Dose Calculator developed by McGinnis (2002-2009). Using X-ray empirical data from British Standard BS 4094-2:1971 (Recommendation for data shielding from ionizing radiation – Part 2: Shielding from X-radiation), all that is required for the estimation of sample dose is a basic understanding of the scanning parameters and filters utilised. When we sought to estimate dose from previously published work it was often necessary to infer sample to X-ray source distance from the scanners used because the actual distance was not provided. Furthermore filter thickness and material were commonly unreported, but have a large influence on the resultant X-ray exposure of samples.

4.3.2 *X-ray Dose and Plants*

4.3.2.1 *Growth of plants exposed to X-rays before germination*

X-ray studies involving seeds (imbibed and dry) from 70 plant species showed that exposure to moderate X-ray sources (0.01 Gy to 5 Gy) had a positive influence on shoot and root elongation (Johnson 1936b), as well as increased branching in Colorado wild potato (*Solanum jamesii*) (Johnson 1937). At higher doses (> 15 Gy), significant reduction of seed germination, shoot and root growth, budding, flowering and fruiting were identified in many plant species including field bean (*Phaseolus vulgaris*) (Genter and Brown 1941) and *Nicotiana tabacum* (Goodspeed 1929). Additionally, the influence of X-ray exposure on plant growth is highly dependent on plant type as well as variety. Sunflowers (*Helianthus annuus L.*) displayed negative growth effects when the imbibed seeds were exposed to doses greater than 33 Gy (Johnson 1936b). In field bean, doses as low as 26 Gy produced inhibition of germination and chlorophyll abnormalities (Genter and Brown 1941). However, much lower doses (0.05 Gy) impaired germination of date palm (*Phoenix dactylifera L.*), reduced DNA production, altered biosynthesis of plant pigment (chlorophyll a, chlorophyll b and xanthophylls) and negatively impacted root and shoot growth of the germinated seeds (Al-Enezi and Al-Khayri 2012).

4.3.2.2 *Growth of plants exposed to X-rays after germination*

In comparison to plants exposed as seeds, plants are less susceptible if exposed to X-rays post-germination. However, as noted previously the impact of X-ray exposure is highly variable and dependent on the plant type, variety and developmental stage. Dhondt et al. (2010b) reported growth inhibition in repeatedly scanned *Arabidopsis thaliana L.* seedlings,

which is consistent with the observations of Johnson (1936b) that X-ray exposure at seedling stage often had a negative influence on growth. However, no indication of X-ray energy was provided by Dhondt et al. (2010b), so dose could not be calculated from the manuscript. Many of the early experiments investigating plant-dose response involved doses that were several orders of magnitude greater than that considered lethal to humans, an acute dose of > 4 Gy (Kauffman 2003). However, these doses do not necessarily impact plant growth and microbial activity, as doses below 33 Gy showed little impact on plant growth (Johnson 1936b). Since 2003, most experiments have involved X-ray exposure equivalent to less than 1.5 Gy (Fig. 4-2), largely as a result of optimised detector response and improvements to acquisition methodologies (Mooney et al. 2012a).

4.3.3 *The influence of X-ray radiation on soil microbial populations*

The irradiation of soil could influence microbial communities through the direct ionisation of cells causing DNA mutation, and the indirect radiolysis of cell water creating damaging free radicals within extra- and intra-cellular fluids (Jackson et al. 1967). Free radicals can cause single or double stranded DNA breaks (McNamara et al. 2003), damaging future cell and plant development. Yet, to date there has been little work to assess the impact of X-ray radiation on soil constituents, with much of the focus being based on γ -rays due to its application in soil sterilisation procedures. Jackson et al. (1967) demonstrated that fungi are more sensitive to radiation than bacteria, with γ -irradiation doses as low as 10 Gy able to alter fungal populations. Responses to radiation continually change as enzymatic activity in soils aid recovery from acute doses, although sensitivity is dependent on a large range of physiological factors such as metabolic activity, organism size and complexity, and life-cycle stage (McNamara et al. 2003). A dose of 10 Gy of X-ray radiation is equivalent to 10 Gy of γ -

ray radiation since X-rays and γ -rays have the same radiation weighting factor, formerly known as quality factor, which is a measure of the expected biological impact of ionising radiation often used in radiation protection (Als-Nielsen and McMorrow 2011). For example, α -particles have a quality factor of 20, meaning on average α -particles are expected to produce 20 times the biological damage of X-rays or γ -rays. Furthermore soil moisture status plays a key role in indirect radiation damage. In wetter soils the ability to form free radicals through the radiolysis of water is increased, requiring a lower dose to harm microbial populations than dry soils (Jackson et al. 1967). These findings are consistent with those of McNamara et al. (2003), who in a meta-analysis of published results suggested that higher irradiation doses may be required to eliminate bacteria in dry soils. Due to the heterogeneity of soil systems, it still remains a challenge to accurately define the impact of radiation on soil-borne populations, although γ -ray doses reported as having impacts on soil constituents are an order of magnitude greater than any found in modern X-ray CT studies. To date, there is controversy surrounding the expected range of X-ray doses thought to impact plant and soil samples analysed via X-ray CT. We aimed to summarise key sources that report the influence of X-ray dose on plant or soil samples, particularly those involving X-ray CT. In addition, two experiments were completed that aimed to assess the potential effect of dose received during X-ray CT on (i) plant growth and (ii) soil microbial activity.

4.4 Materials and Methods

4.4.1 Data Collection

Web of Knowledge (Institute of Scientific Information) was utilised as a search database to find related publications with the search term “plant AND X-ray Computed Tomography” or “soil AND X-ray Computed Tomography”. This identified relevant literature dating back 30

years, 93 plant related publications and 346 soil related works. Papers from earlier than 1982 were found through hard copies at the University of Nottingham library (66 items).

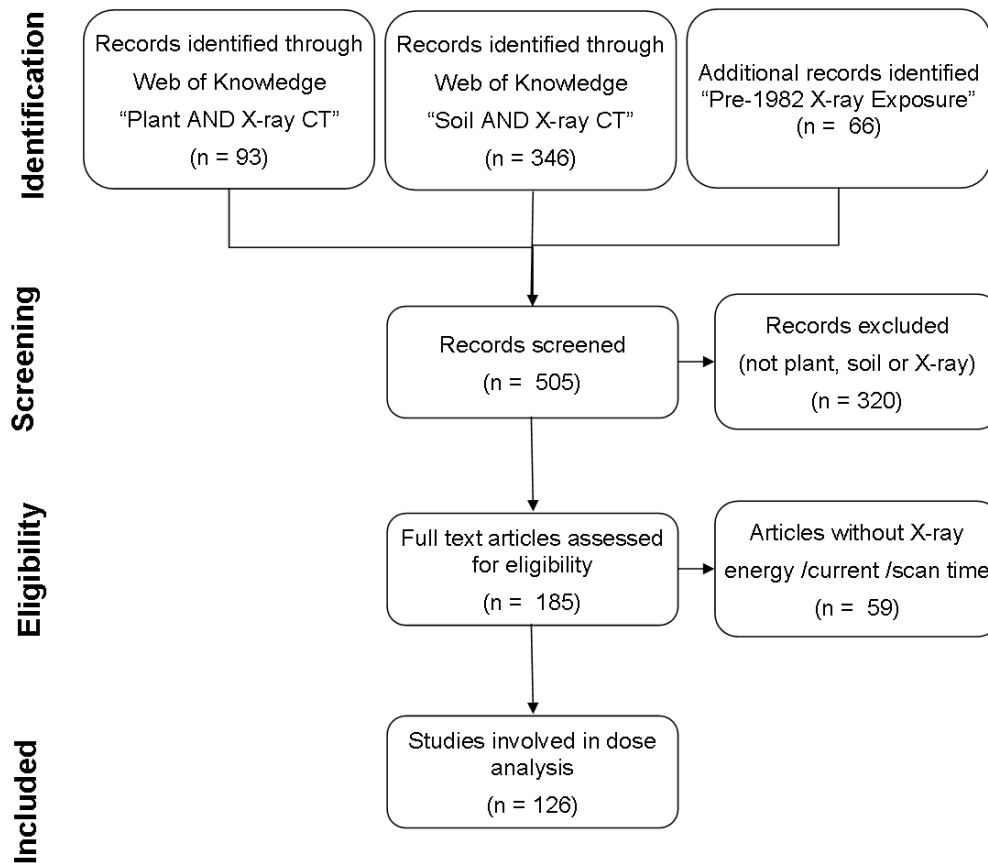


Fig. 4-1: Flowchart depicting meta-analysis protocol.

From the 505 publications identified during the search, 320 were excluded because they did not pertain to plants, soil, X-ray CT or X-ray exposure. From the remaining 185 documents, a database containing data for X-ray energy, current, distance between source and sample, filter utilised, scan timing, total exposure time, sample type and date of publication was created. The 59 publications without information about X-ray energy, current or scan time were excluded from analysis. Reported dose to sample was recorded if provided and compared to Rad Pro X-ray Dose Calculator results, to validate the assumptions made using

online tools. In total 126 publications were included in the dose assessment (Fig. 4-1). The range of calculated X-ray doses from each publication was included in Fig. 4-2.

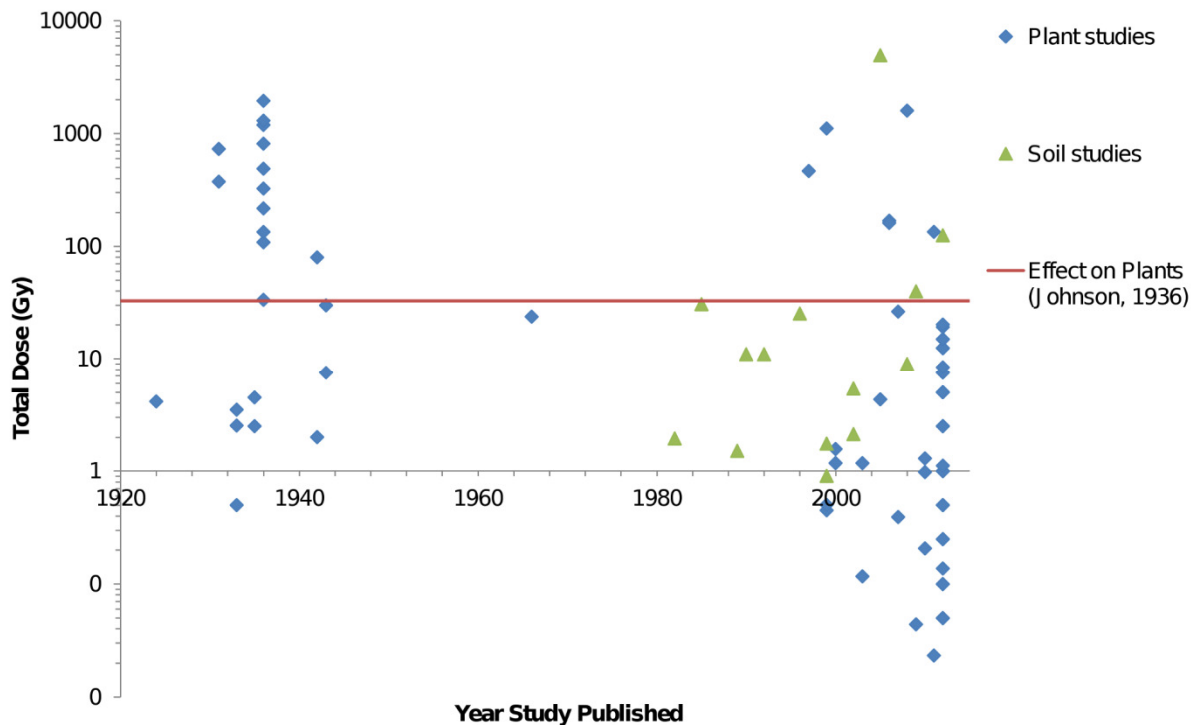


Fig. 4-2: X-ray dose in plant and soil studies. Dose was calculated in Rad Pro with X-ray parameters derived from literature. Most studies involve doses below the 33Gy threshold noted by Johnson (Johnson 1936b), below which she did not observe visible alteration of post-germination plant growth after X-ray exposure. Note the reduction in published studies between 1940 and 1980 and the clear rise in the 1990s.

4.4.2 Dose Calculations derived from the literature

Doses were estimated using the Rad Pro Dose Calculator. Due to restrictions of the dose calculator, X-ray doses were calculated assuming a 30 cm source-detector distance for industrial scanners and 100 cm distance for medical scanners. A 1 mm Be filter was used for the calculation if no data was given in the reviewed literature, as this was the minimum available shielding in the Rad Pro software and hence represents a worst case scenario.

Ultimately, all dose calculations are predictions, rather than actual measurements, due to the inherent randomness of X-ray energy and its interaction with materials. X-ray doses in

this manuscript are expressed as absorbed dose, which reflects the energy absorbed per unit mass for any radiation source and any material. The concept of absorbed dose was adopted by the International Commission on Radiological Protection (ICRP) to enable comparison of potential radiobiological impact from all types of radiation and a variety of sample types. Absorbed dose best meets the goals of the manuscript to provide a means for dose comparison in plant-soil studies involving X-ray CT. Effective dose cannot be used here as it includes a weighting for the sample composition, which is extremely heterogeneous amongst soil-plant-microbe samples, even in replicates using the same soil type and treatment.

4.4.3 *Soil and Plant Sample Preparation and Treatment*

Polypropylene columns (55 mm diameter, 150 mm height and 2.32 mm thick) were packed with sieved (< 2 mm) loamy sand field soil (Newport Series, FAO Class brown soil) at equivalent bulk density of 1.3 g cm^{-3} . The soil was saturated with deionised (DI) water and planted with seeds of *O. sativa* cv. Azucena after germination, when the coleoptile and radicle were approximately 1 cm long. Columns were kept at continuous saturation by providing DI water in a tray ponded with 2 cm of DI water. Rice plants were grown for 29 days on a 12 hour daylight cycle at 28°C daytime temperature and 20°C at night. Four hours before X-ray CT scanning, all columns were taken out of the water tray and not provided with any more water. For each column, gravimetric soil moisture content was measured before and after X-ray CT scanning to catalogue moisture loss. Four treatment columns were X-ray CT scanned daily for nine days to represent the full range of water contents expected during experimentation. Four control columns were treated in exactly the same way with the exception of X-ray CT scanning, to record any potential effects on plant growth incurred

during repeated X-ray exposure. These unscanned control plants were removed from the controlled growth chamber and placed in the dark for the duration of X-ray CT scan time to account for the influence of removal from the growth room.

Plant root systems of the treatment and control columns were destructively sampled on day ten by carefully removing the intact soil cores from the polypropylene columns. The soil-root columns were placed in water and the soil was carefully removed from the root systems. Immediately after cleaning the root systems, root volume was measured with WinRHIZO® 2002c (Regent Instruments, Canada) scanning equipment and software. The root volume measurements were further verified by water displacement (Pang et al. 2011).

4.4.4 *Soil and Microbe Sample Preparation and Treatment*

Four replicate columns (23 mm diameter, 70 mm height and 1.52 mm thick) were uniformly packed with a loamy sand (Newport Series, FAO Class brown soil), silty loam (Batcome Series, FAO Class chromic luvisol) and clay loam (Worcester Series, FAO Class argillic pelosol) to a dry weight bulk density of 1.2 g cm^{-3} , saturated with sterilised DI water and gravimetrically drained to field capacity. The water status of the columns was maintained at field capacity (determined by weight) throughout the investigation by sterile deionised water addition every 1-2 days. The columns were incubated for 24 weeks at 16 °C and a sub-section repeatedly scanned at weeks 0, 2, 4, 8, 16 and 24 of incubation. Scanned and unscanned soils were destructively harvested and microbial biomass carbon assessed at the end of the incubation period by chloroform fumigation extraction (Vance et al. 1987). A value of 0.45 was selected as the conversion coefficient of 'chloroform-labile' carbon to microbial biomass carbon (Jenkinson et al. 2004).

4.4.5 X-ray CT Imaging

A Phoenix Nanotom X-ray CT scanner (GE Sensing and Inspection Technologies, GmbH, Wunstorf, Germany) with a tungsten transmission target obtained 3-D images of each sample column including soil and root structure where applicable. Scan settings for the plant and microbial samples are detailed in Table 4-1. The spot size was approximately 3 μm (Mode Zero). Datos|x 2.0 (GE Sensing and Inspection Technologies, GmbH, Wunstorf, Germany) was used to reconstruct the X-ray CT images into a 3-D volume. Individual adjustments were made for minor sample displacement during scanning.

Table 4-1: X-ray CT scan parameters

Sample	kV	μA	Filter	Source to sample distance (cm)	Time each scan (min)	Total number of scans per sample	Voxel size (μm)
Rice in soil	110	320	0.2 mm Cu	21.5	73	9	57.3
Soil microbes	120	100	0.1 mm Cu	5.5	33	6	12.38

4.4.6 Statistical Analysis

Genstat 15.1 (VSN International Ltd., UK) was used to perform an analysis of variance, containing time and all possible interactions as explanatory variables. Normality was tested by interpreting the plots of residuals; in all cases the data were normally distributed, satisfying the assumptions underlying general analysis of variance.

4.5 Results

4.5.1 Literature analysis

In total, 126 publications were identified that related to plant and/or soil studies involving X-ray CT or X-ray exposure. Three papers (2.4% of total number analysed) using X-ray CT to

visualise soil and plant samples explicitly reported the estimated dose received by the sample. The required information for estimating dose using Rad Pro is i) X-ray energy, ii) X-ray current, iii) distance from source to centre of sample, iv) thickness and type of filter used and v) total exposure time. Fewer than 5% of the publications analysed in this research area contained all the required information to calculate the X-ray dose of each sample. This is primarily due to exclusion from the reports of source to sample distance or filters used. These studies and those with minimum information (X-ray voltage, current and total scan time) to estimate dose using the Rad Pro calculator are presented in Fig. 4-2.

The radiation dose in X-ray CT studies involving plants and microbes in soil generally are an order of magnitude lower than those considered to influence plant growth (33 Gy, Fig. 4-2). From our extensive literature search a value for the influence of X-ray dose on soil microbial populations could not be found, although we envisage that the value that soil microbial populations could sustain would be significantly higher than the 33 Gy suggested for plants. The majority of reported studies involved doses that were lower than the 33 Gy threshold considered to significantly influence plant growth. It should be noted that for plant species considered more sensitive to the influence of X-ray radiation exposure such as field bean (Genter and Brown 1941) and date palm (Al-Khayri et al. 2012), the thresholds for negative influence on growth were 26 Gy and 0.05 Gy respectively.

Prior to 1950, studies investigating the effect of X-ray exposure on plants involved direct exposure of the seed or plant to X-ray radiation (Fig. 4-2). After 1945 there was a sharp decline in studies relating to X-ray dose on plants that included the required information to calculate dose. With the advent of X-ray CT developed by Hounsfield (1972), studies

involving soil microorganisms were undertaken as the possibility for non-destructive imaging of the physical structure of soil became possible. Additionally, X-ray CT was adopted for visualisation of plant root development in soil. Since 2008, technological advancements in X-ray detectors and data storage have contributed to the increase in the number of plant and soil investigations that include the use of X-ray CT.

4.5.2 *Impact of Repeated Scanning on Plant Roots in Soil*

For the study involving rice roots growing in soil, no significant difference was found between scanned and unscanned number of root tips, root volume and total root length measured in WinRhizo (Fig. 4-3). Scanned root systems had an average of 4512 root tips and unscanned root systems had an average of 4571 root tips ($P = 0.928$). Average root volume was 0.765 cm^3 for scanned plants and 0.718 cm^3 for unscanned plants ($P = 0.752$). Total root length averaged 596 cm and 589 cm for scanned and unscanned plants respectively ($P = 0.960$). The dose received by each column for a single scan was 1.4 Gy, equating to a total dose per column of 13 Gy over the ten day investigation (nine scans). Results are consistent with previous studies (Flavel et al. 2012b; Gregory et al. 2003b), who found no significant alteration to root development in cereals at doses of 0.7 Gy and 1 Gy respectively.

4.5.3 *Impact of Repeated Scanning on Microbes in Soil*

The soil microbe experiment involved scanning over a total of 24 weeks with six scanning sessions. No significant difference was found between the scanned and unscanned microbial biomass values after 24 weeks (Fig. 4-4; $P = 0.975$). Interestingly mean biomass values were consistently higher in unscanned compared to scanned treatments across all soil textures (mean values of 451.30 and $416.66 \mu\text{g C g}^{-1}$ soil in the clay loam, 167.57 and $154.32 \mu\text{g C g}^{-1}$

soil in the silty loam and 108.71 and 104.19 $\mu\text{g C g}^{-1}$ soil in the loamy sand for unscanned and scanned respectively), although none were statistically significant. Total dose received by each sample was 23 Gy over six scans.

4.6 Discussion

Hypotheses about the hormetic effects of X-ray radiation on plant productivity drove initial investigations into the impact of X-ray dose on crops such as wheat (Cattell 1931) and potato (Johnson 1937). There was agreement that large X-ray doses impaired plant growth and development; the disagreement arose surrounding the beneficial effects of moderate X-ray doses (Johnson 1936a). Eventually, researchers found that any improvement in growth rate or yield observed in very young plants dissipated at later growth stages (Johnson 1936b). This lack of financial benefit for crops could explain the decline in interest regarding the effects of X-rays on plants that occurred in the late 1930s (Fig. 4-2). In the late 1980s/early 1990s, there was a resurgence of use of X-rays in plant and soil research. This likely occurred due to development of X-ray CT as a 3-D visualisation tool. X-ray CT provided another option for researchers to visualise plant root architecture in soil as well as soil structure and pore geometry.

As X-ray CT becomes more widely adopted in the plant and soil sciences, the demand for greater throughput, larger samples (to analyse field soil cores) and higher resolution will intensify. Advancements in detector technology, computer processing and data storage could both increase and decrease dose received by samples scanned using X-ray CT. For example, reduced scan times will mean that single samples are subject to less X-ray dose per scan. However, less total X-ray scan time means that researchers can complete a set of

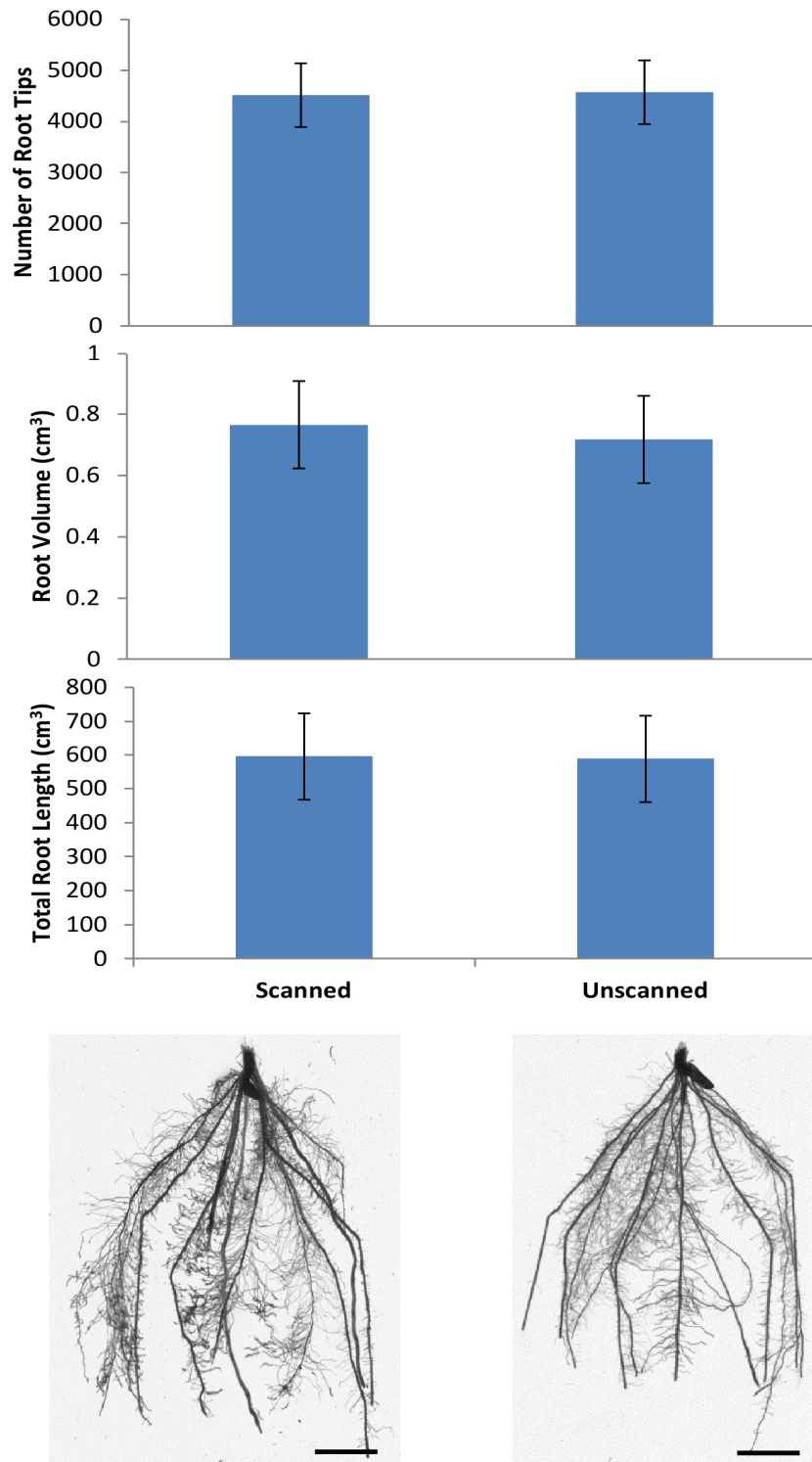


Fig. 4-3: Impact of X-ray CT on rice root growth. Twenty-eight day old rice plants grown in soil were X-ray CT scanned daily for nine days. After day nine of scanning, root systems were destructively sampled via root washing and root volume was measured in WinRHIZO. Repeated exposure to X-rays had no significant effect on the number of root tips, root volume or total root length of rice grown in soil when compared to unscanned plants. Error bars depict standard error of the mean (n=4). Total dose received by each sample was 13 Gy over nine scans. Scale bar represents 1 cm.

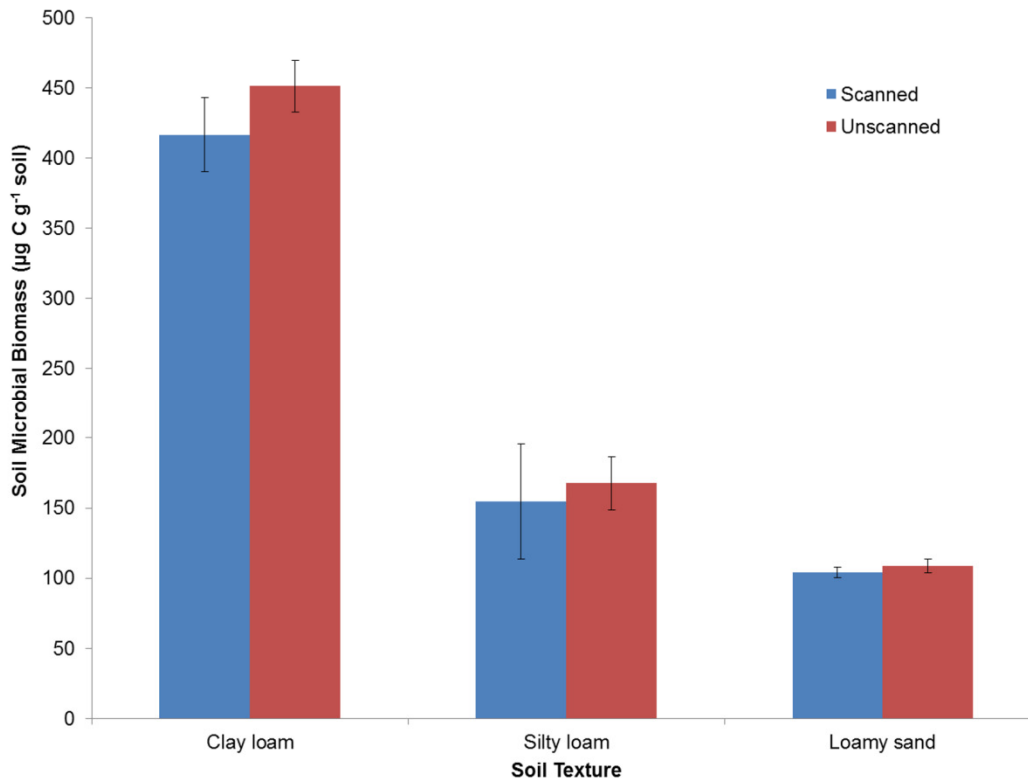


Fig. 4-4: Influence of X-ray CT on soil microbial biomass after 24 weeks of incubation. Microbial biomass was measured with chloroform fumigation and compared between X-ray CT scanned columns and unscanned controls. Total dose received by each sample was 23 Gy over six scans. Error bars depict the standard error of the mean of four replicates.

samples in the time it would have taken for one sample. We envisage that future experiments are more likely to include repeated scanning of the same sample and thus have a total dose much higher than that of a single scan. This is especially true for experiments analysing root phenotypes or soil structural development that investigate changes in these systems over time. Therefore we suggest that experimental studies utilising X-ray CT report the dose received by the sample, or at least the constituent parameters in order to allow others to make informed decisions as to the dose that experimental samples have received.

At present, those studies that have included unscanned controls have reported no significant influence of X-ray CT scanning at moderate energy levels and relatively small (< 30 cm) source to sample distances. However, the vast majority of publications do not

mention dose or include unscanned controls in their experiments. This is not to say that unscanned controls were not included in the experiments, but they were unreported in the published articles. Therefore, unscanned controls are important as a verification method to ensure that the X-ray parameters and resulting dose are not significantly impacting the experimental treatment. Our recent studies have shown that a typical X-ray CT experiment with repeated scanning of the same sample does not have a significant negative impact on plant root development (Fig. 4-3) or microbial activity (Fig. 4-4) in soil.

The main potential contributor to differences between scanned and unscanned plants may be removal from growth chamber if unscanned plants are kept under controlled conditions whilst the scanned plants are not in the growth chamber. For example, total scan time can amount to several hours that a planted sample is removed from the growth room, so in turn less hours photosynthesising. Furthermore, fluctuations in temperature within the scanning chamber itself may induce changes in the moisture content of samples. To minimise this time outside of controlled growth conditions shorter scan times are encouraged, which are becoming increasingly feasible through technological development. However, this is often at the expense of decreased image quality, which may impact on feature identification in the subject of interest. Hence there is a trade-off between scan time and image quality optimisation, which varies dependent upon experimental aims. Alternatively where practical, another largely unexplored option is to set the day/night cycle opposite to real-world conditions, so that during working hours scanning can be carried out during the night cycle for the plant. To be confident that other differences between the X-ray CT laboratory conditions and the field/glasshouse/growth room (e.g. light intensity, humidity, temperature, O₂ / CO₂ levels) are not affecting plant growth, workers could consider leaving

some unscanned controls in the usual place of growth and removing other unscanned control samples. By taking both sets of samples to the X-ray CT laboratory for the duration of the scan time, before returning again to the field/ glasshouse/ growth room, the potential influence of X-ray exposure on plant growth and microbial populations is reduced.

To minimise received dose, samples could possibly be moved further from the source, total scan time can be reduced, or lower energies can be used. However these options all have implications for the quality of the X-ray CT image produced. Due to the relationship between the distance of the sample and the X-ray source, there is a recognised trade-off between the achievable image resolution and received dose. Moving a sample further from the source reduces the magnification of the image received at the detector, and thus limits the achievable image resolution. Additionally, contrast within the image can deteriorate when trying to minimise dose because contrast is dependent on the energy, wavelength and type and thickness of filters used.

A more complicated aspect of assessing the impact of X-ray dose on living samples is that organisms have highly variable responses to exposure. In the case of plants, Al Khayri et al. (2012) found relatively small X-ray exposures of 0.25 Gy had an influence on biochemical aspects of date palm (*Phoenix dactylifera* L.) development (i.e. DNA and pigment synthesis), as well as a negative influence on root and shoot development found by Al-Enezi et al. (2012). Alternatively, Johnson (1936b) found that high X-ray doses (33 Gy) had little or no observable effect on Sunflowers (*Helianthus annus* L.). This variability further validates the need for incorporation of unscanned controls in all X-ray CT experiments. However it is worth noting that the dose currently utilised to γ -sterilise soils (a method often used as a

highly successful biocide and preferable to other sterilisation procedures such as autoclaving due to having a lessened effect on soil chemical and physical properties) is 20 000 - 70 000 Gy (McNamara et al. 2003). This is three orders of magnitude higher than the largest doses reported in X-ray CT investigations to date. Likewise, doses required for routine sterilisation of foodstuffs and medical appliances are ca. 25 000 Gy (Yardin et al. 2000).

4.7 Conclusion

This study supports the use of X-ray CT as a means of quantifying root and soil traits, as the results show no significant impacts on observable growth parameters due to X-ray exposure at the levels used in the study. The advantage of using X-ray CT to non-invasively characterise the 3-D geometry of soil and roots is reinforced by the insignificant impact of X-rays on soil biota and root systems in our two repeated scanning investigations. The doses received by individual samples and the total dose accumulated over the period of repeated scanning were within a range of accepted values that should not significantly influence growth (< 33 Gy). Of particular importance is the fact that at the settings used, multiple scans on the same sample appear to have no effect on root phenotypic traits, confirming the appropriateness of X-ray CT for high-throughput investigations given the right scan settings. As this field of research evolves, it is anticipated that further information can be gained from a greater number of researchers reporting dose received by samples and highlighting any significant alterations to expected growth patterns.

5.0 Phenotyping of OsAUX1 related root system architecture (RSA)

5.1 Introduction

As part of what has been termed the “Second Green Revolution” (Lynch 2007), there has been a relatively recent move toward understanding and manipulating plant root architectures to increase yield and ensure plant adaptation to climate severity and nutrient poor soils (Wollenweber et al. 2005). For this, new techniques are required that link laboratory and field-derived information to incorporate data gleaned from molecular biology about RSA development with field studies that will inform the genetic influences on yield and plant adaptation to abiotic stresses (Zhu et al. 2011). These efforts to link lab and field investigations begins with lab-based study of RSA development performed with plants grown in soil to obtain effects from soil chemistry, soil morphology and physical properties such as compaction (Tracy et al. 2012e). Soil presents a specific challenge for observation of root development because of its opacity.

X-ray CT has been one technique used to analyse root development in soil and provides the ability to visualise roots, water and the soil matrix simultaneously and repeatedly over time. This opens new avenues for in situ investigation of plant water uptake, nutrient uptake and root development (Hinsinger et al. 2009). Further understanding of root architecture, root growth and soil properties at the microscale have become possible with X-ray CT and standardised image analysis methods (Mooney et al. 2012a). Some researchers have increasingly utilised non-destructive techniques such as Nuclear Magnetic Resonance (Iyer-Pascuzzi et al. 2010), Magnetic Resonance Imaging (Stingaciu et al. 2013), Positron Emission Tomography (Nagel et al. 2009) or techniques involving non-soil media in 3-D (Clark et al. 2011) to capture 3-D root development over time. X-ray CT provides the best opportunity to

observe root growth in soil because it is non-destructive and utilises the differences in X-ray absorption to simultaneously visualise roots, soil organic matter, minerals and air/water-filled pores (Perret et al. 2007).

Technological developments in X-ray CT now allow soil and plant scientists to visualise the spatial and temporal development of plant roots in soil at scales of approximately 500 nm (Tracy et al. 2010). Before the introduction of microscale X-ray CT, some workers scanned plant and soil samples in medical grade scanners that were developed for imaging of the human body, which produced low resolution (mm scale) images that made root material difficult to distinguish from the growth medium (Gregory et al. 2003b). Under the right circumstances, X-ray CT allows repeated measurement of root and soil properties over time (Tracy et al. 2012c) and is a good candidate for observing specific root traits related to nutrient acquisition.

This work focuses on the RSA that can influence phosphorus (P) uptake. Root angle and root responses to gravity have been of particular interest for studies involving P uptake and its relationship to root architecture is (Ge et al. 2000; Lynch and Brown 2001). Phenotyping gravitropism in soil has been tackled in the field and in the lab (Zhu et al. 2011). Field techniques that capture 3-D root angle traits primarily include shovelomics (Trachsel et al. 2011) and colander/basket-based measurement (Oyanagi 1994). Lab and glasshouse-based work uses rhizotrons or soil boxes (MacMillan et al. 2006), however the opacity of soil has led researchers toward the use of transparent non-soil media found in hydroponic or gel-based systems (Downie et al. 2012; Hargreaves et al. 2009). This work aimed to evaluate X-

ray CT as a technique to quantify gravitropism in the *OsAUX1* knockout mutants generated by Parker (2010) when they are grown in soil.

5.2 Materials and Methods

Four replicates were planted for each line (wildtype, *Osaux1-1* and *Osaux1-2*). Seeds were prepared as described in Section 2.1 and grown under conditions described in Section 2.2 for four weeks. The germinated seeds were planted in columns containing sandy loam (Newport) soil as described in Section 2.3. One plant each of wildtype and *Osaux1-2* died during the experiment, leaving three replicates for these treatments. Each column was scanned by X-ray CT weekly for four weeks; Section 2.8. The scanner settings were 130 kV, 240 μ A, 1080 projections, 73 min total scan time, sample-source distance of 22.7 cm, 27.3 μ m voxel size with a 0.1 mm copper filter. The relatively long scan time (73 min) was used to obtain the best quality X-ray CT images for the sample size. Columns were allowed to drain for two days before scanning (Zappala et al. 2013b). Each sample received an approximate X-ray dose of 5.9 Gy over the four scans (1.5 Gy each scan) as estimated by the RadPro X-ray Device Dose-Rate Calculator (McGinnis 2002-2009). Root systems were segmented from the X-ray CT generated images using VGStudioMax and measured with VGStudioMax and RooTrak (Mairhofer et al. 2013) software (Section 2.8.3). Destructive measurement of the root washed RSA is described in Section 2.9.

5.3 Results

5.3.1 3-D root volume and comparison of VGSM and RooTrak

The root volume of each root system segmented from X-ray CT images was measured by VGStudioMax (VGSM) and RooTrak (Mairhofer et al. 2012) software. There were no significant differences in root volume between the genotypes. The root systems significantly

($P < 0.001$) grew each week (Fig. 5-1). In week two and three, *Osaux1-2* had a larger root volume than the other lines.

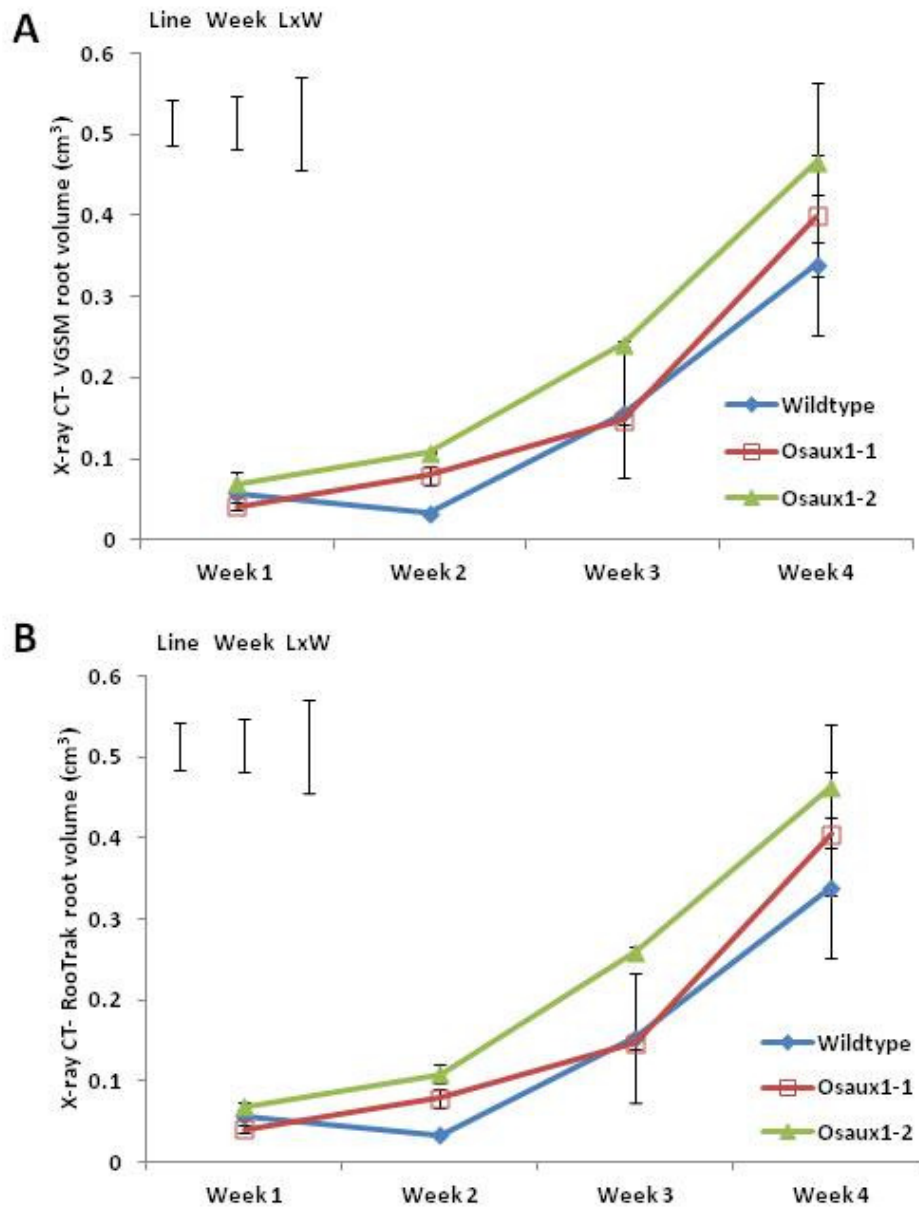


Fig. 5-1: Root volume measurement of root systems segmented from X-ray CT images as measured by VGStudioMax (VGSM) in A and RooTrak (Mairhofer et al. 2012) software in B. Error bars represent standard error of the mean. Least significant difference is represented by bars in the top left.

The root volumes segmented from X-ray CT images were measured using both VGSM and RooTrak software. The resulting root volume measurements were compared to ensure that

they provided sufficient agreement when quantifying 3-D RSA (Fig. 5-2). RooTrak provides information about 3-D RSA that is not obtainable through VGSM such as centroid Z-value, convex hull volume and maximum depth (Section 2.8.3). There was excellent agreement between RooTrak derived root volumes and the VGSM root volume calculation at each of the weekly scan points (Fig. 5-2). This was true for all of the rice lines.

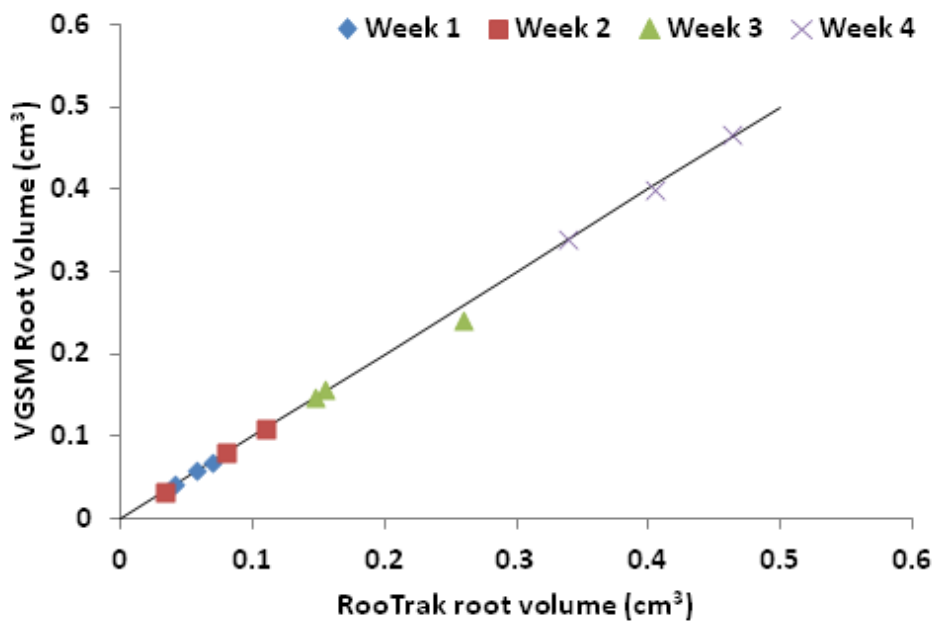


Fig. 5-2: At all weekly measurement points, VG StudioMax 2.0 (VGSM) and RooTrak 0.2 (Mairhofer et al. 2012) produced similar results for root volume. R-squared values for weeks one, two, three and four were 1.0, 0.9998, 0.998 and 0.9959 respectively.

5.3.2 X-ray CT derived indicators of root angle

As seen in agar grown plants under gravistimulation, soil grown *Osaux1-1* and *Osaux1-2* display a shallow root angle in relation to wildtype (Fig. 5-3). This was further reinforced by centroid Z measurements which represent the root volume distribution with depth and were a useful indicator for gravitropism where larger values indicate a deeper root distribution. In general, *Osaux1-1* had a significantly smaller centroid Z value ($P = 0.006$) and thus shallower overall RSA than wildtype and *Osaux1-2* (Fig. 5-4). In week one, wildtype had

the lowest centroid Z. At all subsequent scanning points, *Osaux1-1* had the smallest centroid Z value.

Excluding week one, wildtype and *Osaux1-2* had similar vertical root volume distribution. At week two, there was no significant difference in the centroid of any of the lines ($P = 0.386$). Between week one and four, wildtype centroid Z ranged between 0.38 cm and 1.87 cm, *Osaux1-1* between 0.58 cm and 1.14 cm and *Osaux1-2* between 0.957 cm and 1.59 cm. Wildtype displayed a more linear increase in centroid Z than either of the knockout mutants, which had more of an exponential increase in centroid Z (Fig. 5-4).

Not only does OsAUX1 influence the vertical distribution of the entire root mass, a relationship between OsAUX1 and the maximum extent of the root system was also identified. Maximum root system depth was significantly ($P = 0.010$) different between the genotypes (Fig. 5-5 A). At week two and three, *Osaux1-1* had significantly shallower maximum depth than wildtype and *Osaux1-2* ($P = 0.010$). Over time, maximum depth in wildtype ranged between 1.6 cm and 4.6 cm. *Osaux1-1* had maximum depth between 0.9 cm and 4.5 cm. The depth of the *Osaux1-2* root system was between 1.7 cm and 4.9 cm.

The horizontal extent of the root systems (minimum enclosing circle radius) was significantly wider in week two and week three ($P = 0.021$) for the two knockout mutants, which is indicative of the agravitropic nature of their RSA (Fig. 5-5 B).

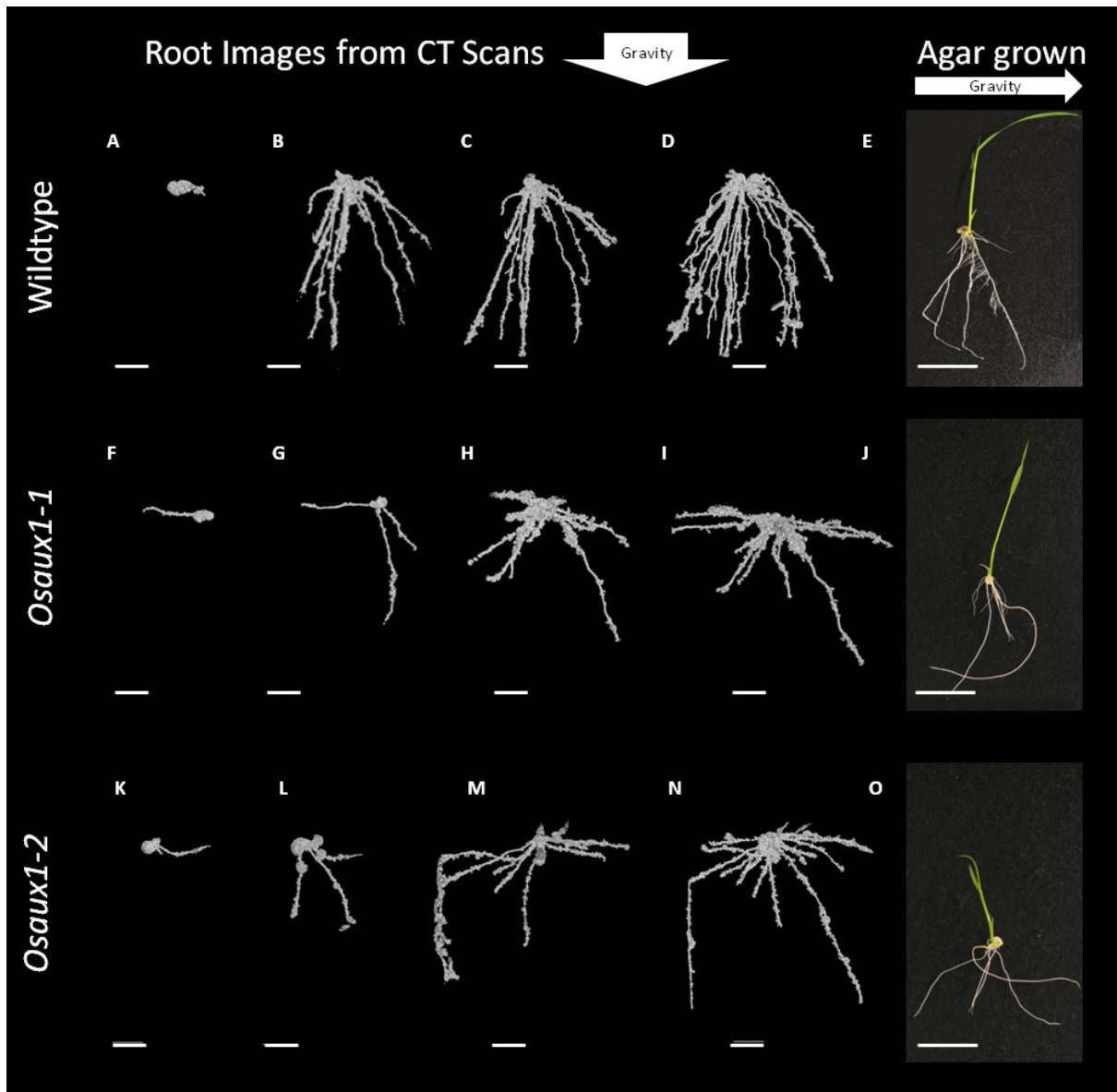


Fig. 5-3: Comparison of root angle from X-ray CT images of soil grown wildtype (A to D), *Osaux1-1* (F to I) and *Osaux1-2* (K to N) plants and those gravistimulated on agar (plate E, J and O). Gravity vectors are provided by white arrows. Scale bar represents 2 cm.

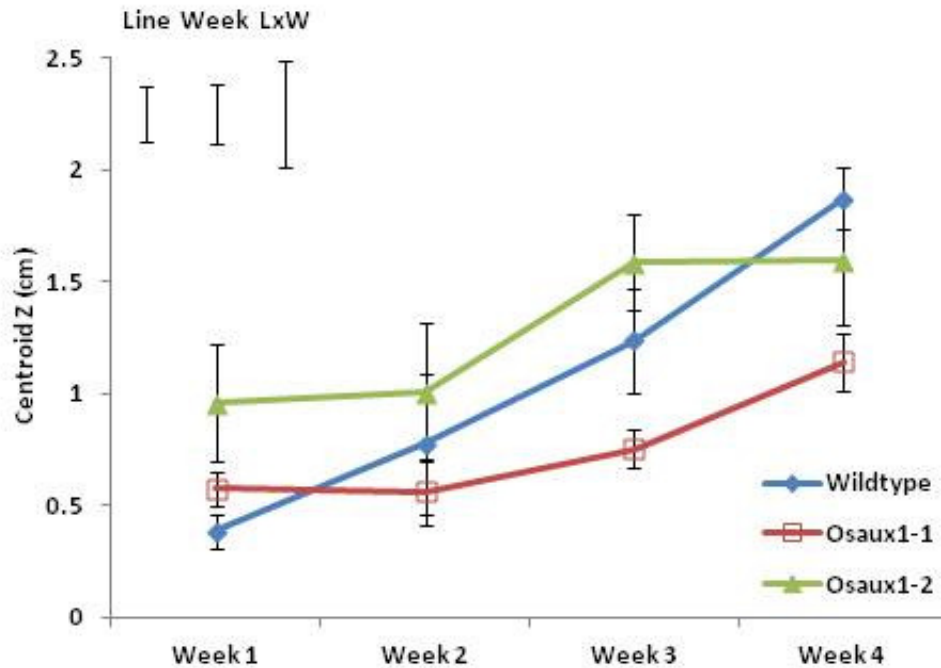


Fig. 5-4: Centroid Z-value for wildtype, *Osaux1-1* and *Osaux1-2* where larger centroid Z indicates a deeper distribution of root volume. Error bars represent standard error of the mean. Least significant difference is represented by bars in the top left.

Wildtype had a much larger range of width values, which is consistent with introduction of new crown roots and was between 0.548 cm and 2.412 cm. The mutants had a more consistent enclosing circle radius from week two to week four, which indicates an agravitropic habit very early in root system development. *Osaux1-1* extended between 0.87 cm and 2.6 cm from week one to week four. Over the experimental period, the *Osaux1-2* root system grew from 1.3 cm to 2.6 cm in width.

5.3.3 Non-root angle related RSA measured by X-ray CT

Three dimensional root distributions were quantified using the convex hull volume, which represents the most conservative soil volume explored by the extent of the root system. Convex hull volume can be coupled with root volume to understand the solidness of a root system by quantifying the amount of root occupied soil volume (convex hull) that actually

contains roots (root volume). Surface area provides an estimate for potential root-soil contact.

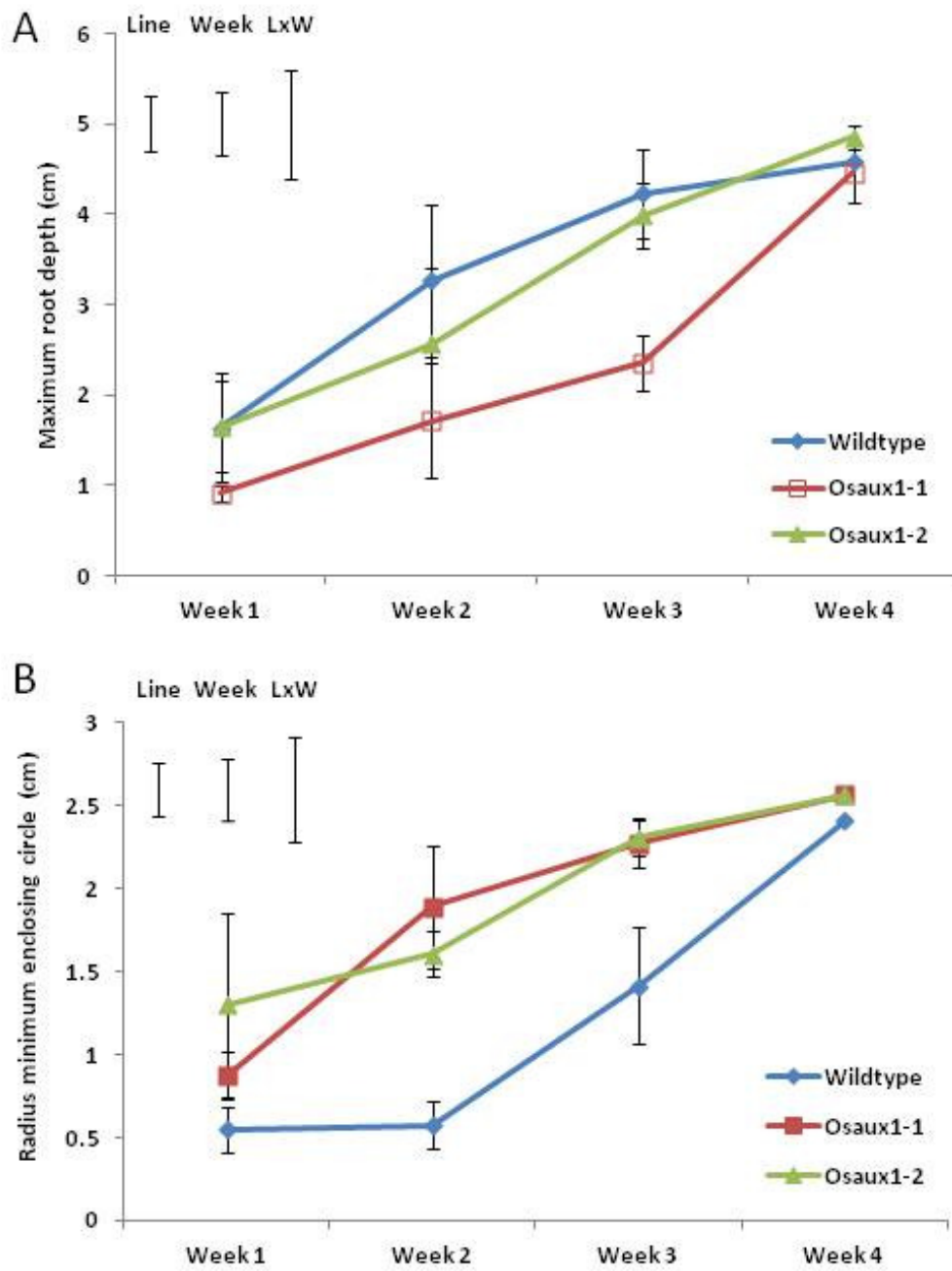


Fig. 5-5: Weekly measurement of maximum root system depth (A) and the minimum enclosing circle (root system width) (B) for wildtype, *Osaux1-1* and *Osaux1-2* obtained from X-ray CT images of soil grown plants. Error bars represent standard error of the mean. LSD represented by bars top left.

Convex hull volume was not significantly different between the genotypes (Fig. 5-6 A). From week one to week four, convex hull volume increased from 9.46 cm³ to 99.4 cm³ for

wildtype. *Osaux1-1* convex hull volume ranged between 5.4 cm³ and 89.4 cm³ and *Osaux1-2* began with the largest convex hull volume at 21.9 cm³ and in week four was 88.3 cm³.

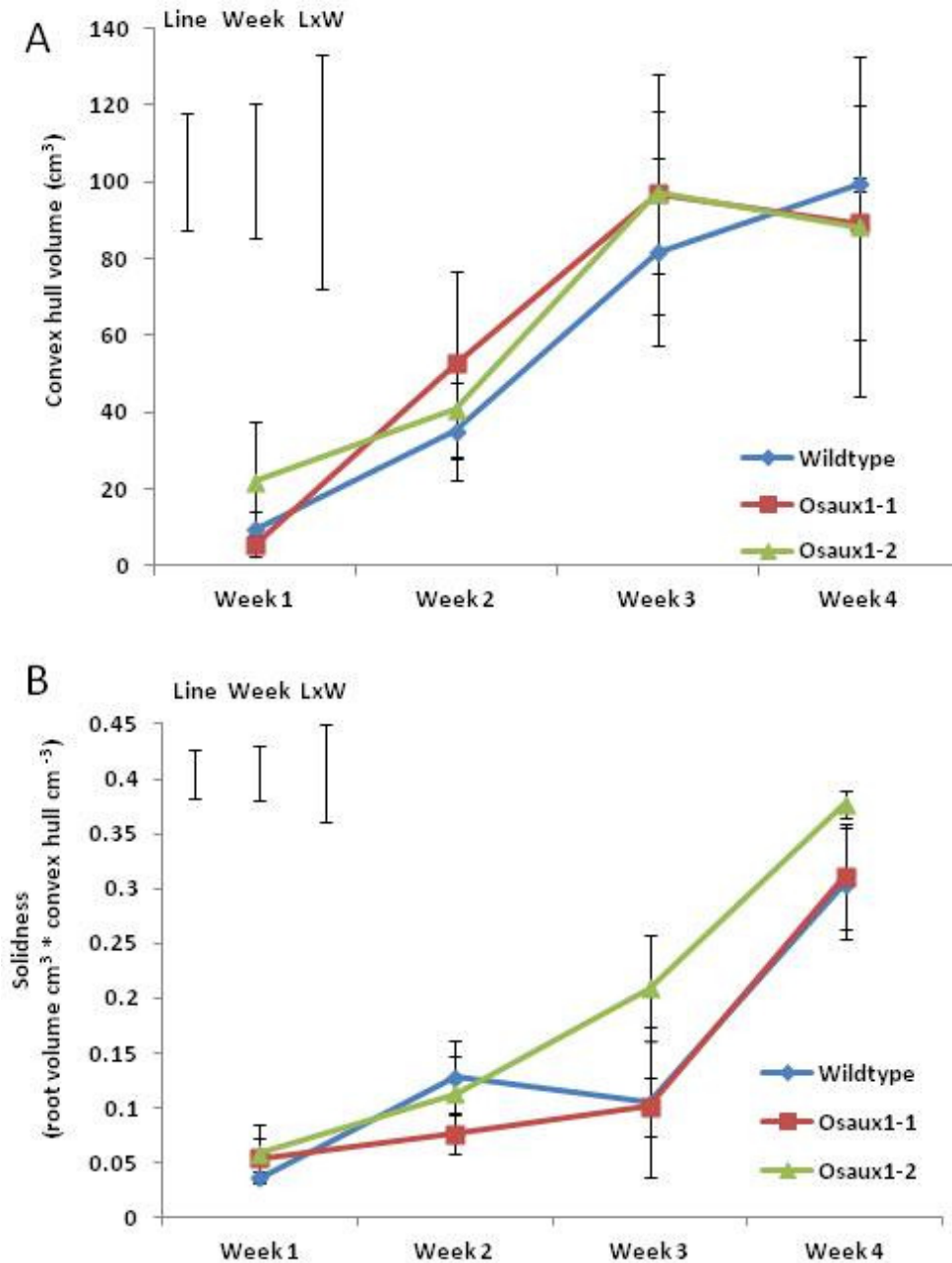


Fig. 5-6: Convex hull (A) and root system solidness (B) derived from X-ray CT. Error bars represent standard error of the mean. Least significant difference is represented by bars in the top left.

There was no significant difference in root system solidness between the three lines ($P = 0.698$) for all weeks (Fig. 5-6 B). In week one, root volume represented between 3.6%

(wildtype) and 5.8% (*Osaux1-2*) of the convex hull volume. By week four, the root systems occupied approximately 35% of the potentially explored soil volume (convex hull). This similarity in solidness at week four provides a justification for assessing the influence of OsAUX1 on P uptake on four week old plants.

Root system surface area was not significantly different between the three lines (Fig. 5-7). In week four, all root systems had similar surface areas ranging between 30.6 cm² for wildtype and 33.5 cm² for *Osaux1-2*.

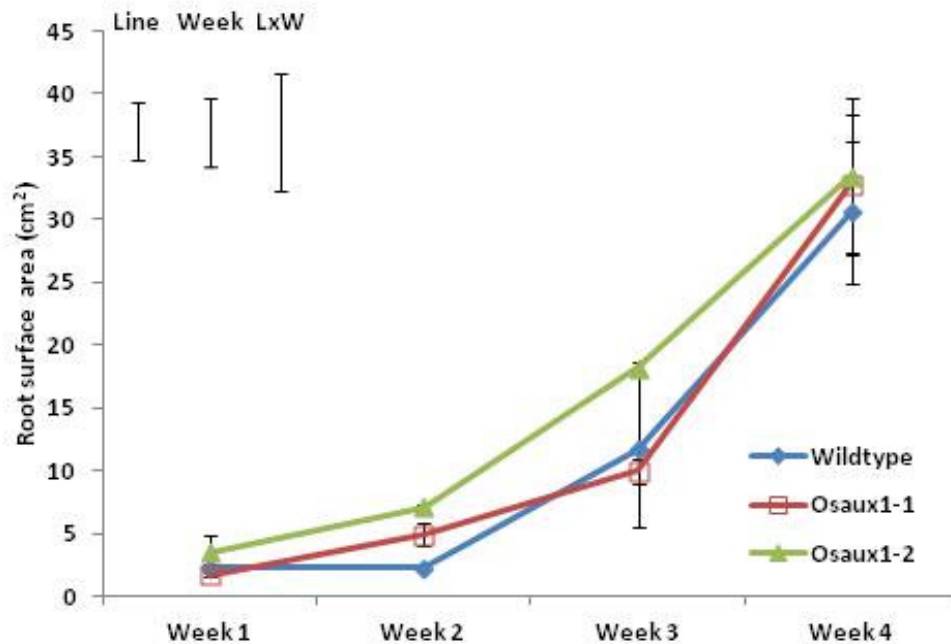


Fig. 5-7: Root system surface area measured by RooTrak from X-ray CT derived images. Error bars represent standard error of the mean. Least significant difference is represented by bars in the top left.

5.3.4 Comparison of X-ray CT and WinRHIZO analysis

To validate the root volumes derived from X-ray CT images, they were compared to the destructively sampled volumes measured in WinRHIZO. Discrepancies between X-ray CT and destructively sampled volume measurements are highlighted in Fig. 5-8. R-squared was 0.824 and considered sufficient to justify comparison of WinRHIZO and X-ray CT derived measurements.

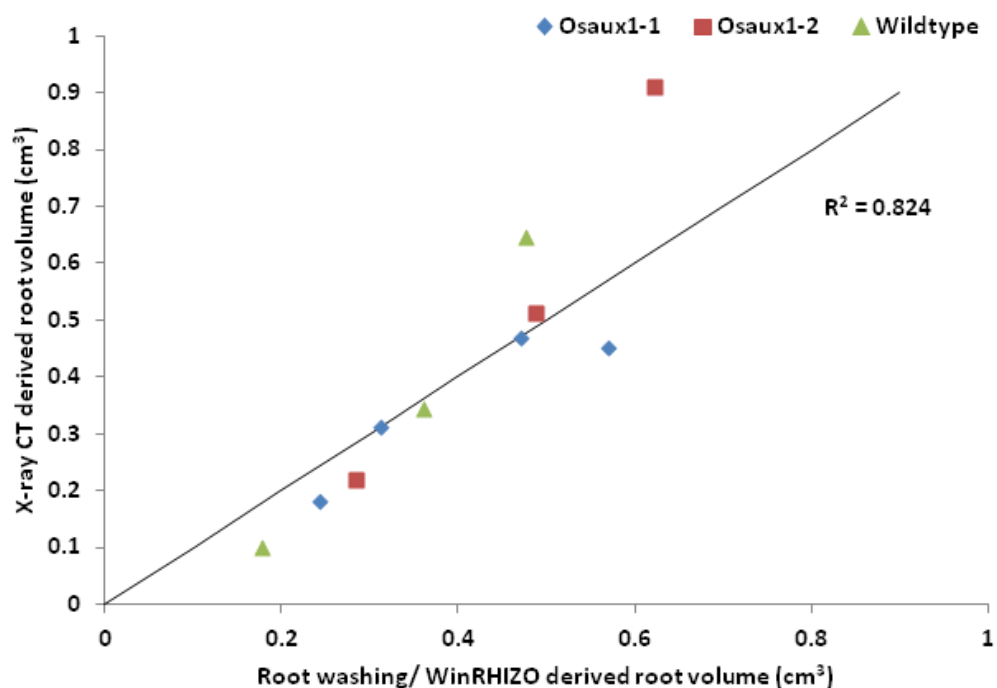


Fig. 5-8: Comparison of X-ray CT and WinRHIZO (root washing derived) root volumes with a 1:1 line for *Osaux1-1* (diamonds), *Osaux1-2* (squares) and wildtype (triangles). Points above the line indicate potential overestimation and points below the line indicate potential underestimation of root volume.

5.3.5 Destructive WinRHIZO analysis

In order to quantify the fine root fraction (particularly large and small lateral roots; Fig. 5-9) destructive sampling was required since fine roots (< 0.5 mm diameter) were not readily visible in the X-ray CT images even with 27.3 μm voxel size. Mean root volume from destructively sampled cores was 0.363 cm^3 , 0.353 cm^3 , and 0.548 cm^3 for wildtype, *Osaux1-*

1 and *Osaux1-2* respectively (Fig. 5-10 A). Although *Osaux1-2* appeared to have a larger root volume, there was no statistically significant difference between the root volumes ($P = 0.503$). Root surface area had similar results with 48.53 cm², 37.16 cm², 74.06 cm² for wildtype, *Osaux1-1* and *Osaux1-2* respectively with no significant ($P = 0.216$) difference (Fig. 5-10 B).

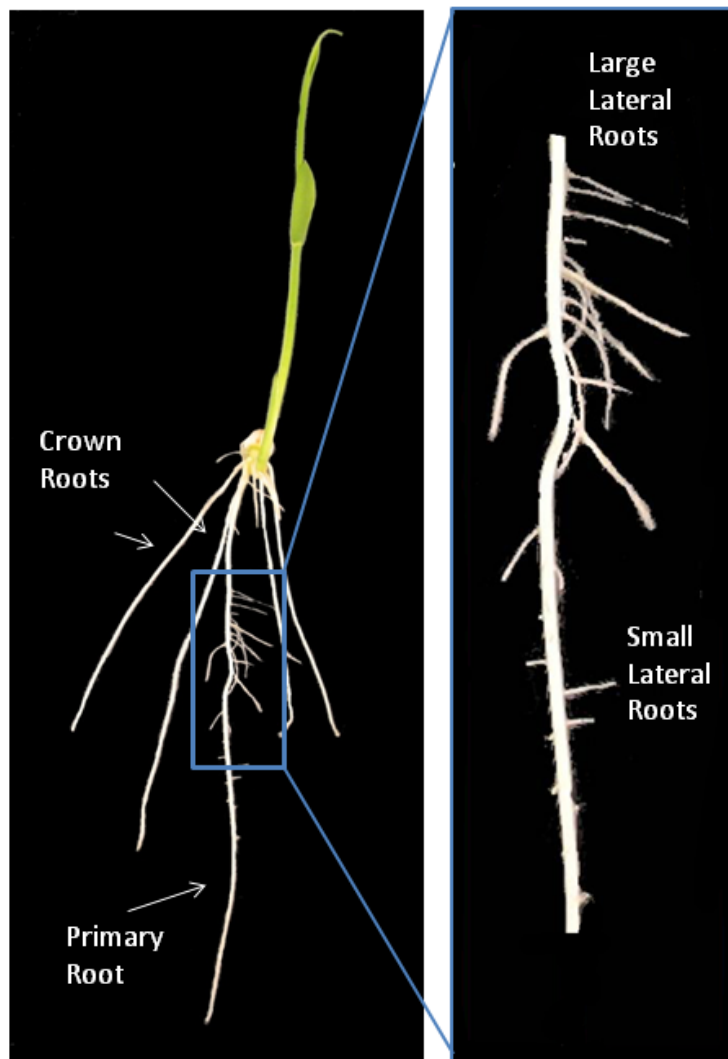


Fig. 5-9: Rice root system components include the primary root, crown roots and fine roots comprised of large and small lateral roots.

Total root length varied more between the genotypes (Fig. 5-11 A), however no significant difference was found ($P = 0.079$). *Osaux1-1* had the smallest total root length with 325.1 cm,

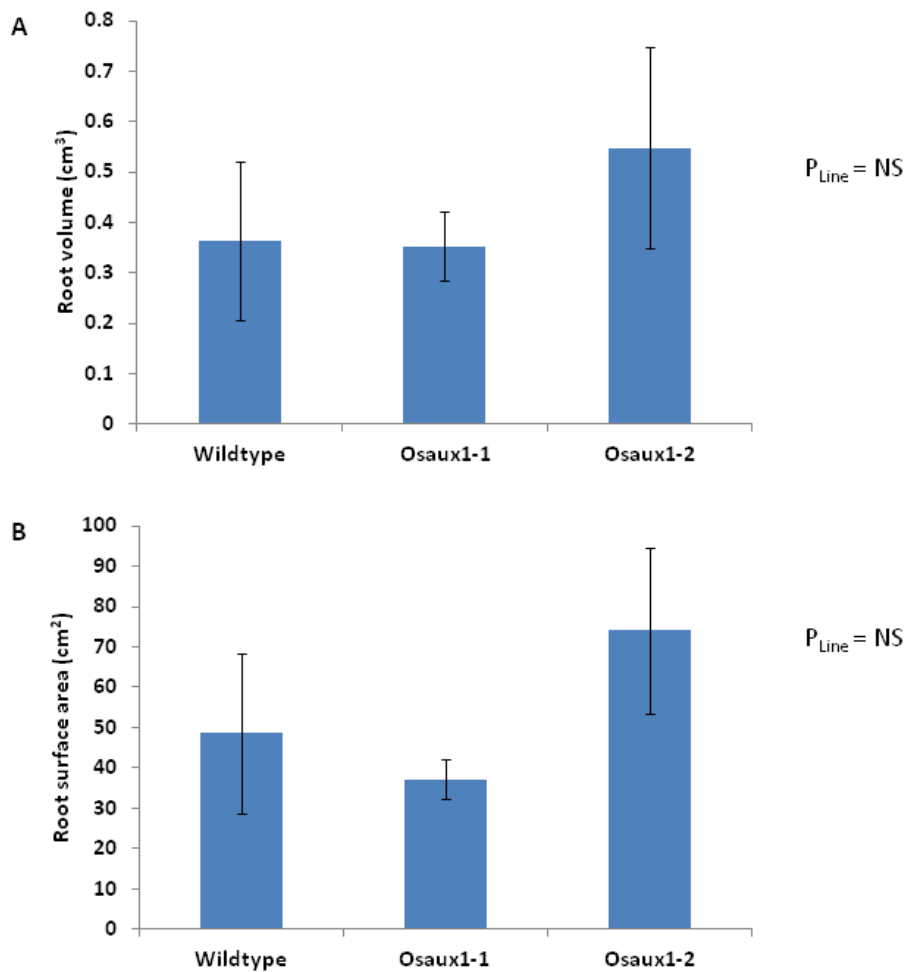


Fig. 5-10: Root washing derived root volume (A) and root surface area (B) of wildtype and the *OsAUX1* knockout mutants. Number of replicates for wildtype, *Osaux1-1* and *Osaux1-2* are three, four and three respectively. Error bars represent standard error of the mean.

whereas wildtype and *Osaux1-2* had much larger values with 518.2 cm and 815.7 cm respectively (Fig. 5-11 A). There was no significant variation in root diameter between the genotypes (Fig. 5-11 B). *Osaux1-1* had the thickest mean root diameter at 0.376 mm. Wildtype and *Osaux1-2* were more similar at 0.288 mm and 0.281 mm respectively. The genotypes had no significant difference in number of root tips. *Osaux1-2* had the most root tips with 4535 with 3735 for wildtype and 3105 for *Osaux1-1* (Fig. 5-12).

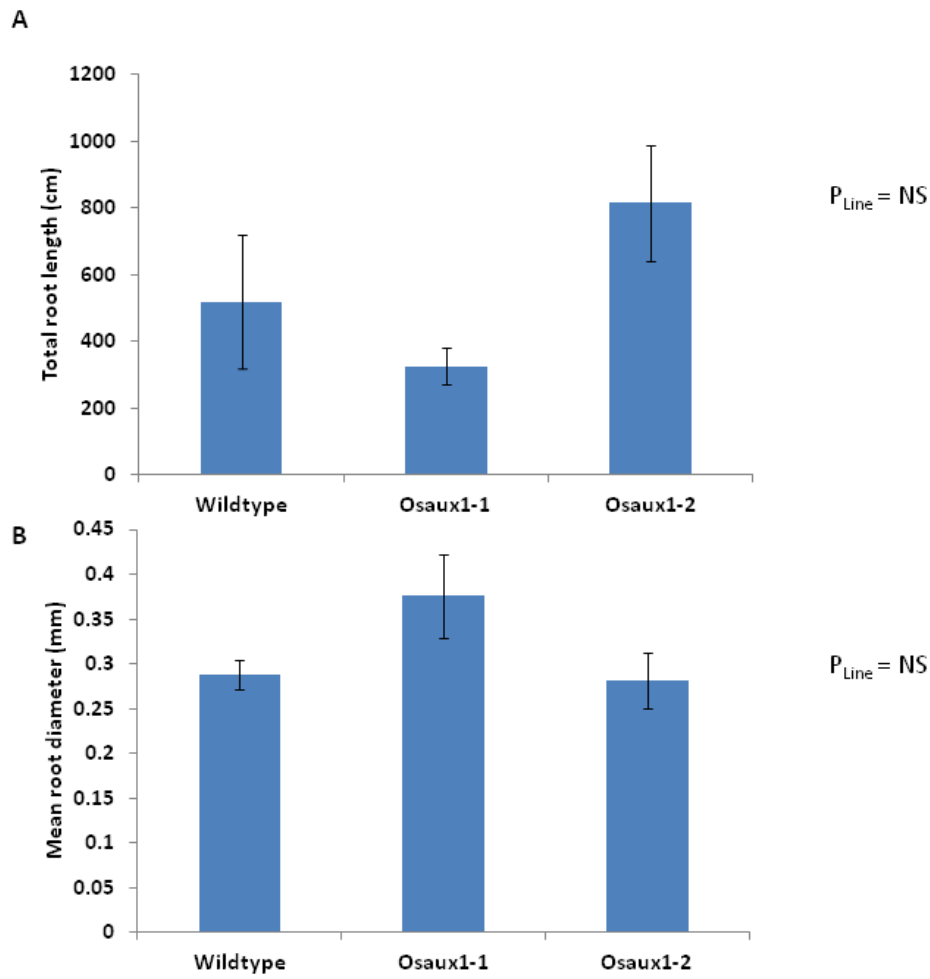


Fig. 5-11: WinRHIZO derived total root length (A) and mean root diameter (B). Error bars represent standard error of the mean.

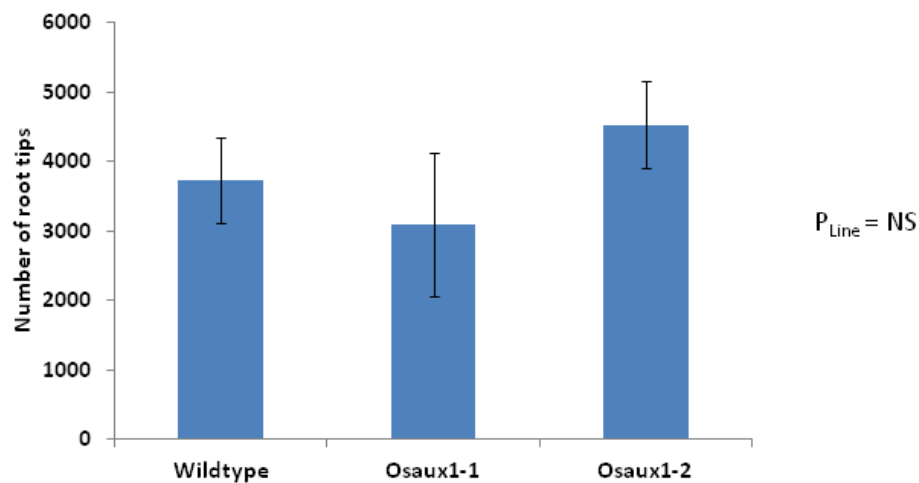


Fig. 5-12: Number of root tips for wildtype, *Osaux1-1* and *Osaux1-2* as determined by WinRHIZO. Error bars represent standard error of the mean.

5.4 Discussion

The shallow root angle influenced by OsAUX1 activity that was identified on agar by Parker (2010) was evident in soil grown rice plants (Fig. 5-3). Additionally, the work characterised other aspects of RSA for soil-grown wildtype plants and the mutants *Osaux1-1* and *Osaux1-2* that have reduced OsAUX1 function (Section 1.4).

Root gravitropic response to low P soil environments has been linked to topsoil foraging in common bean (*Phaseolus vulgaris*) (Lynch and Brown 2001; Rubio et al. 2003), maize (*Zea mays*) (Zhu et al. 2005), oilseed rape (*Brassica oleracea*) (Hammond et al. 2009) This is particularly true in the case of bioavailable inorganic P which resides in the upper five to ten cm of the soil profile depending on soil characteristics and land management techniques (Blake et al. 2000). In a clay loam soil, inorganic phosphate remained in the top two to three cm (Rolston et al. 1975).

There were indications that *Osaux1-1* may have a different RSA than wildtype and *Osaux1-2*. As is indicative of their agravitropic nature, *Osaux1-1* and *Osaux1-2* both had significantly larger enclosing circles than wildtype (Fig. 5-5). The increased minimum enclosing circle radius and reduced centroid Z provided clear indication that knocking out OsAUX1 had influenced the gravitropic response of *Osaux1-1* roots in soil when compared to wildtype (Fig. 5-4 and Fig. 5-6). Variation in response to gravitropic stimulus was consistent with previous observation on agar between *Osaux1-1* and wildtype (Parker 2010).

In addition to gravitropic response, the overall root surface in contact with soil can significantly influence the ability of plants to obtain soil nutrients and water (Dunbabin et al. 2002). RSA factors which increase the amount of root:soil contact that can enhance nutrient

uptake include lateral roots (Bai et al. 2013) and root hairs (Keyes et al. 2013) although the amount of available nutrients such as P can have a significant effect on the development of these fine fractions of the root system (Ma et al. 2001; Pérez-Torres et al. 2008). *OsAUX1* did not significantly influence overall root volume (Fig. 5-1), surface area (Fig. 5-7), total root length (Fig. 5-11 A) or root diameter (Fig. 5-11 B). This is primarily because *Osaux1-1* had the smallest total root length and thickest average root diameter, which would translate into similar root volume and surface area measurements when compared to root systems with a longer total root length and thinner roots. In most cases, *Osaux1-2* performed similarly or even better than wildtype and thus did not provide the appropriate contrast with wildtype to analyse the effects of AUX1 on P uptake.

This work also demonstrated that for assessing global agravitropism of a soil grown root system, X-ray CT was a useful technique. X-ray CT provided an appropriate tool to quantify root characteristics in soil in 3-D and can be used to study the influence of P in conjunction with *OsAUX1*. For 3-D RSA quantification, RooTrak and VGSM provided sufficient agreement in measurement of roots segmented from X-ray CT images. The most meaningful measurements occurred around week four where the most significant differences in centroid Z were observed thus, further studies will focus on four week old plants. Additionally, finer root characteristics such as lateral roots and root hairs were not readily visible at the minimum X-ray CT resolution appropriate for the sample size. Thus, in the P study, faster imaging could be obtained by decreasing the resolution to 57.3 μm voxel size whilst retaining the gross root architecture characteristics required for assessing gravitropism and overall soil exploration potential.

5.5 Conclusion

Through X-ray CT imaging, global RSA characteristics such as gravitropism were non-destructively measured in 3-D for the first time for the knockout mutants *Osaux1-1* and *Osaux1-2* when grown in soil. The agravitropic tendencies of the soil grown knockout mutants were consistent with agravitropism observed for plants grown on agar. Destructive sampling (root washing) was required to obtain further measurements of fine root structures with WinRHIZO. There were no significant differences observed in root volume, total root length, root diameter or number of root tips. Whilst growing in sufficient nutrient conditions in soil, wildtype displayed variations in centroid and 2-D characteristics when compared to *Osaux1-1*. However, *Osaux1-2* had very similar performance to wildtype and in some cases exceeded wildtype performance. It was decided to focus on wildtype and the known OsAUX1 knockout, *Osaux1-1*, to isolate the influence of OsAUX1 on P uptake from soil.

6.0 Influence of root gravitropism and OsAUX1 on RSA and subsequent P uptake

6.1 Introduction

Root plasticity is critical for nutrient acquisition and has been linked to heterogeneity of the soil environment by enabling plants to adapt to changes in nutrient availability (Hutchings and John 2004; Kembel and Cahill 2005). When encountering nutrient patches in soil, changes in RSA are representative of this plasticity. Common RSA variations involve increased initiation of adventitious roots, changes in lateral root density, and alterations to primary root elongation (Hodge 2004; Lynch 1995). RSA can be measured by topological and morphological parameters (Fitter 1987). A root's morphology can be characterised by variation in root length, root hair density and elongation, root radius, vascular differentiation and colour. Whereas root topology is described by branching and placement of roots in soil, thus the centroid, root angle, number of adventitious roots and total root depth are linked to topological quantification.

Of particular interest here are RSA adaptations with respect to soil P availability whether at deficient, replete or toxic levels. Root P acquisition results in many plant reactions which ultimately influence primary root length, lateral root growth, root hair development and root exudation (Lynch 2011; Lynch and Brown 2008). In order to manipulate these changes in RSA and potentially create higher yielding or stress tolerant crops, genetic controls must be identified (Smith and De Smet 2012). One candidate gene that warrants investigation of root system plasticity under P stress is AUX1, which was first characterised in *Arabidopsis* by Bennett et al. (1996). In order to perceive nutrients in the heterogeneous soil environment

and then react once they are encountered, a gene with high affinity to RSA regulation is required. AUX1 controls both phloem and polar indole-3-acetic acid (IAA) transport in the root (Swarup et al. 2001), which in turn has been associated with several changes in RSA such as gravitropism and lateral root initiation (Bennett et al. 1996; Marchant et al. 2002).

IAA, the major form of plant auxin, has been linked to lateral root growth and root gravitropism, two critical aspects of RSA adaptation to P stress. As an instigator of ethylene production, auxin has been correlated with an arrest in primary root elongation of *Arabidopsis* (López-Bucio et al. 2002). IAA accumulation in the root apex can impact on lateral root initiation (Casimiro et al. 2001) and influences lateral root emergence (Péret et al. 2012). Root gravitropism in *Arabidopsis* is controlled by AUX1 because of its influence on localised auxin distribution in the root (Swarup et al. 2005). Upon gravistimulation (plant turned 90° from root growth vector), auxin is released from the gravity sensing columella cells resulting in a transient lateral auxin gradient which induces bending in the root elongation zone (Band et al. 2012; Brunoud et al. 2012). This bending is caused by auxin induced differential growth and thus modifies root angle (Ottenschläger et al. 2003). The typical response under normal auxin transport is for the bending root to tend toward the gravity vector, however in plants with disturbed AUX1 expression an agravitropic phenotype is evident (Swarup et al. 2005). Gravisensing and the relation to auxin is thoroughly reviewed in Baldwin et al. (2013).

In *Arabidopsis*, responses to P stress have been linked to auxin redistribution. Under P starvation, lateral root length increased in plants with unaltered auxin transport (Nacry et al. 2005). It should be noted that by week two lateral root growth slowed. Nacry et al. (2005)

hypothesised the altered lateral root phenotype was due to localised changes in auxin distribution induced in the wildtype plant under low P. Al-Ghazi et al. (2003) linked auxin to root plasticity and in particular temporal variation in lateral root elongation when the auxin-resistant mutant *axr4* was subject to P deprivation. A key question is whether auxin induced responses to P stress could be a conserved trait in crop plants.

Recently AUX1 was characterised in the crop species rice (*Oryza sativa* ssp. Japonica cv. Dongjin) (Parker 2010), which is commonly grown on P deficient soils. When grown on nutrient agar, OsAUX1 was linked to lateral root initiation, primary root length and root gravitropic response. These are aspects of RSA which change under varying soil P conditions in crop species. Genotypes related to P uptake and tolerance to limiting concentrations of soil P have been investigated in maize (Liu et al. 2004), barley (*Hordeum vulgare* L.) (Gahoonia and Nielsen 1996), oilseed rape (*Brassica napus* L.) (Zhang et al. 2009), durum wheat (*Triticum durum* L.) (Ozturk et al. 2005), common bean (Beebe et al. 2006) and rice (Chin et al. 2010; Li et al. 2007; Wissuwa and Ae 2001). However, the influence of OsAUX1 on rice root system plasticity and plant P uptake has not been characterised. By utilising a T-DNA insertion knockout mutant, this work quantified RSA in soil under varying P conditions for plants with full and reduced OsAUX1 expression.

6.2 Materials and Methods

A combination of X-ray CT and destructive sampling were used to quantify root traits under seven soil P distributions with three P levels. Soil was collected from the Hoosfield Exhaustion Land experimental plot 014 at RRes, United Kingdom because of its unusually

low P content of 4 mg kg⁻¹ (RRes 2006). Soil collection, preparation and descriptions are covered in Section 2.3 and 2.4.

There were three uniform column treatments (No P, Sufficient P and High P), two treatments with P amendments in the top 4 cm (Split top sufficient and Split top high) and two treatments with P in the bottom 6 cm (Split bottom sufficient and Split bottom high); these are detailed in Section 2.5.1. There were ten replicates for each column setup and this was implemented with two rice lines; one line was the unaltered wildtype and the other was an OsAUX1 T-DNA insertion knockout line *Osaux1-1* (Parker 2010) which is detailed in Section 1.4. This produced a total of 140 columns that were measured. High P was repeated twice because of poor plant growth.

Five randomly selected soil and root columns from each treatment (P Treatment X Line) were X-ray CT scanned with a Phoenix Nanotom (GE Sensing and Inspection Technologies, GmbH, Wunstorf, Germany) fitted with a diamond transmission target. The X-ray CT scanning was performed with the following settings: mode zero, fast scans, 180 kV, 110 µA, 1200 projections, 40 min total scan time, sample-source distance of 19.9 cm, 57.3 µm voxel size with a 0.2 mm copper filter. Each column was drained for two days before scanning (Zappala et al. 2013b) and scanned at week four. Each sample received an approximate X-ray dose of 1.1 Gy each scan, which was estimated using the RadPro X-ray Device Dose-Rate Calculator (McGinnis 2002-2009). VGSM and RooTrak software was used to quantify RSA extracted from X-ray CT images. VGSM was used to measure root volume by pixel counting. RooTrak provided values for root volume, surface area, centroid, maximum depth, minimum enclosing circle and convex hull (Section 2.8.3). RooTrak implements voxel counting or area

calculations from a triangle mesh generated around the segmented root system for these measurements. Root system “solidness” was calculated from the ratio of root volume to convex hull volume. Specific root length was calculated from the ratio between total root length obtained in WinRHIZO and the root dry mass. After scanning destructive measurements of the root system were performed using WinRHIZO (Section 2.9.1) and P analysis of plant tissues was completed (Section 2.10.2).

6.3 Results

6.3.1 Biomass accumulation and P uptake

Under all uniform P soil distributions there was not a significant difference between the genotypes for shoot dry mass or root dry mass. Under low P and sufficient P, the root:shoot ratio and amount of plant P as a proportion of dry mass was similar between the two genotypes. However, under high P conditions, wildtype had a lower root:shoot ratio and proportion of P than *Osaux1-1* (Table 6-1).

Table 6-1: Biomass and colorimetric P measurements for wildtype and *Osaux1-1* under uniform P distribution for low, sufficient and high P. All values are shown with \pm standard error of the mean. * designates significance where ANOVA $P < 0.05$ for interaction between genotype and soil P level.

	4 mg kg ⁻¹		50 mg kg ⁻¹		150 mg kg ⁻¹	
	Wildtype	<i>Osaux1-1</i>	Wildtype	<i>Osaux1-1</i>	Wildtype	<i>Osaux1-1</i>
Shoot dry mass (g)	0.021 \pm 0.011	0.033 \pm 0.010	0.133 \pm 0.047	0.112 \pm 0.025	0.036 \pm 0.025	0.029 \pm 0.025
Root dry mass (g)	0.011 \pm 0.003	0.016 \pm 0.002	0.042 \pm 0.010	0.036 \pm 0.006	0.002 \pm 0.007	0.005 \pm 0.007
Root:shoot	0.48 \pm 0.07	0.46 \pm 0.04	0.34 \pm 0.02	0.33 \pm 0.02	0.08 \pm 0.03*	0.40 \pm 0.03
Plant P (mg g ⁻¹ dry mass)	0.87 \pm 0.10	0.91 \pm 0.08	0.92 \pm 0.19	0.80 \pm 0.11	0.64 \pm 0.23*	1.09 \pm 0.23*

Under stratified P conditions (see split top P and split bottom P in Fig. 2-2), there was more variation in biomass accumulation between the genotypes than for the plants grown in the

soil with uniform P distribution (Table 6-2). Wildtype had the greatest root and shoot dry mass when grown in columns with 50 mg kg⁻¹ P in the top 4 cm of soil (split top sufficient; P_{Shoot} = 0.003; P_{Root} = 0.002). When 50 mg kg⁻¹ P was in the bottom 6cm of the soil column (split bottom sufficient), *Osaux1-1* had less root and shoot biomass than wildtype (P_{Root} = 0.014; P_{Shoot} = 0.040). However, at the higher P level, wildtype and *Osaux1-1* had similar biomass accumulation. Genotype and P level in soil did not affect root:shoot ratio. Genotype did not influence P accumulation for any of the stratified P treatments (Table 6-2).

Table 6-2: Biomass and colorimetric P measurements for wildtype and *Osaux1-1* under uniform P distribution for low, sufficient and high P. All values are shown with ± standard error of the mean. For interaction between genotype and soil P level, ** represents P<0.001 and * designates P< 0.05.

	Top 50 mg kg ⁻¹		Top 150 mg kg ⁻¹		Bottom 50 mg kg ⁻¹		Bottom 150 mg kg ⁻¹	
	Wildtype	<i>Osaux1-1</i>	Wildtype	<i>Osaux1-1</i>	Wildtype	<i>Osaux1-1</i>	Wildtype	<i>Osaux1-1</i>
Shoot dry mass (g)	0.289 ± 0.001*	0.138 ± 0.003*	0.064 ± 0.027	0.049 ± 0.015	0.155 ± 0.006	0.074 ± 0.015*	0.158 ± 0.006	0.163 ± 0.012
Root dry mass (g)	0.076 ± 0.013*	0.044 ± 0.006*	0.012 ± 0.002	0.010 ± 0.002	0.035 ± 0.008	0.016 ± 0.008*	0.036 ± 0.005	0.040 ± 0.005
Root:shoot	0.26 ± 0.03	0.33 ± 0.02	0.18 ± 0.01	0.23 ± 0.07	0.22 ± 0.01	0.26 ± 0.04	0.24 ± 0.02	0.26 ± 0.03
Plant P (mg g⁻¹ dry mass)	0.39 ± 0.01	0.48 ± 0.04	4.53 ± 0.34	3.82 ± 0.21	0.77 ± 0.05	1.08 ± 0.17	0.81 ± 0.05	1.01 ± 0.07

6.3.2 3-D root exploration in relation to soil P concentration and distribution

As seen in Fig. 6-1 and Table 6-3, under uniform soil P at 50 mg kg⁻¹, wildtype had larger root X-ray CT measured volume than *Osaux1-1* (P = 0.027). This was also true for root surface area measured from X-ray CT images (P = 0.038). There was no difference between the genotypes for all other 3-D parameters including convex hull, centroid Z, maximum depth and maximum width within a given P level (Table 6-3).

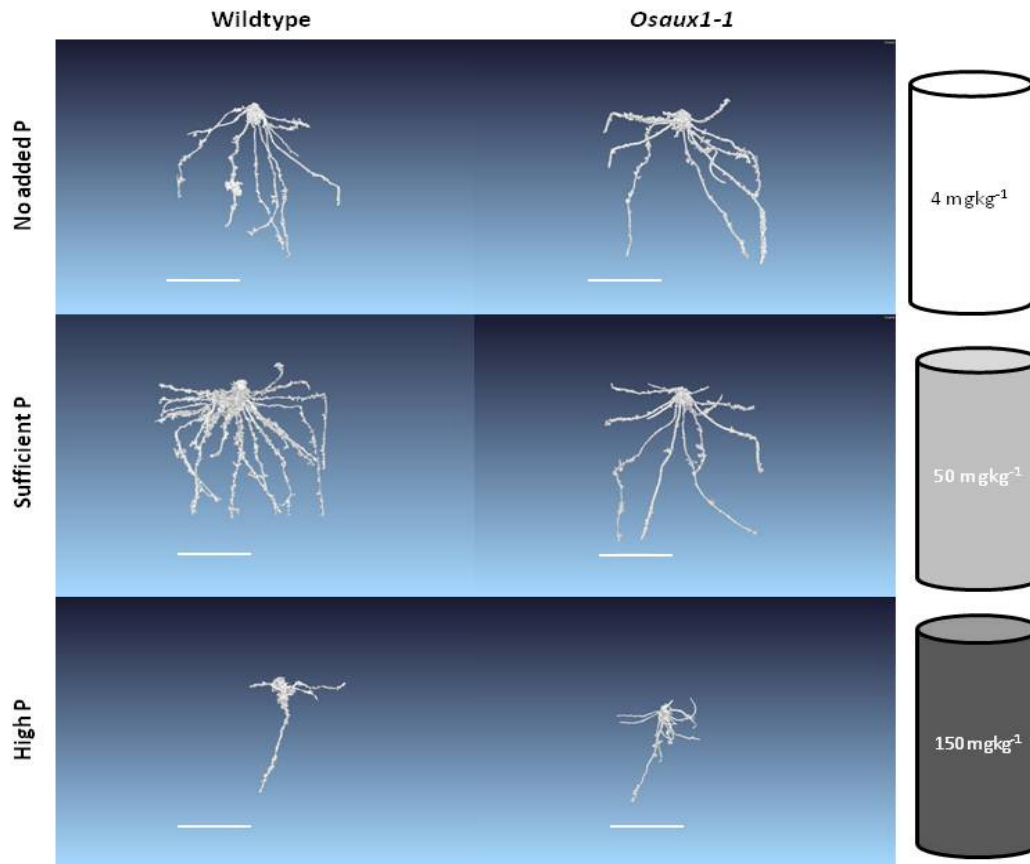


Fig. 6-1: Representative images of root systems obtained by X-ray CT for plants grown under uniform P distribution. Scale bar is equivalent to 3 cm.

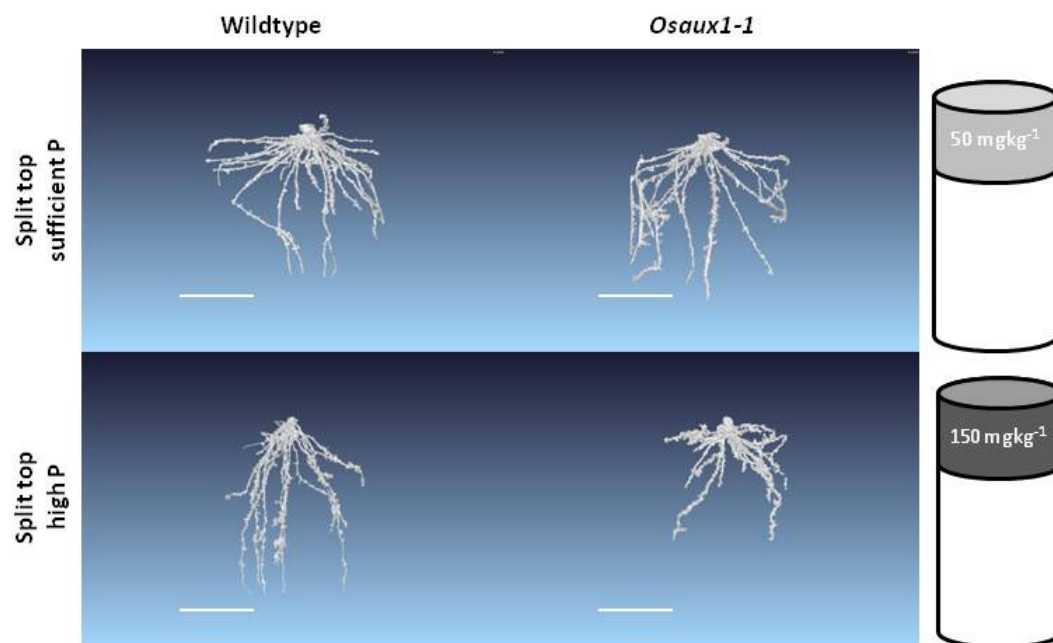


Fig. 6-2: Representative images obtained by X-ray CT of root systems grown in stratified soil P distributions. Extra P was provided in the top 4 cm at sufficient and high P soil concentrations. Scale bar is equivalent to 3 cm.

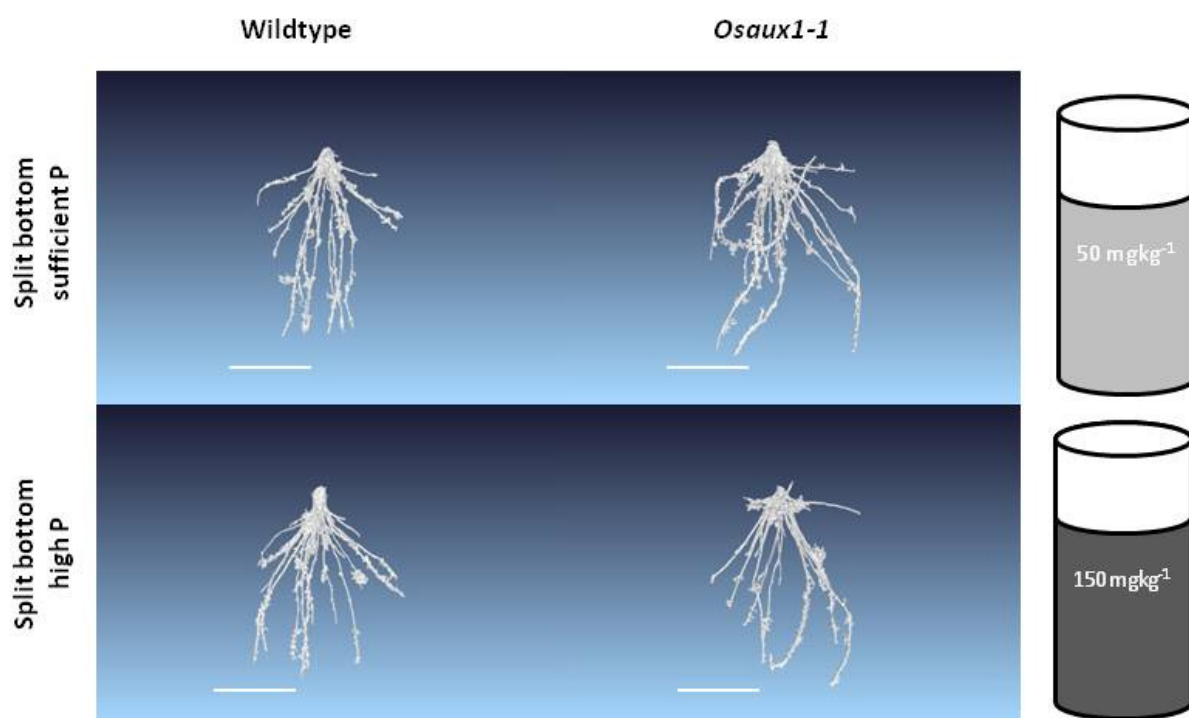


Fig. 6-3: Representative images obtained by X-ray CT of root systems grown in stratified soil P distributions. At sufficient and high P soil concentrations, extra P was provided in the bottom 6 cm (split bottom) of the 10 cm columns. Scale bar is 3 cm.

Table 6-3: X-ray CT derived measurements for wildtype and *Osaux1-1* under uniform P distribution for low, sufficient and high P. All values are shown with \pm standard error of the mean. * designates significance where ANOVA $P < 0.05$ for interaction between genotype and soil P level.

	4 mg kg ⁻¹		50 mg kg ⁻¹		150 mg kg ⁻¹	
	Wildtype	<i>Osaux1-1</i>	Wildtype	<i>Osaux1-1</i>	Wildtype	<i>Osaux1-1</i>
Mesh Root Volume (cm ³)	0.29 \pm 0.01	0.29 \pm 0.07	0.67 \pm 0.07*	0.36 \pm 0.05	0.14 \pm 0.06	0.18 \pm 0.06
Convex Hull Volume (cm ³)	58.5 \pm 5.7	50.7 \pm 6.0	66.0 \pm 3.7	74.8 \pm 3.0	8.6 \pm 5.4	21.0 \pm 7.9
Solidness (cm ³ * cm ⁻³)	0.005 \pm 0.0005	0.006 \pm 0.0007	0.010 \pm 0.0015	0.005 \pm 0.0007	0.023 \pm 0.0068*	0.009 \pm 0.0006
Mesh Surface area (cm ²)	18.6 \pm 1.5	17.7 \pm 2.6	34.1 \pm 4.3*	19.3 \pm 3.3	7.0 \pm 3.3	10.1 \pm 2.9
Centroid Z (cm)	3.01 \pm 0.56	3.83 \pm 0.11	1.68 \pm 0.07	2.27 \pm 0.58	1.44 \pm 0.26	1.49 \pm 0.49
Max Depth (cm)	5.38 \pm 0.19	5.28 \pm 0.01	5.33 \pm 0.12	5.63 \pm 0.10	3.38 \pm 1.08	4.81 \pm 0.20
Max Width (cm)	5.37 \pm 0.28	5.28 \pm 0.11	4.74 \pm 0.13	5.63 \pm 0.28	3.91 \pm 0.23	3.77 \pm 0.60

Under stratified conditions where added P was segregated to the top 4 cm (Fig. 6-2) or bottom 6 cm (Fig. 6-3) of the soil column, there was little variation between the genotypes for a given P level. Interestingly, centroid Z, maximum root depth and maximum root system width showed no difference between the genotypes. *Osaux1-1* did have a larger root volume than wildtype when grown in soil with 50 mg kg⁻¹ P in the bottom 6 cm of the soil column (Table 6-4).

Table 6-4: X-ray CT derived root measurements for wildtype and *Osaux1-1* under stratified P distribution for sufficient and high P. All values are shown with \pm standard error of the mean. For interaction between genotype and soil P level, * designates $P < 0.05$.

	Top 50 mg kg ⁻¹		Top 150 mg kg ⁻¹		Bottom 50 mg kg ⁻¹		Bottom 150 mg kg ⁻¹	
	Wildtype	<i>Osaux1-1</i>	Wildtype	<i>Osaux1-1</i>	Wildtype	<i>Osaux1-1</i>	Wildtype	<i>Osaux1-1</i>
Mesh Root Volume (cm³)	0.84 \pm 0.20	0.61 \pm 0.02	0.04 \pm 0.01	0.16 \pm 0.01	0.53 \pm 0.01	0.79 \pm 0.03*	0.61 \pm 0.01	0.61 \pm 0.03
Convex Hull Volume (cm³)	74.9 \pm 10.7	66.3 \pm 11.0	41.4 \pm 5.2	31.1 \pm 5.6	57.0 \pm 8.2	96.8 \pm 6.5	43.8 \pm 8.2	77.0 \pm 6.5
Solidness (cm³ * cm⁻³)	0.011 \pm 0.0020	0.010 \pm 0.0016	0.001 \pm 0.0002	0.005 \pm 0.0007	0.005 \pm 0.0012	0.008 \pm 0.0002	0.014 \pm 0.0012	0.008 \pm 0.0002
Mesh Surface area (cm²)	39.6 \pm 7.4	35.9 \pm 2.8	5.9 \pm 0.3	12.4 \pm 0.6	32.7 \pm 5.1	40.1 \pm 0.1	27.5 \pm 5.1	30.6 \pm 0.1
Centroid Z (cm)	1.33 \pm 0.08	1.52 \pm 0.10	1.77 \pm 0.14	1.59 \pm 0.20	1.84 \pm 0.09	1.88 \pm 0.02	1.72 \pm 0.09	1.91 \pm 0.02
Max Depth (cm)	5.44 \pm 0.18	5.36 \pm 0.09	5.05 \pm 0.06	4.60 \pm 0.12	5.08 \pm 0.04	5.73 \pm 0.26	5.64 \pm 0.04	5.54 \pm 0.26
Max Width (cm)	4.75 \pm 0.12	4.75 \pm 0.34	4.76 \pm 0.57	5.05 \pm 0.33	5.32 \pm 0.24	5.64 \pm 0.05	5.11 \pm 0.24	5.54 \pm 0.05

6.3.3 Destructively sampled RSA and P soil concentration

Representative images of the washed root systems grown in uniform P (Fig. 6-4), split top P (Fig. 6-5) and split bottom P (Fig. 6-6) treatments show the variation of RSA with P distribution. With uniform P distribution there was no discernible variation between

genotypes for the measured parameters including root volume, total root length and number of root tips (Table 6-5).

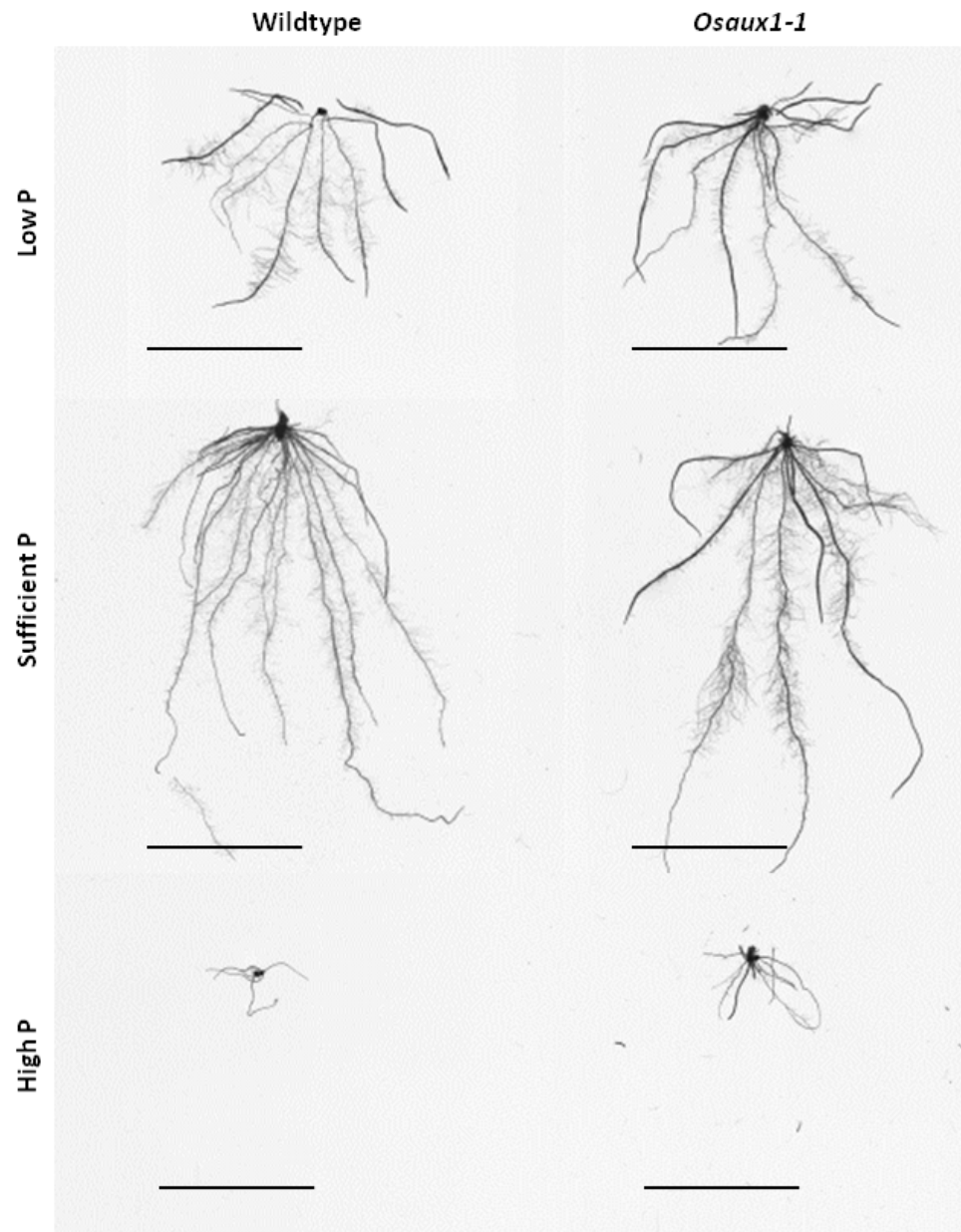


Fig. 6-4: Representative images of roots washed after being grown in uniform low P, sufficient P and high P. Scale bars are equivalent to 5 cm.

Table 6-5: WinRHIZO measurements for wildtype and *Osaux1-1* under uniform P distribution for low, sufficient and high P. The root systems were destructively sampled. Values are shown with \pm standard error of the mean. No significant interactions between genotype and P level were recorded.

	4 mg kg ⁻¹		50 mg kg ⁻¹		150 mg kg ⁻¹	
	Wildtype	<i>Osaux1-1</i>	Wildtype	<i>Osaux1-1</i>	Wildtype	<i>Osaux1-1</i>
WinRhizo Root Volume (cm³)	0.10 \pm 0.03	0.13 \pm 0.02	0.66 \pm 0.18	0.44 \pm 0.11	0.09 \pm 0.07	0.16 \pm 0.05
Surface area (cm²)	17.0 \pm 4.7	20.3 \pm 3.3	87.9 \pm 22.8	65.2 \pm 16.2	9.1 \pm 5.6	19.2 \pm 4.9
Root Diameter (mm)	0.29 \pm 0.009	0.27 \pm 0.026	0.26 \pm 0.015	0.27 \pm 0.014	0.33 \pm 0.016	0.33 \pm 0.008
Total Root Length (cm)	222 \pm 90	249 \pm 57	948 \pm 335	773 \pm 249	75 \pm 31	185 \pm 44
Specific root length (cm root g⁻¹ root dry mass)	198 \pm 82	161 \pm 43	225 \pm 112	217 \pm 91	357 \pm 17	385 \pm 211
Number Root Tips	1760 \pm 540	2147 \pm 397	3334 \pm 404	3309 \pm 383	447 \pm 129	759 \pm 113

However, in stratified P conditions, there was more variation between the genotypes when compared within a given P level. This was particularly true for the soil columns with 50 mg kg⁻¹ P in the top 4 cm of the soil column (Split top sufficient; Fig. 6-5) and when 150 mg kg⁻¹ P was added to the bottom 6 cm of the soil column (Split bottom high; Fig. 6-6) as seen in the flatbed scanned images of the destructively sampled root systems. The destructive root system measurements for stratified P conditions are presented in Table 6-6. Under split top sufficient conditions, wildtype had more root volume, surface area, total root length and number of root tips than *Osaux1-1* (all $P < 0.001$). There appears to be linkage between these values and an increased proportion of fine roots (< 0.5 mm diameter). The split top high P treatment produced smaller root systems in both genotypes.

Under split bottom sufficient P (50 mg kg⁻¹ in bottom 6 cm of soil column), *Osaux1-1* had greater root volume ($P = 0.036$) than wildtype but less surface area ($P = 0.004$). When high P

was present in the bottom 6 cm of the soil profile, *Osaux1-1* had larger total root length ($P < 0.001$), surface area ($P = 0.003$) and root diameter ($P = 0.004$) than wildtype.

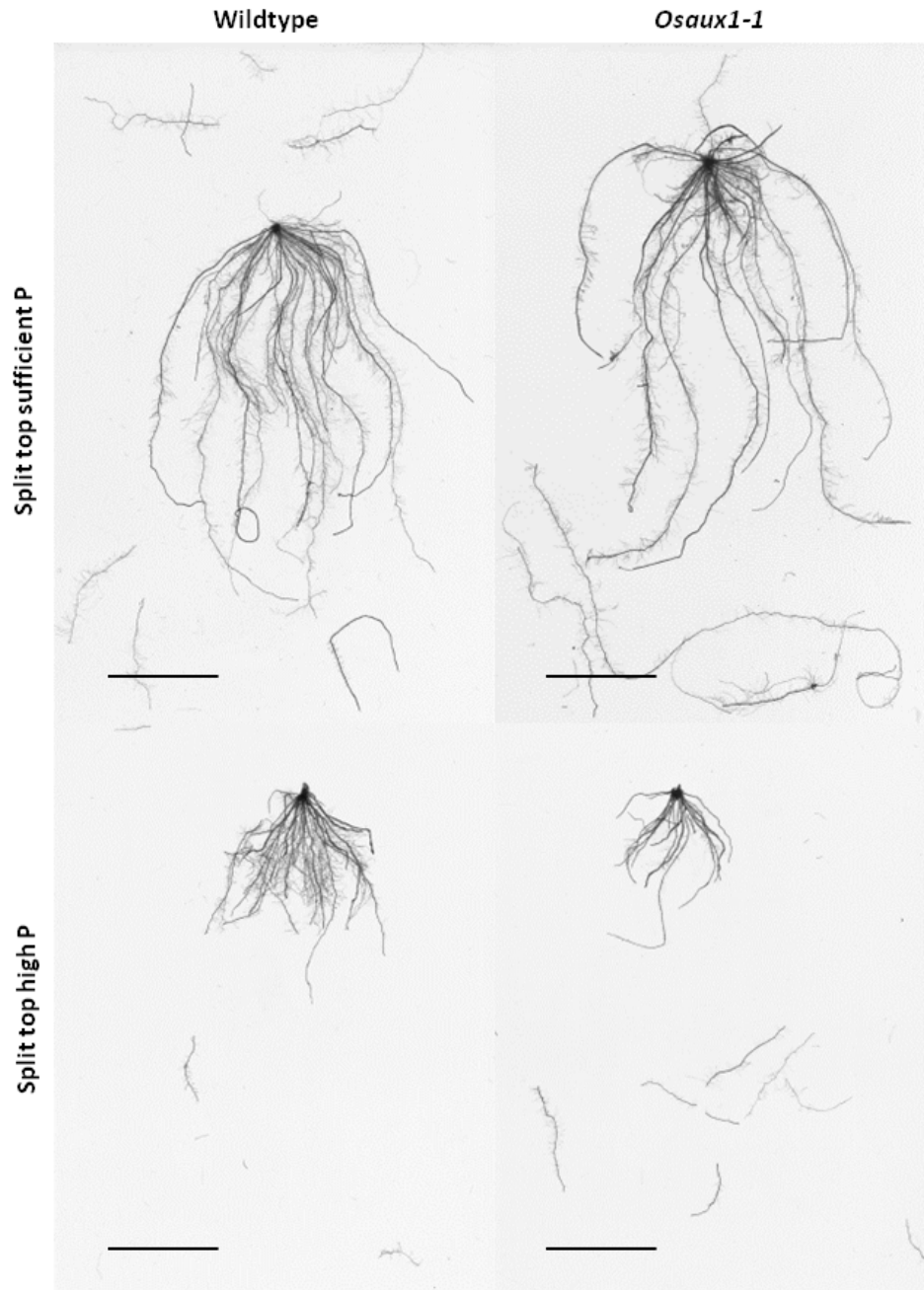


Fig. 6-5: Washed root systems of plants grown in sufficient and high P sequestered to the top 4 cm of the soil column. Scale bars are equivalent to 5 cm.

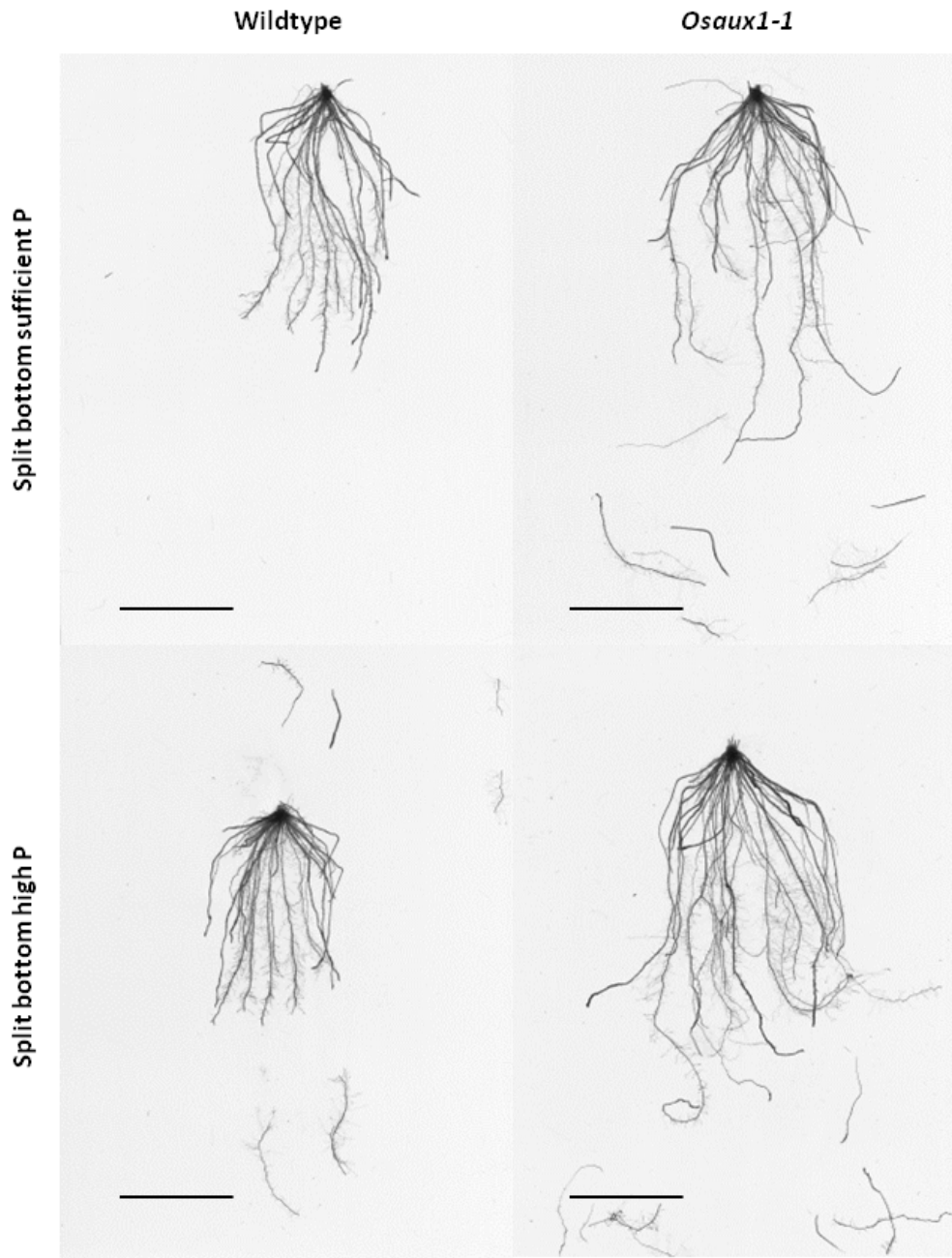


Fig. 6-6: Representative images of RSA for plants grown with P in the bottom 6 cm of the soil column. Scale bars are equivalent to 5 cm.

Table 6-6: WinRHIZO derived measurements for wildtype and *Osaux1-1* under stratified P distribution for sufficient and high P. Root systems were destructively sampled. All values are shown with \pm standard error of the mean. For interaction between genotype and soil P level, ** represents $P < 0.001$ and * designates $P < 0.05$.

Destructive Sampling	Top 50 mg kg ⁻¹		Top 150 mg kg ⁻¹		Bottom 50 mg kg ⁻¹		Bottom 150 mg kg ⁻¹	
	Wildtype	<i>Osaux1-1</i>	Wildtype	<i>Osaux1-1</i>	Wildtype	<i>Osaux1-1</i>	Wildtype	<i>Osaux1-1</i>
WinRhizo Root Volume (cm ³)	1.27 \pm 0.21**	0.69 \pm 0.10**	0.14 \pm 0.03	0.12 \pm 0.02	0.68 \pm 0.14	0.34 \pm 0.12*	0.70 \pm 0.08	0.71 \pm 0.08
Surface area (cm ²)	181.9 \pm 22.0**	98.8 \pm 13.8**	17.8 \pm 3.4	15.1 \pm 2.3	63.3 \pm 11.7	35.9 \pm 14.9*	69.4 \pm 8.6	86.6 \pm 6.3*
Root Diameter (mm)	0.27 \pm 0.015	0.28 \pm 0.014	0.32 \pm 0.014	0.32 \pm 0.017	0.42 \pm 0.014	0.39 \pm 0.032	0.40 \pm 0.014	0.32 \pm 0.026*
Total Root Length (cm)	2090 \pm 159**	1130 \pm 169**	181 \pm 34	155 \pm 27	470 \pm 74	311 \pm 146	554 \pm 62	869 \pm 107**
Specific root length (cm root g ⁻¹ root dry mass)	274 \pm 49	255 \pm 8	157 \pm 48	158 \pm 44	135 \pm 19	192 \pm 17	156 \pm 10	215 \pm 32
Number Root Tips	6196 \pm 165**	3214 \pm 523**	770 \pm 154	578 \pm 115	1503 \pm 304	1180 \pm 418	1816 \pm 199	2838 \pm 375*

6.4 Discussion

Here we began to unravel some of the complexities of nutrient acquisition from soil by exploring the relationship between gravitropism and P uptake for rice plants with and without full *Osaux1* expression. Soil P presents a particular challenge because it is rarely mobile (Larsen 1967) and has a tendency to become unavailable to the plant through sorption to soil particles (Borggaard et al. 1990), complexation with aluminium or iron oxides in paddy soils (Kögel-Knabner et al. 2010) and transformation to forms unsuitable for plant uptake (Blake et al. 2000). Often, bioavailable P resides in the upper 5 cm of topsoil (Section 1.2.2). Encouraging root traits such as shallow rooting angle to increase yield under P stress has been gathering interest with plant breeders and plant scientists alike (Lynch 2011).

Each of the soil P treatments provided its own challenges for rice root system development. The uniform treatments where P level was distributed throughout the vertical soil profile provided an indication of the influence of OsAUX1 under limiting (no P), sufficient and toxic (high P) soil P levels. The columns with P treatment in the upper 4 cm of the soil column allowed assessment of root interaction under variable soil P conditions. The split bottom treatments provided clues as to what happens with root development when the initial stages of growth are in limiting conditions and then followed by an increase in available P. Generally, as found in the split top P distribution, P is considered to reside in the top 5 to 10 cm of the soil profile (Owens et al. 2008).

Of particular interest was the vertical root distribution of each genotypes under the various P treatments. The strong influence of OsAUX1 on a gravitropic response observed by Parker (2010) for agar grown plants was overridden in this work. In most cases, wildtype displayed similar vertical root distribution as *Osaux1-1* when characterised by centroid z-value. It appears OsAUX1 does influence root development under varying P conditions and subsequent P uptake, but this is likely linked to factors other than root gravitropism. The complex feedback between nutrient acquisition and nutrient concentration in tissues may be part of the explanation. It would be prudent to investigate non-geometric root characteristics which have been linked to phosphorus starvation such as root hair length (Mackay and Barber 1985) and density (Ma et al. 2001), aerenchyma formation (Drew et al. 1989; Postma and Lynch 2011), iron rhizosheath formation (Zhang et al. 1999) and seed P content (Hedley et al. 1994).

For rice, levels of available soil Pi between 2 and 8 mg P kg⁻¹ are considered to be limiting (De Datta et al. 1990) and as expected the uniform low P treatment produced the smallest root systems (Fig. 6-1). In limiting conditions, the wildtype was able to capture a similar amount of P as *Osaux1-1*. This is consistent with low P conditions where primary root growth was impeded under low P for *Arabidopsis* (López-Bucio et al. 2002). This is not necessarily true for all crop plants. Maize plants subjected to P deficient nutrient solution for four weeks had twice as much total root length as those with sufficient P (Sachay et al. 1991). Hammond et al. (2009) observed longer primary roots under low P (0.006 mM) for soil grown *Brassica oleracea*.

Uniform high P produced very stunted root systems for both genotypes which affected the amount of soil explored and the potential for P uptake from soil by root tissues. Rice plants in general found it difficult to grow in the uniform high P treatment and thus had high variability between replicates. Despite the highly variable response, *Osaux1-1* had a propensity to accumulate more P and to continue root growth even under these toxic conditions.

In particular the split top sufficient P treatment was meant to reflect field-like conditions where most P resides in the upper portion of the soil profile (Owens et al. 2008). As hypothesised, root volume and surface area were significantly higher for both genotypes under split top P sufficient than split top high P. *Osaux1-1* displayed a limited response to toxic soil P concentrations in comparison to wildtype when P was allocated to the top portion of the soil column as indicated by solidness of the root system.

Although tissue concentrations of P were similar between the lines, root and shoot biomass accumulation of P for wildtype was almost twice that of *Osaux1-1*. In comparison to X-ray CT derived data, WinRHIZO measurements highlighted the increased proliferation of fine roots in wildtype which had ca. twice the surface area, total root length and number of root tips when compared with *Osaux1-1* under split top sufficient conditions. This is consistent with other studies where proliferation of lateral roots is affected by available P (Bai et al. 2013) and AUX1 activity (Lavenus et al. 2013). There was a similar trend for wildtype in the split top high treatment as in split top sufficient, however the total accumulated P and tissue P concentrations were higher than those measured in *Osaux1-1*.

The split bottom treatments seemed to inhibit root growth by exposing the developing root system to limiting P conditions. With sufficient P in the bottom portion of the column, wildtype had larger biomass accumulation but similar total root length to the knockout mutant. The wildtype had a reduced area of soil exploration and combined with the smaller overall root volume is indicative of a reaction to low P. Wildtype had significantly lower root volume under split bottom sufficient conditions than *Osaux1-1*. Although wildtype explored less of the soil volume than *Osaux1-1* under split bottom conditions, when soil P concentrations were high, wildtype had more root volume solidness within the explored area showing a localised response to available P.

With high P in the bottom of the soil column, wildtype performed similarly in biomass, but took up less overall P and had lower tissue P concentrations than *Osaux1-1*. This may be attributed to the increased root diameter which was larger in wildtype and combined with similar mass may be indicative of aerenchyma formation. Aerenchyma formation has been

linked to phosphorus starvation in maize (Drew et al. 1989) and is indicative of the 'steep, cheap and deep' phenotype proposed by Lynch (2013) which enables plants under stress to increase root length and diameter with minimum carbon input.

The allocation of root and shoot biomass by both wildtype and the *OsAUX1* knockout were unexpected. Commonly root:shoot ratio increases when P is low (Lynch and Brown 2008). However in this work, the lowest observed root:shoot ratios occurred under high P and the largest under the no P treatment. The high P treatment result could be explained by the reduced overall plant growth and high standard error between replicates, although it is notably four-fold lower than the low P result.

Further investigation is required to determine whether there was an influence of *OsAUX1* on the allocation of resources for root and shoot biomass accumulation. Root:shoot ratio was reduced in wildtype in comparison to *Osaux1-1* for split top sufficient P and high P which highlights the role of *OsAUX1* for adaptation to variation in P levels. For example, wildtype was able to alter root:shoot ratios under uniform toxic conditions, whereas *Osaux1-1* showed no variation in response. In conditions where the soil the roots initially developed in was toxic, but that underlying layers contained insufficient P, wildtype was again able to alter root:shoot to ensure better allocation of carbon for P uptake that would ensure biomass accumulation for the whole plant.

6.5 Conclusion

This work explored the candidate gene *OsAUX1* for its influence on RSA under differing soil P concentrations and distributions. In these experiments, *OsAUX1* could be linked to P uptake, but it was not clear what role gravitropism and topsoil foraging played in P uptake of rice, if

any. OsAUX1 appears integral to some aspects of root growth and development in relation to the fine root fraction when P is uniformly distributed throughout the vertical soil profile. However, in terms of vertical and horizontal distribution of the root system, wildtype and *Osaux1-1* had similar phenotypes when P was uniformly distributed throughout the soil. In split top conditions, wildtype had a significantly larger root volume, surface area and overall plant biomass. The split top sufficient treatment wildtype plants also had the greatest biomass accumulation with a relatively moderate uptake of total P whereas plants grown with high/toxic P treatments had the greatest P uptake. This could be indicative of a further relationship between OsAUX1 with P translocation and regulation in addition to proliferation of lateral roots independent of P availability. The work has provided a justification for further investigation into the aspects of root development such as lateral root growth and root hair elongation, their relationship to OsAUX1 and potential influence on P uptake in rice.

7.0 Unravelling the role of OsAUX1 in P uptake

7.1 Introduction

Although fertiliser application can augment the available nutrients in soil, the ability to acquire these nutrients is primarily determined by the plant root system architecture (RSA) and capability to actually take up the available nutrients (Richardson et al. 2009). Most P taken up by plants is acquired through diffusion; mass flow accounts for between 1 and 5% of plant P demand (Lambers et al. 2006). Plants are considered to respond to nutrient status in soil through changes in RSA or through exudation of organic acids that alter rhizosphere chemistry. These changes include root foraging responses such as increased root branching (Desnos 2008) and root hair density (Bates and Lynch 2000), root proliferation in P rich patches (Robinson 1994), variation in gravitropism (Ge et al. 2000), the ability to alter rhizosphere pH (Jianguo and Shuman 1991), and through association with microorganisms (Rodríguez and Fraga 1999) and increasing P solubility via root exudates (Bais et al. 2006).

7.1.1 *Increasing the likelihood of encountering soil P*

Generally, plants increase root:shoot ratios in response to P deficits through root foraging and slowing shoot growth (Kirk et al. 1998). In split chamber experiments, it has been shown that 75% of rice root biomass was located in the high P medium side when compared with the growth limiting side, although P was distributed throughout root tissues (He et al. 2003). In common bean, plants with a higher P uptake efficiency (PUE) had more adventitious rooting under low P conditions than under replete P (Lynch and Brown 2008). P uptake efficiencies have been related to increased root length, overall root biomass and number of roots, but this varies with plant species and even cultivar (Ni et al. 1998). Increased lateral root production is also related to PUE (Lynch and Brown 2001). In Arabidopsis, plants with a

limited ability to initiate lateral roots had a reduced PUE when compared to wildtype plants (Fitter et al. 2002; Waisel et al. 2002).

Root hairs increase the available surface area per unit root length which can influence potential for P accumulation in P deficient conditions. Development of longer root hairs or a higher density of root hairs has been identified as a mechanism for adaptation to variations in nutrient availability, specifically P (Bates and Lynch 2000). Root hair initiation has also been correlated with reduced P availability, which provides further evidence for the role of root hairs in P acquisition (Schmidt and Schikora 2001). A computer model simulating root hair uptake of P in P starved plants showed that uptake occurs within minutes and an order of magnitude greater in soils than in solution for plants with more root hair surface area (Leitner et al. 2010). However, through mathematical modelling of the influence of root hairs versus the root itself in uptake of P, Keyes et al. (2013) determined that in wheat, the root surface took up more P than the root hairs because of the larger root surface area.

7.1.2 Root induced changes to the rhizosphere to make P more available

In rice, P uptake is correlated with pH changes in the rhizosphere as pH can alter the availability of organic and inorganic forms of P through transformation of the P compounds (Jianguo and Shuman 1991; Kirk et al. 1998). Often these pH changes are related to plant alteration of the rhizosphere depending on soil conditions such as waterlogging induced by flooding. In rice growing in waterlogged soils, pH changes are attributed to oxygen transport to the rhizosphere through aerenchyma, which are specialised root structures formed through programmed cell death to create channels for gas transport (Fig. 7-1). Oxygenation of the rhizosphere in flooded soils has also been linked to changes in soil P concentration

and P availability (Kirk and Saleque 1995). Rice has also been shown to increase solubility of P in soils that were not saturated or anoxic (Kirk et al. 1999).

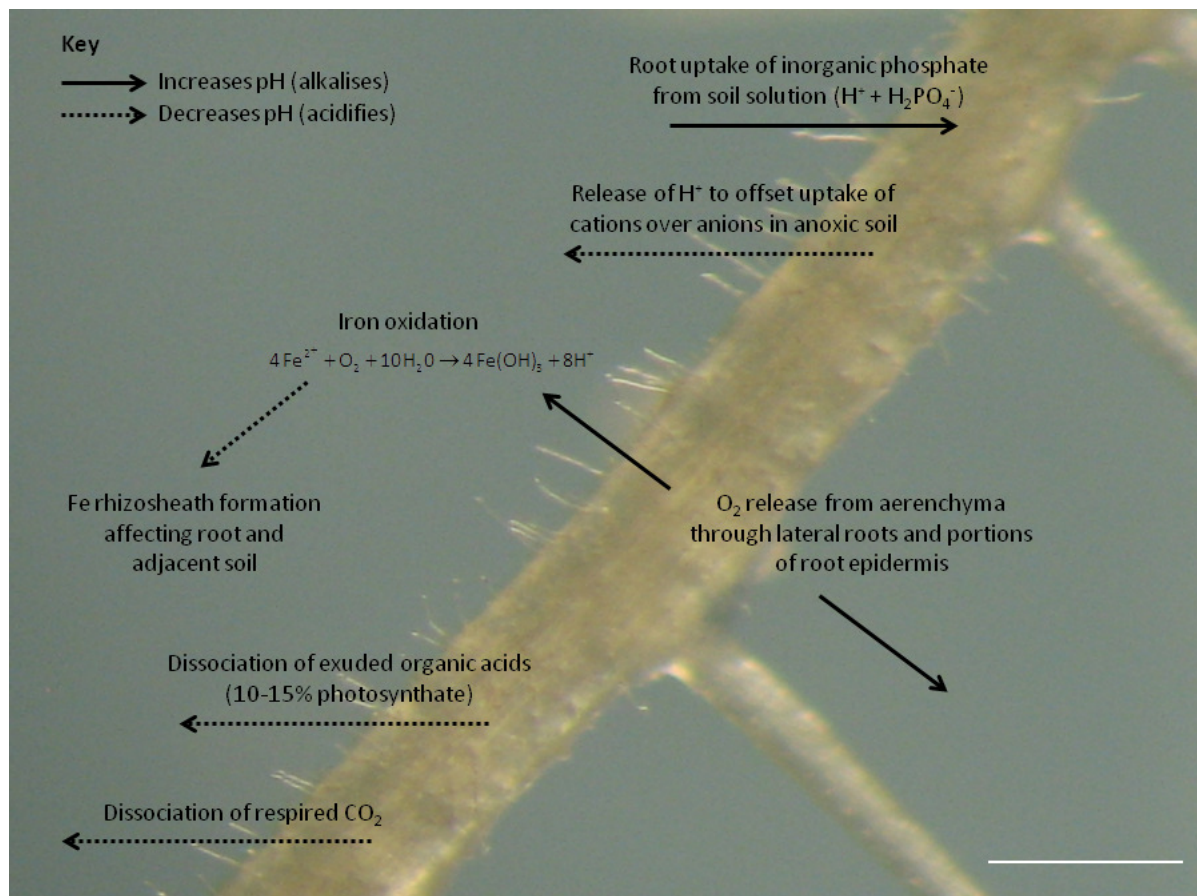


Fig. 7-1: Influence of P uptake itself, release of O_2 from aerenchyma and root exudates on the pH of the rhizosphere in submerged soils. Information compiled from Kirk (2004); image and figure generated by S. Zappala. Scale bar = 500 μm .

Plant roots can add compounds and molecules to soils that increase the availability of P for plant uptake. These root exudates such as malate and citrate can alter the pH of soil within the vicinity (0.1 to 4 cm) of the root system (Oburger et al. 2009). Liu et al. (1990) correlated a 37-61% increase in excretion of citric acid with P stress dependent on variety, which was considered to increase availability of inorganic P forms. This exudation and direct influence on pH and oxygenation of the rhizosphere can result in development of iron rhizosheaths which impact nutrients available to rice under flooded conditions (Benckiser et al. 1984).

The aim of the following experiments was to elucidate the aspects of OsAUX1 related changes in root development and growth related to the trends in P uptake observed in the soil-based experiments. In particular, to investigate how the root system influences P uptake as available soil P increases as well as the root variations which would influence total P uptake in the split column top treatments. Additionally, to examine the potential role of AUX1 in these adaptations to the availability of soil P.

7.2 Materials and Methods

7.2.1 OsAUX1: pro β -glucuronidase marker

The *E. Coli* enzyme β -glucuronidase (GUS) was used as a reporter for the OsAUX1 promoter as described in Jefferson et al. (1987) and the OsAUX1:proGUS ligation is detailed in Parker (2010). The blue colour developed when the enzyme reacted with the (5-bromo-4-chloro-3-indolyl glucuronide) substrate indicated promotion of the OsAUX1 at a cellular level.

OsAUX1:proGUS plants were grown on 25% MS agar media (pH 5.8). All plants were placed in deep well trays and covered in X-Gluc solution. The plants in X-Gluc were vacuum infiltrated for 15 min at room temperature and then incubated at 37°C for three hours. The tissue was then incubated at 37°C for 72 h in chloral hydrate solution (8 g chloral hydrate: 2 ml water: 1ml glycerol) to clear the roots. The cleared roots were mounted on glass slides and observed under a stereo microscope (10x magnification for primary root and crown root, 20x magnification for large lateral and 25x magnification for small lateral root).

7.2.2 Real time quantitative polymerase chain reaction (RT-qPCR)

Plants were grown on 25% MS agar (pH 5.8) after seeds were sterilised. There were ten replicates for each tissue type. Coleoptile and radicle were harvested at three days after

sterilisation (DAS). Primary root, crown root and lateral roots at ten DAS. Leaves were excised during crown root emergence (Leaf CR) at five DAS and when lateral roots began to develop on crown roots (Leaf Lat) at ten DAS. Tissues were immediately frozen in liquid nitrogen and stored at -80°C in preparation for RNA extraction. RNA was extracted using the RNeasy® Mini Kit (Qiagen) protocol which was slightly modified by using TRIzol Reagent (Invitrogen Cat. No. 15596-026) for cell lysis. A NanoDrop 1000 Spectrophotometer, Thermo Fisher Scientific) was used to verify RNA concentration and purity. cDNA was synthesised by reverse transcribing the RNA (500 ng RNA per 40 µL reaction; 100 µM Oligo dT, 500 µM dNTPs, 5X Buffer, 0.01M DTT and reverse transcriptase (Invitrogen SuperScript® II) at 42°C for 50 min and neutralised by holding at 70°C for 5 min.

Expression profiles were based on cDNA generated from RNA extracted from excised tissues. RT-qPCR was performed using SYBR® Green I dye (Invitrogen) in 384-well optical reaction plates. The plate was heated to 95°C over 5 min followed by 50 extension cycles of 10 sec denaturation at 95°C and annealing for 30 sec at 60°C. All reactions had four replicates. There was significant variability in actin (ACT11) expression between the *Osaux1* mutants and wildtype. Actin is commonly used as the housekeeping gene in RT-qPCR rice studies, but can vary under various hormone and stress treatments (Jain et al. 2006). β -Tubulin (Accession No. AK072502) was used as a housekeeping gene because it was found to be stable between the three lines (forward primer (GCTGACCACACCTAGCTTTGG) and reverse (AGGGAACCTTAGGCAGCATGT)). Primers used to quantify OsAUX1 expression were OsAUX1 forward (AGTTTTGGTCGCCTTGTA) and OsAUX1 reverse (AGATCGTAGGGACCCATGC).

7.2.3 *Root hair and RSA characterisation on agar with varying P*

Plants were grown for seven days on P-free nutrient agar (pH 5.8) with differing amounts of phosphate added as potassium phosphate at low (3.12 $\mu\text{M P}$), replete (31.2 $\mu\text{M P}$), high (62.4 $\mu\text{M P}$) and toxic (312 $\mu\text{M P}$) levels. Two of each line (wildtype, *Osaux1-1* and *Osaux1-2*) were grown on each plate and arranged as assigned by random number. There were five replicate plates for each P level. The plates were imaged with a digital camera (Section 2.9.3) for assessment of coarse root architecture (primary root, number of crown roots and lateral roots). The picture was taken from the back of the plate to minimise any influence from condensation. The cover was removed and the plate was placed under a stereo microscope with 20x magnification and pictures of root hairs were obtained with a digital camera mounted onto the microscope.

7.2.4 *Iron rhizosheath SEM/EDX*

Six week old plants grown in P-free compost were fed weekly with a phosphate and iron supplemental solution. Compost was used instead of soil to enable full control of P and Fe content of the original mix. There were ten replicates for each plant line (wildtype, *Osaux1-1* and *Osaux1-2*). The plants were destructively harvested and root washed. Ten roots were chosen from each plant then frozen at -80°C overnight. The frozen root sections were then freeze dried (Edwards Freeze Dryer Modulgo M143, 10^{-3} mbar) for 48 h. Freeze dried samples of root tip and a 1 cm section taken from an area 5 cm above the root tip were mounted on 25 mm diameter carbon sticky discs. There were four replicates for each treatment (line X root section) making a total of 24 samples. The mounted samples were spray coated with ca. 30 nm carbon and imaged by Scanning Electron Microscopy (SEM; FEI XL30 with INCA X-sight 6650, Oxford Instruments). Elemental analysis was performed with

energy dispersive X-ray microanalysis (EDX) in relation to carbon fraction. The EDX was performed at two locations on each sample at 400x zoom.

7.2.5 pH under varying phosphate

Agar growth media (pH 5.8) with four P concentrations (as described in Section 6.2.5) was doped with bromocresol green at 0.006% (CAS 76-60-8). Bromocresol green is a pH indicator that changes yellow at pH 3.8 and darkens to blue at pH 5.4. Sterilised and germinated rice seed was planted onto the plates and grown for seven days. One seedling of each line was planted in each of the plates in randomly assigned positions. The plants were imaged with a digital camera from the back of the plate. The images were then cropped to the same size (2.5 cm wide 7 cm high) in Image J.

Colours were segmented into areas similar to the main root, root tips, rhizosphere (most yellow) and bulk (darkest, uninfluenced area) using the Image J Colour Segmentation Plugin (Daniel Sage, Ecole Polytechnique Fédérale de Lausanne ([EPFL](https://www.epfl.ch))). Colours were chosen by selecting several points of representative colour within each region (root tip, root, rhizosphere and bulk) and averaging the red-green-blue (RGB) colour values (Fig. 7-2).

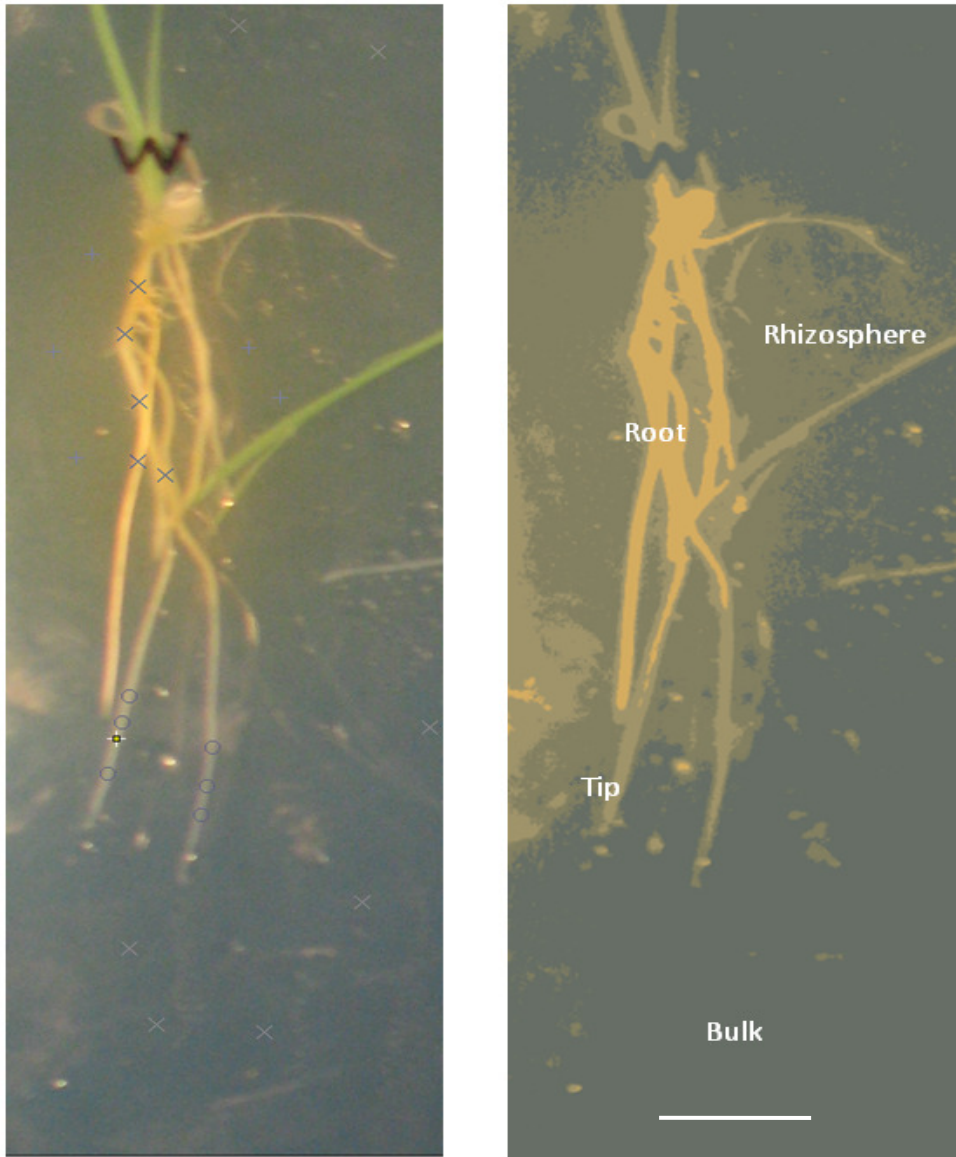


Fig. 7-2: Colour segmentation setup. Four areas of colour segmentation related to pH were distinguished: Root, Tip, Rhizosphere and Bulk (uninfluenced). The areas were defined by selection of several representative colour points (marked X in left image) and the Plugin produced a colour coded area for each of the four segmented areas (right hand image). Scale bar = 1 cm.

Table 7-1: Comparison of colour segmentation algorithms. An image of rice roots grown on pH indicator containing agar was analysed using the Image J Colour Segmentation Plugin (Daniel Sage). The K-Mean algorithm was faster and also produced a more conservative result for the influence of the root system on pH of surrounding media as determined by the percentage of total picture area.

	Original	K-Mean Algorithm	Hidden Markov Model
			
% Colour A-Root	N/A	4.47	5.00
% Colour B-Root Tips	N/A	9.74	18.75
% Colour B-Rhizosphere	N/A	26.36	27.04
% Colour D-Bulk	N/A	59.43	49.22

These were then segmented using the Joint Colour Channel and K-Mean algorithm to provide the most conservative colour segmentation. The Joint Colour Channel algorithm presumes there is a potential overlap of the colours and this was appropriate because the pH colour changes are gradated in the agar medium. The K-Mean clusters the image into groups based on the pixels chosen to represent each region. The K-Mean algorithm also ensures that similar colours are near each other in distance and that dissimilar colours are as far away as possible from the section of similar colour.

Although considered a disadvantage in some colour segmentation applications, K-mean also requires the number of segmentation areas to be defined (Dong and Xie 2005), which ensured that the pH colour change area could be classified as desired into root, root tip, rhizosphere and bulk areas. This produces regions as dissimilar to each other as possible both spatially and colour-wise. As shown in Table 7-1 the Joint Colour Channel-K-Mean segmentation method provided the most consistent and discrete segmentation as well as a faster calculation time when compared to the only other grouping option in the Image J Colour Segmentation Plugin, the Hidden Markov Model (Celeux et al. 2003; Jain and Dubes 1988; Ramos and Muge 2000). Segmented areas of colour were expressed as a percentage of total image size to provide an indication of the amount of colour/pH change contributed by the root, root tip, rhizosphere and bulk.

7.2.6 *Aerenchyma measurement*

Images of the root systems obtained via X-ray CT (from Section 6.2.4) were used to measure intro-root air-filled pore space within the root systems. Air-filled pore space volume was measured in the VGSM Volume Analyser tool by manually thresholding near-black air-filled

pores from lighter grey root material (Fig. 7-3). There was no thresholding algorithm available in VGSM thus manual segmentation was required. This air space was considered as aerenchyma for the purposes of this comparison. The air space could also be non-aerenchymatous air-filled pores within the root, but these are uncommon.

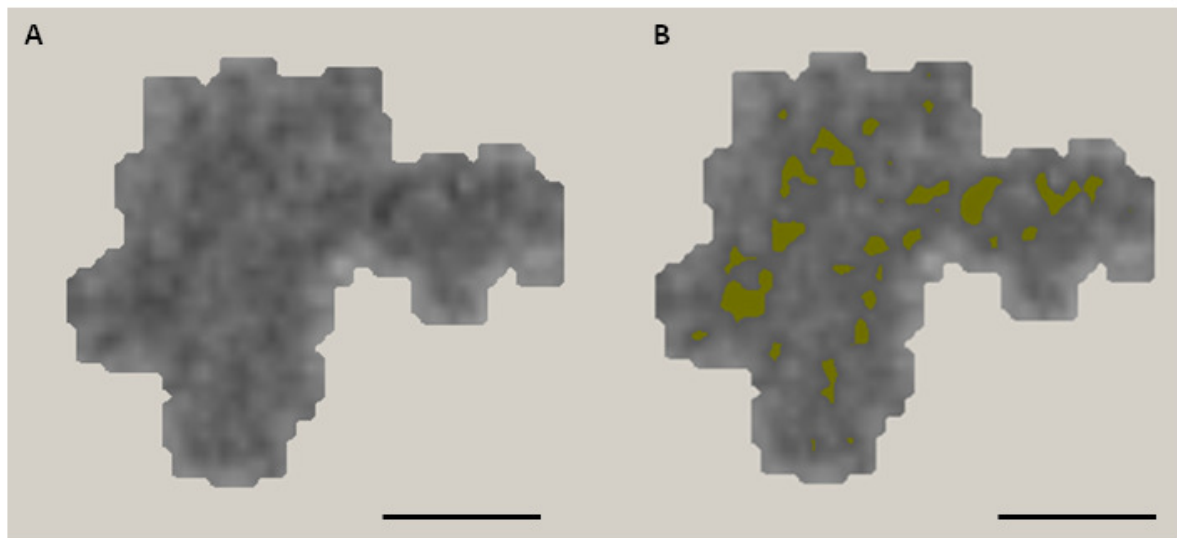


Fig. 7-3: X-ray CT cross section of a segmented rice root (A) and subsequent isolation of intra-root air space (aerenchyma) as shown by yellow areas (B). Air space is designated by near-black pixels in the greyscale X-ray CT image. Scale bar is equivalent to 0.5 mm.

7.3 Results

7.3.1 *Osaux1* genotype and potential indicators for P uptake

7.3.1.1 *OsAUX1:GUS* expression

The rice primary root (Fig. 7-4 A), crown root (Fig. 7-4 B) and large lateral root (Fig. 7-4 C) displayed *OsAUX1* expression in the tip as determined by presence of blue colour from GUS signalling. The stele and cells adjacent to emerged lateral roots displayed GUS expression on crown roots (Fig. 7-4 D). Small lateral roots did not have a positive GUS signal (Fig. 7-4 D).

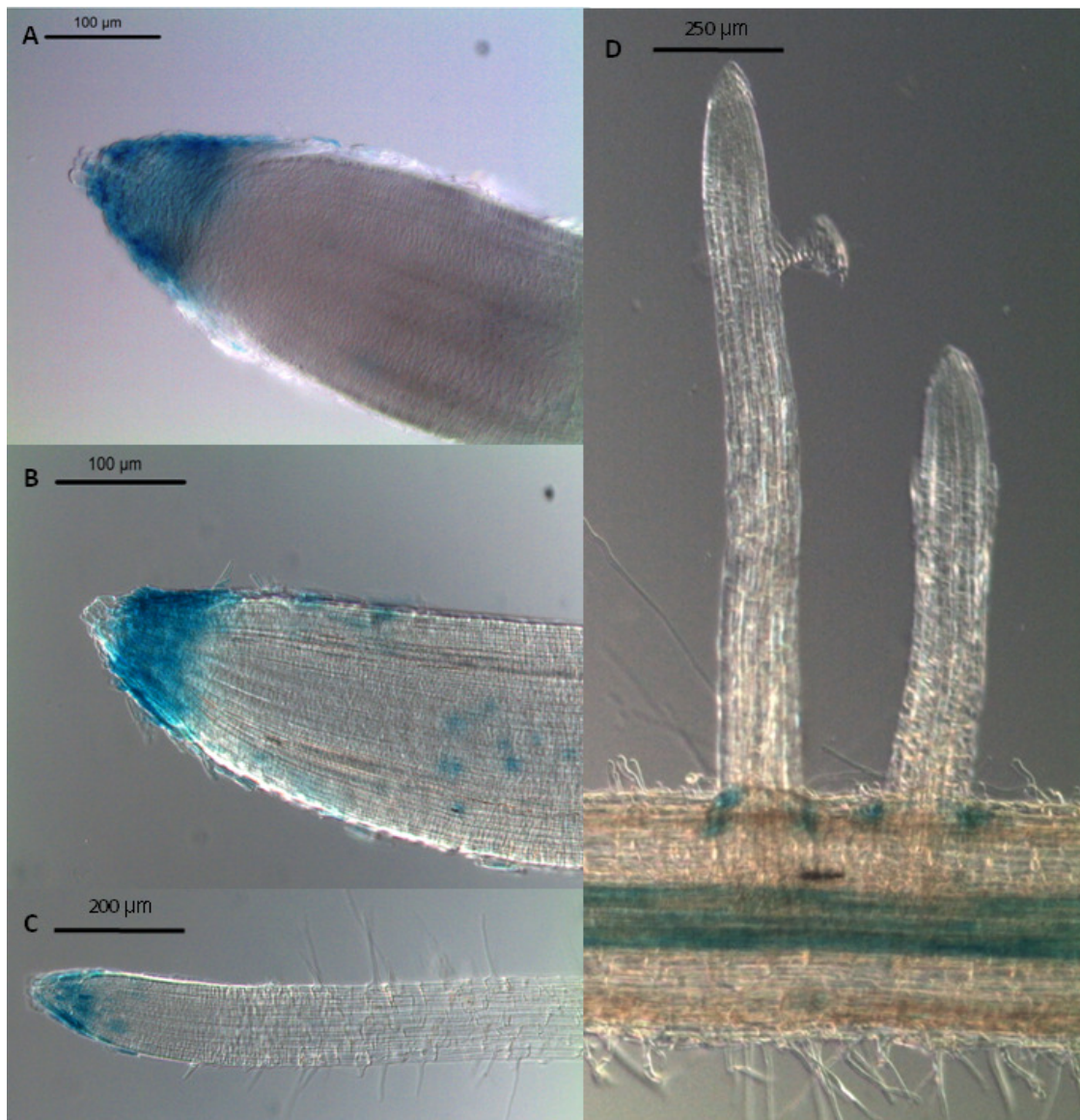


Fig. 7-4: *OsAux1*:GUS expression delineated by blue colour was observed in the tip of the primary root (A), crown root (B) and large lateral root (C). GUS expression was also identified in the cells adjacent to the emergence location of lateral roots and in the stele of crown roots (D). Note Panel D also shows no *OsAUX1* expression in small lateral roots.

7.3.1.2 *OsAUX1* RT-qPCR

The *Osaux1* loss of function mutants had relatively lower *OsAUX1* expression as determined by RT-qPCR in both root and shoot when compared to wildtype. Shoot expression was lowest in *Osaux1-1*. Both mutants had a similar level of *OsAUX1* expression in shoot tissues. There was no discernible difference in wildtype root and shoot expression of *OsAUX1*.

However, in the mutants, shoot OsAUX1 expression was significantly ($P = 0.010$) higher than expression in the root (Fig. 7-5 A).

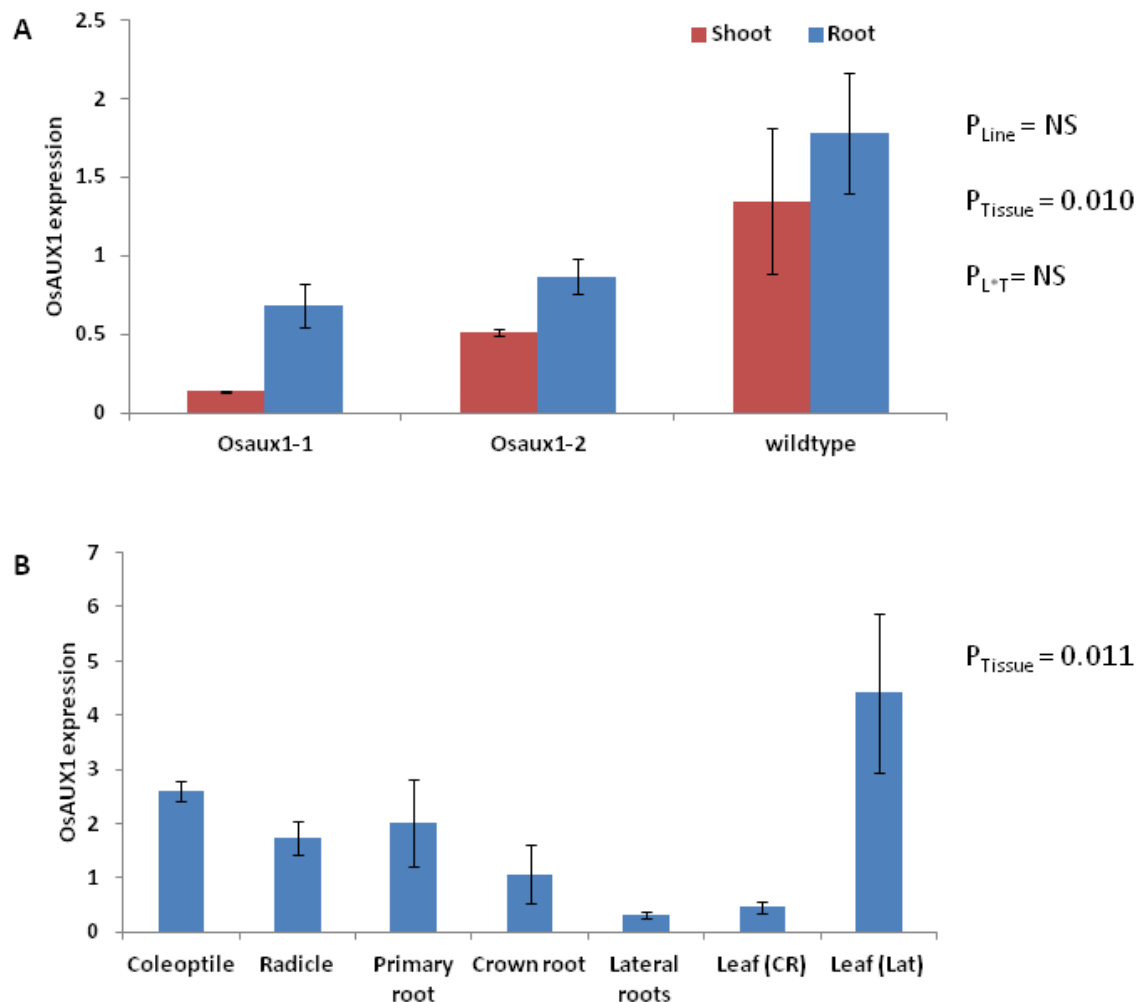


Fig. 7-5: Expression of OsAUX1 in both shoot and root (A). Expression in above and below-ground wildtype tissues (B). Leaf (CR) is leaf tissue after crown root initiation and Leaf (Lat) is leaf material harvested after lateral roots are visible on the primary root. Error bars represent standard error of the mean.

When comparing various wildtype tissues at different time points, there was a significant ($P = 0.011$) difference between root and shoot tissues (Fig. 7-5 B). Generally the main root structures had similar OsAUX1 expression. Three days after sterilisation, the radicle (embryonic root) had significantly ($P = 0.011$) less OsAUX1 expression than the coleoptile (embryonic shoot). Primary root and crown root tissues had similar expression to the

radicle. Most notably, lateral roots had a significantly ($P = 0.011$) lower OsAUX1 expression at day ten.

The shoot had large variation in OsAUX1 expression over time. Initially, coleoptile expression was on par with root tissues. At day five, there was a dramatic decrease in OsAUX1 expression for shoot tissues at crown root emergence. By day ten, leaf tissues showed a marked increase in expression which coincided with early stages of lateral root development on the primary root and crown roots.

7.3.2 *Primary root elongation and lateral root development on agar*

There was no significant difference between the length of primary roots of agar grown plants under varying P concentration. Additionally, OsAUX1 did not significantly influence the ultimate length of the primary root after seven days of growth (Fig. 7-6 A). Primary root length ranged between 46.3 mm (*Osaux1-1*, 3.12 μM) and 72.6 mm (*Osaux1-2*, 31.2 μM).

Lateral root number was significantly ($P = 0.017$) affected by the amount of phosphate present in the growing media as well as the expression of OsAUX1 ($P < 0.001$) (Fig. 7-6 B). The number of lateral roots on the primary root was consistently high in *Osaux1-2*; this was significant for the two highest P treatments. At 3.12 μM P, all lines showed a relatively low number of lateral roots ranging between 6.9 (*Osaux1-1*) and 11.6 (*Osaux1-2*). *Osaux1-1* had a consistently low number of lateral roots over all P treatments. In the highest P treatments, wildtype and *Osaux1-1* had a similar number of lateral roots. Wildtype had the most lateral roots in the replete P treatment at 31.2 μM . Higher P concentrations had a negative effect on wildtype lateral root number.

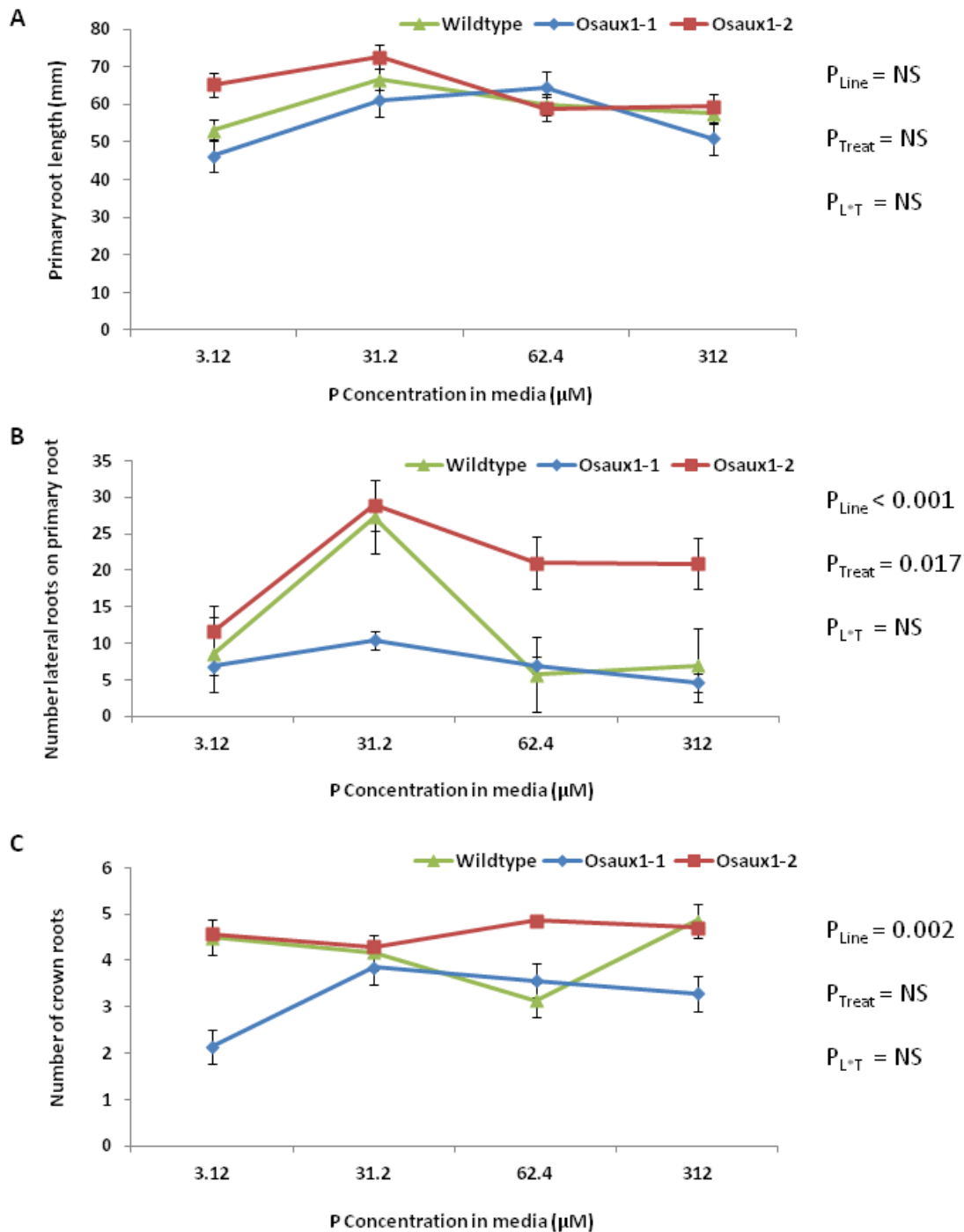


Fig. 7-6: Coarse root development under uniform P conditions. Measurements were taken from seven day old plants of wildtype (triangles), *Osaux1-1* (diamonds) and *Osaux1-2* (squares). Error bars represent standard error of the mean, $n = 10$.

Overall, there was a significant difference in crown root number between the genotypes ($P = 0.002$) but no significant influence from the level of P present (Fig. 7-6 C). The number of crown roots at day seven was lowest for *Osaux1-1* at 3.12 μM P. In general, crown root

number remained consistent along the replete and excessive P treatments for the reduced OsAUX1 function mutants. Wildtype crown root number dipped at 62.4 μM P, but was not significantly different to other P treatments. Mean number of crown roots ranged between 2.14 (*Osaux1-1*, 3.12 μM P) and 4.86 (wildtype, 312 μM P).

7.3.3 Root hair phenotype in agar

Wildtype had significantly ($P = 0.014$) longer root hairs under all P treatments except the highest at 312 μM . Wildtype root hair length increased between low P (3.12 μM) and replete P (31.2 μM) and then steadily decreased as P concentration increased (Fig. 7-7 A). *Osaux1-2* showed a similar variation in root hair length with P concentration where the length increased between low and replete P and then steadily declined as P concentrations increased above 31.2 μM . The knockout mutant *Osaux1-1* had highly variable reaction to P concentration. As with the other lines, *Osaux1-1* root hair length increased between low and replete P treatments, but then decreased at 62.4 μM P and then decreased again at the highest P level.

Wildtype had significantly ($P = 0.009$) higher root hair density in all P treatments except the highest level (Fig. 7-7 B). The wildtype root hair density decreased as P concentration increased. Root hair density for wildtype ranged between 110 and 150 root hairs mm^{-1} . At the lowest P concentration, the mutants had root hair density between 73 and 78 root hairs mm^{-1} . Under replete P *Osaux1-1* had the lowest root hair density of the three lines which

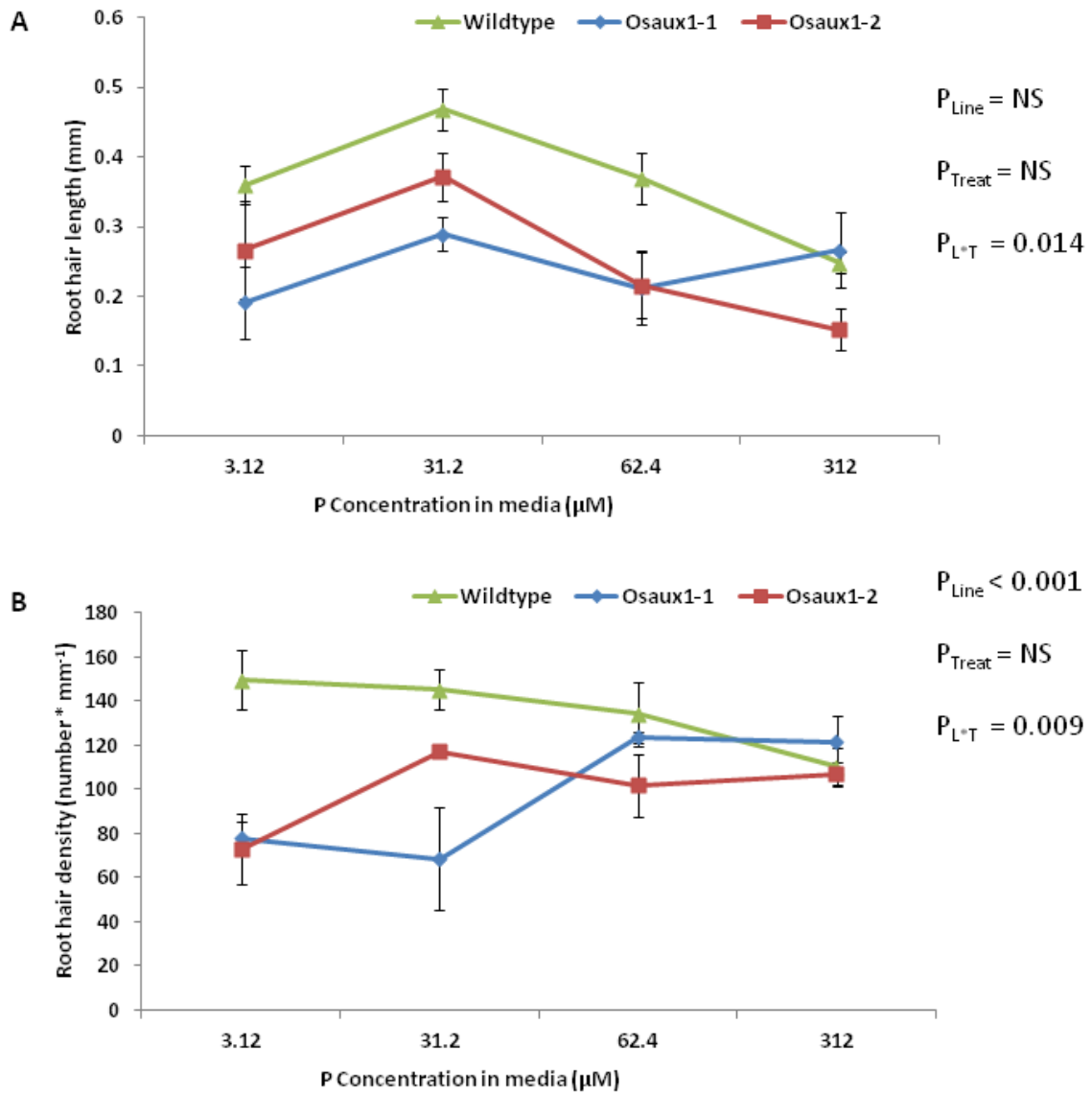


Fig. 7-7: Root hair length (A) and root hair density (B) in response to available phosphate for Wildtype (triangles), *Osaux1-1* (diamonds) and *Osaux1-2* (squares). Error bars represent standard error of the mean and $n = 10$.

was 68 root hairs mm^{-1} that then increased under the higher P levels from between 122 and 124 root hairs mm^{-1} for 62.4 μM P and 312 μM P respectively. *Osaux1-2* had a similar stabilisation at the highest P levels with 102 and 107 root hairs mm^{-1} for 62.4 μM P and 312 μM P respectively. In contrast, wildtype root hair density decreased between 62.4 μM P and 312 μM P. Fig. 7-8 contains representative images of the root hair density and length under the various P conditions.

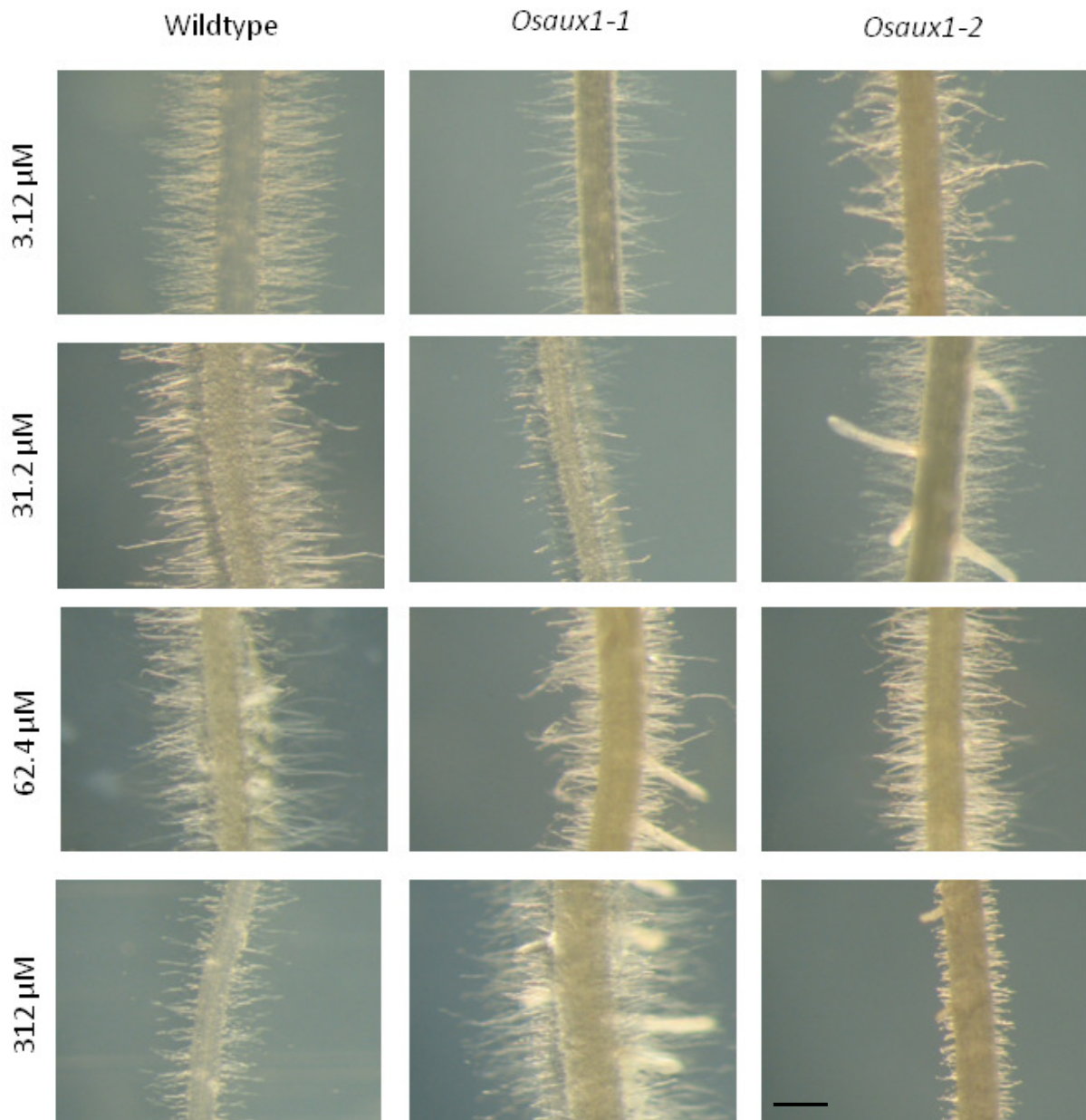


Fig. 7-8: Variation in rice root hair length under varying phosphate concentration when grown on agar. Scale bar represents 200 μm .

7.3.4 Iron rhizosphere development in soil grown plants

As measured by EDX, there was no significant difference between the proportion of P at the root tip for wildtype and *Osaux1-2* with 16.6 and 18.0 % respectively (Fig. 7-9 A). The proportion of P present on the root surface was significantly ($P < 0.001$) higher in the mid root section (5 cm from root tip) than at the root tip. Mid root P was not significantly

different between the three lines. The proportion of P on the mid root surface ranged between 1.7 (wildtype) and 3.3% (*Osaux1-1*).

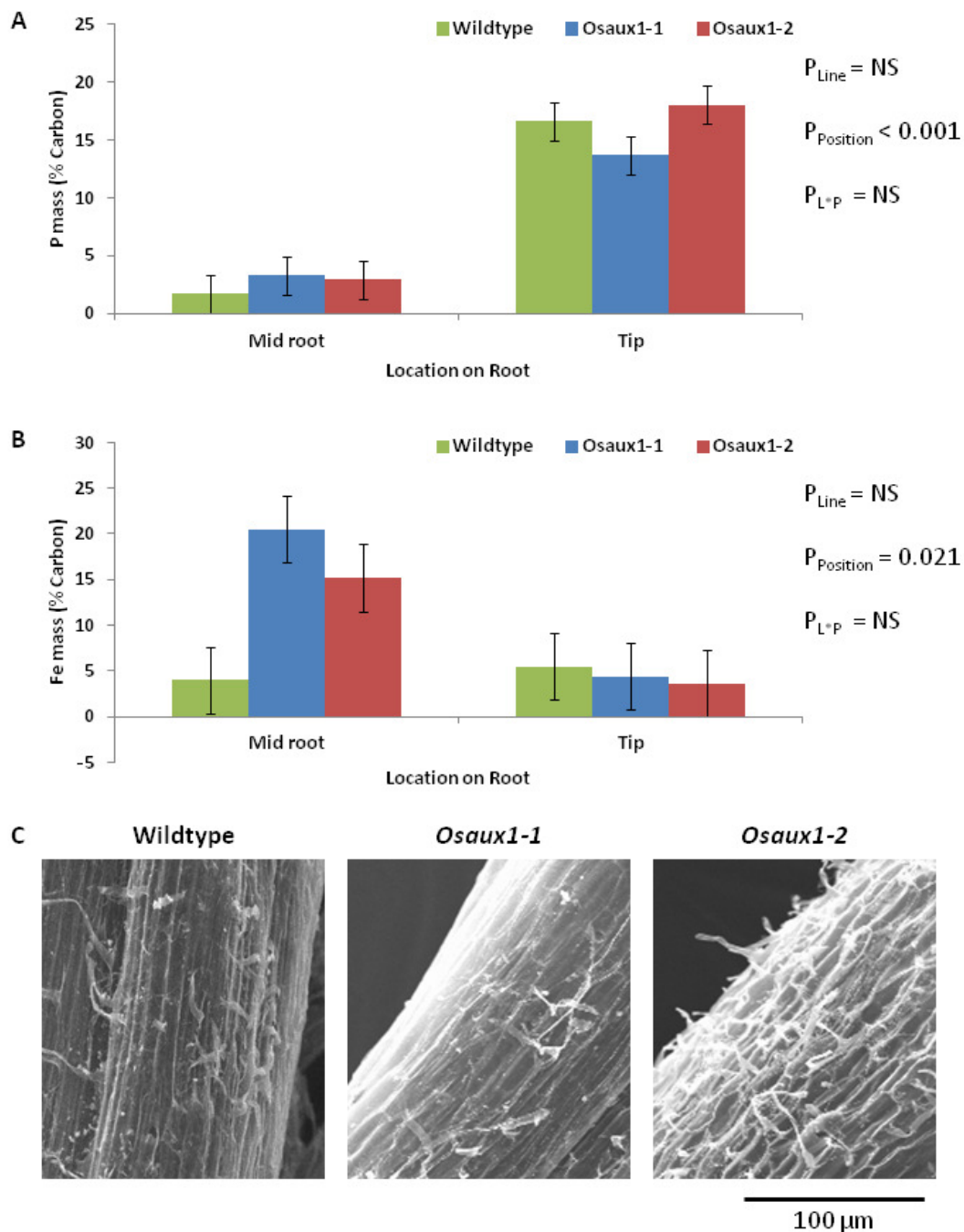


Fig. 7-9: EDX measured concentrations of elemental P (A) and Fe (B) on root surfaces. Root hairs visualised with SEM (C). Error bars represent standard error of the mean, n = 4.

Fe at the root tip was not significantly different between the three lines and was an order of magnitude lower than P found at the root tip (Fig. 7-9 B). There was a significant ($P = 0.021$)

difference between Fe concentrations at mid root and the tip in the mutants. Iron at the tip ranged between 3.6% (*Osaux1-2*) and 5.5% (wildtype). In contrast, wildtype had lower Fe at mid root than *Osaux1-1* or *Osaux1-2*. Wildtype Fe was significantly lower ($P = 0.021$) at 4% whereas *Osaux1-1* and *Osaux1-2* had 20.5% and 15.2% respectively. In SEM images, the mid root sections of *Osaux1-2* had the greatest number of visible root hairs (Fig. 7-9 C). Wildtype had less visible root hairs than *Osaux1-2*. *Osaux1-1* had the fewest amount of root hairs. It should be noted that the roots were grown in soil, root washed and then freeze-dried in preparation for SEM/EDX. Exploded cells and damaged root hairs were observed and are a common difficulty when freeze drying roots (Campbell and Rovira 1973), which could skew the results. Exploded cells can mean that the EDX results are for the inside surface of the cell rather than the outside of the epidermis and would reduce the amount of observed Fe if not the P that would be expected in a rhizosheath.

7.3.5 pH under varying P concentration in agar

Wildtype, *Osaux1-1* and *Osaux1-2* had no significantly different changes in pH when grown on agar doped with bromocresol green, a pH indicator (Fig. 7-10). Under 312 μM P, *Osaux1-2* had a smaller proportion of the image occupied by pH similar to the main root (Fig. 7-10 A). Under the lowest P concentration, areas with similar pH to the root tips represented a lower proportion in *Osaux1-1* than in wildtype or *Osaux1-2* (Fig. 7-10 B). However, under these same low P conditions, areas with similar pH adjacent to the root (rhizosphere) were higher in *Osaux1-1* than in wildtype (Fig. 7-10 C). In replete (31.2 μM P) conditions, wildtype had slightly more area classed as rhizosphere than *Osaux1-2*. Under low P, the uninfluenced, bulk area was higher in wildtype than *Osaux1-2* and lower under replete P (Fig. 7-10 D).

Wildtype had smaller uninfluenced area than *Osaux1-1* under the highest P treatments (62.4 and 312 μ M P).

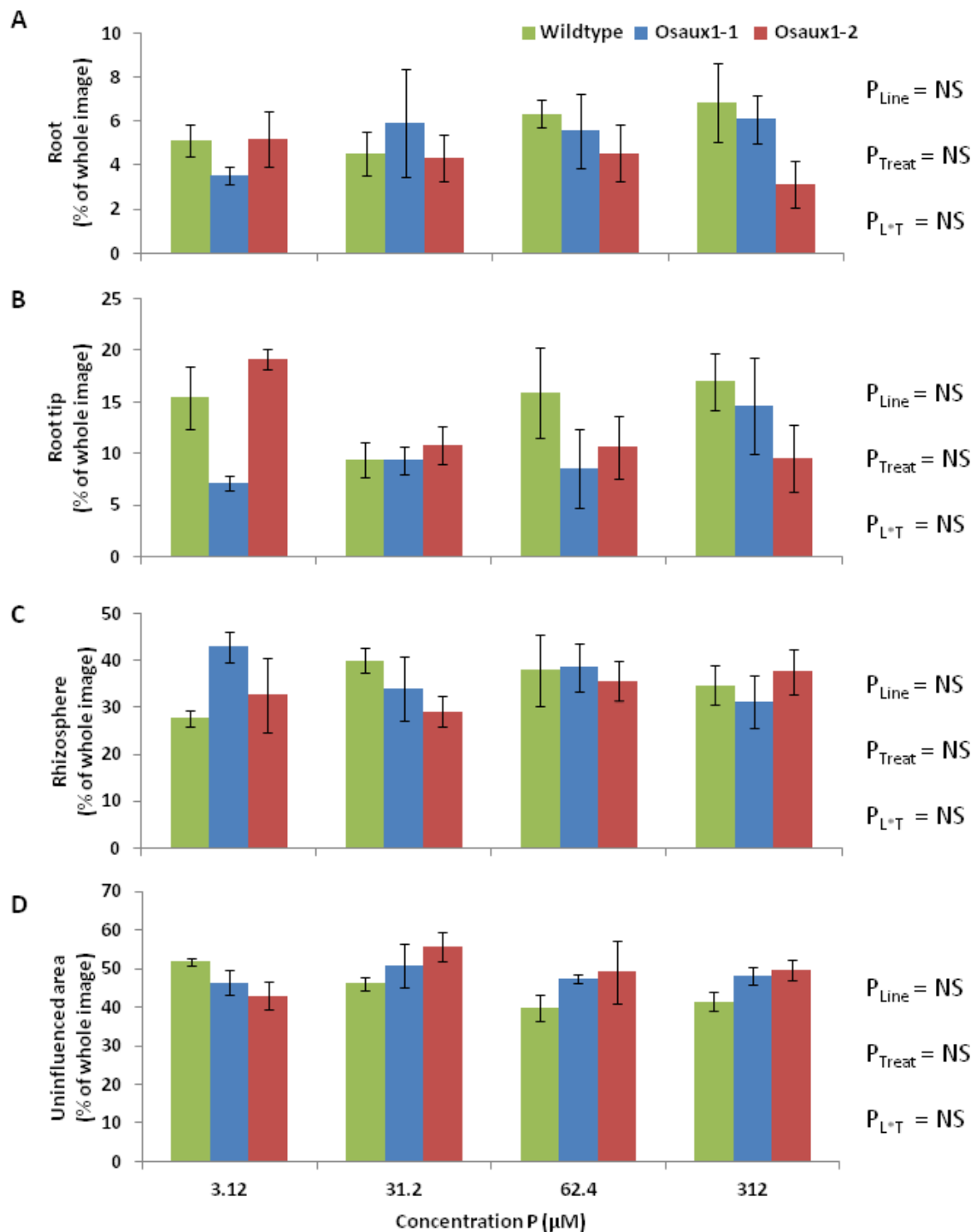


Fig. 7-10: Area of root system influence in agar doped with pH indicator (Bromocresol green) under varying P conditions. Error bars represent standard error of the mean, n = 4.

7.3.6 *Aerenchyma in soil grown plants*

Under the uniform P treatments, wildtype and *Osaux1-1* had no significant difference in total intra-root air space volume (Fig. 7-11 A). The lowest total intra-root air space was found in *Osaux1-1* under high P with 41.1 cm³. There was a significant (P = 0.024) difference in air space between uniform P treatments with sufficient P yielding the highest volume of root air space.

As found under the uniform P treatments, there was no significant difference in intra-root air space between wildtype and *Osaux1-1*. The level of P significantly (P = 0.010) reduced the amount of intra-root air space in both plant (Fig. 7-11 B). The split top treatments produced roots with more intra-root air space than the uniform treatments; for example, wildtype had an average air space under split top sufficient of 204.6 cm³. Also, there was a significantly (P = 0.010) higher total air space under split top sufficient conditions in comparison to split top high P.

For both split bottom treatments, *Osaux1-1* had significantly (P = 0.011) higher total air volume within the roots (Fig. 7-11 C). The highest total intra-root air space was measured in *Osaux1-1* under split bottom high P at 258.1 cm³. Wildtype had its highest air space volumes under the split bottom P treatments which were ca. 170 cm³. There was no significant difference in accumulated air space between split bottom P levels.

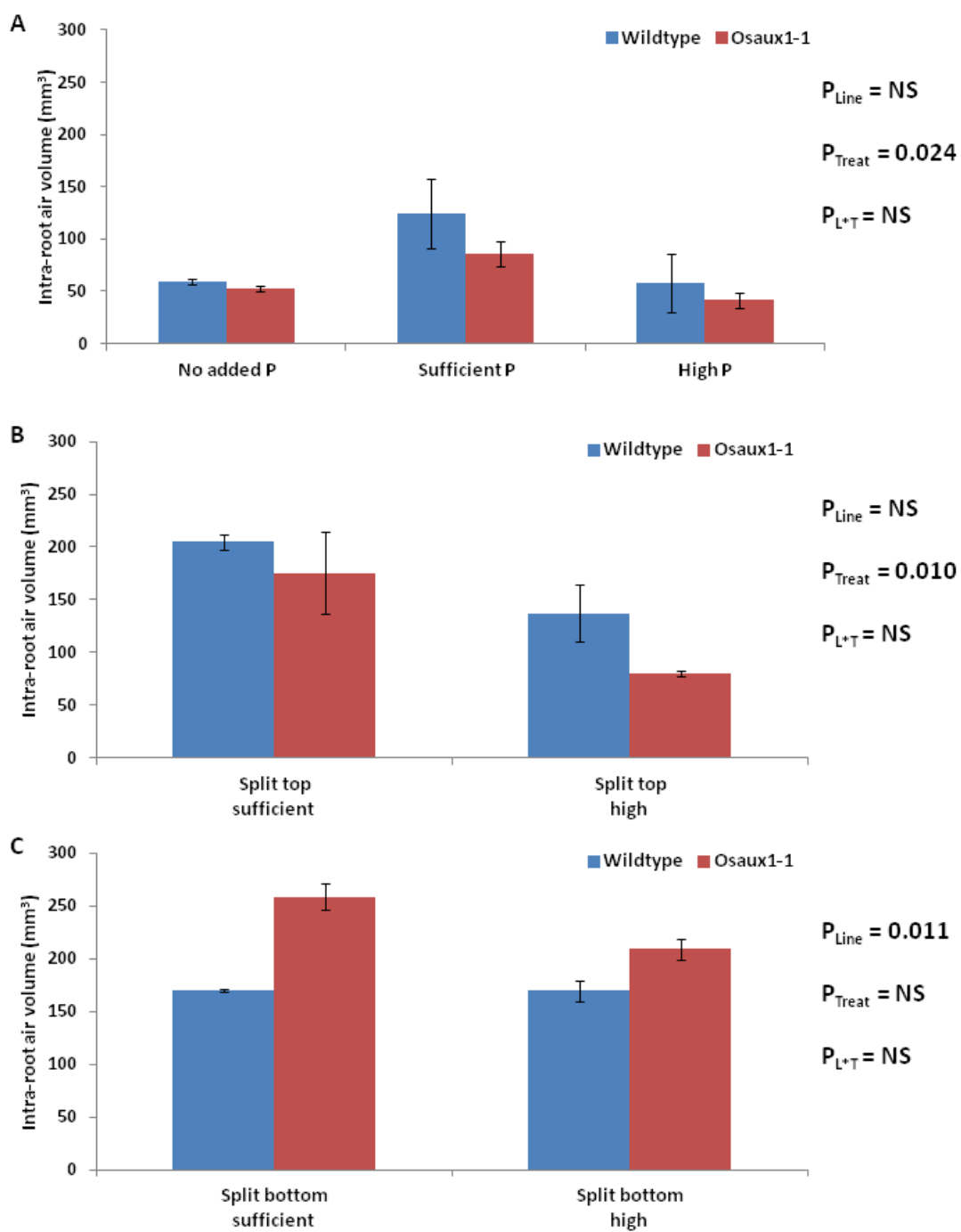


Fig. 7-11: The total volume of air space within roots grown in P amended soil for uniform P (A), split top sufficient (P in top 4 cm) (B), and split bottom (P in bottom 6 cm) conditions (C). Error bars represent standard error of the mean.

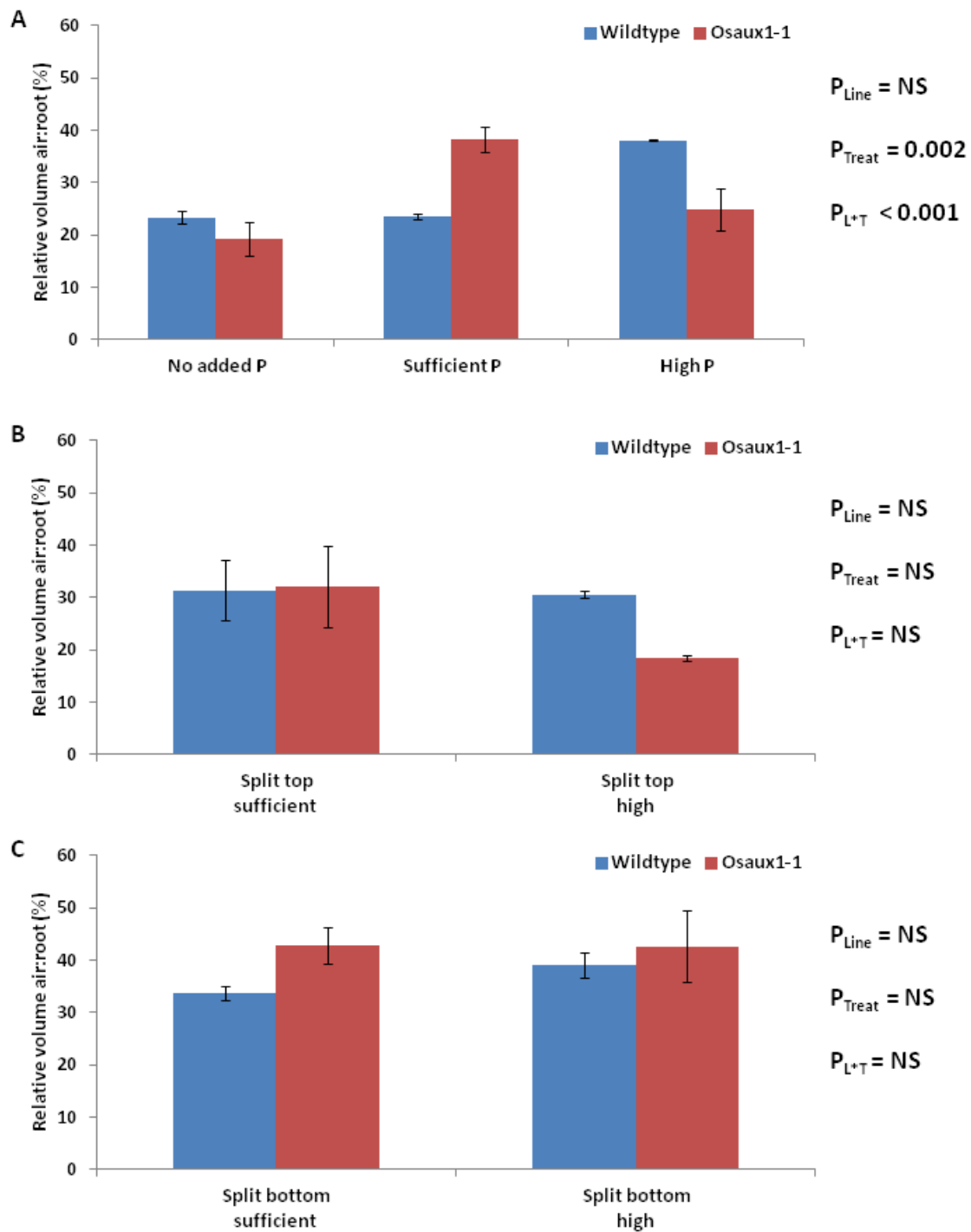


Fig. 7-12: Root air space as a proportion of total root volume air under uniform P (A), split top (B) and split bottom (C) treatments. Error bars represent standard error of the mean.

When measured as a proportion of total root volume, the intra-root air space showed a different pattern from total intra-root air volume (Fig. 7-12). In replete (sufficient P)

conditions, *Osaux1-1* designated significantly ($P < 0.001$) more root system volume to aerenchyma than wildtype (Fig. 7-12 A). When subject to toxic P levels at initial stages of root system development, wildtype had a significantly ($P < 0.001$) higher proportion of total root volume occupied by air space than *Osaux1-1* (Fig. 7-12 A). The proportion of air under split top conditions was higher in wildtype (Fig. 7-12 B). Under split bottom P, there was no significant difference between the proportion of air between the lines or under the sufficient and high P (Fig. 7-12 C). However, the highest proportion of air in roots was found under the split bottom P treatments.

7.4 Discussion

From this work, it is clear that OsAUX1 significantly enhances root hair length and root hair density on agar as well as Fe accumulation on the root surface for plants grown in soil. Root hairs were often 30 to 50% longer (ca. 100 μm) in wildtype than *Osaux1-1* except under the toxic P conditions, where wildtype would be expected to reduce carbon allocation to roots (Fig. 7-8). Root hair density was also almost twice as large in wildtype when compared to *Osaux1-1*. This variation in root hair characteristics impacts root surface area and thus potential root:soil contact, which would be expected improve phosphorus uptake. Fe accumulation on the root surface as measured by EDX was much lower in wildtype than in the *Osaux1* reduced function mutants. The link of OsAUX1 with root hair formation was reinforced by the *OsAUX1:proGUS* expression observed (Fig. 7-4), which indicates that OsAUX1 could be expected to have many traits observed in AtAUX1 such as influences on lateral root growth (Marchant et al. 2002) and root hair elongation (Rahman et al. 2002). Additionally, OsAUX1 could be linked to variation in aerenchyma formation under P stress.

OsAUX1 expression indicated a link to root morphology that definitely involves gravitropism and could be adaptation to P stress through root hair developmental changes (Fig. 7-5). OsAUX1:proGUS expression patterning was similar to AtAUX1:proGUS observed in *Arabidopsis* columella cells, stele and lateral root cap (Swarup et al. 2001). OsAUX1:proGUS tissue expression revealed the importance of OsAUX1 even in early stages of rice development (Fig. 7-4). Perhaps this is linked to subsequent gravitropic response of shoots at early stages of plant development. It is feasible that OsAUX1 could be linked to a gravitropic response in the shoot soon after germination. This gravitropic response of the coleoptile as well as circumnutation is required to ensure shoot growth above the water-line or soil surface to acquire sunlight for photosynthetic activity and carbon accumulation (Yoshihara and Iino 2005). Kutschera et al. (1991) showed that in comparison to air-grown plants, rice germinated under water (anaerobically) has greater shoot elongation in comparison to root elongation and a severe gravitropic response in the shoot. This could also be indicative of shoot derived auxin/IAA synthesis required for distribution through root and shoot tissues. As more auxin is required to regulate gravitropic response in primary roots, crown roots and initiation and elongation of both lateral roots and root hairs, auxin/IAA production should increase. In this study, roots had less OsAUX1 promotion, particularly in lateral roots which are generally considered agravitropic (Fig. 7-4). At these initial stages of growth that require auxin for gravitropic response and initiation of lateral roots and root hairs, shoot derived auxin distribution to the roots may be significantly influenced by OsAUX1.

Rice has a secondary challenge of dealing with variable soil chemistry induced by flooding. Perhaps this is part of the reason for variation in root hair elongation and density observed

in the wildtype that was not evident in the *Osaux1-1* plants. Chemical changes induced by roots within the rhizosphere are critical for nutrient uptake by rice (Jianguo and Shuman 1991; Wang and Shuman 1994), particularly in flooded conditions. Alterations in pH and the influence of root hair length and density could not be discerned by the agar doped with pH indicator because the range was too coarse to detect small differences in pH. This method has been shown to measure pH to 0.2 pH units (Liu et al. 2004). Finer methods such as micro-electrodes (Rudolph et al. 2013) or planar optodes (Blossfeld 2013) may prove more useful for detecting subtle differences in rhizosphere pH between wildtype and the mutants grown on agar or soil.

Although direct measurement of pH was not successful in distinguishing between the *OsAUX1* genotypes, iron rhizosheath formation indicated changes in the chemistry of soil adjacent to the roots. The rice rhizosphere has been linked to iron oxide accumulation under flooded conditions (Begg et al. 1994). P solubilisation and iron oxide accumulation have been correlated with rice root induced acidification with a radial influence of 4 to 6 mm (Saleque and Kirk 1995). In this work, there was a clear difference in iron and phosphorus accumulation on root surfaces as measured by EDX. Wildtype had less iron accumulation but was able to take up the same amount of P as *Osaux1-1*. There were a significantly higher number of root hairs in wildtype as observed on agar as well as in the SEM images. More root hairs in wildtype could mean higher local acidity through root exudation and thus less Fe accumulation on the root. However at these low pH levels (< pH 5), P has a tendency to complex with Fe and become insoluble and thus, unavailable to plants (Shen et al. 2011).

Curiously, *Osaux1-2* had the most visible number of root hairs (Fig. 7-8), but had similar Fe accumulation on the root surface to *Osaux1-1* (Fig. 7-9). This could indicate that it is not the presence of the root hairs, but possibly the activity of the root hairs that is impacting surface Fe accumulation. This in turn would affect how much P is trapped in the Fe rhizosheath since inactive root hairs would exude less organic acids and thus not acidify the rhizosphere as severely. Iron rhizosheath formation also depends on soil type, flooding (Ponnamperuma 1972) and the microbiological activity in the soil which all affect adsorption of Fe (Benckiser et al. 1984; Gotoh and Patrick 1974; Liu et al. 1990) and thus adsorption of P (Borggaard et al. 1990).

Another factor that has been linked to both P stress and auxin in this work is aerenchyma formation. Traditionally, aerenchyma are associated with anoxia stress induced by flooding such as that seen in maize (Mano et al. 2006), soybean (Thomas et al. 2005) and *Rumex* species (Laan et al. 1989). Aerenchyma formation has also been linked to N and P stress in maize (Drew et al. 1989). In this work, patterns of aerenchyma formation could be linked to soil P status and even P stress. Under sufficient P, wildtype allocated less of the root volume to air space than *Osaux1-1* and under toxic P, allocated significantly more than *Osaux1-1* (Fig. 7-12 A). The wildtype also had a larger proportion of aerenchyma than *Osaux1-1* when high P was allocated to the top portion of the soil column (Fig. 7-12 B). It should be noted that in rice, lysigenous aerenchyma form as a normal part of root development and is not solely part of a stress response to anoxia or nutrient stress. Rice aerenchyma formation does not vary in four week old seedlings whether they are grown in flooded or aerobic soil environments (John 1977).

Although there were differences in aerenchyma formation under some P conditions, particularly the high P, several of the treatments showed no difference between genotypes including no P (Fig. 7-12 A), split top sufficient (Fig. 7-12 B) and the split bottom treatments (Fig. 7-12 C). Aerenchyma formation is considered part of the 'steep, cheap and deep' root ideotype proposed for maize water and N acquisition by Lynch (2013); this ideotype could equally be applicable for efficient uptake of other mobile nutrients. Under the low initial P levels seen in uniform no P and the split bottom experiments, plants would be expected to allocate as little carbon to root growth as possible to reach the largest amount of soil and potentially reach soil with higher P. Aerenchyma provide a way to increase root surface area with a minimum of carbon used to build the root structure (Lynch 2013).

Can aerenchyma formation be linked to AUX1 expression? *OsAUX1* expression has been displayed in cortical cells where lysigenous aerenchyma formation occurs (Fig. 7-4). In maize, Rajhi et al. (2011) identified down-regulation of *OsIAA10* in cortical cells as a response to flooding; *OsIAA10* is an auxin responsive Aux/IAA gene family member. Additionally, the GUS results in this work and Parker (2010) support expression of *OsAUX1* in cortical cells. Aerenchyma formation is also associated with auxin induced ethylene production causes for a range of species (Visser and Voeselek 2005) but not necessarily in rice (Jackson et al. 1985).

7.5 Conclusions

The nature of the interaction between *OsAUX1* and P stress is complex because (i) *OsAUX1* influences the overall amount of soil occupied by roots through control of root angle (Parker 2010) which impacts the likelihood of encountering P in soil and (ii) *OsAUX1* is involved in development of fine root structures such as lateral roots (Chhun et al. 2003; Sreevidya et al. 2010) and root hairs which alter the ability of the plant to extract P from soil that roots occupy (Bates and Lynch 2000; Keyes et al. 2013; Liu et al. 2013). From this work it was found that rice root hair elongation and density were reduced with a loss of *OsAUX1* expression, which reinforces the importance of *OsAUX1* for potential P uptake. For wildtype plants with fully functioning *OsAUX1*, the amount of available P present also influenced root hair elongation with the longest root hairs present in replete P conditions and a steady decline in root hair length as P increased. This provides further evidence for the feedback between available P and plasticity required in RSA development for adaptation to changes in P availability (Lynch and Brown 2012).

Additionally, *OsAUX1* has potential to play a role in the influence of roots on nutrient availability in soil. Changes in rhizosphere chemistry were evident between wildtype and *Osaux1-1* as indicated by Fe rhizosheath formation for soil grown plants. In particular, wildtype had less Fe accumulation 5 cm from the root tip than the *Osaux1-1* reduced function mutant. Despite this, for agar grown plants grown in pH indicating media, a link between *OsAUX1*, P level and rhizosphere acidification was not identified. The differences in aerenchyma formation between the genotypes also provided evidence that *OsAUX1* was linked to RSA adaptation to P stress.

8.0 General discussion and conclusion

8.1 OsAUX1 as a target gene for improvement of phosphorus uptake in paddy rice

This work explored how soil P status influences RSA development with and without OsAUX1 expression, which can impact the amount of soil explored and the root surface area in contact with soil (Fig. 8-1). OsAUX1 clearly influences root angle, lateral root elongation, root hair density and root hair elongation in soil grown rice. Whether these OsAUX1 related root traits positively influenced P uptake from soil remains unclear.

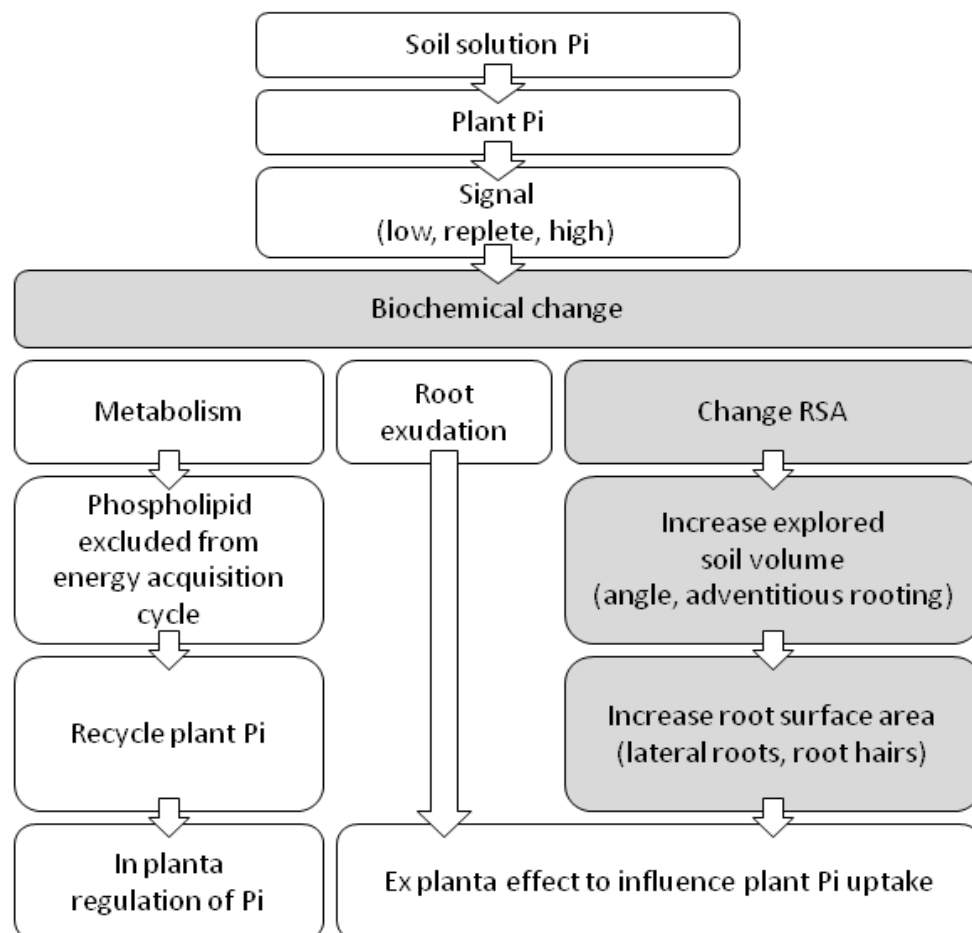


Fig. 8-1: Representation of P signalling pathway and in planta and ex planta responses to P stress. Parts of the P signalling pathway linked to OsAUX1 in this work are shaded.

Linking plant P status, soil P availability and the influence of a pleiotropic gene such as OsAUX1 is challenging. Additionally, there is the influence of available P, plant P status, soil microbes and the feedback with root system development to consider.

Assessing the effects of a gene influencing many phenotypic traits becomes particularly complicated when comparing soil to non-soil systems because of their differences in water status (agar being ca. 98% water) and buffering capacity for nutrient availability. For example, Clark et al. (2000) identified QTLs that were related to drought resistance and could involve several genes that impact adaptation to water stress. The group compared the ability of rice cultivars with varying degrees of drought resistance (identified by the QTLs) to penetrate a hardpan in both lab conditions (sand with a wax layer simulating the hardpan) and field conditions (fields with hardpan). Downie et al. (2012) found that cultivars which were able to penetrate the wax layer in controlled conditions had more variable penetration of the field hardpan.

8.1.1 *Root angle effects on encountering soil P in rice paddies*

Shallow root angle has been proven to be a positive trait for improving P uptake efficiency (Ge et al. 2000) in several plants including common bean (Rubio et al. 2003), pasture grasses (Abel et al. 2002) and maize (Liu et al. 2004). Since plant available P resides in the topsoil (Borggaard et al. 1990; Owens et al. 2008), these shallow root systems likely encounter more available P and thus are more efficient at P acquisition.

For rice, particularly paddy rice grown in waterlogged conditions, the role of root angle in P acquisition is less clear. The chemistry of paddy soils because of flooding could mean that shallow root angle is not an adaptation to P stress. P is quickly transformed into soluble

forms immediately upon flooding (Ponnamperuma 1984; Shahandeh et al. 1995) and then becomes much less available during adsorption to Fe and Mn in the subsequent anoxic soil conditions (Bodegom et al. 2001; Shahandeh et al. 2003). Since plant available P is soluble and initially increases in the flooded soil (Kristoffersen and Riley 2005), P transport is increased in paddy systems in comparison to non-waterlogged soils (Justin and Armstrong 1987). Rice paddies which have water flow mean that available P moves through the soil and is quickly depleted by root uptake (Chapagain and Yamaji 2010). Thus, rice root systems must proactively pursue avenues such as fine root development (He et al. 2003), association with fungi (Hajiboland et al. 2009a) and alteration of rhizosphere pH (Begg et al. 1994) through release of O₂ and organic acids (Bodegom et al. 2001) to facilitate P uptake under anoxic soil conditions.

As seen in Chapter Five, with complete supplementation of nutrients in a loamy sand soil (Newport Series), the *Osaux1* knockout mutants retained the agravitropic phenotype. However from the work performed in low P silty clay loam soil (Chapter Six) it was not evident that shallow root angle induced by knockout of OsAUX1 could be retained for rice in soil with varying P concentration and distribution.

In comparison to root volume distribution with soil depth as defined by centroid z values found during the phenotyping study (Chapter Five) where *Osaux1-1* had a mean of 1.14 cm and wildtype was 1.87 cm, the root system volume distributions under varying P conditions (Chapter Six) were in a comparable range. In the P experiments, wildtype centroid ranged between 1.33 cm (split top sufficient) and 3.0 cm (no added P); *Osaux1-1* centroid z was between 1.49 cm (high P) and 3.8 cm (no added P). However, wildtype had much shallower

root volume distribution than *Osaux1-1*, which was unexpected given the reduced gravitropic response of the knockout mutant displayed in Chapter Five. One explanation for why wildtype appeared less gravitropic than *Osaux1-1* under varying soil P could be that P stress reduces primary root elongation as well as adventitious root formation. In *Arabidopsis*, low soil phosphate can impact lateral root angle (Bai et al. 2013), root hair density (Ma et al. 2001), root branching (Desnos 2008) and primary root elongation (López-Bucio et al. 2002). Common bean has reduced root angle when soil is P deficient (Bonser et al. 1996). In maize, low soil phosphorus can increase root hair density although Mackay and Barber (1985) found no correlation between root hair length and soil P concentration. In Chapter Six, wildtype had reduced primary root length and root elongation under low P which would have contributed to a shallower root system and smaller root angle.

8.1.2 *Fine roots: Increasing the ability to take-up phosphate from soil*

In addition to shallow root angle, fine root proliferation (lateral roots and root hairs) has also been linked to more efficient P uptake from soil (Bates and Lynch 2000; Beebe et al. 2006; Desnos 2008; Gahoonia and Nielsen 1996). These traits are often linked to auxin distribution and AUX1. Auxin redistribution (and potentially the gene AUX1) has been considered a conserved trait between both monocots and dicots for lateral root initiation (Sreevidya et al. 2010). Although the shallow root angle induced by knockout of *OsAUX1* did not appear to confer an advantage for uptake of soil P under waterlogged conditions (Chapter Six), *OsAUX1* related fine root traits showed more promising results for adaptability to variations in P availability (Chapter Seven).

In this work, root angle as defined by centroid Z-value was less important for P acquisition than other traits which increase P uptake when available P is in proximity of the root system such as root hair length and root activity that alters rhizosphere chemistry. This result could be expected for rice plants acquiring P from waterlogged soils. OsAUX1 was linked to variations in the root hair phenotype for agar grown rice plants (Chapter Six) which could be useful for P acquisition from soil by increasing root surface area. Keyes et al. (2013) found that wheat root hairs take up 15% less P than the root surface itself, but that root hairs increase overall uptake of the root system by 85%. Zygalkis et al. (2011) established that root hair length, rather than root hair density, was the primary driver for P uptake under P limiting conditions and that root length has a critical length where after this point longer root hairs do not induce a linear increase in P uptake.

When comparing results from agar-based and soil-based experiments by available P concentrations (No added P: 3.12 μ M P, sufficient P: 31.2 μ M P and high/toxic P: 312 μ M P), root hairs could not be linked to actual P uptake observed in soil grown plants. With longer root hairs and a higher density of root hairs, wildtype would be expected to take up more phosphate. In Chapter Six, both genotypes had no significant difference in tissue P concentration when grown in soil with similar P concentration and distribution. However, in the split top P distribution, wildtype had significantly ($P < 0.001$) more total P accumulated (mg) likely because there was significantly ($P < 0.001$) more biomass accumulation than *Osaux1-1*. The unexpected result in P tissue concentration could be due to the plants not reaching their ideal P concentration at such an early growth stage (four weeks old) and thus would mask the effects of root hairs which might be evident in older plants.

Root hairs are also integral to bacterial and fungal interaction with crop plants such as barley (Baon et al. 1993; Haling et al. 2013a; Zhu et al. 2003), maize (Anderson et al. 1987) and Arabidopsis (Kapulnik et al. 2011) as well as rice in wetland ecosystems (Khan 2004b). P solubilising bacteria proliferate near roots because they use root exudates as readily available energy sources (Gyaneshwar et al. 2002). The presence of the bacteria increases the size of the rhizosphere in flooded soils by releasing previously unavailable P from surrounding soils (Osorio and Nelson 2007; Raghu and MacRae 1966; Richardson et al. 2009). In addition to transporting P directly to plant tissues from soil unoccupied by a plant's roots, AMF influence expression of P transporters in rice which increases P uptake and plant tissue P concentrations (Chen et al. 2012b).

8.1.3 *OsAUX1 and RSA plasticity in relation to P uptake*

Roots are critical to crops because they drive the plant's plastic response to environmental change and variation in nutrient and water availability in the soil environment (Fitter 1994; Hodge 2004). This work indicates that for rice, *OsAUX1* could be involved in root plasticity related to increasing root surface area and uptake of P from paddy soils. This was demonstrated by the greater variation of phenotypes produced by wildtype when P concentration varied or had a different distribution as seen in Chapter Six. *Osaux1-1* appeared to have a more determinate phenotype under the various P conditions. However some root traits which could be adaptations to stresses may become determinate over time. Kato et al. (2006) found that a steep root angle in rice, which could increase drought tolerance, was a determinate trait that occurred independent of soil water status.

Additionally, the reduced gravitropic response observed in wildtype centroid Z values under P stress further implicate OsAUX1 as a driver of plasticity under varying soil P. Under P stress, OsAUX1 function in wildtype increased elongation of lateral roots as well as initiation and elongation of root hairs in P deficient conditions (Chapter Seven). Additionally, under P toxic conditions, lateral root growth, root hair density and root hair length were decreased. With impaired OsAUX1 function, *Osaux1-1* may have had a delayed reaction to the P stress and continued typical root growth for a much longer period than wildtype which would explain the phenotype observed where root hairs were short under low P and longer under high P. Complete OsAUX1 function would manifest as a quicker response to P stress in wildtype than *Osaux1-1*, making the wildtype root system appear less extensive and have smaller values for centroid, root depth and root system width as observed in Chapter Six.

In agar, wildtype had a larger root area (more roots and more lateral roots) than *Osaux1-1* under extreme low and high P. Wildtype had more crown roots under low P and more lateral roots under replete P. Wildtype had more crown roots under High P; perhaps indicative of plasticity and trying to explore more soil to avoid the unsatisfactory soil conditions. *Osaux1-1* had a low number of lateral roots and a low number of crown roots under all except replete conditions. This could explain the unexpected tissue P concentration results since loss of OsAUX1 regulatory control for P uptake in *Osaux1-1* could result in hyper-accumulation of P despite the plant having less biomass and reduced potential root:soil contact.

8.1.4 *Optimisation of X-ray CT for imaging soil-grown rice roots*

As seen in Chapter Three, soil moisture can play a critical part in segmentation of roots from soil in X-ray CT images. Rice roots in particular are challenging to visualise in soil using X-ray CT because of their similar X-ray attenuation properties to soil; the rice roots were composed of carbon, water and air in similar proportions to the surrounding soil. RooTrak (Mairhofer et al. 2012) had not yet been optimised for rice root images because of X-ray attenuation density similarities between rice and soil. Thus the work was restricted to semi-automated segmentation with the VGSM region-growing tool. RooTrak relies on creating an updateable model of the greyscale histogram within the root that must contrast with the greyscale histogram of the voxels directly outside of the root. The similarity of greyscale distributions both within the root and outside of the root restricted the usefulness of RooTrak software for segmenting these roots from soil in the X-ray CT images although it is hoped further revisions will address this.

There was excellent agreement between root volume values derived from root washing and X-ray CT images however, there were also some discrepancies. In the X-ray CT images, mis-estimation of root volume likely occurred where pores were misclassified as root material or where root material was designated as part of the soil fractions. This is a commonly encountered challenge when visualising roots in field soils using X-ray CT and can confuse automated segmentation software (Flavel et al. 2012a; Mairhofer et al. 2013). Root volume was underestimated where the X-ray CT images did not capture the finer root fraction, particularly for wildtype and *Osaux1-1*. In addition, the measurement of root-washed samples involved extrapolation of root volume from the actual projected surface area of the root system. This can introduce error to WinRHIZO calculation and result in overestimation

of average root diameter and subsequently, exaggerate the root volume calculated from root diameter and surface area (Wang and Zhang 2009).

Improvements in X-ray CT technology could reduce the negative influence that rice root anatomy (internal air and water-filled spaces) has on the contrast between X-ray attenuation density of the rice roots and soil matrix. These advancements could improve automated segmentation tools such as RooTrak would be useful for segmentation of rice roots. For example, enhanced X-ray detector technology has already increased the ability of researchers to move from mm scale of medical grade X-ray CT scanners to microscale (μm) investigations performed today (Mooney et al. 2012b).

8.2 Conclusions

The following major conclusions can be made from the research presented in this thesis:

- The gene AUX1 and its ortholog in rice, OsAUX1, have been linked to root angle, lateral root initiation and elongation and root hair elongation through control of auxin efflux. It is clear that without fully functioning OsAUX1, rice plants have a more deterministic root development which does not vary with P distribution or concentration except under toxic P conditions. In rice, there is potential for enhancement of OsAUX1 expression to enable paddy rice to increase the adaptability of its RSA development to changing soil P availability. This increased root plasticity has the potential to improve P uptake under flooded conditions by increasing lateral root and root hair development.
- As an ortholog of the Arabidopsis gene AUX1, OsAUX1 influences root gravitropism in soil grown rice plants. 3-D root gravitropism and vertical distribution of root

volume was characterised through centroid Z-value for rice plants grown on loamy sand (Newport) with a replete nutrient supply. In reduced *OsAUX1* function mutants (*Osaux1-1* and *Osaux1-2*) grown for four weeks, the plants had relatively shallow vertical distribution of the root volume with centroid Z values of 1.1 cm and 1.6 cm respectively. In contrast, wildtype had a deeper root volume distribution with a significantly ($P = 0.006$) larger centroid Z of 1.9 cm.

- When grown under varying P conditions and distributions, *OsAUX1* induced agravitropism was reduced in the knockout mutants. Centroid Z-value, an indicator of overall root volume distribution with depth, was not significantly smaller in *Osaux1-1* than wildtype. However, *OsAUX1* function was required for fine root proliferation. Particularly when sufficient P conditions were partitioned to the top 4 cm of the soil profile, wildtype had a significantly greater root volume, surface area, total root length and number of root tips than *Osaux1-1*. This reinforces the role that *OsAUX1* plays in rice for fine root development in relation to P distribution and availability.
- In waterlogged soils, P availability for rice was more dependent on the influence that the root system had on the immediate soil environment than root angle. In particular, P availability had a significant effect on root hair density and elongation in both wildtype and the *Osaux1* knockout mutants. Wildtype had significantly longer root hairs ($P = 0.014$) and a significantly higher density of root hairs ($P = 0.009$) than the mutants under replete P when grown on agar. This could influence rhizosphere pH and the development of iron rhizosheaths which have been known to influence P uptake in paddy rice (Kögel-Knabner et al. 2010). However in this work, *OsAUX1*

expression could not be linked to a difference in iron rhizosheath formation or rhizosphere pH acidification.

- X-ray CT is becoming more widely utilised for studies involving root development in soil (Mooney et al. 2012b). Segmentation of root material from soil in X-ray CT images is influenced by soil moisture content. The optimal X-ray density contrast between root material and the soil matrix (minerals, organic matter and water/air-filled pores) is achieved by allowing soils to reach an approximated field capacity (ca. 3 days drainage) (Zappala et al. 2013b).
- As X-ray CT technology improves and higher throughput analysis become possible, there is a greater likelihood that X-ray studies may impact the living rhizosphere through exposure to X-radiation. Low level X-ray doses (< 30 Gy) did not impact rice root growth or soil microbial populations in relatively long term studies (4 weeks for rice, 24 weeks for soil microbes) (Zappala et al. 2013a). X-ray dose is often under-reported in current X-ray CT studies and the parameters to estimate dose or the dose itself should be reported.

8.3 Further investigation

- Building on this work that used sieved and sterilised soil, the influence of OsAUX1 on P uptake and root gravitropism should be investigated under field conditions. OsAUX1 clearly has the potential to influence P uptake through root hair proliferation which should be investigated in a field situation. Additionally, OsAUX1 induced shallow root angle could be more advantageous for P acquisition in the field because of interaction between plants which could not be replicated in the column setup utilised for this work. The use of a field setting would also allow introduction

of feedback from soil microbes and fungi such as AMF to be included in experimental designs.

- The investigation of localised P uptake through use of microelectrodes would enhance understanding of the microscale influence of OsAUX1 related root traits on P uptake in the rhizosphere. This work was restricted to quantification of root architectural properties in relation to OsAUX1, but the chemical influence of OsAUX1 induced root traits on the rhizosphere of rice in flooded soils are poorly understood and should be investigated.
- Use of X-ray CT to observe rice root development required a balance between column size and image resolution to ensure that the rice root architecture could be reasonably quantified. In order to achieve voxel sizes of 27 to 54 μm , sample diameters were restricted to 5.5 cm, which in turn meant that the maximum plant age that could be analysed was four weeks. Future study should investigate older plants which would be in later stages of plant development such as flowering and grain-filling.
- In agar-based systems, several rice genes have been linked to root angle such as OsCLR4 (Kitomi et al. 2008) and OsDRO1 (Uga et al. 2011). Additionally, there are rice genes that control lateral root initiation (Zhu et al. 2012) and elongation (Zhang et al. 2008). Understanding how OsAUX1 and these other genes are expressed under varying P concentrations in agar and eventually soil could help further the likelihood of identifying key genes for improvement of paddy rice as a crop in relation to P uptake.

9.0 Bibliography

Abel S, Ticconi CA, Delatorre CA (2002) Phosphate sensing in higher plants. *Physiologia Plantarum* 115: 1-8

Al-Enezi NA, Al-Khayri JM (2012) Alterations of DNA, ions and photosynthetic pigments content in date palm seedlings induced by X-irradiation. *International Journal of Agriculture and Biology* 14: 329-336

Al-Khayri J, Al-Enezi N, Al-Bahrany A (2012) Effect of X-irradiation on date palm seed germination and seedling growth. *Emirates Journal of Food and Agriculture* 24

Al-Ghazi Y, Muller B, Pinloche S, Tranbarger T, Nacry P, Rossignol M, Tardieu F, Dumas P (2003) Temporal responses of *Arabidopsis* root architecture to phosphate starvation: evidence for the involvement of auxin signalling. *Plant, Cell & Environment* 26: 1053-1066

Als-Nielsen J, McMorro D (2011) *Elements of modern X-ray physics*. John Wiley & Sons, Ltd., Chichester, UK

Anderson E, Millner P, Kunishi H (1987) Maize root length density and mycorrhizal infection as influenced by tillage and soil phosphorus. *Journal of Plant Nutrition* 10: 1349-1356

Bai H, Murali B, Barber K, Wolverton C (2013) Low phosphate alters lateral root setpoint angle and gravitropism. *American Journal of Botany* 100: 175-182

Bais HP, Weir TL, Perry LG, Gilroy S, Vivanco JM (2006) The role of root exudates in rhizosphere interactions with plants and other organisms. *Annual Review of Plant Biology* 57: 233-266

Bakker MG, Manter DK, Sheflin AM, Weir TL, Vivanco JM (2012) Harnessing the rhizosphere microbiome through plant breeding and agricultural management. *Plant and Soil* 360: 1-13

Balasubramanian V, Sie M, Hijmans R, Otsuka K (2007) Increasing rice production in Sub-Saharan Africa: Challenges and opportunities. *Advances in Agronomy* 94: 55-133

Baldwin KL, Strohm AK, Masson PH (2013) Gravity sensing and signal transduction in vascular plant primary roots. *American Journal of Botany* 100: 126-142

Baluška F, Volkmann D (2011) Mechanical aspects of gravity-controlled growth, development and morphogenesis. In: Wojtaszek P (ed) *Mechanical Integration of Plant Cells and Plants*. Springer Berlin Heidelberg, pp 195-223

Band LR, Wells DM, Larrieu A, Sun J, Middleton AM, French AP, Brunoud G, Sato EM, Wilson MH, Peret B, Oliva M, Swarup R, Sairanen I, Parry G, Ljung K, Beeckman T, Garibaldi JM, Estelle M, Owen MR, Vissenberg K, Hodgman TC, Pridmore TP, King JR, Vernoux T, Bennett MJ (2012) Root gravitropism is regulated by a transient lateral auxin gradient controlled by a tipping-point mechanism. *Proceedings of the National Academy of Sciences of the United States of America* 109: 4668-4673

Baon J, Smith S, Alston A (1993) Mycorrhizal responses of barley cultivars differing in P efficiency. *Plant and Soil* 157: 97-105

- Bates TR, Lynch JP (2000) Plant growth and phosphorus accumulation of wild type and two root hair mutants of *Arabidopsis thaliana* (Brassicaceae). *American Journal of Botany* 87: 958-963
- Beebe SE, Rojas-Pierce M, Yan X, Blair MW, Pedraza F, Muñoz F, Tohme J, Lynch JP (2006) Quantitative trait loci for root architecture traits correlated with phosphorus acquisition in common bean. *Crop Science* 46: 413-423
- Begg C, Kirk G, Mackenzie A, Neue HU (1994) Root-induced iron oxidation and pH changes in the lowland rice rhizosphere. *New Phytologist* 128: 469-477
- Benckiser G, Santiago S, Neue H, Watanabe I, Ottow J (1984) Effect of fertilization on exudation, dehydrogenase activity, iron-reducing populations and Fe⁺⁺ formation in the rhizosphere of rice (*Oryza sativa* L.) in relation to iron toxicity. *Plant and Soil* 79: 305-316
- Bennett MJ, Marchant A, Green HG, May ST, Ward SP, Millner PA, Walker AR, Schulz B, Feldmann KA (1996) *Arabidopsis* AUX1 gene: a permease-like regulator of root gravitropism. *Science* 273: 948-950
- Blake L, Mercik S, Koerschens M, Moskal S, Poulton P, Goulding K, Weigel A, Powlson D (2000) Phosphorus content in soil, uptake by plants and balance in three European long-term field experiments. *Nutrient Cycling in Agroecosystems* 56: 263-275
- Blossfeld S (2013) Light for the dark side of plant life: Planar optodes visualizing rhizosphere processes. *Plant and Soil* 369: 29-32
- Bodegom Pv, Groot T, den Hout B, Leffelaar P, Goudriaan J (2001) Diffusive gas transport through flooded rice systems. *Journal of Geophysical Research: Atmospheres* (1984–2012) 106: 20861-20873
- Bonser AM, Lynch J, Snapp S (1996) Effect of phosphorus deficiency on growth angle of basal roots in *Phaseolus vulgaris*. *New Phytologist* 132: 281-288
- Borggaard O, Jørgensen S, Moberg J, Raben-Lange B (1990) Influence of organic matter on phosphate adsorption by aluminium and iron oxides in sandy soils. *Journal of Soil Science* 41: 443-449
- Bouckaert L, Van Loo D, Ameloot N, Buchan D, Van Hoorebeke L, Sleutel S (2012) Compatibility of X-ray micro-computed tomography with soil biological experiments. *Soil Biology and Biochemistry* 56: 10-12
- Brunoud G, Wells DM, Oliva M, Larrieu A, Mirabet V, Burrow AH, Beeckman T, Kepinski S, Traas J, Bennett MJ (2012) A novel sensor to map auxin response and distribution at high spatio-temporal resolution. *Nature* 482: 103-106
- Cai H, Chen Q (2000) Rice production in China in the early 21st century. *Chinese Rice Research Newsletter* 8: 14-16
- Campbell B, Grime J, Mackey J (1991) A trade-off between scale and precision in resource foraging. *Oecologia* 87: 532-538
- Campbell R, Rovira A (1973) The study of the rhizosphere by scanning electron microscopy. *Soil Biology and Biochemistry* 5: 747-750

- Carminati A, Moradi AB, Vetterlein D, Vontobel P, Lehmann E, Weller U, Vogel H-J, Oswald SE (2010) Dynamics of soil water content in the rhizosphere. *Plant and Soil* 332: 163-176
- Carminati A, Vetterlein D, Weller U, Vogel HJ, Oswald SE (2009) When roots lose contact. *Vadose Zone Journal* 8: 805-809
- Carpenter SR (2005) Eutrophication of aquatic ecosystems: Bistability and soil phosphorus. *Proceedings of the National Academy of Sciences of the United States of America* 102: 10002-10005
- Carter DO, Yellowlees D, Tibbett M (2007) Autoclaving kills soil microbes yet soil enzymes remain active. *Pedobiologia* 51: 295-299
- Casimiro I, Marchant A, Bhalerao RP, Beeckman T, Dhooge S, Swarup R, Graham N, Inzé D, Sandberg G, Casero PJ (2001) Auxin transport promotes *Arabidopsis* lateral root initiation. *The Plant Cell Online* 13: 843-852
- Cattell W (1931) The effects of X-rays on the growth of wheat seedlings. *Science* 73: 531-533
- Cavell A (1955) The colorimetric determination of phosphorus in plant materials. *Journal of the Science of Food and Agriculture* 6: 479-480
- Celeux G, Forbes F, Peyrard N (2003) EM procedures using mean field-like approximations for Markov model-based image segmentation. *Pattern Recognition* 36: 131-144
- Chapagain T, Yamaji E (2010) The effects of irrigation method, age of seedling and spacing on crop performance, productivity and water-wise rice production in Japan. *Paddy and Water Environment* 8: 81-90
- Chen X, Li H, Chan W, Wu F, Wu S, Wong M (2012a) Phosphate Transporters Expression in Rice (*Oryza sativa* L.) Associated with Arbuscular Mycorrhizal Fungi (AMF) Colonization under Different Levels of Arsenate Stress. *Environmental and Experimental Botany*
- Chen X, Li H, Chan W, Wu F, Wu S, Wong M (2012b) Phosphate transporters expression in rice (*Oryza sativa* L.) associated with arbuscular mycorrhizal fungi (AMF) colonization under different levels of arsenate stress. *Environmental and Experimental Botany* 87: 92-99
- Chhun T, Taketa S, Tsurumi S, Ichii M (2003) The effects of auxin on lateral root initiation and root gravitropism in a lateral rootless mutant Lrt1 of rice (*Oryza sativa* L.). *Plant Growth Regulation* 39: 161-170
- Chin JH, Lu X, Haefele SM, Gamuyao R, Ismail A, Wissuwa M, Heuer S (2010) Development and application of gene-based markers for the major rice QTL phosphorus uptake 1. *Theoretical and Applied Genetics* 120: 1073-1086
- Clark L, Aphale S, Barraclough P (2000) Screening the ability of rice roots to overcome the mechanical impedance of wax layers: importance of test conditions and measurement criteria. *Plant and Soil* 219: 187-196
- Clark RT, MacCurdy RB, Jung JK, Shaff JE, McCouch SR, Aneshansley DJ, Kochian LV (2011) Three-dimensional root phenotyping with a novel imaging and software platform. *Plant Physiology* 156: 455-465

- Conley DJ, Paerl HW, Howarth RW, Boesch DF, Seitzinger SP, Havens KE, Lancelot C, Likens GE (2009) Controlling eutrophication: Nitrogen and phosphorus. *Science* 323: 1014-1015
- Cordell D, Drangert J-O, White S (2009) The story of phosphorus: Global food security and food for thought. *Global Environmental Change* 19: 292-305
- Coudert Y, Bès M, Le TVA, Pré M, Guiderdoni E, Gantet P (2011) Transcript profiling of crown rootless1 mutant stem base reveals new elements associated with crown root development in rice. *BMC Genomics* 12: 387
- De Datta S, Biswas T, Charoenchamratcheep C (1990) Phosphorus requirements and management for lowland rice. Phosphorus requirements for sustainable agriculture in Asia and Oceania. International Rice Research Institute, Manila, Philippines, pp 307-323
- de Dorlodot S, Forster B, Pagès L, Price A, Tuberosa R, Draye X (2007) Root system architecture: opportunities and constraints for genetic improvement of crops. *Trends in Plant Science* 12: 474-481
- Desnos T (2008) Root branching responses to phosphate and nitrate. *Current Opinion in Plant Biology* 11: 82-87
- Dhondt S, Vanhaeren H, Van Loo D, Cnudde V, Inze D (2010a) Plant structure visualization by high-resolution X-ray computed tomography. *Trends in Plant Science* 15: 419-422
- Dhondt S, Vanhaeren H, Van Loo D, Cnudde V, Inzé D (2010b) Plant structure visualization by high-resolution X-ray computed tomography. *Trends in Plant Science* 15: 419-422
- Dong G, Xie M (2005) Color clustering and learning for image segmentation based on neural networks. *IEEE Transactions on Neural Networks* 16: 925-936
- Downie H, Holden N, Otten W, Spiers AJ, Valentine TA, Dupuy LX (2012) Transparent soil for imaging the rhizosphere. *PloS One* 7: e44276
- Drew MC, He C-J, Morgan PW (1989) Decreased ethylene biosynthesis, and induction of aerenchyma, by nitrogen-or phosphate-starvation in adventitious roots of *Zea mays L.* *Plant Physiology* 91: 266-271
- Drew MC, He C-J, Morgan PW (2000) Programmed cell death and aerenchyma formation in roots. *Trends in Plant Science* 5: 123-127
- Dunbabin VM, Diggle AJ, Rengel Z, van Hugten R (2002) Modelling the interactions between water and nutrient uptake and root growth. *Plant and Soil* 239: 19-38
- Dutilleul P, Prasher SO, Lontoc-Roy M (2005) Branching out with a CT scanner. *Trends in Plant Science* 10: 411-412
- Eghball B, Binford G, Baltensperger DD (1996) Phosphorus movement and adsorption in a soil receiving long-term manure and fertilizer application. *Journal of Environmental Quality* 25: 1339-1343
- Eissenstat DM (1992) Costs and benefits of constructing roots of small diameter. *Journal of Plant Nutrition* 15: 763-782

- Fang S, Yan X, Liao H (2009) 3D reconstruction and dynamic modeling of root architecture in situ and its application to crop phosphorus research. *Plant Journal* 60: 1096-1108
- Ferreira SJ, Senning M, Sonnewald S, Kessling PM, Goldstein R, Sonnewald U (2010) Comparative transcriptome analysis coupled to X-ray CT reveals sucrose supply and growth velocity as major determinants of potato tuber starch biosynthesis. *BMC Genomics* 11: 93-109
- Fitter A (1987) An architectural approach to the comparative ecology of plant root systems. *New Phytologist* 106: 61-77
- Fitter A (1991) Characteristics and functions of root systems. *Plant roots: The hidden half*. Marcel Dekker, Inc., New York, NY, pp 1-29
- Fitter A (1994) Architecture and biomass allocation as components of the plastic response of root systems to soil heterogeneity. *Exploitation of environmental heterogeneity by plants*. Academic Press, Inc., London, UK, pp 305-323
- Fitter A, Williamson L, Linkohr B, Leyser O (2002) Root system architecture determines fitness in an *Arabidopsis* mutant in competition for immobile phosphate ions but not for nitrate ions. *Proceedings of the Royal Society of London. Series B: Biological Sciences* 269: 2017-2022
- Flavel RJ, Guppy CN, Tighe M, Watt M, McNeill A, Young IM (2012a) Non-destructive quantification of cereal roots in soil using high-resolution X-ray tomography. *Journal of Experimental Botany* 63: 2503-2511
- Flavel RJ, Guppy CN, Tighe M, Watt M, McNeill A, Young IM (2012b) Non-destructive quantification of cereal roots in soil using high-resolution X-ray tomography. *Journal of Experimental Botany*: Online only at present
- Gahoonia TS, Nielsen NE (1996) Variation in acquisition of soil phosphorus among wheat and barley genotypes. *Plant and Soil* 178: 223-230
- Ge Z, Rubio G, Lynch JP (2000) The importance of root gravitropism for inter-root competition and phosphorus acquisition efficiency: Results from a geometric simulation model. *Plant and Soil* 218: 159-171
- Genter CF, Brown HM (1941) X-ray studies on the field bean. *Journal of Heredity* 32: 39-44
- Goff SA, Ricke D, Lan T-H, Presting G, Wang R, Dunn M, Glazebrook J, Sessions A, Oeller P, Varma H (2002) A draft sequence of the rice genome (*Oryza sativa* L. ssp. japonica). *Science* 296: 92-100
- Goodspeed TH (1929) The effects of X-rays and radium on species of the genus *Nicotiana*. *Journal of Heredity* 20: 243-259
- Gotoh S, Patrick W (1974) Transformation of iron in a waterlogged soil as influenced by redox potential and pH. *Soil Science Society of America Journal* 38: 66-71
- Gregory P, Hutchison D, Read D, Jenneson P, Gilboy W, Morton E (2003a) Non-invasive imaging of roots with high resolution X-ray micro-tomography. *Roots: The dynamic interface between plants and the Earth*. Springer, pp 351-359
- Gregory PJ (2006) *Plant roots: growth, activity and interactions with the soil*. Blackwell, Oxford, UK

- Gregory PJ, Hutchison DJ, Read DB, Jenneson PM, Gilboy WB, Morton EJ (2003b) Non-invasive imaging of roots with high resolution X-ray micro-tomography. *Plant and Soil* 255: 351-359
- Grime J, Campbell B, Mackey J, Crick J (1991) Root plasticity, nitrogen capture and competitive ability. *Plant root growth: An ecological perspective*. Blackwell, London, UK, pp 381-397
- Gyaneshwar P, Kumar GN, Parekh L, Poole P (2002) Role of soil microorganisms in improving P nutrition of plants. *Plant and soil* 245: 83-93
- Hajiboland R, Aliasghar zad N, Barzeghar R (2009a) Phosphorus mobilization and uptake in mycorrhizal rice (*Oryza sativa* L.) plants under flooded and non-flooded conditions. *Acta Agriculturae Slovenica* 93: 153-161
- Hajiboland R, Aliasghar zad N, Barzeghar R (2009b) Phosphorus mobilization and uptake in mycorrhizal rice (*Oryza sativa* L.) plants under flooded and non-flooded conditions.
- Haling RE, Brown LK, Bengough AG, Young IM, Hallett PD, White PJ, George TS (2013a) Root hairs improve root penetration, root-soil contact, and phosphorus acquisition in soils of different strength. *Journal of Experimental Botany* 64: 3711-3721
- Haling RE, Tighe MK, Flavel RJ, Young IM (2013b) Application of X-ray computed tomography to quantify fresh root decomposition in situ. *Plant and Soil* 372: 619-627
- Hammond JP, Broadley MR, White PJ, King GJ, Bowen HC, Hayden R, Meacham MC, Mead A, Overs T, Spracklen WP (2009) Shoot yield drives phosphorus use efficiency in *Brassica oleracea* and correlates with root architecture traits. *Journal of Experimental Botany* 60: 1953-1968
- Hammond JP, White PJ (2008) Diagnosing phosphorus deficiency in crop plants. *The ecophysiology of plant-phosphorus interactions*. Springer, Dordrecht, The Netherlands, pp 225-246
- Hamza MA, Anderson SH, Aylmore LAG (2007) Computed tomographic evaluation of osmotic shrinkage and recovery of lupin (*Lupinus angustifolius* L.) and radish (*Raphanus sativus* L.) roots. *Environmental and Experimental Botany* 59: 334-339
- Hamza MA, Anderson SH, Aylmore LAG (2008) Water drawdown by radish (*Raphanus sativus* L.) multiple-root systems evaluated using computed tomography. *Australian Journal of Soil Research* 46: 228-236
- Hargreaves C, Gregory P, Bengough AG (2009) Measuring root traits in barley (*Hordeum vulgare* ssp. *vulgare* and ssp. *spontaneum*) seedlings using gel chambers, soil sacs and X-ray microtomography. *Plant and Soil* 316: 285-297
- Harrison BR, Masson PH (2008) ARL2, ARG1 and PIN3 define a gravity signal transduction pathway in root statocytes. *The Plant Journal* 53: 380-392
- Hazen SP, Pathan MS, Sanchez A, Baxter I, Dunn M, Estes B, Chang H-S, Zhu T, Kreps JA, Nguyen HT (2005) Expression profiling of rice segregating for drought tolerance QTLs using a rice genome array. *Functional & Integrative Genomics* 5: 104-116
- He Y, Liao H, Yan X (2003) Localized supply of phosphorus induces root morphological and architectural changes of rice in split and stratified soil cultures. *Structure and functioning of cluster roots and plant responses to phosphate deficiency*. Springer, Netherlands, pp 247-256

- Hedley M, Kirk G, Santos M (1994) Phosphorus efficiency and the forms of soil phosphorus utilized by upland rice cultivars. *Plant and Soil* 158: 53-62
- Heeraman DA, Hopmans JW, Clausnitzer V (1997) Three dimensional imaging of plant roots in situ with X-ray computed tomography. *Plant and Soil* 189: 167-179
- Helliwell J, Sturrock C, Grayling K, Tracy S, Flavel R, Young I, Whalley W, Mooney S (2013) Applications of X-ray computed tomography for examining biophysical interactions and structural development in soil systems: A review. *European Journal of Soil Science* 64: 279-297
- Himmelbauer M (2004) Estimating length, average diameter and surface area of roots using two different image analyses systems. *Plant and Soil* 260: 111-120
- Hinsinger P, Bengough AG, Vetterlein D, Young IM (2009) Rhizosphere: Biophysics, biogeochemistry and ecological relevance. *Plant and Soil* 321: 117-152
- Hodge A (2004) The plastic plant: Root responses to heterogeneous supplies of nutrients. *New Phytologist* 162: 9-24
- Hounsfield G (1972) British Patent No. 1283915. British Patent Office, London
- Hutchings M, John E (2003) Distribution of roots in soil, and root foraging activity. *Root Ecology*. Springer, Berlin Heidelberg, pp 33-60
- Hutchings MJ, John EA (2004) The effects of environmental heterogeneity on root growth and root/shoot partitioning. *Annals of Botany* 94: 1-8
- Hutchings MJ, John EA, Wijesinghe DK (2003) Toward understanding the consequences of soil heterogeneity for plant populations and communities. *Ecology* 84: 2322-2334
- Inukai Y, Sakamoto T, Ueguchi-Tanaka M, Shibata Y, Gomi K, Umemura I, Hasegawa Y, Ashikari M, Kitano H, Matsuoka M (2005) Crown rootless1, which is essential for crown root formation in rice, is a target of an AUXIN RESPONSE FACTOR in auxin signaling. *The Plant Cell Online* 17: 1387-1396
- Irshad A, Cheema ZA, Farooq M (2008) Influence of nitrogen on the interference of barnyard grass (*Echinochloa crus-galli*) with fine grain aromatic rice. *Archives of Agronomy and Soil Science* 54: 493-505
- Ismail AM, Heuer S, Thomson MJ, Wissuwa M (2007) Genetic and genomic approaches to develop rice germplasm for problem soils. *Plant Molecular Biology* 65: 547-570
- Iyer-Pascuzzi AS, Symonova O, Mileyko Y, Hao Y, Belcher H, Harer J, Weitz JS, Benfey PN (2010) Imaging and analysis platform for automatic phenotyping and trait ranking of plant root systems. *Plant Physiology* 152: 1148-1157
- Jackson M, Armstrong W (1999) Formation of aerenchyma and the processes of plant ventilation in relation to soil flooding and submergence. *Plant Biology* 1: 274-287
- Jackson MB, Fenning TM, Jenkins W (1985) Aerenchyma (gas-space) formation in adventitious roots of rice (*Oryza sativa* L.) is not controlled by ethylene or small partial pressures of oxygen. *Journal of Experimental Botany* 36: 1566-1572

- Jackson NE, Corey JC, Frederick LR, Picken JC (1967) Gamma irradiation and the microbial population of soils at two water contents. *Soil Science Society Journal of America* 31: 491-494
- Jain AK, Dubes RC (1988) Algorithms for clustering data. Prentice-Hall, Inc.
- Jain M, Nijhawan A, Tyagi AK, Khurana JP (2006) Validation of housekeeping genes as internal control for studying gene expression in rice by quantitative real-time PCR. *Biochemical and Biophysical Research Communications* 345: 646-651
- Jefferson RA, Kavanagh TA, Bevan MW (1987) GUS fusions: Beta-glucuronidase as a sensitive and versatile gene fusion marker in higher plants. *The EMBO Journal* 6: 3901-3907
- Jenkinson DS, Brookes PC, Powlson DS (2004) Measuring soil microbial biomass. *Soil Biology & Biochemistry* 36: 5-7
- Jenneson P, Gilboy W, Morton E, Gregory P (2003) An X-ray micro-tomography system optimised for the low-dose study of living organisms. *Applied Radiation and Isotopes* 58: 177-181
- Jianguo H, Shuman L (1991) Phosphorus status and utilization in the rhizosphere of rice. *Soil Science* 152: 360-364
- Jing J, Cheng Z, Hong-xin Z, Zong-xiu S (2004) Preliminary study on a gravity-insensitive rice mutant. *Journal of Zhejiang University Science* 5: 144-148
- John C (1977) The structure of rice roots grown in aerobic and anaerobic environments. *Plant Soil* 47: 269-274
- Johnson EL (1936a) Effects of X-rays upon green plants. *Biological effects of radiation*. McGraw-Hill Book Company Inc., New York, NY, pp 961-985
- Johnson EL (1936b) Susceptibility of seventy species of flowering plants to X-radiation. *Plant Physiology* 11: 319
- Johnson EL (1937) Tuberization of the Colorado wild potato as affected by X-radiation. *Plant Physiology* 12: 547-551
- Justin S, Armstrong W (1987) The anatomical characteristics of roots and plant response to soil flooding. *New Phytologist* 106: 465-495
- Kapulnik Y, Delaux P-M, Resnick N, Mayzlish-Gati E, Wininger S, Bhattacharya C, Séjalon-Delmas N, Combier J-P, Bécard G, Belausov E (2011) Strigolactones affect lateral root formation and root-hair elongation in *Arabidopsis*. *Planta* 233: 209-216
- Karahara I, Umemura K, Soga Y, Akai Y, Bando T, Ito Y, Tamaoki D, Uesugi K, Abe J, Yamauchi D (2012) Demonstration of osmotically dependent promotion of aerenchyma formation at different levels in the primary roots of rice using a 'sandwich' method and X-ray computed tomography. *Annals of Botany* 110: 503-509
- Kato Y, Abe J, Kamoshita A, Yamagishi J (2006) Genotypic variation in root growth angle in rice (*Oryza sativa* L.) and its association with deep root development in upland fields with different water regimes. *Plant and Soil* 287: 117-129

- Kauffman JM (2003) Radiation hormesis: demonstrated, deconstructed, denied, dismissed, and some implications for public policy. *Journal of Scientific Exploration* 17: 389-407
- Kembel Steven W, Cahill James FJ (2005) Plant phenotypic plasticity belowground: A phylogenetic perspective on root foraging trade-offs. *The American Naturalist* 166: 216-230
- Keyes SD, Daly KR, Gostling NJ, Jones DL, Talboys P, Pinzer BR, Boardman R, Sinclair I, Marchant A, Roose T (2013) High resolution synchrotron imaging of wheat root hairs growing in soil and image based modelling of phosphate uptake. *New Phytologist* 198: 1023-1029
- Khan A (2004a) Mycotrophy and its significance in wetland ecology and wetland management. *Developments in ecosystems* 1: 95-114
- Khan A (2004b) Mycotrophy and its significance in wetland ecology and wetland management. *Developments in ecosystems*. Elsevier B.V., Amsterdam, pp 95-114
- Khush GS (2005) What it will take to feed 5.0 billion rice consumers in 2030? *Plant Molecular Biology* 59: 1-6
- Kirk G (2004) *The biogeochemistry of submerged soils*. John Wiley & Sons, Chichester, UK
- Kirk G, George T, Courtois B, Senadhira D (1998) Opportunities to improve phosphorus efficiency and soil fertility in rainfed lowland and upland rice ecosystems. *Field Crops Research* 56: 73-92
- Kirk G, Saleque M (1995) Solubilization of phosphate by rice plants growing in reduced soil: Prediction of the amount solubilized and the resultant increase in uptake. *European Journal of Soil Science* 46: 247-255
- Kirk G, Santos E, Findenegg G (1999) Phosphate solubilization by organic anion excretion from rice (*Oryza sativa* L.) growing in aerobic soil. *Plant and Soil* 211: 11-18
- Kirkby EA, Johnston AEJ (2008) Soil and fertilizer phosphorus in relation to crop nutrition. *The ecophysiology of plant-phosphorus interactions*. Springer, pp 177-223
- Kitomi Y, Inahashi H, Takehisa H, Sato Y, Inukai Y (2012) OsIAA13-mediated auxin signaling is involved in lateral root initiation in rice. *Plant Science* 190: 116-122
- Kitomi Y, Ogawa A, Kitano H, Inukai Y (2008) CRL4 regulates crown root formation through auxin transport in rice. *Plant Root* 2: 19-28
- Kleine-Vehn J, Ding Z, Jones AR, Tasaka M, Morita MT, Friml J (2010) Gravity-induced PIN transcytosis for polarization of auxin fluxes in gravity-sensing root cells. *Proceedings of the National Academy of Sciences* 107: 22344-22349
- Kögel-Knabner I, Amelung W, Cao Z, Fiedler S, Frenzel P, Jahn R, Kalbitz K, Kölbl A, Schloter M (2010) Biogeochemistry of paddy soils. *Geoderma* 157: 1-14
- Kravchenko A, Falconer RE, Grinev D, Otten W (2011) Fungal colonization in soils with different management histories: modeling growth in three-dimensional pore volumes. *Ecol. Appl.* 21: 1202-1210

- Kristoffersen AØ, Riley H (2005) Effects of soil compaction and moisture regime on the root and shoot growth and phosphorus uptake of barley plants growing on soils with varying phosphorus status. *Nutrient Cycling in Agroecosystems* 72: 135-146
- Kutschera U, Siebert C, Sievers A, Masuda Y (1991) Effects of submergence on development and gravitropism in the coleoptile of *Oryza sativa* L. *Planta* 183: 112-119
- Laan P, Berrevoets M, Lythe S, Armstrong W, Blom C (1989) Root morphology and aerenchyma formation as indicators of the flood-tolerance of *Rumex* species. *The Journal of Ecology* 77: 693-703
- Lambers H, Shane MW, Cramer MD, Pearse SJ, Veneklaas EJ (2006) Root structure and functioning for efficient acquisition of phosphorus: Matching morphological and physiological traits. *Annals of Botany* 98: 693-713
- Larsen S (1967) Soil phosphorus. *Advances in Agronomy* 19: 151-210
- Lavenus J, Goh T, Roberts I, Guyomarc'h S, Lucas M, De Smet I, Fukaki H, Beeckman T, Bennett M, Laplace L (2013) Lateral root development in *Arabidopsis*: Fifty shades of auxin. *Trends in Plant Science* 18: 450-458
- Leitner D, Klepsch S, Ptashnyk M, Marchant A, Kirk G, Schnepf A, Roose T (2010) A dynamic model of nutrient uptake by root hairs. *New Phytologist* 185: 792-802
- Li Y, Luo A, Wei X, Yao X (2007) Genotypic variation of rice in phosphorus acquisition from iron phosphate: Contributions of root morphology and phosphorus uptake kinetics. *Russian Journal of Plant Physiology* 54: 230-236
- Lin H, Zhu M, Yano M, Gao J, Liang Z, Su W, Hu X, Ren Z, Chao D (2004) QTLs for Na⁺ and K⁺ uptake of the shoots and roots controlling rice salt tolerance. *Theoretical and Applied Genetics* 108: 253-260
- Linkohr BI, Williamson LC, Fitter AH, Leyser H (2002) Nitrate and phosphate availability and distribution have different effects on root system architecture of *Arabidopsis*. *The Plant Journal* 29: 751-760
- Liu Y, Donner E, Lombi E, Li R, Wu Z, Zhao F-J, Wu P (2013) Assessing the contributions of lateral roots to element uptake in rice using an auxin-related lateral root mutant. *Plant and Soil* 372: 125-136
- Liu Y, Mi G, Chen F, Zhang J, Zhang F (2004) Rhizosphere effect and root growth of two maize (*Zea mays* L.) genotypes with contrasting P efficiency at low P availability. *Plant Science* 167: 217-223
- Liu Z, Shi W, Fan X (1990) The rhizosphere effects of phosphorus and iron in soils. *Transactions 14th International Congress of Soil Science, Kyoto, Japan*, pp 147-152
- López-Bucio J, Hernández-Abreu E, Sánchez-Calderón L, Nieto-Jacobo MaF, Simpson J, Herrera-Estrella L (2002) Phosphate availability alters architecture and causes changes in hormone sensitivity in the *Arabidopsis* root system. *Plant Physiology* 129: 244-256
- Lynch J (1995) Root architecture and plant productivity. *Plant Physiology* 109: 7-13
- Lynch J, Brown K (2001) Topsoil foraging – an architectural adaptation of plants to low phosphorus availability. *Plant and Soil* 237: 225-237

- Lynch JP (2007) Turner review no. 14. Roots of the second green revolution. *Australian Journal of Botany* 55: 493-512
- Lynch JP (2011) Root phenes for enhanced soil exploration and phosphorus acquisition: Tools for future crops. *Plant Physiology* 156: 1041-1049
- Lynch JP (2013) Steep, cheap and deep: an ideotype to optimize water and N acquisition by maize root systems. *Annals of Botany* 122: 347-357
- Lynch JP, Brown KM (2008) Root strategies for phosphorus acquisition. The ecophysiology of plant-phosphorus interactions. Springer, pp 83-116
- Lynch JP, Brown KM (2012) New roots for agriculture: Exploiting the root phenome. *Philosophical Transactions of the Royal Society B-Biological Sciences* 367: 1598-1604
- Ma Z, Bielenberg D, Brown K, Lynch J (2001) Regulation of root hair density by phosphorus availability in *Arabidopsis thaliana*. *Plant, Cell & Environment* 24: 459-467
- MacDonald GK, Bennett EM, Potter PA, Ramankutty N (2011) Agronomic phosphorus imbalances across the world's croplands. *Proceedings of the National Academy of Sciences* 108: 3086-3091
- Mackay A, Barber S (1985) Effect of soil moisture and phosphate level on root hair growth of corn roots. *Plant and Soil* 86: 321-331
- MacMillan K, Emrich K, Piepho H-P, Mullins C, Price A (2006) Assessing the importance of genotype x environment interaction for root traits in rice using a mapping population. I: A soil-filled box screen. *Theoretical and Applied Genetics* 113: 977-986
- Mairhofer S, Zappala S, Tracy S, Sturrock C, Bennett MJ, Mooney SJ, Pridmore TP (2013) Recovering complete plant root system architectures from soil via X-ray μ -computed tomography. *Plant Methods* 9: 1-7
- Mairhofer S, Zappala S, Tracy SR, Sturrock C, Bennett M, Mooney SJ, Pridmore T (2012) RooTrak: Automated recovery of three-dimensional plant root architecture in soil from X-ray microcomputed tomography images using visual tracking. *Plant Physiology* 158: 561-569
- Mano Y, Omori F, Takamizo T, Kindiger B, Bird RM, Loaisiga C (2006) Variation for root aerenchyma formation in flooded and non-flooded maize and teosinte seedlings. *Plant and Soil* 281: 269-279
- Manske G, Ortiz-Monasterio J, van Ginkel R, Rajaram S, Vlek P (2002) Phosphorus use efficiency in tall, semi-dwarf and dwarf near-isogenic lines of spring wheat. *Euphytica* 125: 113-119
- Marchant A, Bhalerao R, Casimiro I, Eklöf J, Casero PJ, Bennett M, Sandberg G (2002) AUX1 promotes lateral root formation by facilitating indole-3-acetic acid distribution between sink and source tissues in the *Arabidopsis* seedling. *The Plant Cell Online* 14: 589-597
- Marchant A, Kargul J, May ST, Muller P, Delbarre A, Perrot-Rechenmann C, Bennett MJ (1999) AUX1 regulates root gravitropism in *Arabidopsis* by facilitating auxin uptake within root apical tissues. *The EMBO Journal* 18: 2066-2073
- Martin SL, Mooney SJ, Dickinson MJ, West HM (2012) The effects of simultaneous root colonisation by three *Glomus* species on soil pore characteristics. *Soil Biology and Biochemistry* 49: 167-173

- McGinnis R (2002-2009) Rad Pro X-ray device dose-rate calculator online. Massachusetts Institute of Technology
- McNamara NP, Black HIJ, Beresford NA, Parekh NR (2003) Effects of acute gamma irradiation on chemical, physical and biological properties of soils. *Applied Soil Ecology* 24: 117-132
- Mees F, Swennen R, Van Geet M, Jacobs P (2003) Applications of X-ray computed tomography in the geosciences. Geological Society, London, Special Publications 215: 1-6
- Mengel K (1985) Dynamics and availability of major nutrients in soils. *Advances in soil science*. Springer, pp 65-131
- Miller CR, Ochoa I, Nielsen KL, Beck D, Lynch JP (2003) Genetic variation for adventitious rooting in response to low phosphorus availability: Potential utility for phosphorus acquisition from stratified soils. *Functional Plant Biology* 30: 973-985
- Monshausen GB, Haswell ES (2013) A force of nature: molecular mechanisms of mechanoperception in plants. *Journal of Experimental Botany*
- Monshausen GB, Miller ND, Murphy AS, Gilroy S (2011) Dynamics of auxin-dependent Ca^{2+} and pH signaling in root growth revealed by integrating high-resolution imaging with automated computer vision-based analysis. *The Plant Journal* 65: 309-318
- Mooney S, Pridmore T, Helliwell J, Bennett M (2012a) Developing X-ray computed tomography to non-invasively image 3-D root systems architecture in soil. *Plant and Soil* 352: 1-22
- Mooney SJ, Morris C (2008) A morphological approach to understanding preferential flow using image analysis with dye tracers and X-ray computed tomography. *CATENA* 73: 204-211
- Mooney SJ, Pridmore TP, Helliwell J, Bennett MJ (2012b) Developing X-ray computed tomography to non-invasively image 3-D root systems architecture in soil. *Plant and Soil* 352: 1-22
- Moran C, Pierret A, Stevenson A (2000) X-ray absorption and phase contrast imaging to study the interplay between plant roots and soil structure. *Plant and Soil* 223: 101-117
- Mori I, Machida Y, Osanai M, Iinuma K (2012) Photon starvation artifacts of X-ray CT: their true cause and a solution. *Radiological Physics and Technology* 6: 1-12
- Mulkey TJ, Evans ML (1981) Geotropism in corn roots: Evidence for its mediation by differential acid efflux. *Science* 212: 70-71
- Munkholm LJ, Heck RJ, Deen B (2012) Soil pore characteristics assessed from X-ray micro-CT derived images and correlations to soil friability. *Geoderma* 181-182: 22-29
- Nacry P, Canivenc G, Muller B, Azmi A, Van Onckelen H, Rossignol M, Doumas P (2005) A role for auxin redistribution in the responses of the root system architecture to phosphate starvation in *Arabidopsis*. *Plant Physiology* 138: 2061-2074
- Nagel KA, Kastenholz B, Jahnke S, Van Dusschoten D, Aach T, Mühlich M, Truhn D, Scharf H, Terjung S, Walter A (2009) Temperature responses of roots: Impact on growth, root system architecture and implications for phenotyping. *Functional Plant Biology* 36: 947-959

- Nakamura A, Umemura I, Gomi K, Hasegawa Y, Kitano H, Sazuka T, Matsuoka M (2006) Production and characterization of auxin-insensitive rice by overexpression of a mutagenized rice IAA protein. *The Plant Journal* 46: 297-306
- Nguyen T, Klueva N, Chamareck V, Aarti A, Magpantay G, Millena A, Pathan M, Nguyen H (2004) Saturation mapping of QTL regions and identification of putative candidate genes for drought tolerance in rice. *Molecular Genetics and Genomics* 272: 35-46
- Ni J, Wu P, Lou A, Tao Q (1998) Rice seedling tolerance to phosphorus stress in solution culture and soil. *Nutrient Cycling in Agroecosystems* 51: 95-99
- Nibau C, Gibbs D, Coates J (2008) Branching out in new directions: The control of root architecture by lateral root formation. *New Phytologist* 179: 595-614
- Nunan N, Ritz K, Rivers M, Feeney DS, Young IM (2006) Investigating microbial micro-habitat structure using X-ray computed tomography. *Geoderma* 133: 398-407
- Oburger E, Kirk GJ, Wenzel WW, Puschenreiter M, Jones DL (2009) Interactive effects of organic acids in the rhizosphere. *Soil Biology and Biochemistry* 41: 449-457
- Ohno T, Hoskins BR, Erich MS (2007) Soil organic matter effects on plant available and water soluble phosphorus. *Biology and Fertility of Soils* 43: 683-690
- Osorio V, Nelson W (2007) A review on beneficial effects of rhizosphere bacteria on soil nutrient availability and plant nutrient uptake. *Revista Facultad Nacional de Agronomía, Medellín* 60: 3621-3643
- Ottenschläger I, Wolff P, Wolverton C, Bhalerao RP, Sandberg G, Ishikawa H, Evans M, Palme K (2003) Gravity-regulated differential auxin transport from columella to lateral root cap cells. *Proceedings of the National Academy of Sciences* 100: 2987-2991
- Owens PN, Deeks LK, Wood GA, Betson MJ, Lord EI, Davison PS (2008) Variations in the depth distribution of phosphorus in soil profiles and implications for model-based catchment-scale predictions of phosphorus delivery to surface waters. *Journal of Hydrology* 350: 317-328
- Oyanagi A (1994) Gravitropic response growth angle and vertical distribution of roots of wheat (*Triticum aestivum* L.). *Plant and Soil* 165: 323-326
- Ozturk L, Eker S, Torun B, Cakmak I (2005) Variation in phosphorus efficiency among 73 bread and durum wheat genotypes grown in a phosphorus-deficient calcareous soil. *Plant and Soil* 269: 69-80
- Page T, Haygarth PM, Beven KJ, Joynes A, Butler T, Keeler C, Freer J, Owens PN, Wood GA (2005) Spatial variability of soil phosphorus in relation to the topographic index and critical source areas. *Journal of Environmental Quality* 34: 2263-2277
- Pálsdóttir A-M, Alsanus B, Johannesson V, Ask A (2005) Prospects of non-destructive analysis of root growth and geometry using computerized tomography (CT-X-Ray). *International Symposium on Growing Media* 779, pp 155-160
- Pang W, Crow W, Luc J, McSorley R, Giblin-Davis R, Kenworthy K, Kruse J (2011) Comparison of water displacement and WinRHIZO software for plant root parameter assessment. *Plant Disease* 95: 1308-1310

Parker H (2010) The characterisation of the AUX/LAX family in rice. University of Nottingham. Theses. Biosciences: 234

Patrick Jr WH, Mahapatra I (1968) Transformation and availability to rice of nitrogen and phosphorus in waterlogged soils. *Advances in Agronomy* 20: 323-359

Patrick W, Mikkelsen DS, Wells B (1985) Plant nutrient behavior in flooded soil. Fertilizer technology and use. Soil Science Society of America, Madison, WI, pp 197-228

Pearson D (1976) General methods-determination of phosphate by the vanado-molybdate colorimetric method. *The chemical analysis of foods*. Churchill Livingstone, Edinburgh, UK, pp 23-24

Peng S, Tang Q, Zou Y (2009) Current status and challenges of rice production in China. *Plant Production Science* 12: 3-8

Péret B, Li G, Zhao J, Band LR, Vos U, Postaire O, Luu D-T, Da Ines O, Casimiro I, Lucas M (2012) Auxin regulates aquaporin function to facilitate lateral root emergence. *Nature Cell Biology* 14: 991-998

Pérez-Torres C-A, López-Bucio J, Cruz-Ramírez A, Ibarra-Laclette E, Dharmasiri S, Estelle M, Herrera-Estrella L (2008) Phosphate availability alters lateral root development in *Arabidopsis* by modulating auxin sensitivity via a mechanism involving the TIR1 auxin receptor. *The Plant Cell Online* 20: 3258-3272

Perret J, Al-Belushi M, Deadman M (2007) Non-destructive visualization and quantification of roots using computed tomography. *Soil Biology and Biochemistry* 39: 391-399

Pheav S, Bell R, Kirk G, White P (2005) Phosphorus cycling in rainfed lowland rice ecosystems on sandy soils. *Plant and Soil* 269: 89-98

Pires LF, Borges JA, Bacchi OO, Reichardt K (2010) Twenty-five years of computed tomography in soil physics: A literature review of the Brazilian contribution. *Soil and Tillage Research* 110: 197-210

Ponnamperuma F (1972) *The chemistry of submerged soils*. Academic Press New York, NY and London, UK

Ponnamperuma F (1984) Effects of flooding on soils. *Flooding and plant growth*. International Rice Research Institute, Laguna, Phillipines, pp 9-45

Postma JA, Lynch JP (2011) Root cortical aerenchyma enhances the growth of maize on soils with suboptimal availability of nitrogen, phosphorus, and potassium. *Plant Physiology* 156: 1190-1201

Potter P, Ramankutty N, Bennett EM, Donner SD (2010) Characterizing the spatial patterns of global fertilizer application and manure production. *Earth Interactions* 14: 1-22

Price AH (2006) Believe it or not, QTLs are accurate! *Trends in Plant Science* 11: 213-216

Raghu K, MacRae I (1966) Occurrence of phosphate-dissolving micro-organisms in the rhizosphere of rice plants and in submerged soils. *Journal of Applied Microbiology* 29: 582-586

Rahman A, Hosokawa S, Oono Y, Amakawa T, Goto N, Tsurumi S (2002) Auxin and ethylene response interactions during *Arabidopsis* root hair development dissected by auxin influx modulators. *Plant Physiology* 130: 1908-1917

- Rajhi I, Yamauchi T, Takahashi H, Nishiuchi S, Shiono K, Watanabe R, Mliki A, Nagamura Y, Tsutsumi N, Nishizawa NK (2011) Identification of genes expressed in maize root cortical cells during lysigenous aerenchyma formation using laser microdissection and microarray analyses. *New Phytologist* 190: 351-368
- Ramos V, Muge F (2000) Map segmentation by colour cube genetic k-mean clustering. In: Borbinha J, Baker T (eds) *Research and advanced technology for digital libraries*. Springer, Berlin Heidelberg, pp 319-323
- Rani Debi B, Chhun T, Taketa S, Tsurumi S, Xia K, Miyao A, Hirochika H, Ichii M (2005) Defects in root development and gravity response in the *aem1* mutant of rice are associated with reduced auxin efflux. *Journal of Plant Physiology* 162: 678-685
- Ren Z-H, Gao J-P, Li L-G, Cai X-L, Huang W, Chao D-Y, Zhu M-Z, Wang Z-Y, Luan S, Lin H-X (2005) A rice quantitative trait locus for salt tolerance encodes a sodium transporter. *Nature Genetics* 37: 1141-1146
- Richardson AE, Barea J-M, McNeill AM, Prigent-Combaret C (2009) Acquisition of phosphorus and nitrogen in the rhizosphere and plant growth promotion by microorganisms. *Plant and Soil* 321: 305-339
- Robinson D (1994) Tansley review no. 73. The responses of plants to non-uniform supplies of nutrients. *New Phytologist* 127: 635-674
- Robinson D (1996) Resource capture by localized root proliferation: Why do plants bother? *Annals of Botany* 77: 179-186
- Rodríguez H, Fraga R (1999) Phosphate solubilizing bacteria and their role in plant growth promotion. *Biotechnology Advances* 17: 319-339
- Rolston DE, Rauschkolb RS, Hoffman DL (1975) Infiltration of organic phosphate compounds in soil. *Soil Science Society of America Journal* 39: 1089-1094
- Rothamsted R (2006) *Guide to the classical and other long-term experiments, datasets and sample archive*. Lawes Agricultural Trust Ltd., p 56
- Rubio G, Liao H, Yan X, Lynch JP (2003) Topsoil foraging and its role in plant competitiveness for phosphorus in common bean. *Crop Science* 43: 598-607
- Rudolph N, Voss S, Moradi AB, Nagl S, Oswald SE (2013) Spatio-temporal mapping of local soil pH changes induced by roots of lupin and soft-rush. *Plant and Soil* 369: 669-680
- Ryser P (2006) The mysterious root length. *Plant and Soil* 286: 1-6
- Sachay JE, Wallace RL, Johns MA (1991) Phosphate stress response in hydroponically grown maize. *Plant and Soil* 132: 85-90
- Saleque M, Kirk G (1995) Root-induced solubilization of phosphate in the rhizosphere of lowland rice. *New Phytologist* 129: 325-336
- Schmidt S, Bengough A, Gregory P, Grinev D, Otten W (2012) Estimating root-soil contact from 3D X-ray microtomographs. *European Journal of Soil Science* 63: 776-786

- Schmidt W, Schikora A (2001) Different pathways are involved in phosphate and iron stress-induced alterations of root epidermal cell development. *Plant Physiology* 125: 2078-2084
- Seigneur N, Gauthier A, Mess F, Brunel C, Dubois M, Potdevin JL (2010) Development of plant root networks in polluted soils: An X-ray computed microtomography investigation. *Water Air and Soil Pollution* 209: 199-207
- Shahandeh H, Hossner L, Turner F (1995) Evaluation of soil phosphorus tests for flooded rice soils under oxidized and reduced soil conditions. *Communications in Soil Science & Plant Analysis* 26: 107-121
- Shahandeh H, Hossner L, Turner F (2003) Phosphorus relationships to manganese and iron in rice soils. *Soil Science* 168: 489-500
- Shen J, Yuan L, Zhang J, Li H, Bai Z, Chen X, Zhang W, Zhang F (2011) Phosphorus dynamics: From soil to plant. *Plant Physiology* 156: 997-1005
- Shepherd M, Withers P (1999) Applications of poultry litter and triple superphosphate fertilizer to a sandy soil: effects on soil phosphorus status and profile distribution. *Nutrient Cycling in Agroecosystems* 54: 233-242
- Shimizu A, Yanagihara S, Kawasaki S, Ikehashi H (2004) Phosphorus deficiency-induced root elongation and its QTL in rice (*Oryza sativa* L.). *Theoretical and Applied Genetics* 109: 1361-1368
- Sims JT, Sharpley AN (2005) Phosphorus: Agriculture and the environment. *American Society of Agronomy*
- Smil V (2000) Phosphorus in the environment: Natural flows and human interferences. *Annual Review of Energy and the Environment* 25: 53-88
- Smith S, De Smet I (2012) Root system architecture: Insights from *Arabidopsis* and cereal crops. *Philosophical Transactions of the Royal Society B: Biological Sciences* 367: 1441-1452
- Smith VH, Tilman GD, Nekola JC (1999) Eutrophication: Impacts of excess nutrient inputs on freshwater, marine, and terrestrial ecosystems. *Environmental Pollution* 100: 179-196
- Solaiman MZ, Hirata H (1995) Effects of indigenous arbuscular mycorrhizal fungi in paddy fields on rice growth and N, P, K nutrition under different water regimes. *Soil Science and Plant Nutrition* 41: 505-514
- Song Y, You J, Xiong L (2009) Characterization of OsIAA1 gene, a member of rice Aux/IAA family involved in auxin and brassinosteroid hormone responses and plant morphogenesis. *Plant Molecular Biology* 70: 297-309
- Sreevidya V, Hernandez-Oane RJ, Gyaneshwar P, Lara-Flores M, Ladha JK, Reddy PM (2010) Changes in auxin distribution patterns during lateral root development in rice. *Plant Science* 178: 531-538
- Stanga J, Neal C, Vaughn L, Baldwin K, Jia G (2009) Signaling in plant gravitropism. *Signaling in plants*. Springer-Verlag, Berlin Heidelberg, pp 209-237
- Stevenson FJ, Cole MA (1999) Cycles of soils: carbon, nitrogen, phosphorus, sulfur, micronutrients. John Wiley & Sons, Danvers, MA

Stingaciu L, Schulz H, Pohlmeier A, Behnke S, Zilken H, Javaux M, Vereecken H (2013) In situ root system architecture extraction from magnetic resonance imaging for water uptake modeling. *Vadose Zone Journal* 12: 1-9

Stupian GW (2007) X-Ray dose in microfocus radiographic inspections. Aerospace Corp. Electronics Research Lab, El Segundo, CA, p 34

Stuppy WH, Maisano JA, Colbert MW, Rudall PJ, Rowe TB (2003) Three-dimensional analysis of plant structure using high-resolution X-ray computed tomography. *Trends in Plant Science* 8: 2-6

Swarup R, Friml J, Marchant A, Ljung K, Sandberg G, Palme K, Bennett M (2001) Localization of the auxin permease AUX1 suggests two functionally distinct hormone transport pathways operate in the *Arabidopsis* root apex. *Genes & Development* 15: 2648-2653

Swarup R, Kramer EM, Perry P, Knox K, Leyser HO, Haseloff J, Beemster GT, Bhalerao R, Bennett MJ (2005) Root gravitropism requires lateral root cap and epidermal cells for transport and response to a mobile auxin signal. *Nature Cell Biology* 7: 1057-1065

Syers J, Poulton P, Johnston A, International Fertiliser Society Y (2001) Phosphorus, potassium and sulphur cycles in agricultural soils. The International Fertiliser Society

Thomas A, Guerreiro S, Sodek L (2005) Aerenchyma formation and recovery from hypoxia of the flooded root system of nodulated soybean. *Annals of Botany* 96: 1191-1198

Trachsel S, Kaeppler SM, Brown KM, Lynch JP (2011) Shovelomics: High throughput phenotyping of maize (*Zea mays* L.) root architecture in the field. *Plant and Soil* 341: 75-87

Tracy SR, Black C, Roberts J, McNeill A, Davidson R, Tester M, Samec M, Korošak D, Sturrock C, Mooney S (2012a) Quantifying the effect of soil compaction on three varieties of wheat (*Triticum aestivum* L.) using X-ray micro computed tomography (CT). *Plant and Soil* 353: 195-208

Tracy SR, Black CR, Roberts JA, McNeill A, Davidson R, Tester M, Samec M, Korošak D, Sturrock C, Mooney SJ (2012b) Quantifying the effect of soil compaction on three varieties of wheat (*Triticum aestivum* L.) using X-ray micro computed tomography (CT). *Plant and Soil* 353: 195-208

Tracy SR, Black CR, Roberts JA, Mooney SJ (2013) Exploring the interacting effect of soil texture and bulk density on root system development in tomato (*Solanum lycopersicum* L.). *Environmental and Experimental Botany* 91: 38-47

Tracy SR, Black CR, Roberts JA, Sturrock C, Mairhofer S, Craigon J, Mooney SJ (2012c) Quantifying the impact of soil compaction on root system architecture in tomato (*Solanum lycopersicum*) by X-ray micro-computed tomography. *Annals of Botany*: Online only at present

Tracy SR, Black CR, Roberts JA, Sturrock C, Mairhofer S, Craigon J, Mooney SJ (2012d) Quantifying the impact of soil compaction on root system architecture in tomato (*Solanum lycopersicum*) by X-ray micro-computed tomography. *Annals of Botany* 110: 511-519

Tracy SR, Black CR, Roberts JA, Sturrock C, Mairhofer S, Craigon J, Mooney SJ (2012e) Quantifying the impact of soil compaction on root system architecture in tomato (*Solanum lycopersicum*) by X-ray micro-computed tomography. *Annals of Botany* 110: 511-519

- Tracy SR, Roberts JA, Black CR, McNeill A, Davidson R, Mooney SJ (2010) The X-factor: Visualizing undisturbed root architecture in soils using X-ray computed tomography. *Journal of Experimental Botany* 61: 311-313
- Uga Y, Okuno K, Yano M (2011) Dro1, a major QTL involved in deep rooting of rice under upland field conditions. *Journal of Experimental Botany* 62: 2485-2494
- Vallino M, Greppi D, Novero M, Bonfante P, Lupotto E (2009) Rice root colonisation by mycorrhizal and endophytic fungi in aerobic soil. *Annals of Applied Biology* 154: 195-204
- Van Nguyen N, Ferrero A (2006) Meeting the challenges of global rice production. *Paddy and Water Environment* 4: 1-9
- Vance ED, Brookes PC, Jenkinson DS (1987) An extraction method for measuring soil microbial biomass C. *Soil Biology and Biochemistry* 19: 703-707
- Visser EJ, Voesenek LA (2005) Acclimation to soil flooding—sensing and signal-transduction. *Plant and Soil* 274: 197-214
- Waisel Y, Eshel A, Waisel Y, Eshel A (2002) Functional diversity of various constituents of a single root system. *Plant roots: The hidden half*. CRC Press, pp 157-174
- Wang J, Shuman LM (1994) Transformation of phosphate in rice (*Oryza sativa* L.) rhizosphere and its influence on phosphorus nutrition of rice. *Journal of Plant Nutrition* 17: 1803-1815
- Wang M-B, Zhang Q (2009) Issues in using the WinRHIZO system to determine physical characteristics of plant fine roots. *Acta Ecologica Sinica* 29: 136-138
- Wells CE, Eissenstat DM (2002) Beyond the roots of young seedlings: The influence of age and order on fine root physiology. *Journal of Plant Growth Regulation* 21: 324-334
- Whalley WR, Watts CW, Gregory AS, Mooney SJ, Clark LJ, Whitmore AP (2008) The effect of soil strength on the yield of wheat. *Plant and Soil* 306: 237-247
- White PJ, Hammond JP (2008) Phosphorus nutrition of terrestrial plants. *The ecophysiology of plant-phosphorus interactions*. Springer, pp 51-81
- White PJ, Hammond JP (2009) The sources of phosphorus in the waters of Great Britain. *Journal of Environmental Quality* 38: 13-26
- Wijesinghe DK, John EA, Beurskens S, Hutchings MJ (2001) Root system size and precision in nutrient foraging: responses to spatial pattern of nutrient supply in six herbaceous species. *Journal of Ecology* 89: 972-983
- Wildenschild D, Vaz C, Rivers M, Rikard D, Christensen B (2002) Using X-ray computed tomography in hydrology: Systems, resolutions, and limitations. *Journal of Hydrology* 267: 285-297
- Wissuwa M, Ae N (2001) Genotypic variation for tolerance to phosphorus deficiency in rice and the potential for its exploitation in rice improvement. *Plant Breeding* 120: 43-48

- Wissuwa M, Wegner J, Ae N, Yano M (2002) Substitution mapping of Pup1: A major QTL increasing phosphorus uptake of rice from a phosphorus-deficient soil. *Theoretical and Applied Genetics* 105: 890-897
- Wollenweber B, Porter JR, Lübberstedt T (2005) Need for multidisciplinary research towards a second green revolution. *Current Opinion in Plant Biology* 8: 337-341
- Xu M, Zhu L, Shou H, Wu P (2005) A PIN1 family gene, OsPIN1, involved in auxin-dependent adventitious root emergence and tillering in rice. *Plant and Cell Physiology* 46: 1674-1681
- Yang WN, Xu XC, Duan LF, Luo QM, Chen SB, Zeng SQ, Liua QA (2011) High-throughput measurement of rice tillers using a conveyor equipped with X-ray computed tomography. *Review of Scientific Instruments* 82: 02512-025107
- Yardin MR, Kennedy IR, Thies JE (2000) Development of high quality carrier materials for field delivery of key microorganisms used as bio-fertilisers and bio-pesticides. *Radiation Physics and Chemistry* 57: 565-568
- Yoshihara T, Iino M (2005) Circumnutation of rice coleoptiles: its occurrence, regulation by phytochrome, and relationship with gravitropism. *Plant, Cell & Environment* 28: 134-146
- Yu J, Hu S, Wang J, Wong GK-S, Li S, Liu B, Deng Y, Dai L, Zhou Y, Zhang X (2002) A draft sequence of the rice genome (*Oryza sativa* L. ssp. indica). *Science* 296: 79-92
- Zappala S, Helliwell JR, Tracy SR, Mairhofer S, Sturrock CJ, Pridmore T, Bennett M, Mooney SJ (2013a) Effects of X-ray dose on rhizosphere studies using X-ray computed tomography. *PloS One* 8: e67250
- Zappala S, Mairhofer S, Tracy S, Sturrock CJ, Bennett M, Pridmore T, Mooney SJ (2013b) Quantifying the effect of soil moisture content on segmenting root system architecture in X-ray computed tomography images. *Plant and Soil* 370: 35-45
- Zhang H, Huang Y, Ye X, Shi L, Xu F (2009) Genotypic differences in phosphorus acquisition and the rhizosphere properties of *Brassica napus* in response to low phosphorus stress. *Plant and Soil* 320: 91-102
- Zhang J, Peng Y, Guo Z (2008) Constitutive expression of pathogen-inducible OsWRKY31 enhances disease resistance and affects root growth and auxin response in transgenic rice plants. *Cell Research* 18: 508-521
- Zhang X, Zhang F, Mao D (1999) Effect of iron plaque outside roots on nutrient uptake by rice (*Oryza sativa* L.): Phosphorus uptake. *Plant and Soil* 209: 187-192
- Zhu J, Ingram PA, Benfey PN, Elich T (2011) From lab to field, new approaches to phenotyping root system architecture. *Current Opinion in Plant Biology* 14: 310-317
- Zhu J, Kaeppler SM, Lynch JP (2005) Topsoil foraging and phosphorus acquisition efficiency in maize (*Zea mays*). *Functional Plant Biology* 32: 749-762
- Zhu Y-G, Smith AF, Smith SE (2003) Phosphorus efficiencies and responses of barley (*Hordeum vulgare* L.) to arbuscular mycorrhizal fungi grown in highly calcareous soil. *Mycorrhiza* 13: 93-100

Zhu Z-X, Liu Y, Liu S-J, Mao C-Z, Wu Y-R, Wu P (2012) A gain-of-function mutation in OsIAA11 affects lateral root development in rice. *Molecular Plant* 5: 154-161

Zobel RW (2008) Hardware and software efficacy in assessment of fine root diameter distributions. *Computers and Electronics in Agriculture* 60: 178-189

Zygalakis K, Kirk G, Jones D, Wissuwa M, Roose T (2011) A dual porosity model of nutrient uptake by root hairs. *New Phytologist* 192: 676-688